Western Graduate&PostdoctoralStudies

Western University
Scholarship@Western

Electronic Thesis and Dissertation Repository

3-7-2019 2:00 PM

Cortical Plasticity following Adult-Onset Hearing Loss

Ashley L. Schormans
The University of Western Ontario

Supervisor
Allman, Brian L.
The University of Western Ontario

Graduate Program in Anatomy and Cell Biology
A thesis submitted in partial fulfillment of the requirements for the degree in Doctor of Philosophy
© Ashley L. Schormans 2019

Follow this and additional works at: https://ir.lib.uwo.ca/etd

Part of the Systems Neuroscience Commons

Recommended Citation

Schormans, Ashley L., "Cortical Plasticity following Adult-Onset Hearing Loss" (2019). *Electronic Thesis and Dissertation Repository*. 6050.
https://ir.lib.uwo.ca/etd/6050

This Dissertation/Thesis is brought to you for free and open access by Scholarship@Western. It has been accepted for inclusion in Electronic Thesis and Dissertation Repository by an authorized administrator of Scholarship@Western. For more information, please contact wlswadmin@uwo.ca.

Abstract

The consequences of hearing loss are not confined to how the central auditory system processes sound; crossmodal plasticity also occurs, which is characterized by an increased responsiveness of neurons in auditory areas to visual and/or tactile stimuli. In the primary auditory cortex, partial hearing loss causes a decrease in the number of auditory-responsive neurons, as well as an increase in multisensory neurons. However, it was relatively unknown how adult-onset hearing loss affected cortical areas that are already capable of integrating multisensory information, such as the lateral extrastriate visual cortex (V2L). Using a combination of *in vivo* electrophysiology, neuropharmacology and behavioural testing, this thesis investigated the nature and extent that crossmodal plasticity occurs within higher-order sensory cortices, and its perceptual consequences. At the level of single neurons, hearing loss increased the proportion of visually-responsive neurons, and decreased the number of neurons activated by both auditory and visual stimuli in V2L; findings inconsistent with the plasticity observed in the neighbouring dorsal auditory cortex (AuD), where the proportion of multisensory neurons nearly doubled. Subsequent analyses of the microcircuits within these higher-order cortices, revealed a layer-specific enhancement of auditory input (i.e., central gain enhancement) within the granular layer of AuD. In contrast, crossmodal plasticity was evident across multiple cortical layers within V2L, and also manifested in AuD. Despite the extensive plasticity in the higher-order sensory cortices, hearing loss lead to behavioural changes in audiovisual perception, characterized by a rapid recalibration of temporal sensitivity to the audiovisual stimuli. Next, a neurophysiological assessment revealed that adult-onset hearing loss did not cause a loss of temporally-precise audiovisual processing, but rather a shift in the cortical region displaying the capacity for temporal sensitivity. Lastly, using pharmacological manipulations, hearing loss was found to cause a layer-specific enhancement of visual-evoked input within the granular layer of the V2L cortex, indicative of thalamocortical plasticity. Overall, this work demonstrates that adult-onset hearing loss induces plasticity at the level of single neurons, local cortical microcircuits and sensory perception, all of which are associated with a complex assortment of crossmodal and intramodal changes across the layers of higher-order sensory cortices.

Keywords

Hearing loss, crossmodal plasticity, sensory reorganization, lateral extrastriate visual cortex, extracellular electrophysiology, audiovisual integration, audiovisual perception, rat

Co-Authorship Statement

Chapter 2 of this thesis was published in a special issue of *Hearing Research* and was co-authored by M. Typlt and B.L. Allman. I performed all electrophysiological recordings, data analyses, and wrote/edited the manuscript. M. Typlt helped to design the experimental procedures and assisted with data analysis. B.L. Allman was involved in experimental design and edited the manuscript.

Chapter 3 of this thesis was published in *Cerebral Cortex* and was co-authored by M. Typlt and B.L. Allman. I performed all electrophysiological recordings, data analyses, and wrote/edited the manuscript. M. Typlt edited the manuscript and B.L. Allman was involved in experimental design and edited the manuscript.

Chapter 4 of this thesis was published in *Frontiers of Behavioral Neuroscience* and was co-authored by B.L. Allman. I conducted all behavioural testing, analyzed all data and wrote/edited the manuscript. B.L. Allman assisted with the development and validation of the behavioural tasks and edited the manuscript.

Chapter 5 of this thesis was accepted for publication in *Neural Plasticity* and was co-authored by B.L. Allman. I performed all electrophysiological recordings, conducted all behavioural testing, analyzed all data and wrote/edited the manuscript. B.L. Allman edited the manuscript.

Acknowledgments

First and foremost, I would like to thank my supervisor Dr. Brian Allman. You took me on as your first graduate student at Western University without any research experience and not knowing whether I wanted a scientific career. Over the past 5 years, you have taught me numerous invaluable skills, such as critical thinking, scientific problem solving, research excellence, and how to be a dedicated and influential mentor. Your passion for science and dedication to your students, made you an exceptional mentor and scientific advisor. I cannot begin to thank you for all the opportunities and experiences that you have provided over the course of my degree, I just hope that I will be as good of a mentor to others, as you have been to me.

Secondly, I would like to thank Drs. Marei Typlt and Daniel Stolzberg who provided vital advice and mentoring in my first few years of grad school. Between assisting in setting up our lab and providing advice on experimental techniques, both of you served as scientific role models and played a large role in the scientist I have become today.

I am also grateful to the past and present members of the Allman lab. In particular, I would like to thank Kaela Scott, Krystal Beh and Greg Sigel for their support and friendship over the past 3 years. You helped to fill the long days and late nights in the lab with laughter and friendship and made getting through the hard times so much easier. I would also like to thank all of the undergraduate volunteers that have assisted with various aspects of my research. Principally, I would like to recognize Albert Vo and Anna Tyker for their assistance in setting up the audiovisual perceptual behaviours and their constant support and dedication during this process.

I would also like to thank the members of my advisory committee: Dr. Susanne Schmid, Dr. Raj Rajakumar and Dr. Shawn Whitehead for their guidance and support throughout my graduate studies.

I am grateful to the students, staff and faculty of the Department of Anatomy and Cell Biology, in particular the administrative and support staff. I would also like to thank the Animal Care and Veterinary Services for all their support and assistance over the years, it has been a pleasure to work with everyone.

I would also like to thank all of the friends that I have made during my graduate studies, as well as my friends from the University of Waterloo. There are few people that understand what you are going through as a graduate student, unless they are going through the same thing, and having each and every one of you around made my time at Western so much better. In particular, I would like to thank Dr. Erin Azzopardi. You have been an amazing friend ever since the first time I walked into our office, and have provided me with countless support and advice, and you continue to be my major source of strength as we both move forward with our scientific careers.

Lastly, I would like to thank my family for all the support that you have given me over the years. Parents, I would like to thank you for the unwavering support, confidence and patience over the past 5 years. I know it was never easy trying to understand the life of a graduate student, but you were always there with positive comments and a million questions about my next paper. To my sister Erin, thank you for being there to talk to when I needed and keeping the rest of the family company, especially since I was always in the lab over the holidays. To Rob Dunbar and Ann Fudge-Schormans, thank you for providing me with advice when I was trying to decide to do a PhD, your support and suggestions helped to make my decision much easier. To Jeff Schormans, thank you for always asking me the hard questions, you have always pushed me to become a better and more thoughtful person and taught me the importance of continuing to learn as much as I can.

Table of Contents

Abstract i

Co-Authorship Statement iii

Acknowledgments iv

Table of Contents vi

List of Tables xiv

List of Figures xv

List of Appendices xix

List of Abbreviations and Symbols xx

Chapter 1 1

1 General Introduction 1

1.1 Overview 1

1.2 Sensory Processing 2

1.2.1 Multisensory Processing 2

1.2.2 Multisensory Perception 6

1.3 Sensory Deprivation and Cortical Plasticity 8

1.3.1 Visual Deprivation 8

1.3.2 Auditory Deprivation 10

1.4 Experience-Dependent Neuroplasticity 15

1.4.1 Central Gain Enhancement 16

1.4.2 Crossmodal Plasticity 17

1.5 Thesis Overview 20

1.5.1 Chapter 2: Crossmodal Plasticity in Auditory, Visual and Multisensory Cortical Areas following Noise-Induced Hearing Loss 21

1.5.2 Chapter 3: Adult-Onset Hearing Impairment Induces Layer-Specific Cortical Reorganization: Evidence of Crossmodal Plasticity and Central Gain Enhancement 22

1.5.3 Chapter 4: Behavioural Plasticity of Audiovisual Perception: Rapid Recalibration of Temporal Sensitivity but not Perceptual Binding following Adult-Onset Hearing Loss 23

1.5.4 Chapter 5: Compensatory Plasticity in the Lateral Extrastriate Visual Cortex Preserves Audiovisual Temporal Processing following Adult-Onset Hearing Loss 25

1.5.5 Chapter 6: Noise-Induced Crossmodal Plasticity within the Audiovisual Cortex: Layer-Specific Enhancement and Rapid Manifestation of Visual-Evoked Activity.....26

1.6 References 28

Chapter 2.....45

2 Crossmodal Plasticity in Auditory, Visual and Multisensory Cortical Areas Following Noise-Induced Hearing Loss in Adulthood 45

2.1 Introduction 45

2.2 Material and Methods 47

2.2.1 Animals.....47

2.2.2 Hearing Assessment with an Auditory Brainstem Response.....47

2.2.3 Noise Exposure 48

2.2.4 Surgical Procedure 49

2.2.5 Electrophysiological Recordings.....49

2.2.6 Audiovisual Stimulation Paradigm 52

2.2.7 Offline Sorting of Single- and Multi-Units.....52

2.2.8 Single-Unit Analysis & Neuron Classification.....53

2.2.9 Multi-Unit Analysis & Sensory Responsiveness 57

2.2.10 Statistics.....58

2.2.11 Histology.....59

2.3 Results 60

2.3.1 Noise-Induced Hearing Loss.....60

2.3.2 Single-Unit Firing Rates & Neuron Classification 61

2.3.3 Multi-Unit Activity & Sensory Responsiveness 69

2.4 Discussion.....70

2.4.1 Audiovisual Processing in the Lateral Extrastriate Visual Cortex (V2L) .72

2.4.2 Noise-Induced Crossmodal Plasticity.....73

2.4.3 Multisensory Integration Following Noise Exposure.....75

2.4.4 Transition of the Functional Border of the Audiovisual Cortex 75

2.4.5 Possible Mechanisms of Crossmodal Plasticity.....76

2.4.6 Behavioural Consequences of Partial Hearing Loss on Audiovisual Integration 78

2.5 References 80

Chapter 3.....86

3 Adult-Onset Hearing Impairment Induces Layer-Specific Cortical Reorganization: Evidence of Crossmodal Plasticity and Central Gain Enhancement 86

3.1 Introduction 86

3.2 Methods.....88

3.2.1 Animals.....88

3.2.2 Hearing Assessment 89

3.2.3 Noise Exposure 90

3.2.4 Surgical Procedure 90

3.2.5 Electrophysiological Recordings.....91

3.2.6 Sensory Stimulation.....92

3.2.7 Current Source Density Analysis 94

3.2.8 Average Rectified CSD Analysis.....95

3.2.9 Statistics.....97

3.2.10 Histology.....97

3.3 Results 98

3.3.1 Noise-Induced Hearing Loss.....98

3.3.2 Response Profile of Auditory, Visual and Audiovisual Cortices.....100

3.3.3 Crossmodal Plasticity Occurred across Multiple Layers of the Higher-Order Sensory Cortices.....101

3.3.4 Central Gain Enhancement was Layer-Specific and Did Not Extend Beyond the Auditory Cortex.....103

3.3.5 Noise Exposure Caused a Differential Effect on AVREC Peak Amplitude in the Auditory, Visual and Audiovisual Cortices 105

3.3.6 Audiovisual Responsiveness was Preserved Despite the Co-Existence of Central Gain Enhancement and Crossmodal Plasticity in Higher-Order Sensory Cortices.....108

3.4 Discussion.....110

3.4.1 Cortical Region- and Layer-Specific Plasticity Following Partial Hearing Loss.....111

3.4.2 Putative Mechanisms of Central Gain Enhancement and Crossmodal Plasticity.....113

3.4.3 Audiovisual Processing and Partial Hearing Loss 114

3.5 References 116

Chapter 4.....122

4 Behavioural Plasticity of Audiovisual Perception: Rapid Recalibration of Temporal Sensitivity but not Perceptual Binding Following Adult-Onset Hearing Loss 122

4.1 Introduction 122

4.2 Methods.....125

4.2.1 Behavioural Apparatus and Sensory Stimuli 126

4.2.2 Overview of Behavioural Training Procedures for the TOJ and SJ Tasks 128

4.2.3 Experiment 1- Modulation of Sound Intensity 130

4.2.4 Experiment 2- Noise Exposure and Audiovisual Temporal Acuity.....132

4.2.5 Statistics and Data Presentation 134

4.3 Results 135

4.3.1 Experiment 1A- Modulation of Sound Intensity Shifted the Perception of Simultaneity during the TOJ Task....135

4.3.2 Experiment 2A- Rapid Recalibration of Audiovisual Temporal Order Perception following Hearing Loss....137

4.3.3 Experiment 2A- Audiovisual Temporal Order Perception in Noise-Exposed Rats Remained Sensitive to Sound Intensity Modulation....141

4.3.4 Experiment 1B- Modulation of Sound Intensity Altered the Detection of Asynchronous Stimulus during the SJ Task....143

4.3.5 Experiment 2B- Persistent Impairments in the Ability to Judge the Synchrony of Audiovisual Stimuli following Adult-Onset Hearing Loss....145

4.3.6 Experiment 2B- Impairments in Asynchrony Detection Resulted in Altered Perceptual Binding of Audiovisual Stimuli following Hearing Loss....149

4.4 Discussion....152

4.4.1 Stimulus Intensity Predicts Audiovisual Temporal Acuity....152

4.4.2 Hearing Loss and Audiovisual Temporal Acuity....154

4.4.3 Behavioural Plasticity of Audiovisual Temporal Acuity following Adult-Onset Hearing Loss....155

4.5 References....157

Chapter 5....163

5 Compensatory Plasticity in the Lateral Extrastriate Visual Cortex Preserves Audiovisual Temporal Processing Following Adult-Onset Hearing Loss....163

5.1 Introduction....163

5.2 Methods....166

5.2.1 Experiment 1: Role of V2L in Audiovisual Temporal Acuity....166

5.2.2 Experiment 2: Electrophysiological Investigation of Audiovisual Temporal Processing following Noise-Induced Hearing loss....171

5.2.3 Histology....178

5.2.4 Statistics....180

5.3 Results....180

5.3.1 Inactivation of the V2L Cortex Shifted the Perception of Simultaneity and Perceived Synchrony 180

5.3.2 Noise-Induced Hearing Loss 182

5.3.3 Crossmodal Plasticity Increases Audiovisual Responsiveness within the Multisensory Zone of the V2L Cortex across a Range of SOAs 183

5.3.4 Audiovisual Responsiveness within the Auditory Zone of the V2L Cortex following Adult-Onset Hearing Loss 187

5.3.5 A Shift in the Temporal Profile following Noise-Induced Crossmodal Plasticity 190

5.4 Discussion 195

5.4.1 The Role of the V2L Cortex in Audiovisual Temporal Processing and Perception 196

5.4.2 Effects of Hearing Loss on Audiovisual Temporal Processing 197

5.4.3 Compensatory Plasticity following Hearing Loss 198

5.4.4 Conclusions 199

5.5 References 200

Chapter 6 205

6 Noise-Induced Crossmodal Plasticity within the Audiovisual Cortex: Layer-Specific Enhancement and Rapid Manifestation of Visual-Evoked Activity 205

6.1 Introduction 205

6.2 Methods 207

6.2.1 Animals 207

6.2.2 Hearing Assessment & Noise Exposure 207

6.2.3 Experiment 1: Thalamocortical Contributions to Noise-Induced Crossmodal Plasticity 208

6.2.4 Experiment 2: Onset of Crossmodal Plasticity 214

6.2.5 Statistics and Data Presentation 218

6.3 Results 218

6.3.1 Experiment 1: Thalamocortical Contributions to Noise-Induced Crossmodal Plasticity 218

6.3.2 Experiment 2: Onset of Crossmodal Plasticity 228

6.4 Discussion.....237

6.4.1 Layer-Specific Effects of Sensory Deprivation 238

6.4.2 The Audiovisual Cortex: Spared or Deprived Cortical Region? 240

6.4.3 Rapid Manifestation of Crossmodal Plasticity following Sensory Deprivation 241

6.5 References 243

Chapter 7.....249

7 General Discussion 249

7.1 Summary of Main Findings.....249

7.1.1 Mapping the Sensory Domains within the V2L Cortex in the Rat 249

7.1.2 Crossmodal Plasticity in Auditory, Visual and Multisensory Cortical Areas following Noise-Induced Hearing Loss.....250

7.1.3 Adult-Onset Hearing Impairment Induces Layer-Specific Cortical Reorganization: Evidence of Crossmodal Plasticity and Central Gain Enhancement.....251

7.1.4 Behavioural Plasticity of Audiovisual Perception: Rapid Recalibration of Temporal Sensitivity but not Perceptual Binding following Adult-Onset Hearing Loss 252

7.1.5 Compensatory Plasticity within the Lateral Extrastriate Visual Cortex Preserves Audiovisual Temporal Processing Following Adult-Onset Hearing Loss 253

7.1.6 Noise-Induced Crossmodal Plasticity within the Audiovisual Cortex: Layer-Specific Enhancement, and Rapid Manifestation of Visual-Evoked Activity 254

7.2 Experimental Limitations 255

7.3 Future Directions 257

7.3.1 Effect of Perceptual Training on Temporal Perception following Noise-Induced Hearing Loss.....258

7.3.2 Is a Loss of Inhibition Sufficient to Induce Crossmodal Plasticity? 258

7.4 Conclusion.....259

7.5 References 260

Appendices 266

Curriculum Vitae 308

List of Tables

Table 4.1. Effect of auditory intensity and hearing loss on audiovisual temporal perception at all stimulus onset asynchronies when compared to 75 dB SPL testing sessions 138

Table 4.2. Effect of auditory intensity and hearing loss on audiovisual synchrony perception at all stimulus onset asynchronies when compared to 75 dB SPL testing sessions 146

Table 6.1. Statistical analysis of auditory-evoked data by two-way rmANOVA 232

Table 6.2. Statistical analysis of visual-evoked data by two-way rmANOVA.....235

List of Figures

Figure 2.1. Representative recording penetrations in the V2L cortex and AuD cortex in the rat. 51

Figure 2.2. Responses of a bimodal neuron in the V2L cortex to auditory, visual and combined audiovisual stimuli. 54

Figure 2.3. Responses of unisensory and multisensory (bimodal and subthreshold) neurons in the V2L cortex and AuD cortex in the rat. 56

Figure 2.4. Spiking activity of multi-unit clusters to auditory and visual stimuli was used to assess sensory responsiveness. 58

Figure 2.5. Noise-induced hearing loss as assessed with an auditory brainstem response (ABR) to a click stimulus. 61

Figure 2.6. The proportion of unisensory and multisensory (bimodal and subthreshold) neurons in the V2L cortex and AuD cortex in normal hearing and noise-exposed rats. 63

Figure 2.7. Maximum firing rates per trial of unisensory and multisensory (bimodal and subthreshold) neurons in the V2L cortex and AuD cortex of normal hearing and noise-exposed rats. 66

Figure 2.8. The effect of noise exposure on multisensory integration in bimodal-integrating and subthreshold multisensory neurons in the V2L cortex and AuD cortex. 68

Figure 2.9. Sensory responsiveness in the V2L cortex and AuD cortex of normal hearing and noise-exposed rats. 71

Figure 2.10. Ventral shift of sensory responsiveness across the V2L cortex and AuD cortex in noise-exposed rats. 73

Figure 3.1. Electrode penetrations across all recording locations within V1, V2L and the AuD cortex. 93

Figure 3.2. Visual- and auditory-evoked CSD profiles within the multisensory zone of the lateral extrastriate visual cortex (V2L-Mz)..... 96

Figure 3.3. Assessment of the auditory brainstem response (ABR) to a click stimulus in control and noise exposed rats. 99

Figure 3.4. Increased visual responsiveness occurred across the cortical layers within higher-order sensory regions. 102

Figure 3.5. Noise-induced hearing loss caused region- and layer-specific plasticity in the auditory-evoked CSD profiles across auditory, visual and audiovisual cortices. 104

Figure 3.6. Neighbouring cortical regions were differentially affected by noise-induced hearing loss as measured by the stimulus-evoked AVREC peak amplitudes. 106

Figure 3.7. Audiovisual responsiveness was not affected by noise induced-hearing loss within the auditory, visual and audiovisual cortices.....109

Figure 4.1. Rat audiovisual behavioural tasks and chamber set up. 127

Figure 4.2. Effect of sound intensity on audiovisual temporal order perception. 136

Figure 4.3. Altered auditory- and visual-first performance during TOJ training sessions following noise exposure. 140

Figure 4.4. Preserved audiovisual temporal perception following adult-onset hearing loss. 142

Figure 4.5. Effect of sound intensity on audiovisual synchrony perception as measured during an SJ task.....144

Figure 4.6. Hearing loss impaired performances during SJ training sessions. 147

Figure 4.7. Impaired audiovisual synchrony perception following adult-onset hearing loss. 151

Figure 5.1. Pharmacological silencing of the V2L cortex disrupts audiovisual temporal acuity in rats. 169

Figure 5.2. Recording site reconstruction, and audiovisual-evoked CSD analysis in the multisensory zone of the V2L cortex (V2L-Mz). 175

Figure 5.3. Audiovisual-evoked CSD profiles within the multisensory zone of the V2L cortex in response to 3 different SOAs. 179

Figure 5.4. A loss of the characteristic audiovisual temporal profile was observed across the majority of layers of the multisensory zone of the V2L cortex in noise exposed rats. 184

Figure 5.5. Noise-induced hearing loss enhanced the audiovisual-evoked AVREC amplitudes at select SOAs within the multisensory zone of the V2L cortex. 186

Figure 5.6. A decrease in audiovisual-evoked CSD amplitudes was generally observed within the auditory zone of the V2L cortex in noise exposed rats. 188

Figure 5.7. Audiovisual-evoked AVREC amplitude and latency within the auditory zone of the V2L cortex following noise-induced hearing loss. 190

Figure 5.8. The magnitude of the multisensory response interactions varied across the regions of the V2L cortex before- and after noise exposure. 192

Figure 5.9. Compensatory plasticity in the auditory zone of the V2L cortex preserved audiovisual temporal processing following moderate hearing loss. 194

Figure 6.1. Electrophysiological recordings within the multisensory zone of the V2L cortex (V2L-Mz). 210

Figure 6.2. Recordings from an ECoG electrode positioned over the V2L cortex of the rat. 216

Figure 6.3. Auditory-evoked sink amplitudes following cortical silencing in control and noise-exposed rats. 221

Figure 6.4. Visual-evoked sink amplitudes following cortical silencing in control and noise-exposed rats 224

Figure 6.5. Preservation of audiovisual-evoked responses following pharmacological silencing following noise-induced hearing loss. 226

Figure 6.6. Total strength of audiovisual-evoked postsynaptic input preserved following adult-onset hearing loss. 228

Figure 6.7. Decrease in auditory-evoked amplitudes following noise-induced hearing loss across the higher-order sensory cortices. 231

Figure 6.8. Enhancement of visual-evoked amplitudes following adult-onset hearing loss within higher-order sensory cortices. 234

Figure 6.9. Effect of stimulus intensity on sensory-evoked activity following noise-induced hearing loss. 237

List of Appendices

Appendix A: Development and validation of a rodent model of audiovisual temporal and synchrony perception.....266

Appendix B: Ethics Approvals.....305

Appendix C: Copyright Permissions 307

List of Abbreviations and Symbols

2AFC	Two-Alternative Forced Choice
A1	Primary Auditory Cortex
AAF	Anterior Auditory Field
ABR	Auditory Brainstem Response
aCSF	Artificial Cerebrospinal fluid
ANOVA	Analysis of Variance
AuD	Dorsal Auditory Cortex
AVREC	Average Rectified Current Source Density
CI	Cochlear Implant
cm	centimeters
CN	Cochlear Nucleus
CSD	Current Source Density
CTRL	control
DAPI	4′,6-diamidino-2-phenylindole
DB	Davies-Bouldin
dB SPL	decibels per Sound Pressure Level
DiI	1,1′-Dioctadecyl-3,3,3′,3′-tetramethylindocarbocyanine perchlorate
DZ	Dorsal Zone of the Auditory Cortex
ECoG	Electrocorticography
EEG	Electroencephalography
EPSPs	Excitatory Post-Synaptic Potentials
FAES	Auditory field of the Anterior Ectosylvian Sulcus
fMRI	Functional Magnetic Resonance Imaging
g	grams
G	Gauge
GABA	Gamma-aminobutyric acid
GAD	Glutamate Decarboxylase
gSk	granular sink
Hz	Hertz
IC	Inferior Colliculus
IM	Intramuscular
IP	Intraperitoneal
IP	Intraparietal complex
IR	infrared
iSk-upper	Infragranular-upper
iSk-lower	Infragranular-lower

JND	Just Noticeable Difference
kg	kilograms
kHz	kilohertz
LD	Lateral Dorsal
LED	Light-Emitting Diode
LFP	Local Field Potential
LP	Lateral Posterior
lux	luminous flux per unit area
mg	milligrams
MGB	Medial Geniculate Body
MLR	Middle Latency Response
mm	millimeters
mM	milli-molar
ms	milliseconds
MST	Middle Superior Temporal area
MT	Middle Temporal area
MU	Multi-Unit
NE	noise-exposed
NIHL	Noise-Induced Hearing Loss
OC	Occipital Cortex
P2P	Peak-to-Peak
PAF	Posterior Auditory Field
PB	Phosphate buffer
PLLS	Posterolateral Lateral Suprasylvian
PsF	Pseudo-F
PSS	Point of Subjective Simultaneity
PSTH	Peri-Stimulus Time Histogram
PV+	Parvalbumin-positive
rmANOVA	repeated-measures Analysis of Variance
SEM	Standard Error of the Mean
SC	Superior Colliculus
SD	Standard Deviation
SGC	Spiral Ganglion Cells
SJ	Synchrony Judgments
SL	Sensation Level
SOA	Stimulus Onset Asynchrony
SpontR	Spontaneous firing rate
sSk	supragranular sink
STG	Superior Temporal Gyrus
STS	Superior Temporal Sulcus

SU	Single-Unit
TBW	Temporal Binding Window
TDT	Tucker Davis Technologies
TMS	Transcranial Magnetic Stimulation
TOJ	Temporal Order Judgments
V1	Primary Visual Cortex
V2L	Lateral Extrastriate Visual Cortex
V2L-Mz	Multisensory zone of the Lateral Extrastriate Visual Cortex
V2L-Az	Auditory zone of the Lateral Extrastriate Visual Cortex
V2L-Vz	Visual zone of the Lateral Extrastriate Visual Cortex
VIP	Vasoactive Intestinal Polypeptide
µl	microliters
µm	micrometers
µV	microvolts
°	degrees
°C	degrees Celsius
%	percent

Chapter 1

1 General Introduction

1.1 Overview

Within the mammalian brain, there are distinct regions that are capable of processing sensory information from highly specialized sensory organs (e.g., cochlea), ultimately allowing us to interact with objects or events within our external environment. This environmental interaction is enhanced by the brain's ability to also successfully integrate sensory information from more than one modality (Merabet and Pascual-Leone, 2010). Research over the past 25 years has demonstrated the critical role of sensory experience on the development and integration of stimuli from multiple sensory modalities (i.e., multisensory processing). Moreover, following alterations in sensory experience (e.g., loss of one sensory modality), it is well-established that the brain is able to adapt to the loss of sensory input (i.e., plasticity) by altering sensory responsiveness within numerous cortical regions. Perhaps not surprisingly, the degree of plasticity observed is dependent on the nature and extent of sensory deprivation, as well as the age of the individual at which deprivation occurred.

Research on deprivation-induced plasticity has predominantly focused on examining the perceptual enhancements in specific behavioural tasks observed in individuals with sensory loss, as well as attempts to characterize the changes in sensory responsiveness that occur within the primary sensory regions. For example, sensory deprivation often results in an increase in the responsiveness of the remaining, intact sensory modalities within the deprived cortex; a phenomenon known as crossmodal plasticity. That said, it is important to note that the majority of studies investigating crossmodal plasticity and its perceptual enhancements have been focused on the consequences of complete sensory deprivation (e.g., deafness). Nevertheless, recent studies have begun to demonstrate that individuals with a partial loss of sensory input (i.e., moderate hearing loss), which preserves some residual sensory processing, also show evidence of crossmodal plasticity within the deprived sensory cortex (Campbell and Sharma, 2014; Cardon and Sharma, 2018). In

addition to the recruitment of the intact sensory modalities, partial sensory deprivation also results in various changes throughout the impaired sensory system, which can ultimately manifest as hyperactivity in the core regions of the deprived cortex (e.g., hyperactivity to acoustic stimuli in the primary auditory cortex following moderate hearing loss).

Given that we interact with a complex mixture of sensory information within our daily lives, and that sensory deprivation can result in an assortment of intramodal and crossmodal changes throughout our sensory systems, valuable insights will be gained by improving our understanding of the physiological and perceptual changes that occur when the brain experiences a partial loss of sensory input. As this thesis focuses on how multisensory processing within higher-order sensory cortices are affected by adult-onset hearing loss, the next sections will review the known principles of multisensory processing and perception, as well as outlining our current knowledge of the intramodal and crossmodal consequences of sensory deprivation, with an emphasis on a partial loss of auditory input.

1.2 Sensory Processing

1.2.1 Multisensory Processing

To provide us with a complete sensory experience, our brain is capable of integrating stimuli from more than one sensory modality (i.e., hearing and vision). The ability to accurately integrate or bind stimuli from more than one sensory modality allows for several behavioural and perceptual benefits, such as the accurate detection, localization and identification of external events (Cappe et al., 2010a; Diederich and Colonius, 2004; Gleiss and Kayser, 2012; Hershenson, 1962; Hirokawa et al., 2008; Raposo et al., 2012; Siemann et al., 2015). For example, both humans (Calvert et al., 2000; Diederich and Colonius, 2004) and rodents (Gleiss and Kayser, 2012; Hirokawa et al., 2008) are able to detect auditory and visual stimuli faster, when the stimuli are presented in combination compared to when either cue is presented alone. As discussed below, such behavioural improvements are suggested to arise because of the ability of neurons to effectively integrate the multisensory stimuli.

1.2.1.1 Multisensory Integration

Over the past 25 years, there has been a large emergence of studies investigating multisensory processing. Many of the governing principles of multisensory processing were first characterized from studies conducted on single neurons in the deep layers of the cat superior colliculus (SC) (Stein and Meredith, 1993). Based on this work, multisensory integration is defined as the process by which stimuli from different sensory modalities produces a response that is different from that evoked by an individual sensory component (Stein and Rowland, 2011). More specifically, at the level of single neurons, multisensory integration is computationally defined as a statistically significant difference between the response evoked by the multisensory stimuli (i.e., a combination of two or more sensory modalities) and the response evoked by the most effective individual modality (Stein and Meredith, 1993). As a result, multisensory integration can be described as either *enhancement* where the response to the multisensory stimulus is increased, or *depression* where the response to the combined multisensory stimulus is decreased when compared to the response of the individual sensory modality. Importantly, the magnitude of integration can vary greatly between neurons and even within the same neuron depending on the combination of stimuli presented (Stein and Rowland, 2011).

Stein and Meredith (1993) observed that multisensory neurons – neurons that respond to or whose response is influenced by stimuli from more than one sensory modality – appear to follow a set of operational principles. In general, multisensory stimuli that are presented at the same time and place within their respective receptive fields (i.e., the area of sensory space that leads to a response in a particular neuron following the presentation of a stimulus) demonstrate an enhanced response magnitude, whereas stimuli that are presented at different locations or times inhibit or do not affect the response magnitude (Alais et al., 2010; Stein and Meredith, 1993; Stein and Rowland, 2011). These response features are described as the “spatial” and “temporal” principles of multisensory integration. Put simply, stimuli that are presented from the same location or at the same moment in time generate the greatest degree of multisensory integration. In addition to multisensory neurons demonstrating responsiveness that is dependent on the temporal and/or spatial features of the stimuli, the strength of the response is dependent on the effectiveness (i.e.,

intensity) of the individual sensory components; a principle referred to as *inverse effectiveness* (Stein and Meredith, 1993). More specifically, the degree to which a multisensory response is enhanced or depressed is inversely related to the effectiveness of the individual sensory stimuli. For example, a quiet auditory stimulus and a dim visual stimulus will result in a greater degree of multisensory integration than a loud auditory stimulus and a bright visual stimulus. Overall, it is generally regarded that multisensory stimuli which occur from a common event result in enhanced activity and behavioural performance, whereas stimuli that arise from different events can degrade activity and performance (Stein and Rowland, 2011).

1.2.1.2 Multisensory Processing in the Cortex

Although the majority of the initial characterization studies were conducted in the SC, several studies have demonstrated that multisensory processing occurs within numerous regions of the mammalian brain (Ghazanfar and Schroeder, 2006). More specifically, recent studies have demonstrated that multisensory processing occurs in primary sensory cortices, such as the primary auditory cortex (A1) (Bizley and King, 2008; Bizley et al., 2007; Foxe et al., 2002; Kayser et al., 2009; Schroeder et al., 2001) and the primary visual cortex (V1) (Cappe et al., 2010b; Iurilli et al., 2012; Mercier et al., 2013; Molholm et al., 2002; Murata et al., 1965), as well as higher-order association cortices, such as the superior temporal sulcus (STS) and the intraparietal complex (IP) (for review see, Foxe and Schroeder, 2005; Ghazanfar and Schroeder, 2006). Consistent across species, the higher-order association regions that are capable of processing stimuli from more than one sensory modality are often located at the borders of the primary sensory regions (Wallace et al., 2004a).

Multisensory cortical regions are heterogenous, with the majority of constituent neurons being responsive to a single sensory stimulus (i.e., unisensory neurons), and approximately 20 – 40% of neurons being responsive to more than one modality (i.e., multisensory neurons) (Allman and Meredith, 2007; Foxworthy et al., 2013a; Meredith and Allman, 2009; Wallace et al., 2004a, 2006; Xu et al., 2014). Within these regions, multisensory neurons are classified based on their responsiveness to individual sensory stimuli (i.e., unimodal stimuli) as well as a combined multisensory stimulus (e.g., a combination of

auditory and visual stimuli). For example, neurons that demonstrate overt responses to two different sensory modalities would be classified as *bimodal neurons* (Stein and Meredith, 1993), whereas those neurons that solely respond to an individual sensory stimulus but show multisensory integration (i.e., facilitation or suppression) when presented with a multisensory stimulus would be classified as *subthreshold multisensory neurons* (Allman and Meredith, 2007; Allman et al., 2008a, 2008b; Foxworthy et al., 2013b; Meredith and Allman, 2009). As described above, when combined multisensory (e.g., auditory and visual) stimuli are presented, select multisensory neurons generate response enhancement or depression, which is characterized by an increase or decrease in spiking activity when compared to the activity evoked from a single sensory stimulus (i.e., multisensory integration) (Allman et al., 2008a; Stein and Meredith, 1993; Stein and Stanford, 2008; Stein et al., 2014; Wallace et al., 2006). Furthermore, whether or not neurons demonstrate multisensory enhancement or depression is dependent on the temporal, spatial, and/or effectiveness of the unimodal stimuli (Stein and Meredith, 1993). Although the principles of multisensory integration are well-established and have been documented in numerous brain regions, the mechanisms which regulate the nature and extent of multisensory integration have not been fully elucidated.

1.2.1.2.1 The Lateral Extrastriate Visual Cortex (V2L)

A well-established example of a cortically-mediated multisensory behaviour is the ability of mammals to more quickly detect auditory and visual cues when the stimuli are presented together, compared to when either stimulus is presented alone (i.e. improved reaction time) (Gleiss and Kayser, 2012; Hirokawa et al., 2008). Furthermore, the degree of multisensory facilitation of reaction time is largest when the quality of the auditory (e.g., loudness of a noise burst) and visual (e.g., brightness of a light) stimuli are “weak”. In contrast, when the intensity of the stimuli are increased (i.e., “strong”), the reaction time to detect the combined audiovisual stimuli is no faster than when either the auditory- or visual stimulus is presented alone. In rodents, the lateral extrastriate visual cortex (V2L) has been identified as the cortical area mediating this improved reaction time to detect audiovisual stimuli, as deactivation of this region results in a loss of multisensory facilitation (Hirokawa et al., 2008). Consistent with work on various species, the V2L cortex is known to contain

neurons that respond to both unisensory and multisensory stimuli, and show evidence of multisensory integration (Barth et al., 1995; Hirokawa et al., 2008; Toldi et al., 1986; Wallace et al., 2004a; Xu et al., 2014).

In order for the V2L cortex to facilitate behaviours that rely on successful audiovisual integration, its constituent neurons must receive converging inputs from numerous brain regions. In rodents, the V2L cortex predominantly receives corticocortical projections from auditory, visual and other association cortices, as well as some non-specific thalamic inputs (Budinger et al., 2006; Laramée et al., 2011; Liang et al., 2012). Anatomical studies have shown direct connections from A1 (Budinger and Scheich, 2009; Budinger et al., 2006) and V1 (Laing et al., 2012; Laramée et al., 2011, 2013; Olavarria and Montero, 1981) to the V2L cortex. In addition to these cortical projections, the V2L cortex receives thalamic input from the lateral posterior (LP), pulvinar, and lateral dorsal (LD) nuclei, with the majority of the thalamic projections to multisensory cortex following a feedforward pattern of innervation with targets focusing in layers III/IV (Barth et al., 1995; Burkhalter, 2016; Olsen and Witter, 2016). While thalamic projections preferentially target the granular layer, demonstrating feedforward pattern (target layer III/IV, granular layer), intracortical projections target all cortical layers, indicative of feedback (supragranular and infragranular layers) activation patterns (Schroeder et al., 2003). Based on these extensive cortical and sub-cortical inputs, it is reasonable to predict that the V2L cortex would be susceptible to sensory deprivation.

1.2.2 Multisensory Perception

As described above, the ability to integrate multisensory information is known to be highly dependent upon the temporal relationship of the unimodal stimuli, such that both stimulus modalities must be presented in close proximity in order to have the greatest likelihood of being integrated (Meredith et al., 1987). Electrophysiological studies have demonstrated that the timing of the stimuli influences the magnitude of multisensory integration, such that visual stimuli must be presented 20 to 50 ms prior to the auditory stimuli in order to show the greatest degree of multisensory integration (King and Palmer, 1985; Meredith and Stein, 1986; Miller et al., 2015; Perrault et al., 2005; Stanford et al., 2005). Moreover, behavioural studies have demonstrated a similar phenomenon, where individuals report

audiovisual stimuli as being temporally aligned when the auditory and visual stimuli occur within approximately 100 ms of each other (Boenke et al., 2009; Stevenson et al., 2014; Stone et al., 2001; Vatakis and Spence, 2008; Vroomen and Stekelenburg, 2011; Zampini et al., 2005).

The perceptual ability to judge the timing and synchrony of audiovisual stimuli has been well studied in humans using psychophysical testing (van Eijk et al., 2008; Keetels and Vroomen, 2012; Kostaki and Vatakis, 2018; Stekelenburg and Vroomen, 2007; Stevenson and Wallace, 2013; Vroomen and Keetels, 2010). The two most widely used tasks to assess audiovisual perception in humans are temporal order judgments (TOJs) and synchrony judgments (SJs). The TOJ task requires participants to judge the relative timing of the audiovisual stimuli presented at various stimulus onset asynchronies (SOAs) by stating which stimulus came first or which came second (Boenke et al., 2009; Keetels and Vroomen, 2012; Navarra et al., 2005; Spence et al., 2003; Vatakis and Spence, 2008; Vatakis et al., 2007; Zampini et al., 2003). In the SJ task, participants judge whether they perceived the stimuli to have been presented at the same moment in time (i.e., synchronous) or at different moments in time (i.e., asynchronous) when audiovisual stimuli are presented at various SOAs (van Eijk et al., 2008; Stevenson and Wallace, 2013; Stone et al., 2001; Wallace and Stevenson, 2014; Zampini et al., 2005). For both tasks, additional information can be determined in order to provide insight into perceived simultaneity and temporal sensitivity. For example, the *point of subjective simultaneity* (PSS) which is measured as the 50% value along the psychophysical curve, represents the actual timing of the audiovisual stimuli when the participant is most unsure of the temporal order (Keetels and Vroomen, 2012; Kostaki and Vatakis, 2018; Vroomen and Keetels, 2010). Temporal sensitivity can be examined by calculating the *just noticeable difference* (JND), which represents the smallest interval between the separately presented auditory and visual stimuli that can be reliably detected. Finally, the *temporal binding window* (TBW) is a measure of the range of temporal tolerance of audiovisual stimuli within which the stimuli are perceived as a single event (for review see, Vroomen and Keetels, 2010). Although the TOJ and SJ tasks have been commonly used throughout the literature, the specific response properties of single neurons and their local circuits that contribute to audiovisual perception remain unknown. Furthermore, there were no established behavioural tasks in rodents

capable of assessing their perceptual ability to judge the relative timing or synchrony of auditory and visual stimuli (i.e., audiovisual temporal acuity).

1.3 Sensory Deprivation and Cortical Plasticity

In addition to the features of the unimodal stimuli, environmental experience not only plays a large role in development of multisensory integration (Wallace et al., 2006), but also is capable of modulating the degree of multisensory integration in adulthood (Xu et al., 2014, 2015). For example, in animals raised in the absence of visual cues, SC neurons were not able to successfully integrate combined audiovisual stimuli, suggesting that visual experience is critical for the development of multisensory integration in the SC (Wallace et al., 2004b). Although the consequences within the cortex are not as well defined, exposure to audiovisual stimuli over an extended period of time has been shown to increase the proportion of multisensory neurons within the V2L cortex (Xu et al., 2014). The following sections provide an overview of the behavioural and physiological changes in sensory processing that are induced by visual or auditory deprivation, with an emphasis on changes following partial hearing loss.

1.3.1 Visual Deprivation

It has long been suggested that blind individuals compensate for a loss of vision by more effectively using their remaining senses, ultimately affording them with certain perceptual advantages. Several studies have demonstrated that blind individuals (particularly if blind from birth or very early in life) show similar or even superior behavioural skills when compared to sighted individuals (Merabet and Pascual-Leone, 2010). For example, blind subjects demonstrate finer tactile-discriminate thresholds (Alary et al., 2008, 2009; Goldreich and Kanics, 2003), superior performance on auditory-pitch discrimination (Gougoux et al., 2004), and spatial sound localization (Gougoux et al., 2005; Lessard et al., 1998; Röder et al., 1999; Voss et al., 2004). Interestingly, studies investigating spatial auditory representations demonstrate that blind individuals are able to properly map spatial hearing in distant space, and actually outperform sighted individuals when the stimuli were presented in the periphery (Fieger et al., 2006; Voss et al., 2004). Furthermore, Voss et al. (2004) demonstrated that this improved behavioural performance was observed in both

early- and late-blind participants when compared to sighted individuals. Similar to the results observed in humans, animal models of visual deprivation (e.g., lid sutures, dark-rearing or enucleation) have shown that visually-deprived animals possess superior sound localization (King and Parsons, 1999; Rauschecker, 1995; Rauschecker and Kniepert, 1994).

Given that blind individuals demonstrate behavioural and perceptual enhancements that are reliant on their remaining senses, it would seem reasonable to suggest that there is reorganization within regions of the brain responsible for processing the spared sensory modalities. Within the occipital cortex (OC; an area responsible for processing visual information), there is extensive cortical reorganization whereby it becomes responsive to non-visual stimuli in blind individuals (i.e., crossmodal plasticity) (Collignon et al., 2008). For example, advanced neuroimaging techniques have demonstrated that the occipital cortex becomes activated during auditory (Kujala et al., 1997; Röder et al., 1999; Weeks et al., 2000) and tactile tasks (Burton et al., 2004; Gizewski et al., 2003) in blind subjects. Furthermore, using transcranial magnetic stimulation (TMS), several studies have demonstrated that the recruitment of occipital areas is related to the compensatory behaviours in blind individuals (Merabet and Pascual-Leone, 2010). Moreover, the transient and localized disruption of the OC in blind individuals impairs braille reading (Cohen et al., 1997; Hamilton and Pascual-Leone, 1998; Kupers et al., 2007) and verbal processing (Amedi et al., 2004). Taken together, these findings demonstrate that the occipital cortex is recruited by the intact sensory modalities in order to process input from a different sensory modality, all the while maintaining their functional and neural coding abilities.

While the occipital cortex has been the predominant focus of cortical plasticity following blindness, other non-visual brain regions have been shown to change following visual deprivation, such as the regions responsible for processing somatosensory and auditory stimuli. For example, in blind individuals that are proficient with Braille reading, an expansion and reorganization of the cortical finger representation have been reported (Pascual-Leone and Torres, 1993; Sterr et al., 1998a, 1998b).Within auditory cortical areas, tonotopic mapping studies and responsiveness to tonal stimuli have revealed an expansion

of the cortical areas which respond to auditory stimuli in the blind as compared to sighted controls, as well as shorter response latencies (Elbert et al., 2002). Overall, these studies demonstrate that extensive cortical reorganization occurs following visual deprivation which could underlie the enhanced performance reported during specific behavioural and perceptual tasks.

1.3.2 Auditory Deprivation

Similar to blind individuals, deaf individuals compensate for a loss of audition by heavily relying on their intact senses in order to interact with their surroundings. For example, deaf individuals rely on visual and tactile information to effectively attend to objects within their environment, and many choose to use visuospatial forms of linguistic communication, such as sign language (Merabet and Pascual-Leone, 2010). The behavioural and perceptual enhancements observed in blind individuals are not restricted to subjects with visual deprivation, as deaf individuals have shown superior skills in certain perceptual tasks, such as enhanced tactile sensitivity when compared with normal-hearing controls (Levänen and Hamdorf, 2001). However, to date the majority of studies in deaf individuals have predominantly sought to determine whether they show enhanced visual processing, consistent with the reciprocal perceptual enhancements observed in blind individuals. While deaf subjects do show enhancements in processing visual stimuli, the heightened abilities appear to be limited to specific areas of visual cognition. For example, basic sensory thresholds, such as contrast sensitivity (Finney and Dobkins, 2001), motion velocity (Bosworth and Dobkins, 2002), motion sensitivity (Brozinsky and Bavelier, 2004), brightness discrimination (Bross, 1979), and temporal resolution (Nava et al., 2008; Poizner and Tallal, 1987) are similar to normal-hearing controls. However, enhanced visual processing skills have been observed in more complex tasks, where visual attention and/or processing stimuli within the peripheral visual field are manipulated (Bavelier et al., 2000, 2001; Dye et al., 2007, 2009; Loke and Song, 1991; Neville and Lawson, 1987; Neville et al., 1983; Proksch and Bavelier, 2002; Sladen et al., 2005; Stevens and Neville, 2006). Furthermore, animal models of congenital deafness have also demonstrated similar visual compensation, whereby congenitally deaf cats show superior localization in the peripheral field and lower visual movement detection thresholds (Lomber et al., 2010). It has been

proposed that this re-allocation of resources towards the periphery might be adaptive, and may ultimately serve to direct attention towards objects outside the central field of view (Dye et al., 2009).

Based on the enhanced visual processing skills observed in deaf individuals, it is reasonable to question what changes in the brain actually serve as the neuronal substrate for these behavioural improvements. Of particular interest, researchers have considered whether plasticity occurs throughout the regions of the auditory cortex. Interestingly, unlike blindness, where it is well-established that the occipital cortex is activated by the intact sensory modalities following visual deprivation, there are contradictory reports within the auditory cortex. For example, several human studies have demonstrated that congenitally and post-lingually deaf humans show activation of auditory cortical areas when processing visual motion and complex visual pattern changes, which are not observed in normal hearing control subjects (Auer et al., 2007; Buckley and Tobey, 2011; Doucet et al., 2006; Finney et al., 2001, 2003; Vachon et al., 2013). However, a few studies in humans and animals have demonstrated no crossmodal activation within A1 following congenital deafness (Hickok et al., 1997; Kral et al., 2003). It is worth noting that studies investigating cortical reorganization following deafness have not been limited to the primary auditory cortex, as researchers have also investigated compensatory changes within auditory association regions, as well as the middle temporal (MT) and middle superior temporal (MST) cortex; areas known to be involved in visual motion processing and influenced by attentional processes. More specifically, neuroimaging studies in MT/MST have demonstrated that there are neurophysiological differences between deaf and hearing individuals that only emerge when motion stimuli are attended to in the peripheral visual field, consistent with behavioural observations (Bavelier et al., 2001; Fine et al., 2005).

1.3.2.1 Profound Hearing Loss

The majority of the studies described above were conducted on individuals with profound hearing loss, which typically consists of a hearing loss greater than 90 dB. Similar to the cortical reorganization described above in humans following deafness, animal models have demonstrated that core auditory areas, including A1 and the anterior auditory field (AAF), showed responses to both tactile and visual stimuli (Hunt et al., 2006; Meredith and

Lomber, 2011). While it is still debated whether crossmodal plasticity occurs in A1 (see Kral et al., 2003), auditory regions beyond the core auditory cortex have demonstrated reorganization following early-onset hearing loss. For example, the auditory field of the anterior ectosylvian sulcus (FAES) of the cat, which is largely responsive to acoustic stimulation, demonstrated robust responses to visual stimuli following early-deafening (Meredith et al., 2011). Moreover, the recordings revealed that the visual receptive fields were representative of the contralateral visual field. Additionally, visual reorganization has been observed in the posterior auditory field (PAF) and the dorsal auditory zone (DZ) in the cat brain, which underlies the enhanced performance reported on visual localization of peripheral targets (Lomber et al., 2010).

Numerous studies have examined how profound hearing loss affects the anatomical connections within the deprived and spared sensory systems. Despite the electrophysiological evidence of cortical reorganization, several studies have demonstrated a lack of change in relation to the proportion of intracortical and thalamocortical connections to various auditory cortices of animals with profound hearing loss (Barone et al., 2013; Butler et al., 2016; Chabot et al., 2015; Clemo et al., 2014; Kok et al., 2014; Wong et al., 2015). However, early-onset profound hearing loss in cats did cause an increase in dendritic spine density within the supragranular layers of FAES (Clemo et al., 2014). Despite the extensive research completed on profound sensory deprivation, the cellular/molecular basis of cortical reorganization remains unknown, and as such, future studies are needed in order to provide insight into the underlying mechanisms, as this could have significant implications for sensory protheses (e.g., cochlear implants). It is important to note that functional neuroimaging studies in hearing-impaired humans (Bavelier et al., 2006; Heimler et al., 2014; Pavani and Roder, 2012) and single-unit recordings in animal models (Allman et al., 2009; Hunt et al., 2006; Meredith and Allman, 2012; Meredith and Lomber, 2011; Meredith et al., 2012) have identified that the nature and extent of cortical plasticity depends on the severity of the hearing loss (e.g., profound deafness versus mild hearing impairment), as well as the age at which the deprivation commenced (e.g., congenital/early-onset versus in adulthood).

1.3.2.2 Mild-Moderate Hearing Loss

Studies on humans with mild-moderate hearing loss have reported that, in addition to maintaining some capacity to process auditory information, the neurons within auditory cortical regions show an increased responsiveness to visual and/or tactile stimuli (Campbell and Sharma, 2013, 2014; Cardon and Sharma, 2018). Furthermore, Campbell and Sharma (2013) revealed that individuals with a partial hearing impairment had decreased temporal activation within the superior temporal gyrus (STG), and increased activation in frontal regions in response to passive auditory stimulation. Consistent with human studies, single-unit recordings in partially-deafened ferrets, revealed an increase in the proportion of neurons capable of processing both auditory and non-auditory stimuli (i.e., multisensory neurons) (Meredith et al., 2012).

Contrary to adults with profound hearing loss, individuals with less-severe hearing impairments have been shown to exhibit deficiencies in cognitive performance (Craik, 2007; Tun et al., 2012). It has been proposed that these deficits are due to a greater cognitive load, as more attention is required to process auditory signals following a hearing impairment (Campbell and Sharma, 2013). In addition to requiring a greater cognitive load to process auditory stimuli within everyday life, hearing-impaired individuals rely heavily on visual cues in order to compensate for poorer speech intelligibility. This increased reliance upon visual stimuli may result in better integration of audiovisual speech (Tye-Murray et al., 2007). Interestingly, individuals with a moderate hearing loss demonstrated preserved audiovisual sensitivity to speech stimuli when assessed using an SJ task (Başkent and Bazo, 2011). Consistent with hearing impaired individuals, subjects with cochlear implants (CI) show relatively preserved audiovisual temporal sensitivity (i.e., no difference in the temporal window of integration) (Butera et al., 2018; Hay-McCutcheon et al., 2009). However, Butera et al. (2018) revealed that CI users have a point of subjective simultaneity (PSS) for speech stimuli that was less visual-leading, and they also demonstrated improved visual-only TOJ thresholds. These results are consistent with a greater reliance on visual cues within hearing-impaired individuals. In contrast to the relatively preserved audiovisual temporal acuity, hearing-impaired individuals showed a significantly greater proportion of errors during sensory categorization tasks when presented with distracting

crossmodal stimulation when compared to control groups. Despite the growing evidence of the behavioural consequences of a mild-moderate hearing loss on cognition and sensory processing, little is known about the nature and extent of cortical plasticity that occurs in the brain regions subserving these behaviours.

1.3.2.3 Noise-Induced Hearing Loss

Noise exposure is one of the most common causes of hearing loss, with nearly 10 million Americans suffering from hearing loss related to excessive noise exposure, and the fact that each year, ~22 million workers are exposed to noise levels that could lead to hearing impairment according to the Centers for Disease Control and Prevention. Following exposure to intense sound, noise-induced hearing loss (NIHL) gradually recovers over time for ~2-3 weeks (Miller 1963). Depending on the severity of the exposure, thresholds may fully recover (i.e., temporary threshold shift) or eventually stabilize at an elevated value (i.e., permanent threshold shift).

Permanent NIHL is due to the degradation of cochlear hair cells or from damage to their mechano-sensory hair bundles (Liberman and Dodds, 1984). Following exposure to intense sound, hair cells which normally transduce sound-evoked mechanical motion into receptor potentials, incur damage within minutes, and hair cell death can continue for days (Wang et al., 2002b). In contrast, a loss of spiral ganglion cells (SGCs), which are the cell bodies of the cochlear afferent neurons which contact the hair cells, is delayed for months and can even progress for years following NIHL (Kujawa and Liberman, 2006). Furthermore, the consequences of noise exposure are possibly more insidious than previously thought. For example, Kujawa and Liberman (2009) demonstrated that a noise exposure which caused moderate but reversible effects on hearing thresholds, can actually lead to a loss of afferent nerve terminals and a delayed degeneration of the cochlear nerve.

The consequences of noise exposure are evident in both peripheral and central parts of the auditory system. Damage of the peripheral auditory system is reflected in a hearing threshold shift and in weaker responses to sound at multiple levels of the central auditory system, from the cochlear nucleus to the auditory cortex (for review see Syka, 1989, 2002). Within the central auditory system, NIHL causes neurons in the cochlear nucleus (CN) and

the inferior colliculus (IC) to demonstrate decreased firing rates to sound intensities near threshold, but at intensities above threshold, neurons show increased firing rates (Salvi et al., 1978, 1990; Wang et al., 2002a; Willott and Lu, 1982). This differential responsiveness depending on the intensity of the auditory stimulus is consistent across multiple auditory structures, as noise exposure is also known to result in an enhancement of sound-evoked responses in the IC and middle latency responses (MLRs) recorded from the auditory cortex (Popelar et al., 1987; Salvi et al., 1990; Syka and Rybalko, 2000; Syka et al., 1994).

Within the primary auditory cortex (A1), exposure to a loud noise or a partial loss of sensory input has been shown to result in cortical reorganization characterized by changes in the cortical tonotopic map, alterations in spontaneous firing rates, and hyperactivity (i.e., central gain enhancement; see Section 1.4.1 for further information). In normal hearing subjects, the auditory cortex is tonotopically organized such that specific regions preferentially respond to specific frequencies. However, following peripheral trauma (i.e., hearing loss) there are profound changes in the cortical tonotopic map such that there is an over-representation of frequencies below the trauma frequencies (Komiya and Eggermont, 2000; Popescu and Polley, 2010; Willott et al., 1993). In addition to tonotopic reorganization, spontaneous firing rates within A1 have been observed to be significantly elevated in reorganized cortical regions (Komiya and Eggermont, 2000). Similar observations are seen following adult-onset hearing loss, as Meredith et al. (2012) demonstrated that neurons in A1 and the anterior auditory field (AAF) have a significantly higher spontaneous activity as well as enhanced responsiveness to sensory stimuli. Despite the extensive cortical reorganization within A1, it is unknown whether these factors extend beyond the auditory cortex into neighbouring higher-order cortical regions, such as the audiovisual cortex.

1.4 Experience-Dependent Neuroplasticity

Hearing loss due to noise exposure, aging, or ototoxic drugs that damage the sensory hair cells and/or auditory neurons in the cochlea are known to result in cortical plasticity, the degree to which is dependent on the severity of the hearing loss. In particular, hearing loss alters auditory activity throughout the central auditory system, which ultimately manifests as enhanced neural responsiveness within the auditory cortex (Popelar et al., 1987, 2008;

Salvi et al., 1990, 2000); a phenomenon termed *central gain enhancement*. Separate studies have shown that, following hearing loss, there is also an increased responsiveness to the spared sensory modalities (e.g., visual and/or tactile) within auditory areas (Bavelier and Neville, 2002; Butler and Lomber, 2013; Lomber et al., 2010; Meredith et al., 2012; Puschmann and Thiel, 2017), consistent with *crossmodal plasticity*. The next sections will discuss central gain enhancement and crossmodal plasticity, with an emphasis on the potential underlying mechanisms.

1.4.1 Central Gain Enhancement

Central gain enhancement refers to the hyperactivity and enhancement of sound evoked responses within the auditory pathway following exposure to intense sounds. Similar to crossmodal plasticity, central gain has been well-documented following sensory deprivation and is suggestive to have perceptual implications, such as tinnitus and hyperacusis (for review, see Auerbach et al., 2014). Central gain enhancement is described as a paradoxical increase in gain or neural amplification within the central auditory system (e.g., A1, medial geniculate body (MGB), inferior colliculus (IC)), despite a reduction in the overall neural activity that is transmitted from the cochlea to the central auditory pathway (Chen et al., 2013; Sun et al., 2008, 2012). Although central gain has been observed within various auditory areas, it still remains unknown where the hyperactivity is initiated, and whether this neural amplification is restricted to specific regions corresponding to the damaged areas or if it extends to other regions as well. It has been proposed that central gain enhancement may be due to a decrease in inhibitory synaptic responses, an increase in excitatory synaptic responses, or alterations to intrinsic neuronal excitability (Auerbach et al., 2014).

It is well-established that acoustic trauma disrupts the inhibitory neurotransmission throughout the central auditory system. For instance, altered GABA receptor and GAD expression was observed in the IC following noise exposure, which was restricted to the region of the trauma (Dong et al., 2010). Furthermore, noise trauma has been shown to decrease inhibitory drive within the hearing loss region of the auditory cortex (Yang et al., 2011). A commonly used technique to induce enhancement within the auditory system involves the administration of salicylate, which at high doses induces transient tinnitus and

hearing loss. Using this methodology, several studies have demonstrated that enhancement of sound-evoked responses induced by salicylate may be dependent on changes in inhibition (Lu et al., 2011). For example, salicylate-induced enhancement of auditory cortex neural responses was suppressed after the local application of vigabatrin, which increases GABA levels in the brain (Lu et al., 2011), demonstrating the role of GABAergic transmission in sound-evoked enhancement. While recent studies have begun to examine specific subclasses of inhibitory interneurons in mediating gain control in the auditory cortex, particularly parvalbumin positive (PV+) neurons and vasoactive intestinal polypeptide (VIP) expressing neurons (Moore and Wehr, 2013; Pi et al., 2013), it is not known whether the excitability of specific cell-types is altered following hearing loss.

In addition to altered inhibitory neurotransmission, it has been proposed that homeostatic plasticity may underlie the observed hyperactivity within the central auditory system following noise trauma (Schaette and Kempter, 2006). For example, within the auditory cortex of adult animals, acoustic trauma has been shown to result in a global reduction in the strength of inhibitory synapses, specifically within the region of hearing loss (Yang et al., 2011). Overall, these studies demonstrate that altered auditory input affects neurons within the auditory pathway in a variety of ways, and further work is needed to reveal the behavioural consequences of these deprivation-induced changes.

1.4.2 Crossmodal Plasticity

Unlike central gain enhancement, which is predicated on residual sound processing capacity, and is suggested to lead to aberrant auditory perception (e.g., tinnitus and/or hyperacusis), complete sensory deprivation (e.g., deafness) results in extensive cortical reorganization and often manifests as enhancements in various perceptual tasks. This reorganization is typically described as crossmodal plasticity, as it is characterized by an increased responsiveness to the intact sensory modalities within the deprived sensory regions. For example, Lomber et al. (2010), demonstrated that auditory cortical regions (i.e., PAF, DZ) adapt following early-onset deafness by recruiting the intact sensory modalities to perform visual functions (i.e., sensory substitution). Moreover, PAF maintains its behavioural function, as deaf cats demonstrate enhanced performance on visual localization tasks especially in the periphery, demonstrating that crossmodal

plasticity was responsible for the behavioural enhancements. Although, crossmodal plasticity has been well documented following hearing loss and blindness, the mechanisms remain unknown. Several theories have been proposed such as an increase in the density of the projections from novel and/or existing sources (Rauschecker, 1995), an increase in dendritic spine density (Clemo et al., 2014), altered local GABAergic inhibition (Yang et al., 2011), unmasking of silent inputs (Lee and Whitt, 2015) and synaptic plasticity (Lee and Whitt, 2015).

Crossmodal reorganization is often described as a compensatory or adaptive mechanism to avoid maladaptive consequences (Singh et al., 2018). Compensatory or adaptive plasticity are typically discussed in relation to enhanced behavioural performance following profound sensory deprivation. For instance, tactile thresholds on the index, middle, and ring fingers of blind individuals are smaller when compared to sighted individuals, indicative of great tactile sensitivity (Wong et al., 2011). Interestingly, the compensatory plasticity following profound sensory deprivation results in sensory substitution (Auer et al., 2007; Doucet et al., 2006; Frasnelli et al., 2011; Lambertz et al., 2005; Meredith and Lomber, 2011), while partial deprivation results in multisensory convergence, where crossmodal inputs influence neuronal activity, rather than replace sensory function (Meredith et al., 2012). Meredith et al. (2012) demonstrated that following a moderate hearing loss, the auditory cortex demonstrates a greater proportion of multisensory responsiveness, however the response magnitudes to the multisensory stimuli are reduced, indicative of dysfunctional multisensory integration. While the compensatory effects of profound deprivation are typically described as conferring a behavioural benefit, crossmodal plasticity may also be maladaptive, ultimately resulting in a loss of function. Therefore, future studies are needed in order to examine the full extent of crossmodal plasticity across multiple brain regions following partial hearing loss, to investigate the potential changes in behavioural performance.

Studies on visually-deprived mice have provided extensive evidence of crossmodal synaptic plasticity, such that synaptic changes were triggered by alterations in sensory experience (Goel et al., 2006). Alterations at the synaptic level are referred to as homeostatic plasticity, which is a mechanism that allows neurons to modify their overall

activity level in response to changes in synaptic strength, that ultimately maintains the stability of the neural networks (Turrigiano, 1999). Following visual deprivation, Goel et al. (2006) demonstrated that there is an increase in the strength of the excitatory synapses in the superficial layers in the deprived sensory cortex, but are conversely decreased in the spared cortex. Furthermore, this homeostatic plasticity, which allows neurons to stabilize their own activity following changes in the level of input activity (Whitt et al., 2014), occurred after only a few days of visual deprivation. Interestingly, visual deprivation increased the strength of the lateral inputs to layer 2/3 neurons in V1 without changes in the strength of feedforward connections from layer 4, demonstrating that there is a specific upscaling of lateral intracortical inputs to layer 2/3 (Petrus et al., 2014). Synaptic changes are not restricted to the deprived sensory cortex, as research has demonstrated that the spared sensory cortices also undergo synaptic changes. For example, visual deprivation enhances the strength of thalamocortical synapses in layer 4 neurons of A1 (i.e., spared cortex) (Petrus et al., 2014), as well as potentiation of layer 4 to layer 2/3 synapses in A1 (Petrus et al., 2015). This potentiation of thalamocortical synapses is not sensory specific, as a few days of deafening also potentiates thalamocortical synapses in layer 4 neurons within V1 (Petrus et al., 2014). In contrast, there is no change in the strength of the thalamocortical synapses in layer 4 of V1 neurons following visual deprivation, which is suggested to demonstrate that changes in sensory experience within a modality is not sufficient to alter thalamocortical synaptic strength in adults (Petrus et al., 2014). Taken together, these studies demonstrate that a loss of sensory input results in layer-specific synaptic plasticity across multiple primary sensory regions. Despite this knowledge, it remains unknown whether similar mechanisms exist within higher-order sensory regions following complete or partial sensory deprivation.

Recent studies have demonstrated that the primary sensory regions in healthy individuals are multisensory in nature and receive inputs from multiple thalamic nuclei as well as other primary sensory areas (Driver and Noesselt, 2008; Ghazanfar and Schroeder, 2006). Moreover, neuronal responsiveness within one sensory area can be modulated by projections from a different sensory modality (Iurilli et al., 2012; Lakatos et al., 2007). However, a loss of sensory input could unmask normally dormant connections or increase their inputs to suprathreshold levels (Lee and Whitt, 2015; Rauschecker, 1995; Singh et

al., 2018). Support for this hypothesis comes from short-term visual deprivation studies which revealed multi-modal responses in the visual cortex of normally sighted individuals after a few days of deprivation (Merabet et al., 2008). A few animal studies have also shown evidence consistent with an unmasking of connections within the somatosensory cortex (Faggin et al., 1997; Humanes-Valera et al., 2013). For example, reversible sensory deactivation using pharmacological techniques (i.e., lidocaine injections) within the somatosensory cortex of adult rats revealed immediate and extensive reorganization within the cortex and the thalamus (Faggin et al., 1997). Overall, these studies demonstrate that sensory deprivation may cause previously subthreshold inputs to become strong enough to summate and cross the threshold in order to activate neurons in a different sensory modality.

In conclusion, although several parallels can be drawn between central gain enhancement and crossmodal plasticity, the underlying mechanisms are not fully understood, especially in conditions of partial hearing loss. Furthermore, because no previous studies have examined central gain enhancement and crossmodal plasticity in the same experimental circumstances (e.g., central gain enhancement is typically studied following acoustic trauma, whereas crossmodal plasticity is usually reported following profound hearing loss), it is unknown whether these phenomena compete or co-exist within various sensory regions following adult-onset hearing impairment.

1.5 Thesis Overview

Cortical plasticity is a well-documented phenomenon within primary sensory areas and is known to be dependent on the severity of the deprivation as well as the age at which the deprivation occurred; however, the nature and extent of cortical plasticity within higher-order sensory regions remains unclear. While the complete loss of a sensory modality provides a simple experimental model to examine crossmodal plasticity, a partial loss of sensory input is a far more common neurological phenomenon (Meredith et al., 2012). In fact, even though approximately 20% of Canadian adults have at least a slight hearing loss in one or both ears (Feder et al., 2015), the extent of plasticity beyond the deprived cortical region remains unknown. Therefore, this thesis aims to characterize the electrophysiological consequences and functional implications of cortical plasticity on

multisensory processing within higher-order sensory cortices of the rat following adult-onset noise-induced hearing loss. The following sections outline the research questions and experiments undertaken in Chapters 2 through 6 to accomplish this goal:

1.5.1 Chapter 2: Crossmodal Plasticity in Auditory, Visual and Multisensory Cortical Areas following Noise-Induced Hearing Loss

Rationale & Objectives: Within the primary auditory cortex, adult-onset partial hearing loss results in (1) a decrease in the percentage of neurons that respond solely to auditory stimuli, and (2) a concomitant increase in the percentage of bimodal neurons which respond to both auditory and visual stimuli (i.e., crossmodal plasticity) (Meredith et al., 2012). However, at the time that I commenced my PhD, it was unknown if crossmodal plasticity also occurred beyond the primary sensory cortices following a moderate hearing impairment. Thus, Chapter 2 aimed to determine for the first time whether crossmodal plasticity extended beyond the primary auditory cortex into higher-order sensory cortices, such as the lateral extrastriate visual cortex (V2L) – an area known to integrate audiovisual stimuli in adult rats.

Experimental Approach: Using *in vivo* extracellular electrophysiological recordings, a novel recording approach was implemented where a 32-channel electrode was inserted into the cortex on a dorsal-medial-to-ventral-lateral approach. Using this novel approach, recordings were completed in anaesthetized rats at specific stereotaxic coordinates to consistently and comprehensively map neuronal responses to auditory and visual stimuli in the dorsal auditory cortex (AuD), and area outside the auditory core, as well as in the neighbouring regions of the lateral extrastriate visual cortex (V2L), an area known to respond to audiovisual stimuli. To induce a moderate hearing impairment, adult rats were bilaterally exposed for two hours to a loud broadband noise. Single- and multi-unit activity was recorded in response to auditory, visual and combined audiovisual stimuli in rats two weeks after the noise exposure and the results were compared to age-matched controls.

Predicted Results & Significance: Consistent with the increased visual responsiveness observed in the primary auditory cortex following a moderate hearing loss in adulthood

(Meredith et al., 2012), I predicted that noise exposure would cause neurons in the multisensory cortex (i.e., V2L) to increase their responsiveness to visual stimuli. However, in contrast to the primary auditory cortex, I predicted that crossmodal plasticity in the multisensory cortex would manifest as a decrease in the percentage of neurons that respond to both auditory and visual stimuli because more neurons will now respond only to visual stimuli. Overall, these findings would provide the first evidence of crossmodal plasticity within higher-order sensory cortical areas induced by adult-onset hearing impairments.

1.5.2 Chapter 3: Adult-Onset Hearing Impairment Induces Layer-Specific Cortical Reorganization: Evidence of Crossmodal Plasticity and Central Gain Enhancement

Rationale & Objectives: Non-invasive studies on hearing-impaired individuals and preclinical research using animal models have demonstrated that noise-induced hearing loss can lead to neural plasticity throughout the central auditory system. More specifically, the loss of sensory input results in a paradoxical increase in neural activity at the successive relay nuclei, ultimately manifesting as hyperactivity in the auditory cortex (i.e., central gain enhancement) (Popelar et al., 1987, 2008; Salvi et al., 1990, 2000). However, it was previously unclear to what extent this deprivation-induced hyperactivity in the auditory cortex was relayed to higher-order, multisensory areas of the brain. Thus, Chapter 3 sought to reveal the extent that deprivation-induced hyperactivity in the auditory pathway is relayed beyond the core auditory cortex, and thus, whether central gain enhancement competes or coexists with crossmodal plasticity in the audiovisual cortex following partial hearing loss in adulthood.

Experimental Approach: Using extracellular electrophysiology, advanced laminar recordings were performed in adult rats two weeks after loud noise exposure across several regions of the higher-order sensory cortices. This method involved sampling the local field potential (LFP) across the entire cortical thickness and then applying the current source density (CSD) analysis, which provides a measure of the total current density that enters or leaves the extracellular matrix through the cell membrane, which allows for a description of the activation pattern across all cortical layers (Einevoll et al., 2013; Happel et al., 2010; Mitzdorf, 1985; Nicholson and Freeman, 1975; Schroeder et al., 1998). Auditory-, visual-

, and audiovisual-evoked responses were compared between noise exposed rats and age-matched controls for each of the cortical layers and regions examined.

Predicted Results & Significance: Based on the proposed mechanism that cortical plasticity may be due to changes in intracortical processing (Goel et al., 2006; He et al., 2012; Nys et al., 2015), I predicted that noise-induced hearing loss would result in hyperactivity within the supragranular layers of the auditory cortex during visual stimulation due to increased input from the neighbouring visual cortical areas. Furthermore, I predicted that central gain enhancement would be restricted to auditory cortical regions, as no change in mean firing rates were observed in Chapter 2. Overall, these results would demonstrate for the first time that crossmodal plasticity and central gain enhancement are able to co-exist within higher-order sensory regions, which ultimately results in a complex assortment of intramodal and crossmodal changes across the cortical layers.

1.5.3 Chapter 4: Behavioural Plasticity of Audiovisual Perception: Rapid Recalibration of Temporal Sensitivity but not Perceptual Binding following Adult-Onset Hearing Loss

Rationale & Objectives: The ability to integrate or bind stimuli from more than one sensory modality is highly dependent on the relative timing of the individual sensory stimuli (Meredith et al., 1987; Stein and Meredith, 1993). Psychophysical testing in humans, has demonstrated that the ability to perceptually bind stimuli is impaired in various clinical conditions such as autism, dyslexia, schizophrenia, as well as aging (Bedard and Barnett-Cowan, 2016; Wallace and Stevenson, 2014). However, it was unknown whether audiovisual temporal acuity is affected by adult-onset hearing loss. Therefore, Chapter 4 aimed to examine the nature and extent that audiovisual perception was influenced by noise-induced hearing loss, with a specific focus on the time-course of perceptual changes following loud noise exposure.

Experimental Approach: Prior to investigating the perceptual consequences of noise-induced hearing loss, we first needed to design and validate novel behavioural paradigms for rodents that were capable of assessing their ability to perceive the relative timing of

audiovisual stimuli (i.e., audiovisual perception). Using two-alternative forced-choice paradigms (2AFC), we found that rats are indeed capable of differentiating between auditory and visual stimuli presented at various timing offsets, reaching similar performance levels as those reported in humans (Schormans et al., 2017, Appendix A). Thus, using our novel rodent behavioural paradigms, rats were trained to either determine the temporal order of audiovisual stimuli (TOJ task), or differentiate whether audiovisual stimuli were presented synchronously or not (SJ task). In the first experimental series, psychophysical testing was completed for both behavioural tasks in which the intensity of the auditory stimulus was modulated. In the second experimental series, rats trained on the TOJ and SJ tasks were exposed to a loud noise, and their behavioural performance and associated metrics (i.e., PSS, JND, and TBW) were monitored for the next 3 weeks.

Predicted Results & Significance: Studies in normal-hearing participants have demonstrated that the intensity of the auditory and/or visual stimuli can alter ones' perception of audiovisual stimuli (Boenke et al., 2009; Krueger Fister et al., 2016; Neumann and Niepel, 2004; Smith, 1933). Due to the reduced sensitivity to environmental sounds following moderate hearing loss, I predicted that adult-onset hearing loss would alter perceptual judgments, such that the audiovisual stimuli would be perceived as if the intensity of the auditory stimulus was reduced. That said, it is well-established that the perceptual binding of audiovisual stimuli is highly-adaptive to experience (Fujisaki et al., 2004; Navarra et al., 2005; Powers et al., 2009; De Niear et al., 2016, 2018). Thus, an alternative prediction could be that individuals with adult-onset hearing impairments may show limited changes in audiovisual temporal acuity, owed to a recalibration of their perceptual ability as they adapt to their permanent hearing impairment. Ultimately, these results would reveal for the first time that adult-onset hearing loss could lead to behavioural plasticity of audiovisual perception and could potentially provide additional support for the suggestion that different perceptual processes likely underlie TOJ and SJ task performance.

1.5.4 Chapter 5: Compensatory Plasticity in the Lateral Extrastriate Visual Cortex Preserves Audiovisual Temporal Processing following Adult-Onset Hearing Loss

Rationale & Objectives: Recent studies have confirmed that crossmodal plasticity occurs in individuals who retain some level of residual auditory processing following moderate hearing loss within the auditory cortex (Campbell and Sharma, 2014; Cardon and Sharma, 2018; Meredith et al., 2012) as well as the audiovisual cortices (Chapters 2, 3). However, it is unknown whether adult-onset hearing loss influences the temporal precision of audiovisual processing at the neuronal level or if these effects differ across the neighbouring regions of the multisensory cortex that normally integrate audiovisual stimuli. Thus, Chapter 5 sought to examine the effect of noise-induced crossmodal plasticity on the ability of the multiple regions of the lateral extrastriate visual (V2L) cortex to integrate audiovisual stimuli at various temporal offsets.

Experimental Approach: To do so, adult rats were exposed to loud noise exposure, and two weeks later extracellular electrophysiological recordings were performed within two neighbouring regions of the lateral extrastriate visual cortex (V2L); a multisensory area known to be responsive to audiovisual stimuli (V2L-multisensory zone), and a more predominantly-auditory area (V2L-auditory zone). More specifically, a 32-channel linear electrode was inserted perpendicular to the cortical surface, and audiovisual processing was examined within each cortical region in response to combined audiovisual stimuli presented at various stimulus onset asynchronies (SOAs). Furthermore, the layer-specific effects of crossmodal plasticity were examined at the level of post-synaptic potentials by applying a current source density (CSD) analysis to the mean local field potential (LFP) data.

Predicted Results & Significance: Based on my previous work which revealed that a partial hearing impairment resulted in an expansion of the functional boundary of the audiovisual cortex into the neighbouring auditory regions (Chapter 2,3), I predicted that the auditory zone of the V2L cortex would become more responsiveness to visual stimuli and inherit the capacity to process audiovisual stimuli within the temporal precision that was previously restricted to the audiovisual cortex in normal-hearing rats. Overall, these

results would provide the first demonstration that audiovisual temporal processing is preserved following moderate hearing loss via compensatory plasticity in the higher-order sensory cortices.

1.5.5 Chapter 6: Noise-Induced Crossmodal Plasticity within the Audiovisual Cortex: Layer-Specific Enhancement and Rapid Manifestation of Visual-Evoked Activity

Rationale & Objectives: Studies in visually-deprived mice have revealed layer-specific synaptic changes within both the spared and deprived sensory cortices due to crossmodal plasticity (Goel et al., 2006; He et al., 2012; Lee and Whitt, 2015; Petrus et al., 2014, 2015). Similarly, noise-induced plasticity has been shown to manifest as layer-specific changes in visual-evoked activity (Chapter 3). However, the mechanisms underlying the distinct laminar effects of crossmodal plasticity remain unsolved. Furthermore, it is unknown whether this crossmodal plasticity observed in cortical microcircuits manifests solely from intrinsic changes in the cortex itself, or whether partial hearing impairment leads to increased visual responsiveness via a combination of altered intracortical processing as well as thalamocortical plasticity. Therefore, Chapter 6 aimed to investigate if hearing loss-induced crossmodal plasticity occurs at subcortical loci, as well as reveal the time-course by which crossmodal plasticity emerges following adult-onset hearing loss.

Experimental Approach: To investigate the thalamocortical contributions of crossmodal plasticity, laminar electrophysiological recordings were performed within the multisensory zone of the V2L cortex (V2L-Mz). By using a previously established, pharmacological silencing technique to dissociate the intracortical and thalamocortical contributions of cortical stimulus-evoked excitation (Happel et al., 2010, 2014), we examined alterations in thalamocortical processing following noise-induced hearing loss. Ultimately, using laminar CSD analysis, auditory, visual and audiovisual responses were compared between noise-exposed and age-matched controls before and after pharmacological silencing with muscimol. To investigate the working hypothesis that the characteristic increase in visual responsiveness observed following partial hearing loss occurs, at least in part, because of pre-existing connections becoming unmasked via the auditory deprivation. To that end, we used an epidural electrode array that spanned the higher-order sensory cortices, and

compared the visual-evoked LFP responses before- and immediately after loud noise exposure in the same adult rats.

Predicted Results & Significance: Consistent with studies in visually-deprived mice (Petrus et al., 2014, 2015), I predicted that the multisensory zone of the V2L cortex would show an enhancement of thalamocortical activity in response to visual stimulation. Furthermore, since studies of blind-folded individuals revealed that crossmodal plasticity manifests soon after the onset of the deprivation and was also reversible (Merabet et al., 2008), I predicted that the increased responsiveness to visual stimulation would emerge rapidly following hearing loss, characteristic of an unmasking of pre-existing inputs. Overall, these collective findings would demonstrate for the first time that noise-induced crossmodal plasticity occurs shortly after acoustic trauma, and ultimately results in changes in the thalamocortical input to the higher-order sensory cortices.

1.6 References

Alais, D., Newell, F.N., and Mamassian, P. (2010). Multisensory Processing in Review: from Physiology to Behaviour. *Seeing Perceiving* 23, 3–38.

Alary, F., Goldstein, R., Duquette, M., Chapman, C.E., Voss, P., and Lepore, F. (2008). Tactile acuity in the blind: a psychophysical study using a two-dimensional angle discrimination task. *Exp. Brain Res.* 187, 587–594.

Alary, F., Duquette, M., Goldstein, R., Elaine Chapman, C., Voss, P., La Buissonnière-Ariza, V., and Lepore, F. (2009). Tactile acuity in the blind: A closer look reveals superiority over the sighted in some but not all cutaneous tasks. *Neuropsychologia* 47, 2037–2043.

Allman, B.L., and Meredith, M.A. (2007). Multisensory Processing in "Unimodal" Neurons: Cross-Modal Subthreshold Auditory Effects in Cat Extrastriate Visual Cortex. *J. Neurophysiol*. 98, 545–549.

Allman, B.L., Bittencourt-Navarrete, R.E., Keniston, L.P., Medina, A.E., Wang, M.Y., and Meredith, M.A. (2008a). Do Cross-Modal Projections Always Result in Multisensory Integration? *Cereb. Cortex* 18, 2066–2076.

Allman, B.L., Keniston, L.P., and Meredith, M.A. (2008b). Subthreshold auditory inputs to extrastriate visual neurons are responsive to parametric changes in stimulus quality: Sensory-specific versus non-specific coding. *Brain Res.* 1242, 95–101.

Allman, B.L., Keniston, L.P., and Meredith, M.A. (2009). Adult deafness induces somatosensory conversion of ferret auditory cortex. *Proc. Natl. Acad. Sci*. 106, 5925–5930.

Amedi, A., Floel, A., Knecht, S., Zohary, E., and Cohen, L.G. (2004). Transcranial magnetic stimulation of the occipital pole interferes with verbal processing in blind subjects. *Nat. Neurosci*. 7, 1266–1270.

Auer, E.T., Bernstein, L.E., Sungkarat, W., and Singh, M. (2007). Vibrotactile Activation of the Auditory Cortices in Deaf versus Hearing Adults. *Neuroreport* 18, 645–648.

Auerbach, B.D., Rodrigues, P.V., and Salvi, R.J. (2014). Central gain control in tinnitus and hyperacusis. *Front. Neurol*. 5, 206.

Barone, P., Lacassagne, L., and Kral, A. (2013). Reorganization of the Connectivity of Cortical Field DZ in Congenitally Deaf Cat. *PLOS ONE* 8, e60093.

Barth, D.S., Goldberg, N., Brett, B., and Di, S. (1995). The spatiotemporal organization of auditory, visual, and auditory-visual evoked potentials in rat cortex. *Brain Res*. 678, 177–190.

Başkent, D., and Bazo, D. (2011). Audiovisual asynchrony detection and speech intelligibility in noise with moderate to severe sensorineural hearing impairment. *Ear Hear*. 32, 582–592.

Bavelier, D., and Neville, H.J. (2002). Cross-modal plasticity: where and how? *Nat. Rev. Neurosci*. 3, 443–452.

Bavelier, D., Tomann, A., Hutton, C., Mitchell, T., Corina, D., Liu, G., and Neville, H. (2000). Visual attention to the periphery is enhanced in congenitally deaf individuals. *J. Neurosci.* 20, RC931-6.

Bavelier, D., Brozinsky, C., Tomann, A., Mitchell, T., Neville, H., and Liu, G. (2001). Impact of Early Deafness and Early Exposure to Sign Language on the Cerebral Organization for Motion Processing. *J. Neurosci*. 21, 8931–8942.

Bavelier, D., Dye, M.W.G., and Hauser, P.C. (2006). Do deaf individuals see better? *Trends Cogn. Sci.* 10, 512–518.

Bedard, G., and Barnett-Cowan, M. (2016). Impaired timing of audiovisual events in the elderly. *Exp. Brain Res*. 234, 331–340.

Bizley, J.K., and King, A.J. (2008). Visual–auditory spatial processing in auditory cortical neurons. *Brain Res*. 1242, 24–36.

Bizley, J.K., Nodal, F.R., Bajo, V.M., Nelken, I., and King, A.J. (2007). Physiological and Anatomical Evidence for Multisensory Interactions in Auditory Cortex. *Cereb. Cortex* 17, 2172–2189.

Boenke, L.T., Deliano, M., and Ohl, F.W. (2009). Stimulus duration influences perceived simultaneity in audiovisual temporal-order judgment. *Exp. Brain Res*. 198, 233–244.

Bosworth, R.G., and Dobkins, K.R. (2002). The effects of spatial attention on motion processing in deaf signers, hearing signers, and hearing non-signers. *Brain Cogn*. 49, 152–169.

Bross, M. (1979). Residual sensory capacities of the deaf: a signal detection analysis of a visual discrimination task. *Percept. Mot. Skills* 48, 187–194.

Brozinsky, C.J., and Bavelier, D. (2004). Motion velocity thresholds in deaf signers: changes in lateralization but not in overall sensitivity. *Cogn. Brain Res*. 21, 1–10.

Buckley, K.A., and Tobey, E.A. (2011). Cross-modal Plasticity and Speech Perception in Pre- and Postlingually Deaf Cochlear Implant Users. *Ear Hear*. 32, 2–15.

Budinger, E., and Scheich, H. (2009). Anatomical connections suitable for the direct processing of neuronal information of different modalities via the rodent primary auditory cortex. *Hear. Res*. 258, 16–27.

Budinger, E., Heil, P., Hess, A., and Scheich, H. (2006). Multisensory processing via early cortical stages: Connections of the primary auditory cortical field with other sensory systems. *Neuroscience* 143, 1065–1083.

Burkhalter, A. (2016). "The Network for Intracortical Communication in Mouse Visual Cortex". In *Micro-, Meso- and Macro-Connectomics of the Brain*, eds. H. Kennedy, D.C.V. Essen, and Y. Christen, (London, UK: Springer International Publishing), 31–43.

Burton, H., Sinclair, R.J., and McLaren, D.G. (2004). Cortical activity to vibrotactile stimulation: An fMRI study in blind and sighted individuals. *Hum. Brain Mapp*. 23, 210–228.

Butera, I.M., Stevenson, R.A., Mangus, B.D., Woynaroski, T.G., Gifford, R.H., and Wallace, M.T. (2018). Audiovisual Temporal Processing in Postlingually Deafened Adults with Cochlear Implants. *Sci. Rep.* 8, 11345.

Butler, B.E., and Lomber, S.G. (2013). Functional and structural changes throughout the auditory system following congenital and early-onset deafness: implications for hearing restoration. *Front. Syst. Neurosci*. 7.

Butler, B.E., Chabot, N., and Lomber, S.G. (2016). Quantifying and comparing the pattern of thalamic and cortical projections to the posterior auditory field in hearing and deaf cats. *J. Comp. Neurol.* 524:15, 3042-3063

Calvert, G.A., Campbell, R., and Brammer, M.J. (2000). Evidence from functional magnetic resonance imaging of crossmodal binding in the human heteromodal cortex. *Curr. Biol.* 10, 649–657.

Campbell, J., and Sharma, A. (2013). Compensatory changes in cortical resource allocation in adults with hearing loss. *Front. Syst. Neurosci.* 7, 71.

Campbell, J., and Sharma, A. (2014). Cross-Modal Re-Organization in Adults with Early Stage Hearing Loss. *PLOS ONE* 9, e90594.

Cappe, C., Murray, M.M., Barone, P., and Rouiller, E.M. (2010a). Multisensory Facilitation of Behavior in Monkeys: Effects of Stimulus Intensity. *J. Cogn. Neurosci*. 22, 2850–2863.

Cappe, C., Thut, G., Romei, V., and Murray, M.M. (2010b). Auditory-visual multisensory interactions in humans: timing, topography, directionality, and sources. *J. Neurosci.* 30, 12572–12580.

Cardon, G., and Sharma, A. (2018). Somatosensory Cross-Modal Reorganization in Adults with Age-Related, Early-Stage Hearing Loss. *Front. Hum. Neurosci*. 12.

Chabot, N., Butler, B.E., and Lomber, S.G. (2015). Differential modification of cortical and thalamic projections to cat primary auditory cortex following early- and late-onset deafness. *J. Comp. Neurol*. 523, 2297–2320.

Chen, G.-D., Stolzberg, D., Lobarinas, E., Sun, W., Ding, D., and Salvi, R. (2013). Salicylate-induced cochlear impairments, cortical hyperactivity and re-tuning, and tinnitus. *Hear. Res*. 295, 100–113.

Clemo, H.R., Lomber, S.G., and Meredith, M.A. (2014). Synaptic Basis for Cross-modal Plasticity: Enhanced Supragranular Dendritic Spine Density in Anterior Ectosylvian Auditory Cortex of the Early Deaf Cat. *Cereb. Cortex*, bhu225.

Cohen, L.G., Celnik, P., Pascual-Leone, A., Corwell, B., Faiz, L., Dambrosia, J., Honda, M., Sadato, N., Gerloff, C., Catala´, M.D., et al. (1997). Functional relevance of cross-modal plasticity in blind humans. *Nature* 389, 180–183.

Collignon, O., Voss, P., Lassonde, M., and Lepore, F. (2008). Cross-modal plasticity for the spatial processing of sounds in visually deprived subjects. *Exp. Brain Res*. 192, 343.

Craik, F.I.M. (2007). The Role of Cognition in Age-Related Hearing Loss. *J. Am. Acad. Audiol.* 18, 539-547

De Niear, M.A., Gupta, P.B., Baum, S.H. and Wallace, M.T. (2018). Perceptual training enhances temporal acuity for multisensory speech. *Neurobiol. Learn. Mem.* 147, 9-17

De Niear, M.A., Koo, B., and Wallace, M.T. (2016). Multisensory perceptual learning is dependent upon task difficulty. *Exp. Brain Res.* 234, 3269-3277

Diederich, A., and Colonius, H. (2004). Bimodal and trimodal multisensory enhancement: Effects of stimulus onset and intensity on reaction time. *Percept. Psychophys*. 66, 1388–1404.

Dong, S., Rodger, J., Mulders, W.H.A.M., and Robertson, D. (2010). Tonotopic changes in GABA receptor expression in guinea pig inferior colliculus after partial unilateral hearing loss. *Brain Res*. 1342, 24–32.

Doucet, M.E., Bergeron, F., Lassonde, M., Ferron, P., and Lepore, F. (2006). Cross-modal reorganization and speech perception in cochlear implant users. *Brain* 129, 3376–3383.

Driver, J., and Noesselt, T. (2008). Multisensory Interplay Reveals Crossmodal Influences on ‘Sensory-Specific’ Brain Regions, Neural Responses, and Judgments. *Neuron* 57, 11–23.

Dye, M.W.G., Baril, D.E., and Bavelier, D. (2007). Which aspects of visual attention are changed by deafness? The case of the Attentional Network Test. *Neuropsychologia* 45, 1801–1811.

Dye, M.W.G., Hauser, P.C., and Bavelier, D. (2009). Is Visual Selective Attention in Deaf Individuals Enhanced or Deficient? The Case of the Useful Field of View. *PLOS ONE* 4, e5640.

van Eijk, R.L.J., Kohlrausch, A., Juola, J.F., and Par, S. van de (2008). Audiovisual synchrony and temporal order judgments: Effects of experimental method and stimulus type. *Percept. Psychophys.* 70, 955–968.

Einevoll, G.T., Kayser, C., Logothetis, N.K., and Panzeri, S. (2013). Modelling and analysis of local field potentials for studying the function of cortical circuits. *Nat. Rev. Neurosci. Lond.* 14, 770–785.

Elbert, T., Sterr, A., Rockstroh, B., Pantev, C., Müller, M.M., and Taub, E. (2002). Expansion of the Tonotopic Area in the Auditory Cortex of the Blind. *J. Neurosci.* 22, 9941–9944.

Faggin, B.M., Nguyen, K.T., and Nicolelis, M.A.L. (1997). Immediate and simultaneous sensory reorganization at cortical and subcortical levels of the somatosensory system. *Proc. Natl. Acad. Sci*. 94, 9428–9433.

Feder, K., Michaud, D., Ramage-Morin, P., McNamee, J., and Beauregard, Y. (2015). Prevalence of hearing loss among Canadians aged 20 to 79: audiometric results from the 2012/2013 Canadian Health Measures Survery. *Stat. Can.* 26, 18–25.

Fieger, A., Röder, B., Teder-Sälejärvi, W., Hillyard, S.A., and Neville, H.J. (2006). Auditory spatial tuning in late-onset blindness in humans. *J. Cogn. Neurosci*. 18, 149–157.

Fine, I., Finney, E.M., Boynton, G.M., and Dobkins, K.R. (2005). Comparing the effects of auditory deprivation and sign language within the auditory and visual cortex. *J. Cogn. Neurosci.* 17, 1621–1637.

Finney, E.M., and Dobkins, K.R. (2001). Visual contrast sensitivity in deaf versus hearing populations: Exploring the perceptual consequences of auditory deprivation and experience with a visual language. *Cogn. Brain Res.* 11, 171–183.

Finney, E.M., Fine, I., and Dobkins, K.R. (2001). Visual stimuli activate auditory cortex in the deaf. *Nat. Neurosci.* 4, 1171–1173.

Finney, E.M., Clementz, Brett, A., Hickok, G., and Dobkins, K.R. (2003). Visual stimuli activate auditory cortex in deaf subjects: evidence from MEG. *Neuroreport* 14, 1425–1427.

Foxe, J.J., and Schroeder, C.E. (2005). The case for feedforward multisensory convergence during early cortical processing. *Neuroreport* 16, 419–423.

Foxe, J.J., Wylie, G.R., Martinez, A., Schroeder, C.E., Javitt, D.C., Guilfoyle, D., Ritter, W., and Murray, M.M. (2002). Auditory-Somatosensory Multisensory Processing in Auditory Association Cortex: An fMRI Study. *J. Neurophysiol*. 88, 540–543.

Foxworthy, W.A., Clemo, H.R., and Meredith, M.A. (2013a). Laminar and connectional organization of a multisensory cortex. *J. Comp. Neurol*. 521, 1867–1890.

Foxworthy, W.A., Allman, B.L., Keniston, L.P., and Meredith, M.A. (2013b). Multisensory and unisensory neurons in ferret parietal cortex exhibit distinct functional properties. *Eur. J. Neurosci*. 37, 910–923.

Frasnelli, J., Collignon, O., Voss, P., and Lepore, F. (2011). "Chapter 15 - Crossmodal plasticity in sensory loss". In *Progress in Brain Research*, eds. A.M. Green, C.E. Chapman, J.F. Kalaska, and F. Lepore, (Amsterdam, Netherlands: Elsevier), 233–249.

Fujisaki, W., Shimojo, S., Kashino, M., and Nishida, A. (2004) Recalibration of audiovisual simultaneity. *Nat. Neurosci.* 7, 773-778

Ghazanfar, A.A., and Schroeder, C.E. (2006). Is neocortex essentially multisensory? *Trends Cogn. Sci*. 10, 278–285.

Gizewski, E.R., Gasser, T., de Greiff, A., Boehm, A., and Forsting, M. (2003). Cross-modal plasticity for sensory and motor activation patterns in blind subjects. *NeuroImage* 19, 968–975.

Gleiss, S., and Kayser, C. (2012). Audio-Visual Detection Benefits in the Rat. *PLOS ONE* 7, e45677.

Goel, A., Jiang, B., Xu, L.W., Song, L., Kirkwood, A., and Lee, H.-K. (2006). Cross-modal regulation of synaptic AMPA receptors in primary sensory cortices by visual experience. *Nat. Neurosci*. 9, 1001–1003.

Goldreich, D., and Kanics, I.M. (2003). Tactile Acuity is Enhanced in Blindness. *J. Neurosci.* 23, 3439–3445.

Gougoux, F., Lepore, F., Lassonde, M., Voss, P., Zatorre, R.J., and Belin, P. (2004). Neuropsychology: Pitch discrimination in the early blind. *Nature* 430, 309.

Gougoux, F., Zatorre, R.J., Lassonde, M., Voss, P., and Lepore, F. (2005). A Functional Neuroimaging Study of Sound Localization: Visual Cortex Activity Predicts Performance in Early-Blind Individuals. *PLoS Biol*. 3.

Hamilton, R.H., and Pascual-Leone, A. (1998). Cortical plasticity associated with Braille learning. *Trends Cogn. Sci.* 2, 168–174.

Happel, M.F.K., Jeschke, M., and Ohl, F.W. (2010). Spectral Integration in Primary Auditory Cortex Attributable to Temporally Precise Convergence of Thalamocortical and Intracortical Input. *J. Neurosci*. 30, 11114–11127.

Happel, M.F.K., Deliano, M., Handschuh, J., and Ohl, F.W. (2014). Dopamine-modulated recurrent corticoefferent feedback in primary sensory cortex promotes detection of behaviorally relevant stimuli. *J. Neurosci*. 34, 1234–1247.

Hay-McCutcheon, M.J., Pisoni, D.B., and Hunt, K.K. (2009). Audiovisual Asynchrony Detection and Speech Perception in Hearing-Impaired Listeners with Cochlear Implants: A Preliminary Analysis. Int. *J. Audiol*. 48, 321–333.

He, K., Petrus, E., Gammon, N., and Lee, H.-K. (2012). Distinct Sensory Requirements for Unimodal and Cross-Modal Homeostatic Synaptic Plasticity. *J. Neurosci*. 32, 8469–8474.

Heimler, B., Weisz, N., and Collignon, O. (2014). Revisiting the adaptive and maladaptive effects of crossmodal plasticity. *Neuroscience* 283, 44–63.

Hershenson, M. (1962). Reaction time as a measure of intersensory facilitation. *J. Exp. Psychol*. 63, 289–293.

Hickok, G., Poeppel, D., Clark, K., Buxton, R.B., Rowley, H.A., and Roberts, T.P.L. (1997). Sensory mapping in a congenitally deaf subject: MEG and fRMI studies of cross-modal non-plasticity. *Hum. Brain Mapp*. 5, 437–444.

Hirokawa, J., Bosch, M., Sakata, S., Sakurai, Y., and Yamamori, T. (2008). Functional role of the secondary visual cortex in multisensory facilitation in rats. *Neuroscience* 153, 1402–1417.

Humanes-Valera, D., Aguilar, J., and Foffani, G. (2013). Reorganization of the Intact Somatosensory Cortex Immediately after Spinal Cord Injury. *PLOS ONE* 8, e69655.

Hunt, D.L., Yamoah, E.N., and Krubitzer, L. (2006). Multisensory plasticity in congenitally deaf mice: How are cortical areas functionally specified? *Neuroscience* 139, 1507–1524.

Iurilli, G., Ghezzi, D., Olcese, U., Lassi, G., Nazzaro, C., Tonini, R., Tucci, V., Benfenati, F., and Medini, P. (2012). Sound-Driven Synaptic Inhibition in Primary Visual Cortex. *Neuron* 73, 814–828.

Kayser, C., Petkov, C.I., and Logothetis, N.K. (2009). Multisensory interactions in primate auditory cortex: fMRI and electrophysiology. *Hear. Res*. 258, 80–88.

Keetels, M., and Vroomen, J. (2012). “Perception of Synchrony between the Senses”. In *The Neural Bases of Multisensory Processes*, eds M.M. Murray and M.T. Wallace (Boca Raton, FL: CRC Press/Taylor & Francis), 147-178.

King, A.J., and Palmer, A.R. (1985). Integration of visual and auditory information in bimodal neurons in the guinea-pig superior colliculus. *Exp. Brain Res*. 60, 492–500.

King, A.J., and Parsons, C.H. (1999). Improved auditory spatial acuity in visually deprived ferrets. *Eur. J. Neurosci*. 11, 3945–3956.

Kok, M.A., Chabot, N., and Lomber, S.G. (2014). Cross-modal reorganization of cortical afferents to dorsal auditory cortex following early- and late-onset deafness. *J. Comp. Neurol*. 522, 654–675.

Komiya, H., and Eggermont, J.J. (2000). Spontaneous Firing Activity of Cortical Neurons in Adult Cats with Reorganized Tonotopic Map Following Pure-tone Trauma. *Acta Otolaryngol*. (Stockh.) 120, 750–756.

Kostaki, M., and Vatakis, A. (2018). "Temporal Order and Synchrony Judgments: A Primer for Students". In *Timing and Time Perception: Procedures, Measures, and Applications*, eds. A. Vatakis, F. Balci, M. Di Luca, and A. Correa, (Leiden, Netherlands: Koninklijke Brill), 233-262

Kral, A., Schröder, J.-H., Klinke, R., and Engel, A.K. (2003). Absence of cross-modal reorganization in the primary auditory cortex of congenitally deaf cats. *Exp. Brain Res.* 153, 605–613.

Krueger Fister, J., Stevenson, R.A., Nidiffer, A.R., Barnett, Z.P., and Wallace, M.T. (2016). Stimulus intensity modulates multisensory temporal processing. *Neuropsychologia* 88, 92–100.

Kujala, T., Alho, K., Huotilainen, M., Ilmoniemi, R.J., Lehtokoski, A., Leinonen, A., Rinne, T., Salonen, O., Sinkkonen, J., Standertskjöuld-Nordenstam, C.-G., et al. (1997). Electrophysiological evidence for cross-modal plasticity in humans with early- and late-onset blindness. *Psychophysiology* 34, 213–216.

Kujawa, S.G., and Liberman, M.C. (2006). Acceleration of Age-Related Hearing Loss by Early Noise Exposure: Evidence of a Misspent Youth. *J. Neurosci*. 26, 2115–2123.

Kujawa, S.G., and Liberman, M.C. (2009). Adding Insult to Injury: Cochlear Nerve Degeneration after "Temporary" Noise-Induced Hearing Loss. *J. Neurosci*. 29, 14077–14085.

Kupers, R., Pappens, M., de Noordhout, A.M., Schoenen, J., Ptito, M., and Fumal, A. (2007). rTMS of the occipital cortex abolishes Braille reading and repetition priming in blind subjects. *Neurology* 68, 691–693.

Laing, R. j., Bock, A. s., Lasiene, J., and Olavarria, J. f. (2012). Role of retinal input on the development of striate–extrastriate patterns of connections in the rat. *J. Comp. Neurol.* 520, 3256–3276.

Lakatos, P., Chen, C.-M., O'Connell, M.N., Mills, A., and Schroeder, C.E. (2007). Neuronal Oscillations and Multisensory Interaction in Primary Auditory Cortex. *Neuron* 53, 279–292.

Lambertz, N., Gizewski, E.R., de Greiff, A., and Forsting, M. (2005). Cross-modal plasticity in deaf subjects dependent on the extent of hearing loss. *Cogn. Brain Res.* 25, 884–890.

Laramée, M.E., Kurotani, T., Rockland, K.S., Bronchti, G., and Boire, D. (2011). Indirect pathway between the primary auditory and visual cortices through layer V pyramidal neurons in V2L in mouse and the effects of bilateral enucleation. Eur. *J. Neurosci*. 34, 65–78.

Laramée, M.E., Rockland, K.S., Prince, S., Bronchti, G., and Boire, D. (2013). Principal component and cluster analysis of layer V pyramidal cells in visual and non-visual cortical areas projecting to the primary visual cortex of the mouse. *Cereb. Cortex* N. Y. N 1991 23, 714–728.

Lee, H.-K., and Whitt, J.L. (2015). Cross-modal synaptic plasticity in adult primary sensory cortices. *Curr. Opin. Neurobiol*. 35, 119–126.

Lessard, N., Paré, M., Lepore, F., and Lassonde, M. (1998). Early-blind human subjects localize sound sources better than sighted subjects. *Nature* 395, 278–280.

Levänen, S., and Hamdorf, D. (2001). Feeling vibrations: enhanced tactile sensitivity in congenitally deaf humans. *Neurosci. Lett.* 301, 75–77.

Liberman, M.C., and Dodds, L.W. (1984). Single-neuron labeling and chronic cochlear pathology. III. Stereocilia damage and alterations of threshold tuning curves. *Hear. Res.* 16, 55–74.

Loke, W.H., and Song, S. (1991). Central and peripheral visual processing in hearing and nonhearing individuals. *Bull. Psychon. Soc*. 29, 437–440.

Lomber, S.G., Meredith, M.A., and Kral, A. (2010). Cross-modal plasticity in specific auditory cortices underlies visual compensations in the deaf. *Nat. Neurosci*. 13, 1421–1427.

Lu, J., Lobarinas, E., Deng, A., Goodey, R., Stolzberg, D., Salvi, R.J., and Sun, W. (2011). GABAergic neural activity involved in salicylate-induced auditory cortex gain enhancement. *Neuroscience 189*, 187–198.

Merabet, L.B., and Pascual-Leone, A. (2010). Neural reorganization following sensory loss: the opportunity of change. *Nat. Rev. Neurosci*. 11, 44–52.

Merabet, L.B., Hamilton, R., Schlaug, G., Swisher, J.D., Kiriakopoulos, E.T., Pitskel, N.B., Kauffman, T., and Pascual-Leone, A. (2008). Rapid and Reversible Recruitment of Early Visual Cortex for Touch. *PLOS ONE* 3, e3046.

Mercier, M.R., Foxe, J.J., Fiebelkorn, I.C., Butler, J.S., Schwartz, T.H., and Molholm, S. (2013). Auditory-driven phase reset in visual cortex: Human electrocorticography reveals mechanisms of early multisensory integration. *NeuroImage* 79, 19–29.

Meredith, M.A., and Allman, B.L. (2009). Subthreshold multisensory processing in cat auditory cortex. *Neuroreport* 20, 126–131.

Meredith, M.A., and Allman, B.L. (2012). Early Hearing-Impairment Results in Crossmodal Reorganization of Ferret Core Auditory Cortex. *Neural Plast*. 2012, e601591.

Meredith, M.A., and Lomber, S.G. (2011). Somatosensory and visual crossmodal plasticity in the anterior auditory field of early-deaf cats. *Hear. Res*. 280, 38–47.

Meredith, M.A., and Stein, B.E. (1986). Visual, auditory, and somatosensory convergence on cells in superior colliculus results in multisensory integration. *J. Neurophysiol*. 56, 640–662.

Meredith, M.A., Nemitz, J.W., and Stein, B.E. (1987). Determinants of multisensory integration in superior colliculus neurons. I. Temporal factors. *J. Neurosci*. 7, 3215–3229.

Meredith, M.A., Kryklywy, J., McMillan, A.J., Malhotra, S., Lum-Tai, R., and Lomber, S.G. (2011). Crossmodal reorganization in the early deaf switches sensory, but not behavioral roles of auditory cortex. *Proc. Natl. Acad. Sci*. 108, 8856–8861.

Meredith, M.A., Keniston, L.P., and Allman, B.L. (2012). Multisensory dysfunction accompanies crossmodal plasticity following adult hearing impairment. *Neuroscience* 214, 136–148.

Miller, R.L., Pluta, S.R., Stein, B.E., and Rowland, B.A. (2015). Relative unisensory strength and timing predict their multisensory product. *J. Neurosci.* 35, 5213–5220.

Mitzdorf, U. (1985). Current source-density method and application in cat cerebral cortex: investigation of evoked potentials and EEG phenomena. *Physiol. Rev*. 65, 37–100.

Molholm, S., Ritter, W., Murray, M.M., Javitt, D.C., Schroeder, C.E., and Foxe, J.J. (2002). Multisensory auditory–visual interactions during early sensory processing in humans: a high-density electrical mapping study. *Cogn. Brain Res.* 14, 115–128.

Moore, A.K., and Wehr, M. (2013). Parvalbumin-Expressing Inhibitory Interneurons in Auditory Cortex Are Well-Tuned for Frequency. *J. Neurosci*. 33, 13713–13723.

Murata, K., Cramer, H., and Bach-y-Rita, P. (1965). Neuronal convergence of noxious, acoustic, and visual stimuli in the visual cortex of the cat. *J. Neurophysiol*. 28, 1223–1239.

Nava, E., Bottari, D., Zampini, M., and Pavani, F. (2008). Visual temporal order judgment in profoundly deaf individuals. *Exp. Brain Res*. 190, 179–188.

Navarra, J., Vatakis, A., Zampini, M., Soto-Faraco, S., Humphreys, W., and Spence, C. (2005). Exposure to asynchronous audiovisual speech extends the temporal window for audiovisual integration. *Cogn. Brain Res*. 25, 499–507.

Neumann, O., and Niepel, M. (2004). "Timing of "Perception" and Perception of "Time"," In *Psychophysics Beyond Senstion: Laws and Invariants of Human Cognition*, eds C. Kaerbach, E. Schroger and H. Muller (Mahwah, NJ: Lawrence Erlbaum Associates), 245-269

Neville, H.J., and Lawson, D. (1987). Attention to central and peripheral visual space in a movement detection task: an event-related potential and behavioral study. II. Congenitally deaf adults. *Brain Res*. 405, 268–283.

Neville, H.J., Schmidt, A., and Kutas, M. (1983). Altered visual-evoked potentials in congenitally deaf adults. *Brain Res*. 266, 127–132.

Nicholson, C., and Freeman, J.A. (1975). Theory of current source-density analysis and determination of conductivity tensor for anuran cerebellum. *J. Neurophysiol*. 38, 356–368.

Nys, J., Smolders, K., Laramée, M.-E., Hofman, I., Hu, T.-T., and Arckens, L. (2015). Regional Specificity of GABAergic Regulation of Cross-Modal Plasticity in Mouse Visual Cortex after Unilateral Enucleation. *J. Neurosci*. 35, 11174–11189.

Olavarria, J., and Montero, V.M. (1981). Reciprocal connections between the striate cortex and extrastriate cortical visual areas in the rat. *Brain Res*. 217, 358–363.

Olsen, G.M., and Witter, M.P. (2016). Posterior parietal cortex of the rat: Architectural delineation and thalamic differentiation. *J. Comp. Neurol.* 524:18, 3774-3809

Pascual-Leone, A., and Torres, F. (1993). Plasticity of the sensorimotor cortex representation of the reading finger in Braille readers. *Brain* 116, 39–52.

Pavani, F., and Roder, B. (2012). "Crossmodal plasticity as a consequence of sensory loss: insights from blindness and deafness." In *The New Handbook for Multisensory Processes*, eds. B. Stein (Cambridge, MA: MIT Press) 737–759.

Perrault, T.J., Vaughan, J.W., Stein, B.E., and Wallace, M.T. (2005). Superior Colliculus Neurons Use Distinct Operational Modes in the Integration of Multisensory Stimuli. *J. Neurophysiol.* 93, 2575–2586.

Petrus, E., Isaiah, A., Jones, A.P., Li, D., Wang, H., Lee, H.-K., and Kanold, P.O. (2014). Crossmodal Induction of Thalamocortical Potentiation Leads to Enhanced Information Processing in the Auditory Cortex. *Neuron* 81, 664–673.

Petrus, E., Rodriguez, G., Patterson, R., Connor, B., Kanold, P.O., and Lee, H.-K. (2015). Vision Loss Shifts the Balance of Feedforward and Intracortical Circuits in Opposite Directions in Mouse Primary Auditory and Visual Cortices. *J. Neurosci*. 35, 8790–8801.

Pi, H.-J., Hangya, B., Kvitsiani, D., Sanders, J.I., Huang, Z.J., and Kepecs, A. (2013). Cortical interneurons that specialize in disinhibitory control. *Nature* 503, 521–524.

Poizner, H., and Tallal, P. (1987). Temporal processing in deaf signers. *Brain Lang*. 30, 52–62.

Popelar, J., Syka, J., and Berndt, H. (1987). Effect of noise on auditory evoked responses in awake guina pigs. *Hear. Res*. 26, 239–247.

Popelar, J., Grecova, J., Rybalko, N., and Syka, J. (2008). Comparison of noise-induced changes of auditory brainstem and middle latency response amplitudes in rats. *Hear. Res.* 245, 82–91.

Popescu, M.V., and Polley, D.B. (2010). Monaural Deprivation Disrupts Development of Binaural Selectivity in Auditory Midbrain and Cortex. *Neuron* 65, 718–731.

Proksch, J., and Bavelier, D. (2002). Changes in the spatial distribution of visual attention after early deafness. *J. Cogn. Neurosci*. 14, 687–701.

Powers, A.R. III., Hillock, A.R., and Wallace, M.T. (2009). Perceptual training narrows the temporal window of multisensory binding. *J. Neurosci*. 29, 12265-12274

Puschmann, S., and Thiel, C.M. (2017). Changed crossmodal functional connectivity in older adults with hearing loss. *Cortex* 86, 109–122.

Raposo, D., Sheppard, J.P., Schrater, P.R., and Churchland, A.K. (2012). Multisensory Decision-Making in Rats and Humans. *J. Neurosci*. 32, 3726–3735.

Rauschecker, J.P. (1995). Compensatory plasticity and sensory substitution in the cerebral cortex. *Trends Neurosci*. 18, 36–43.

Rauschecker, J.P., and Kniepert, U. (1994). Auditory Localization Behaviour in Visually Deprived Cats. *Eur. J. Neurosci*. 6, 149–160.

Röder, B., Teder-Sälejärvi, W., Sterr, A., Rösler, F., Hillyard, S.A., and Neville, H.J. (1999). Improved auditory spatial tuning in blind humans. *Nature* 400, 162–166.

Salvi, R.J., Hamernik, R.P., and Henderson, D. (1978). Discharge patterns in the cochlear nucleus of the chinchilla following noise induced asymptotic threshold shift. Exp. *Brain Res*. 32, 301–320.

Salvi, R.J., Saunders, S.S., Gratton, M.A., Arehole, S., and Powers, N. (1990). Enhanced evoked response amplitudes in the inferior colliculus of the chinchilla following acoustic trauma. *Hear. Res*. 50, 245–257.

Salvi, R.J., Wang, J., and Ding, D. (2000). Auditory plasticity and hyperactivity following cochlear damage. *Hear. Res.* 147, 261–274.

Schaette, R., and Kempter, R. (2006). Development of tinnitus-related neuronal hyperactivity through homeostatic plasticity after hearing loss: a computational model. *Eur. J. Neurosci*. 23, 3124–3138.

Schormans, A.L., Scott, K.E., Vo, A.M.Q., Tyker, A., Typlt, M., Stolzberg, D., and Allman, B.L. (2017). Audiovisual Temporal Processing and Synchrony Perception in the Rat. *Front. Behav. Neurosci*. 10.

Schroeder, C.E., Mehta, A.D., and Givre, S.J. (1998). A spatiotemporal profile of visual system activation revealed by current source density analysis in the awake macaque. *Cereb. Cortex* 8, 575–592.

Schroeder, C.E., Lindsley, R.W., Specht, C., Marcovici, A., Smiley, J.F., and Javitt, D.C. (2001). Somatosensory Input to Auditory Association Cortex in the Macaque Monkey. *J. Neurophysiol*. 85, 1322–1327.

Schroeder, C.E., Smiley, J., Fu, K.G., McGinnis, T., O'Connell, M.N., and Hackett, T.A. (2003). Anatomical mechanisms and functional implications of multisensory convergence in early cortical processing. *Int. J. Psychophysiol*. 50, 5–17.

Siemann, J.K., Muller, C.L., Bamberger, G., Allison, J.D., Veenstra-VanderWeele, J., and Wallace, M.T. (2015). A novel behavioral paradigm to assess multisensory processing in mice. *Front. Behav. Neurosci*. 8.

Singh, A.K., Phillips, F., Merabet, L.B., and Sinha, P. (2018). Why Does the Cortex Reorganize after Sensory Loss? *Trends Cogn. Sci*. 22, 569–582.

Sladen, D.P., Tharpe, A.M., Ashmead, D.H., Grantham, D.W., and Chun, M.M. (2005). Visual Attention in Deaf and Normal Hearing Adults: Effects of Stimulus Compatibility. *J. Speech Lang. Hear. Res*. 48, 1529–1537.

Smith, W.F. (1933). The Relative Quickness of Visual and Auditory Perception. *J. Exp. Psychol.* 16, 239–257.

Spence, C., Baddeley, R., Zampini, M., James, R., and Shore, D.I. (2003). Multisensory temporal order judgments: When two locations are better than one. *Percept. Psychophys.* 65, 318–328.

Stanford, T.R., Quessy, S., and Stein, B.E. (2005). Evaluating the operations underlying multisensory integration in the cat superior colliculus. *J. Neurosci.* 25, 6499–6508.

Stein, B.E., and Meredith, M.A. (1993). The merging of the senses (Cambridge, MA, US: The MIT Press).

Stein, B.E., and Rowland, B.A. (2011). "Chapter 10 - Organization and plasticity in multisensory integration: early and late experience affects its governing principles." In *Progress in Brain Research*, eds. A.M. Green, C.E. Chapman, J.F. Kalaska, and F. Lepore, (Amsterdam, Netherlands: Elsevier), 145–163.

Stein, B.E., and Stanford, T.R. (2008). Multisensory integration: current issues from the perspective of the single neuron. *Nat. Rev. Neurosci*. 9, 255–266.

Stein, B.E., Stanford, T.R., and Rowland, B.A. (2014). Development of multisensory integration from the perspective of the individual neuron. *Nat. Rev. Neurosci*. 15, 520–535.

Stekelenburg, J.J., and Vroomen, J. (2007). Neural Correlates of Multisensory Integration of Ecologically Valid Audiovisual Events. *J. Cogn. Neurosci*. 19, 1964–1973.

Sterr, A., Müller, M.M., Elbert, T., Rockstroh, B., Pantev, C., and Taub, E. (1998a). Changed perceptions in Braille readers. *Nature* 391, 134–135.

Sterr, A., Müller, M.M., Elbert, T., Rockstroh, B., Pantev, C., and Taub, E. (1998b). Perceptual Correlates of Changes in Cortical Representation of Fingers in Blind Multifinger Braille Readers. *J. Neurosci*. 18, 4417–4423.

Stevens, C., and Neville, H. (2006). Neuroplasticity as a double-edged sword: deaf enhancements and dyslexic deficits in motion processing. *J. Cogn. Neurosci.* 18, 701–714.

Stevenson, R.A., and Wallace, M.T. (2013). Multisensory temporal integration: task and stimulus dependencies. *Exp. Brain Res*. 227, 249–261.

Stevenson, R.A., Siemann, J.K., Schneider, B.C., Eberly, H.E., Woynaroski, T.G., Camarata, S.M., and Wallace, M.T. (2014). Multisensory temporal integration in autism spectrum disorders. *J. Neurosci.* 34, 691–697.

Stone, J.V., Hunkin, N.M., Porrill, J., Wood, R., Keeler, V., Beanland, M., Port, M., and Porter, N.R. (2001). When is now? Perception of simultaneity. *Proc. R. Soc. Lond. B Bio*l. Sci. 268, 31–38.

Sun, W., Zhang, L., Lu, J., Yang, G., Laundrie, E., and Salvi, R. (2008). Noise exposure–induced enhancement of auditory cortex response and changes in gene expression. *Neuroscience* 156, 374–380.

Sun, W., Deng, A., Jayaram, A., and Gibson, B. (2012). Noise exposure enhances auditory cortex responses related to hyperacusis behavior. *Brain Res.* 1485, 108–116.

Syka, J. (1989). “Experimental Models of Sensorineural Hearing Loss — Effects of Noise and Ototoxic Drugs on Hearing.” In *Progress in Sensory Physiology 9*, eds. H. Autrum, E.R. Perl, R.F. Schmidt, H. Shimazu, W.D. Willis, and D. Ottoson, (Springer Berlin Heidelberg), 97–170.

Syka, J. (2002). Plastic Changes in the Central Auditory System After Hearing Loss, Restoration of Function, and During Learning. *Physiol. Rev*. 82, 601–636.

Syka, J., and Rybalko, N. (2000). Threshold shifts and enhancement of cortical evoked responses after noise exposure in rats. *Hear. Res*. 139, 59–68.

Syka, J., Rybalko, N., and Popelář, J. (1994). Enhancement of the auditory cortex evoked responses in awake guinea pigs after noise exposure. *Hear. Res*. 78, 158–168.

Toldi, J., Fehér, O., and Wolff, J.R. (1986). Sensory interactive zones in the rat cerebral cortex. *Neuroscience* 18, 461–465.

Tun, P.A., Williams, V.A., Small, B.J., and Hafter, E.R. (2012). The Effects of Aging on Auditory Processing and Cognition. *Am. J. Audiol*. 21, 344–350.

Turrigiano, G.G. (1999). Homeostatic plasticity in neuronal networks: the more things change, the more they stay the same. *Trends Neurosci*. 22, 221–227.

Tye-Murray, N., Sommers, M., and Spehar, B. (2007). Audiovisual integration and lipreading of older adults with normal and impaired hearing. *Ear Hear*. 28, 656–668.

Vachon, P., Voss, P., Lassonde, M., Leroux, J.-M., Mensour, B., Beaudoin, G., Bourgouin, P., and Lepore, F. (2013). Reorganization of the auditory, visual and multimodal areas in early deaf individuals. *Neuroscience* 245, 50–60.

Vatakis, A., and Spence, C. (2008). Evaluating the influence of the “unity assumption” on the temporal perception of realistic audiovisual stimuli. *Acta Psychol. (Amst.)* 127, 12–23.

Vatakis, A., Bayliss, L., Zampini, M., and Spence, C. (2007). The influence of synchronous audiovisual distractors on audiovisual temporal order judgments. *Percept. Psychophys.* 69, 298–309.

Voss, P., Lassonde, M., Gougoux, F., Fortin, M., Guillemot, J.-P., and Lepore, F. (2004). Early- and Late-Onset Blind Individuals Show Supra-Normal Auditory Abilities in Far-Space. *Curr. Biol.* 14, 1734–1738.

Vroomen, J., and Keetels, M. (2010). Perception of intersensory synchrony: A tutorial review. *Atten. Percept. Psychophys*. 72, 871–884.

Vroomen, J., and Stekelenburg, J.J. (2011). Perception of intersensory synchrony in audiovisual speech: Not that special. *Cognition* 118, 75–83.

Wallace, M.T., and Stevenson, R.A. (2014). The construct of the multisensory temporal binding window and its dysregulation in developmental disabilities. *Neuropsychologia* 64, 105–123.

Wallace, M.T., Ramachandran, R., and Stein, B.E. (2004a). A revised view of sensory cortical parcellation. *Proc. Natl. Acad. Sci.* 101, 2167–2172.

Wallace, M.T., Perrault, T.J., Hairston, W.D., and Stein, B.E. (2004b). Visual Experience Is Necessary for the Development of Multisensory Integration. *J. Neurosci*. 24, 9580–9584.

Wallace, M.T., Carriere, B.N., Perrault, T.J., Vaughan, J.W., and Stein, B.E. (2006). The Development of Cortical Multisensory Integration. *J. Neurosci*. 26, 11844–11849.

Wang, J., Ding, D., and Salvi, R.J. (2002a). Functional reorganization in chinchilla inferior colliculus associated with chronic and acute cochlear damage. *Hear. Res*. 168, 238–249.

Wang, Y., Hirose, K., and Liberman, M.C. (2002b). Dynamics of Noise-Induced Cellular Injury and Repair in the Mouse Cochlea. *J. Assoc. Res. Otolaryngol*. 3, 248–268.

Weeks, R., Horwitz, B., Aziz-Sultan, A., Tian, B., Wessinger, C.M., Cohen, L.G., Hallett, M., and Rauschecker, J.P. (2000). A positron emission tomographic study of auditory localization in the congenitally blind. *J. Neurosci.* 20, 2664–2672.

Whitt, J.L., Petrus, E., and Lee, H.-K. (2014). Experience-dependent homeostatic synaptic plasticity in neocortex. *Neuropharmacology* 78, 45–54.

Willott, J.F., and Lu, S.M. (1982). Noise-induced hearing loss can alter neural coding and increase excitability in the central nervous system. *Science* 216, 1331–1334.

Willott, J.F., Aitkin, L.M., and McFadden, S.L. (1993). Plasticity of auditory cortex associated with sensorineural hearing loss in adult C57BL/6J mice. *J. Comp. Neurol.* 329, 402–411.

Wong, C., Chabot, N., Kok, M.A., and Lomber, S.G. (2015). Amplified somatosensory and visual cortical projections to a core auditory area, the anterior auditory field, following early- and late-onset deafness. *J. Comp. Neurol*. 523, 1925–1947.

Wong, M., Gnanakumaran, V., and Goldreich, D. (2011). Tactile Spatial Acuity Enhancement in Blindness: Evidence for Experience-Dependent Mechanisms. *J. Neurosci*. 31, 7028–7037.

Xu, J., Sun, X., Zhou, X., Zhang, J., and Yu, L. (2014). The cortical distribution of multisensory neurons was modulated by multisensory experience. *Neuroscience* 272, 1–9.

Xu, J., Yu, L., Stanford, T.R., Rowland, B.A., and Stein, B.E. (2015). What does a neuron learn from multisensory experience? *J. Neurophysiol*. 113, 883–889.

Yang, S., Weiner, B.D., Zhang, L.S., Cho, S.-J., and Bao, S. (2011). Homeostatic plasticity drives tinnitus perception in an animal model. *Proc. Natl. Acad. Sci.* 108, 14974–14979.

Zampini, M., Shore, D.I., and Spence, C. (2003). Audiovisual temporal order judgments. *Exp. Brain Res.* 152, 198–210.

Zampini, M., Guest, S., Shore, D.I., and Spence, C. (2005). Audio-visual simultaneity judgments. *Percept. Psychophys.* 67, 531–544.

Chapter 2

2 Crossmodal Plasticity in Auditory, Visual and Multisensory Cortical Areas Following Noise-Induced Hearing Loss in Adulthood [1]

2.1 Introduction

Hearing loss represents a clinically-relevant form of sensory deprivation which can lead to extensive anatomical and physiological changes throughout the central auditory system (for review, see Chan and Yuan, 2015). The consequences of this experience-dependent neuroplasticity are not restricted to how sound is processed, as crossmodal plasticity can also occur, which is characterized by an increased responsiveness of neurons in the central auditory system to visual and/or tactile stimuli. Functional neuroimaging studies in hearing-impaired humans (for review, see Bavelier et al., 2006; Heimler et al., 2014; Pavani and Roder, 2012) and single-unit recordings in animal models (Allman et al., 2009a; Hunt et al., 2006; Meredith et al., 2012; Meredith and Allman, 2012; Meredith and Lomber, 2011) have identified that the nature and extent of cortical crossmodal plasticity depends on the severity of the hearing loss (e.g., profound deafness versus mild hearing impairment) as well as the age at which the deprivation commenced (e.g., congenital/early-onset versus in adulthood) (Lambertz et al., 2005). For example, studies on humans (Auer et al., 2007; Doucet et al., 2006; Finney et al., 2003, 2001; Vachon et al., 2013), mice (Hunt et al., 2006) and cats (Meredith and Lomber, 2011; but see Kral et al., 2003) have revealed that early-onset profound deafness results in sensory replacement, whereby there is an increased recruitment of the deprived auditory cortex for visual and/or tactile processing. Importantly, such crossmodal plasticity has been shown to underlie the behavioural enhancements that occur in the processing of peripheral visual stimuli and visual motion following congenital deafness (Lomber et al., 2010).

---

[1] A version of this chapter is published as:

Schormans, A.L., Typlt, M., Allman, B.L. (2017) Crossmodal plasticity in auditory, visual and multisensory cortical area following noise-induced hearing loss in adulthood. *Hearing Research*. 343, 92-107.

In contrast to profound deafness which fully deprives the brain of auditory cues from the environment, an incomplete lesion of the cochleae spares some degree of residual auditory processing. To date, relatively few studies have investigated cortical crossmodal plasticity in humans with mild-moderate hearing loss (Campbell and Sharma, 2014, 2013; Musacchia et al., 2009), despite being a fairly common occurrence with nearly one in five adults in the USA having a measurable hearing loss (Agrawal et al., 2008; Lin et al., 2011). In ferrets partially-deafened early in life (Meredith and Allman, 2012) or in adulthood (Meredith et al., 2012), single-unit recordings in the core auditory cortex revealed an increased proportion of neurons capable of processing both auditory and non-auditory stimuli (i.e., multisensory neurons). The neural and behavioural consequences of this increase in multisensory convergence are poorly understood; however, it is reasonable to predict that higher-order areas downstream of the core auditory cortex would also be affected by partial hearing loss.

In the present study, we sought to characterize the nature and extent of crossmodal plasticity induced by adult-onset partial hearing loss in higher-order cortical areas that normally integrate audiovisual information. To that end, we used extracellular electrophysiological recordings in anesthetized rats at specific stereotaxic coordinates to consistently and comprehensively map neuronal responses to auditory and visual stimuli in the dorsal auditory cortex (AuD), an area outside of the auditory core, as well as in the neighbouring region of the lateral extrastriate visual cortex (V2L), an area known to contribute to audiovisual processing (Barth et al., 1995; Hirokawa et al., 2008; Toldi et al., 1986; Wallace et al., 2004; Xu et al., 2014). To induce partial hearing loss, adult rats were bilaterally exposed for two hours to a loud broadband noise. Subsequent electrophysiological testing used auditory stimuli well above each rat's hearing threshold as assessed with auditory brainstem responses to control for differences in audibility caused by the noise exposure. Single- and multi-unit activity was recorded in response to auditory, visual and combined audiovisual stimuli in rats two weeks after noise exposure and the results were compared to age-matched controls. Similar to previous studies in the core auditory cortex of partially-deafened animals (Meredith et al., 2012; Meredith and Allman, 2012), we investigated whether noise-induced crossmodal plasticity manifested in the AuD and V2L cortices as an increased responsiveness to non-auditory stimuli, thereby changing

the relative proportion of multisensory versus unisensory neurons. Related to this, we also examined the prevalence and nature of multisensory integration, a hallmark of multisensory processing in which a multisensory neuron's response to one sensory modality is significantly modulated by stimulation in another modality (for review, see Stein and Meredith, 1993), as this property could greatly influence residual auditory processing and perception following partial hearing loss (Meredith et al., 2012).

2.2 Material and Methods

2.2.1 Animals

Fourteen adult male Sprague-Dawley rats (age: 103 ± 3 days; body mass: 425 ± 8 g) were used in this study. All rats were housed in a temperature-controlled room on a 12-hour light-dark cycle with food and water *ad libitum*. All experimental procedures were approved by the University of Western Ontario Animal Use Subcommittee and were in accordance with the guidelines established by the Canadian Council on Animal Care.

2.2.2 Hearing Assessment with an Auditory Brainstem Response

Hearing levels were assessed using an auditory brainstem response (ABR) which was performed in a double-walled sound attenuating chamber. Rats were anesthetized with ketamine (80 mg/kg; IP) and xylazine (5 mg/kg; IP), and subdermal electrodes (27 gauge; Rochester Electro-Medical, Lutz, FL) were positioned at the vertex (active electrode), over the right mastoid process (reference electrode) and on the mid-back (ground). The animal was not secured in a stereotaxic frame during the ABR testing. Body temperature was maintained at ~37°C using a homeothermic heating pad (507220F; Harvard Apparatus, Kent, UK).

Sound stimuli were generated by a Tucker-Davis Technologies (TDT, Alachua, FL) RZ6 processing module at 100 kHz sampling rate and delivered by a magnetic speaker (MF1; TDT) positioned 10 cm from the animal's right ear. The left ear was occluded with a custom foam earplug. Sound stimuli for the ABR, noise exposure procedure and electrophysiological recording experiments were calibrated with custom Matlab software

(The Mathworks, Natick, MA) using a 1/4-inch microphone (2530; Larson Davis, Depew, NY) and preamplifier (2221; Larson Davis).

The auditory evoked activity was collected using a low-impedance headstage (RA4L1; TDT), preamplified and digitized (RA16SD Medusa preamp; TDT), and sent to a RZ6 processing module via a fiber optic cable. The signal was filtered (300-3000 Hz) and averaged using BioSig software (TDT). Auditory stimuli consisted of a click (0.1 ms) and two tones (4 kHz and 20 kHz; 5 ms duration and 1 ms rise/fall time), which were each presented 1000 times (21 times/second) at decreasing intensities from 90 to 10 dB sound pressure level (SPL) in 10 dB SPL steps. Near threshold, successive steps were decreased to 5 dB SPL, and each sound level was presented twice in order to best determine ABR threshold using the criteria of just noticeable deflection of the averaged electrical activity within the 10-ms window (Popelar et al., 2008).

Rats in the control group (n = 7) underwent an ABR to assess their hearing levels, followed immediately by an electrophysiological recording experiment. Rats in the noise exposure group (n = 7) had their baseline hearing tested with an initial ABR, followed by exposure to a loud broadband noise (see below) that induced a permanent hearing loss. Two weeks after the noise exposure, a final ABR was performed, which was followed immediately by the same electrophysiological recording experiment as performed in control rats.

2.2.3 Noise Exposure

While under ketamine (80 mg/kg; IP) and xylazine (5 mg/kg; IP) anesthesia, rats were bilaterally exposed for two hours to a calibrated broadband noise (0.8-20 kHz) at 120 dB SPL. This noise exposure protocol was similar to one used by Popelar et al. (2008) in rats to induce persistent changes in auditory processing at the level of the ABR as well as the auditory cortex. The broadband noise was generated with TDT software and hardware (RPvdsEx; RZ6 module), and delivered by a super tweeter (T90A; Fostex, Tokyo, Japan) which was placed 10 cm in front of the rat. A homeothermic heating pad was used to maintain body temperature at ~37°C.

2.2.4 Surgical Procedure

Immediately following the final hearing assessment, each rat was maintained under ketamine/xylazine anesthesia, the foam earplug was removed from the left ear, and the animal was fixed in a stereotaxic frame with blunt ear bars. Supplemental doses of ketamine/xylazine were administered IM as needed. A midline incision was made in the skin, and the underlying tissue was reflected from the skull. A headpost was fastened to the skull with dental acrylic, and a stainless-steel screw was inserted into the right frontal bone to serve as an anchor for the headpost as well as an electrical ground. A craniotomy (2.5 x 3 mm; 4-7 mm posterior to bregma) was performed in the left parietal bone in order to expose the cortex. At the end of the surgical procedure, the right ear bar was removed to allow free-field auditory stimulation of the right ear during the electrophysiological recordings in the contralateral cortex. The rat remained securely positioned in the stereotaxic frame using the left ear bar and the headpost for the remainder of the experiment.

2.2.5 Electrophysiological Recordings

Extracellular electrophysiological signals were acquired using a 32-channel electrode array which consisted of a single shank with 32 equally-spaced recording sites, spanning 0.75 mm in length (A1x32-Poly2-10mm-50s-177-A32; NeuroNexus Technologies, Ann Arbor, MI). The electrode array was connected to a high-impedance headstage (NN32AC; TDT), and the neuronal activity was preamplified and digitized (two RA16SD Medusa preamps; TDT), and sent to a RZ5 processing module via a fiber optic cable. For each of the 32 channels, the neuronal activity was digitally sampled at 25 kHz and bandpass filtered online at 300-3000 Hz using a voltage threshold for spike detection of three standard deviations above the noise floor. The timing of the detected spikes and their associated waveforms were stored for offline analyses.

For the first of three recording penetrations in each rat, the electrode array was inserted in the cortex through a small slit in the dura using a dorsomedial-to-ventrolateral approach (40° angle), with the electrode array entering the cortex 5 mm caudal to bregma and 1 mm medial to the temporal ridge of the skull (i.e., ~4.6 mm lateral to midline). Using a high-

precision stereotaxic micromanipulator (World Precision Instruments, Sarasota, FL), the electrode array was advanced at the 40° angle until all recording sites were within the cortex (depth of 0.75 mm) based on visual confirmation using a surgical microscope equipped with a high-resolution camera. A hydraulic microdrive (FHC; Bowdoinham, ME) was then used to slowly advance the electrode array into the cortex until the 32 recording sites spanned the distance of 1.25-2.0 mm from the initial entry in the cortex. At this depth and 40° angle of insertion, the recording sites were located in the dorsomedial region of the lateral extrastriate visual cortex (Paxinos and Watson, 2007), an area where the constituent neurons respond predominantly to visual stimuli (V2L-visual zone; Fig. 2.1).

Overall, in each rat, a quantitative audiovisual stimulation paradigm (described below) was performed at nine cortical locations; three successive depths (i.e., 1.25-2.0 mm, 2.0-2.75 mm and 2.75-3.5 mm) along three penetrations located at 5.0, 5.5 and 6.0 mm caudal to bregma. The electrode array was allowed to settle in place for 45 min before conducting the electrophysiological recordings in each location. Based on extensive pilot testing, the above-listed stereotaxic coordinates and dorsomedial-to-ventrolateral approach (40° angle) were selected as these procedures allowed for a consistent and comprehensive mapping of neuronal responses to visual and auditory stimuli in the different zones of the lateral extrastriate visual cortex (V2L-visual zone; V2L-multisensory zone), as well as the dorsal auditory cortex (AuD). The AuD cortex in rats is considered a higher-order auditory area, as it is not one of the five tonotopically-organized fields within the auditory core (i.e., the primary auditory cortex, the posterior auditory field, the anterior auditory field, the ventral auditory field, and the suprarhinal auditory field) described by Polley et al. (2007). Figure 2.1 shows representative examples of recording penetrations from the pial surface. In both groups, the recording penetrations targeted the granular and supragranular cortical layers.

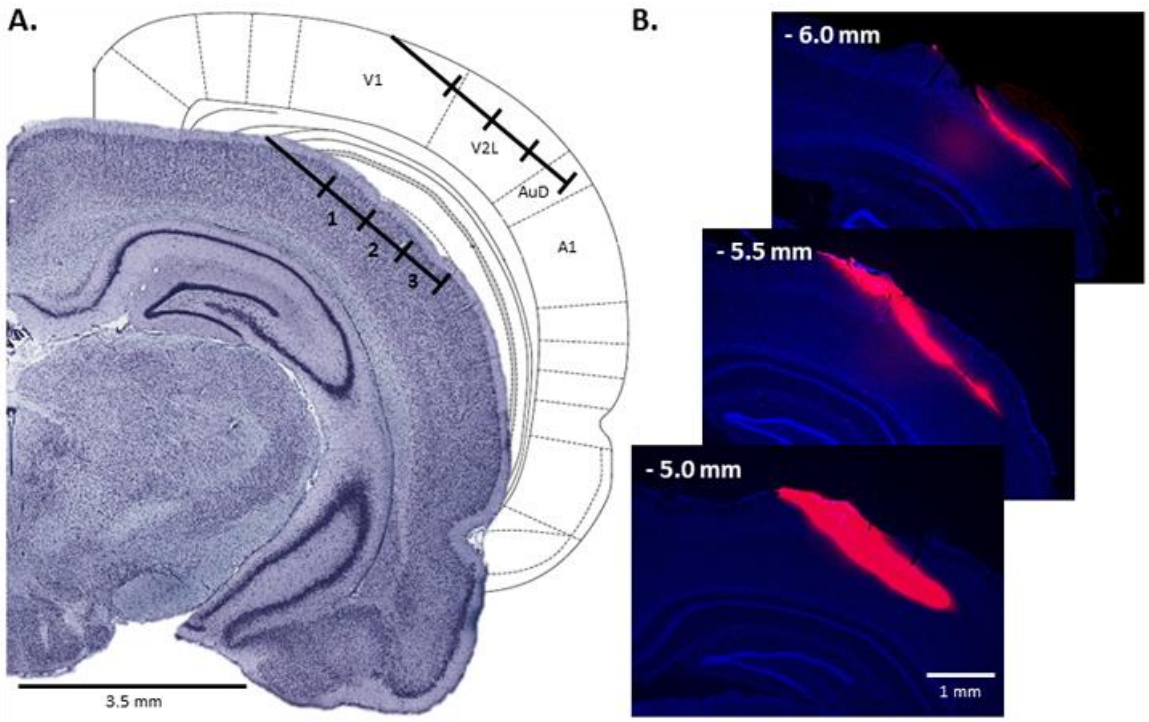

Figure 2.1. Representative recording penetrations in the V2L cortex and AuD cortex in the rat.

Panel A shows a schematic of the location of the three successive recording depths (i.e., 1.25-2.0 mm, 2.0-2.75 mm and 2.75-3.5 mm) from the pial surface when the electrode array was advanced into the cortex at 5.5 mm caudal to bregma using a dorsomedial-to-ventrolateral approach (40° angle). As shown in the coronal sections (Paxinos and Watson, 2007), the electrode array was positioned sequentially throughout the V2L and AuD cortices, typically located within supragranular and granular layers. Within the V2L, there are zones where the neurons are preferentially responsive to visual and/or auditory stimuli (Xu et al., 2014). The predominantly visual area (V2L-visual zone) was targeted at recording depth #1, whereas the recording depth #2 was located in the area responsive to audiovisual stimuli (V2L-multisensory zone). The coronal sections in panel B show the location of the recording penetrations at 5.0, 5.5 and 6.0 mm caudal to bregma in a representative rat. Prior to insertion in the cortex, the electrode array was coated in DiI cell-labeling solution to allow for post-experiment histological reconstruction of the penetrations.

2.2.6 Audiovisual Stimulation Paradigm

At each of the nine recording locations, computer-triggered auditory and visual stimuli were presented alone or in combination using a RZ6 processing module (TDT; 100 kHz sampling rate) and custom Matlab software. Auditory stimuli consisted of noise bursts (1-32 kHz; 50 ms duration) from a magnetic speaker (MF1; TDT) positioned 10 cm above the surface of the stereotaxic frame and 10 cm from the base of the right pinna on a 30° angle from midline in the contralateral space. For each rat, auditory stimuli were presented at two sound levels: 90 dB SPL and 30 dB above the click threshold as determined by the preceding click ABR. In the control group, the sound intensity of the +30 dB Sensation Level (SL) auditory stimulus was 53.6 ± 1.4 dB SPL, whereas it was 65.0 ± 3.6 dB SPL in the noise-exposed group. The visual stimuli consisted of computer-triggered light flashes (11 and 82 lux; 50 ms duration) from an LED positioned adjacent to the speaker. The visual stimuli were presented 40 ms prior to the auditory stimuli during the combined stimulus conditions in order to compensate for differences in modality latencies (Allman et al., 2008a). Each of the auditory (+30 dB SL; 90 dB SPL) and visual (11 lux; 82 lux) stimuli were presented alone or as an audiovisual combination (11 lux & +30 dB SL; 11 lux & 90 dB SPL; 82 lux & +30 dB SL; and 82 lux & 90 dB SPL). A ninth condition was included in which no stimuli were presented to collect spontaneous activity. The nine conditions were presented in random order, separated by an inter-stimulus interval of 3-5 s, and each of the conditions was presented 50 times.

2.2.7 Offline Sorting of Single- and Multi-Units

To isolate single-units, neuronal waveforms were sorted offline using an automated T-distribution Expectation-Maximization algorithm (Plexon Offline Sorter v3, Plexon Inc., Dallas, TX). In accordance with Nicolelis et al. (2003), clusters with a Pseudo-F (PsF) value of less than 30,000 and Davies-Bouldin (DB) value of greater than 0.40 were not considered well isolated, and thus these clusters were combined and classified as multi-unit activity. Furthermore, single-units were identified if they formed a discrete cluster in 2D/3D spaces that were separate from clusters of other units and/or multi-unit activity (Nicolelis et al., 2003). Channels with single-units had mean values of: PsF (2D) = 91,632.3 ± 1835 and a DB (2D) = 0.36 ± 0.002.

2.2.8 Single-Unit Analysis & Neuron Classification

Following classification as a single-unit, the spiking data that were collected during the quantitative audiovisual stimulation paradigm were analyzed using custom scripts in Matlab so that rasters and peri-stimulus time histograms (PSTHs) could be generated in response to the different stimulus conditions. For each single-unit, the average level of spontaneous activity was calculated by first tallying the number of spikes within the 500-ms time window for each of the 50 trials, and then calculating the average spontaneous firing rate per trial over the 50 trials (SpontR; see Fig. 2.2B for representative value). To provide consistency across recording sites and animals, the spiking activity of each single-unit in response to the various stimuli was measured within a 40-ms time window which was time-locked to 90-130 ms from recording onset (narrow grey shading on PSTHs in Fig. 2.2A). The response magnitude of each single-unit was based on the average firing rate per trial, which was determined by tallying the number of spikes within the 40-ms time window for each of the 50 trials, and then calculating the average firing rate per trial over the 50 trials (Hz/trial; see Fig. 2.2B for representative values). Ultimately, each single-unit (neuron) was classified based on its response properties to the auditory, visual and audiovisual stimulus conditions. Consistent with previous studies on various species (Allman et al., 2008a; Allman and Meredith, 2007), to determine if a neuron was indeed responsive to a given stimulus condition, the associated spiking activity (firing rate per trial) over the 50 trials was statistically compared to that of the neuron's spontaneous activity (SpontR) using a paired t-test ($\alpha = 0.05$). In order to be classified as being responsive to a given modality, a neuron needed to show a significantly greater response compared to the spontaneous activity in at least one of the two relevant stimulus conditions (e.g., auditory: +30 dB SL or 90 dB SPL; visual: 11 or 82 lux). Neurons which showed no response to any of the stimulus conditions (i.e., the firing rate per trial computed over the 50 trials of stimulation was not statistically different from the spontaneous activity) were classified as “unresponsive” and were not included in further analysis.

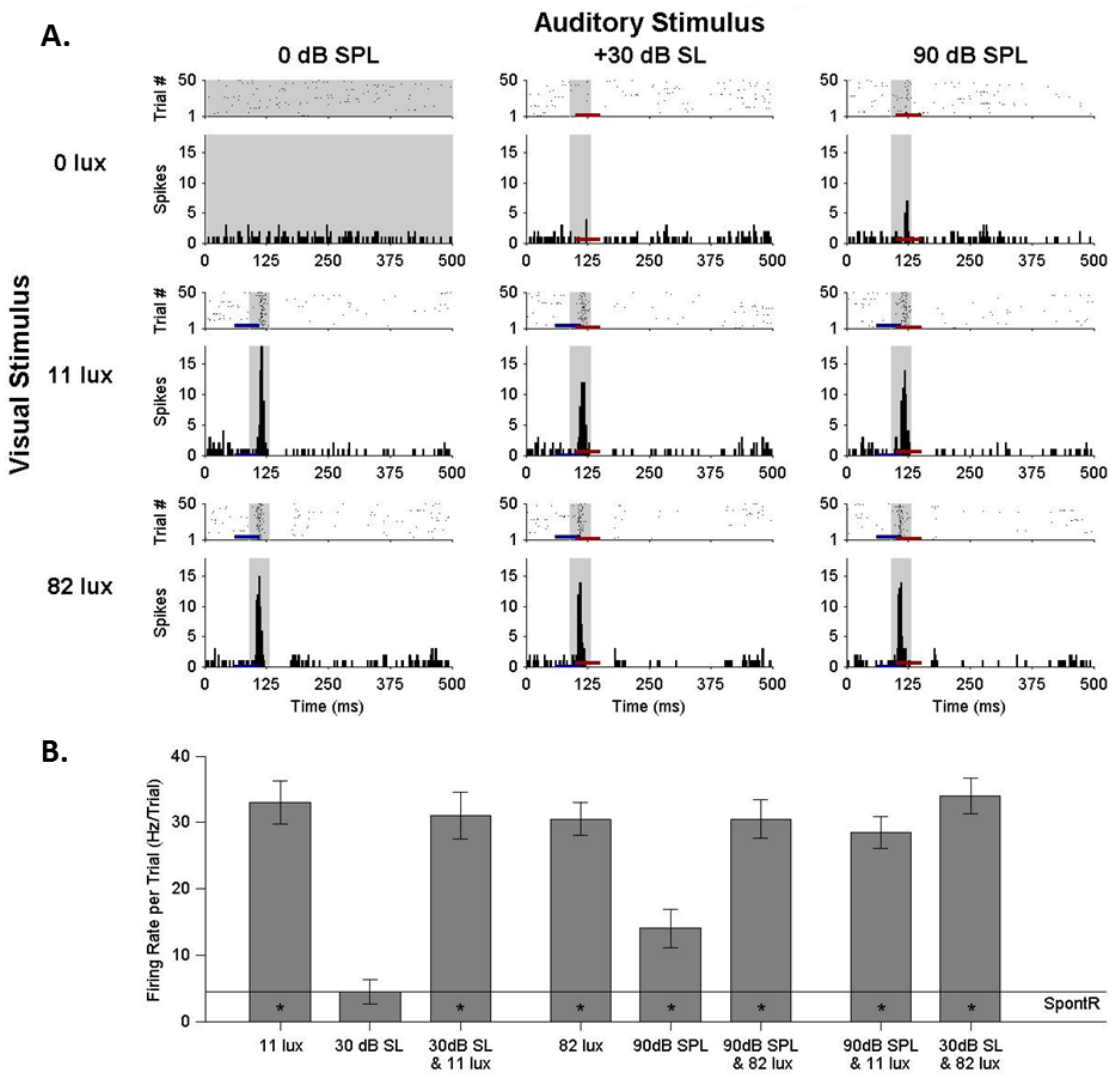

Figure 2.2. Responses of a bimodal neuron in the V2L cortex to auditory, visual and combined audiovisual stimuli.

In panel A, responses to visual stimuli (50 ms LED flash at 11 or 82 lux, denoted by blue horizontal bar), auditory stimuli [50 ms noise burst at 30 dB above sensation level (SL) or 90 dB sound pressure level (SPL), denoted by red horizontal bar], and combined audiovisual stimulation (11 lux & +30 dB SL, located in middle panel; 11 lux & 90 dB SPL; 82 lux & +30 dB SL; and 82 lux & 90 dB SPL, located in the bottom right panel) are shown in the rasters (dot = 1 spike; each row = 1 of the 50 trials) and peri-stimulus time histograms (PSTH; 2.5-ms time bins). For each of the stimulus conditions, the firing rate per trial was calculated within a 40-ms time window which was time-locked to 90-130 ms

from recording onset (narrow grey shading on rasters and PSTHs). Spontaneous activity was determined in the no-stimulus condition (upper left panel). As summarized in the bar graph in panel B (average firing rate per trial ± SEM), the asterisks below the horizontal line (average spontaneous rate of firing per trial; SpontR) denote whether the neuron was responsive to a particular stimulus, as determined by a paired t-test (α = 0.05) that compared the mean firing rate per trial in the given stimulus condition and that of the no-stimulus (spontaneous) condition. Because this representative neuron responded overtly to visual stimuli (11 and 82 lux) as well as an auditory stimulus (90 dB SPL), it was classified as being a bimodal neuron. See Methods for additional details.

Neurons which responded overtly to an auditory stimulus (+30 dB SL and/or 90 dB SPL) as well as a visual (11 and/or 82 lux) stimulus were classified as "bimodal" (see Fig. 2.2 for a representative example). Bimodal neurons were further analyzed to determine if they demonstrated multisensory integration, which was defined as a response to combined audiovisual stimuli that was significantly different (paired t-test, α = 0.05) than that of the most effective single-modality stimulus (Allman et al., 2008a; Allman and Meredith, 2007; Meredith and Stein, 1986; Wallace et al., 2004). Responses to combined stimuli that were significantly greater than the most effective single-modality stimulus were defined as showing response *enhancement* (Fig. 2.3A) whereas those with a significantly reduced response to the combined stimuli were defined as response *depression*.

For each of the neurons that only responded overtly to one of the stimulus modalities, separate comparisons were made to determine whether the combination of the effective modality (e.g., 90 dB SPL) and a seemingly ineffective modality (e.g., 11 or 82 lux) resulted in response facilitation or suppression (Allman et al., 2008a; Allman and Meredith, 2007). Those neurons that only responded overtly to one sensory modality, yet whose response was significantly modulated (paired t-test, α = 0.05) by a stimulus from the other modality were classified as "subthreshold multisensory" neurons (Allman et al., 2009b, 2008b; Allman and Meredith, 2007). "Visual-integrating" neurons were classified as those subthreshold multisensory neurons that only responded overtly to a visual stimulus, yet this

response was facilitated or suppressed when combined with either of the auditory stimuli (+30 dB SL or 90 dB SPL) (Fig. 2.3B). Conversely, "auditory-integrating" neurons only responded overtly to an auditory stimulus, yet they showed a facilitated or suppressed response when this auditory stimulus was combined with a visual stimulus (11 or 82 lux) (Fig. 2.3C). Finally, neurons showing a response to only one of the sensory modalities, and whose response was not significantly modulated by stimuli from the other modality were classified as "unisensory" (Fig. 2.3D).

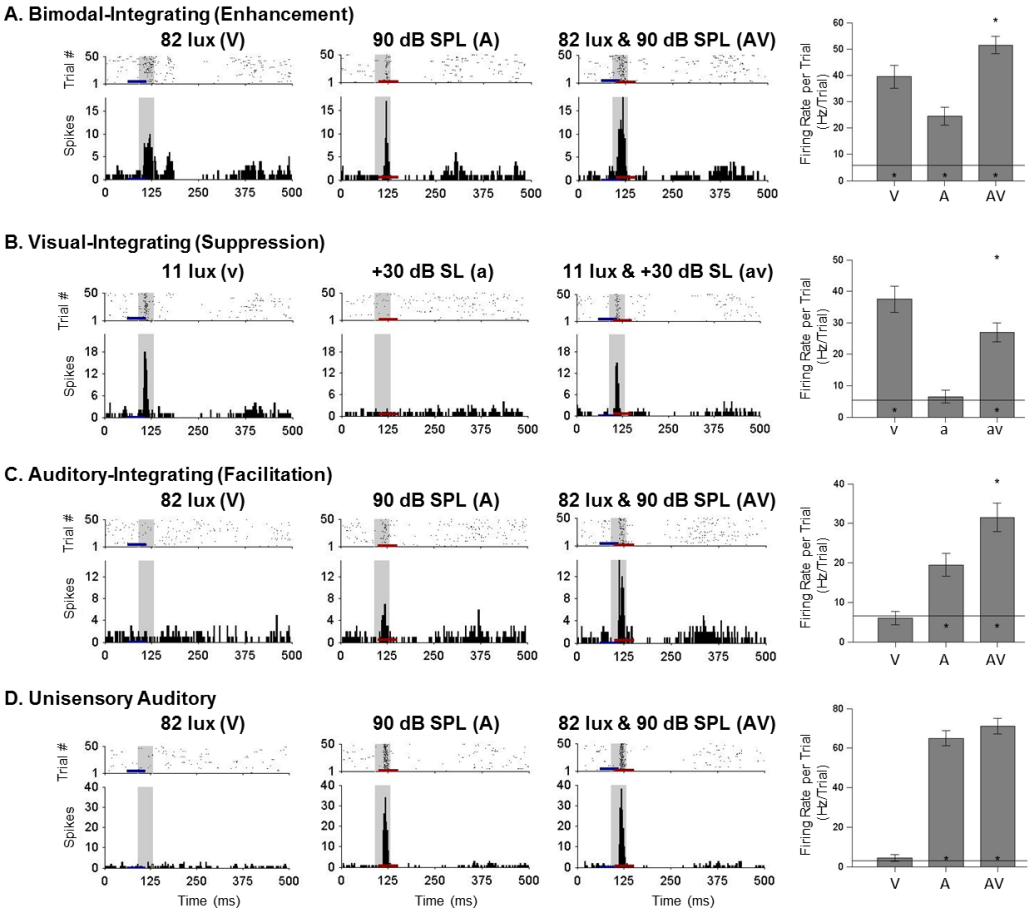

Figure 2.3. Responses of unisensory and multisensory (bimodal and subthreshold) neurons in the V2L cortex and AuD cortex in the rat.

For a representative bimodal, visual-integrating, auditory-integrating and unisensory auditory neuron (panels A-D, respectively), responses to visual (50 ms LED flash denoted by blue horizontal bar), auditory (50 ms noise burst denoted by red horizontal bar) and combined audiovisual stimuli are shown in the rasters (dot = 1 spike; each row = 1 of the

50 trials) and histograms (2.5-ms time bins). The bimodal neuron (panel A) showed overt responses to both the visual and auditory stimuli, as well as a significantly enhanced response in the combined condition. In contrast, the subthreshold multisensory neurons (panels B and C) only responded overtly to a single modality, yet their response was significantly modulated when the effective stimulus was combined with a stimulus from the other modality that failed to elicit a response when presented alone. The visual-integrating neuron (panel B) showed a significantly suppressed response when the visual stimulus was combined with the auditory stimulus, whereas the auditory-integrating neuron (panel C) showed a significantly facilitated response in the combined stimulus condition. For the unisensory auditory neuron (panel D), the auditory stimulus elicited a robust response, whereas the visual stimulus was ineffective. When these same auditory and visual stimuli were combined, the response of this neuron was not significantly changed from the auditory alone condition. In each bar graph (average firing rate per trial ± SEM), the "" appearing near the horizontal line (spontaneous activity) denotes whether a particular stimulus was effective at eliciting an overt response, whereas the "*" above the error bar associated with the combined condition (AV or av) signifies multisensory integration.*

2.2.9 Multi-Unit Analysis & Sensory Responsiveness

Instead of attempting to classify the multi-unit clusters as a particular neuron type like the aforementioned single-units (i.e., unisensory, subthreshold multisensory or bimodal), the spiking activity to the various stimulus conditions was used to describe the overall sensory responsiveness. For each multi-unit cluster, custom scripts in Matlab were used to generate rasters and PSTHs for the stimulus conditions. Similar to the general procedures used on single-units, the average spontaneous activity of the multi-unit cluster was determined (SpontR), as was the firing rate per trial in response to the various stimulus conditions. For a multi-unit cluster to be considered responsive to a given modality, it needed to show a significantly increased firing rate per trial compared to the spontaneous activity as determined with a paired t-test ($\alpha = 0.05$). Figure 2.4 shows representative examples of multi-unit clusters that were broadly categorized as either being responsive to visual (Fig. 2.4A), auditory (Fig. 2.4B) or both visual and auditory stimuli (i.e., multisensory; Fig.

2.4C). No calculations were made regarding multisensory integration in the multi-unit clusters.

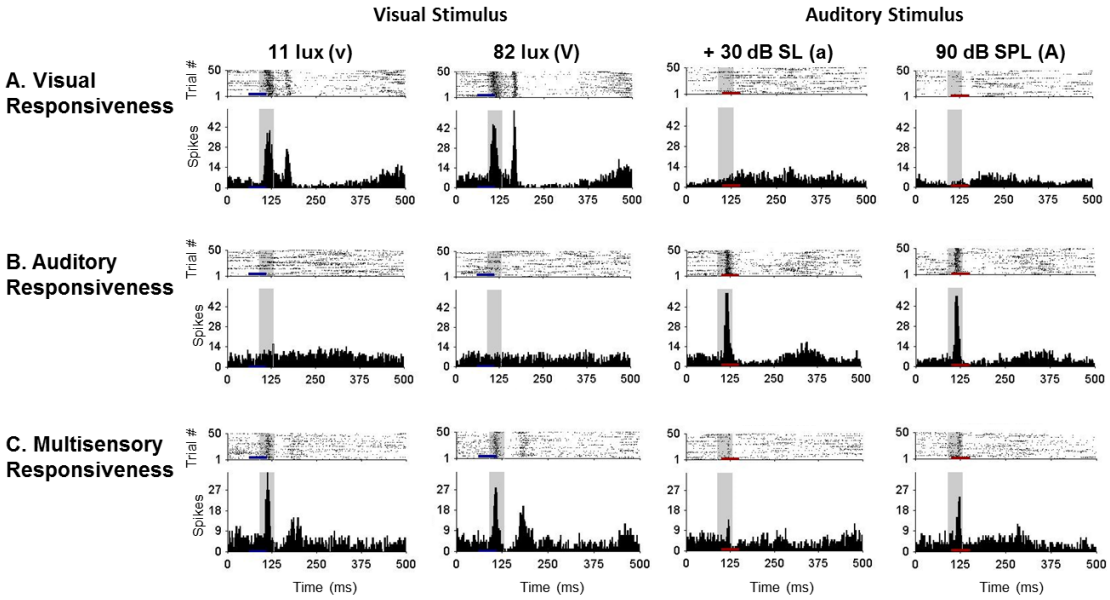

Figure 2.4. Spiking activity of multi-unit clusters to auditory and visual stimuli was used to assess sensory responsiveness.

For representative multi-unit clusters (panels A-C), responses to visual stimuli (50 ms LED flash at 11 or 82 lux, denoted by blue horizontal bar) and auditory stimuli [50 ms noise burst at 30 dB above sensation level (SL) or 90 dB sound pressure level (SPL), denoted by red horizontal bar] are shown in the rasters (dot = 1 spike; each row = 1 of the 50 trials) and histograms (2.5-ms time bins). Representative multi-unit clusters are shown which were categorized as either being responsive to visual (panel A), auditory (panel B) or both visual and auditory stimuli (i.e., multisensory; panel C).

2.2.10 Statistics

Depending on the comparison of interest, a variety of statistical analyses were performed in the present study, including two-way analysis of variance (ANOVA), one-way ANOVA, repeated-measures ANOVA, or paired/unpaired t-tests (see Results section for the details of each specific comparison). The level of statistical significance was set at $\alpha = 0.05$. To

correct for possible ‘family-wise’ error rates when performing multiple comparisons following an ANOVA, the Bonferroni post-hoc test was used (Armstrong, 2014), and the adjusted p-values cited accordingly in the text and Figure legends. SPSS software (version 20, IBM Corporation, Armonk, NY) was used for the various statistical analyses. Matlab and GraphPad Prism (GraphPad Software Inc., La Jolla, CA) were used to plot the data. Throughout the text and figures, data are presented as the mean values ± standard error of the mean (SEM).

2.2.11 Histology

To allow for post-experiment histological reconstruction of the electrode penetrations, the electrode array was coated in DiI cell-labeling solution (V22885; Molecular Probes, Inc., Eugene, OR) prior to insertion in the cortex. At the completion of the electrophysiological experiment, the rat was injected with sodium pentobarbital (100 mg/kg; IP) in preparation for exsanguination via transcardial perfusion of 0.1 M phosphate buffer (PB; 300 ml), followed by 4% paraformaldehyde (400 ml). Next, the brain was removed and post-fixed in paraformaldehyde for 12 hours, followed by storage in 30% sucrose/PB solution for cryoprotection. Using a microtome (HM 430/34; Thermo Scientific, Waltham, MA), frozen sections (50 µm) were cut in the coronal plane and collected serially. The sections were mounted in fluorescent DAPI mounting medium to label DNA (F6057 Fluoroshield™ with DAPI; Sigma, St. Louis, MO), and coverslipped. Sections were imaged with an Axioplan 2 microscope complete with an AxioCam camera (Carl Zeiss Microscopy GmbH, Jena, Germany), and Axiovision Release 4.3 software was used to reconstruct the location and length of the recording penetrations (see Fig. 2.1 for representative images). The average length of the recording penetrations were consistent between the two groups of rats (control 3.45 ± 0.04 mm vs. noise-exposed 3.49 ± 0.03 mm, $p = 0.328$, unpaired t-test); findings which confirm that an equivalent extent of cortical tissue was sampled in the two groups.

2.3 Results

2.3.1 Noise-Induced Hearing Loss

To determine the effect of the noise exposure on hearing sensitivity, the ABR threshold of the 4 kHz, 20 kHz and click stimuli were compared at baseline versus two weeks post-noise in the exposed rats ($n = 7$). A repeated-measures ANOVA with Bonferroni corrected post hoc tests (significant p-value adjusted to $p < 0.017$ to account for multiple comparisons) revealed that the noise exposure caused a significant increase in the ABR threshold of the click (pre-noise 20.7 ± 0.7 dB SPL vs. post-noise 35.0 ± 3.6 dB SPL, $p < 0.017$; Fig. 2.5A), with a trend for an increase in the threshold of the 4 kHz stimulus (pre-noise 22.9 ± 1.0 dB SPL vs. post-noise 39.3 ± 4.6 dB SPL, $p = 0.021$) and 20 kHz stimulus (pre-noise 22.1 ± 1.5 dB SPL vs. post-noise 44.3 ± 8.3 dB SPL, $p = 0.044$). In addition to determining the ABR threshold, the amplitude of the first positive wave of the ABR trace (wave I) in response to the 90 dB SPL click stimulus was used to assess the level of damage to the cochlear hair cell afferents caused by the noise exposure (Kujawa and Liberman, 2009). Compared to baseline, the noise exposure resulted in a 49.6 ± 6.2% reduction of wave I amplitude measured two weeks later (pre-noise 1.5 ± 0.1 mV vs. post-noise 0.7 ± 0.1 mV, $p < 0.001$, paired t-test; Fig. 2.5B), whereas the baseline wave I amplitude in the noise-exposed rats was consistent with that of the controls (1.5 ± 0.1 mV, $p = 0.95$), unpaired t-test; Fig. 2.5B). Furthermore, as revealed with a one-way ANOVA ($F(1,12) = 3.2$, $p = 0.099$) the ABR thresholds did not differ between the control rats and the noise-exposed rats at baseline for the click stimulus (controls 23.6 ± 1.4 dB SPL vs. pre-noise 20.7 ± 0.7 dB SPL), 4 kHz tone (controls 24.0 ± 1.0 dB SPL vs. pre-noise 22.9 ± 1.0 dB SPL) or 20 kHz tone (controls (19.0 ± 1.0 dB SPL vs. pre-noise 22.1 ± 1.5 dB SPL).

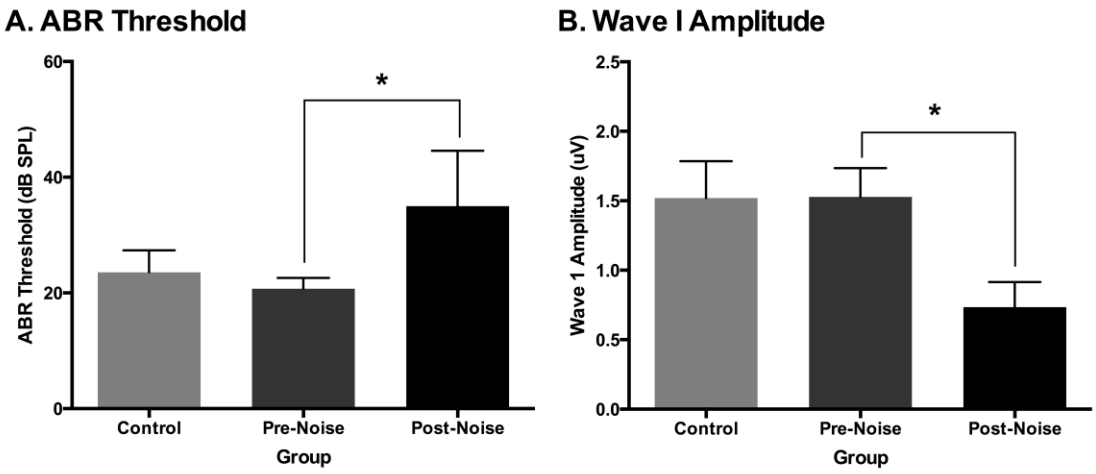

Figure 2.5. Noise-induced hearing loss as assessed with an auditory brainstem response (ABR) to a click stimulus.

ABR threshold (panel A) and the amplitude of the first wave of the evoked response (panel B) to a click stimulus (0.1 ms) were assessed in control rats as well as rats before (pre) and two weeks after (post) exposure to a loud broadband noise (0.8-20 kHz for two hours at 120 dB SPL). At baseline, the ABR click threshold and wave I amplitude did not differ between the control and noise-exposed rats. Compared to their pre-noise values, the rats in the noise exposure group showed a significant increase in their ABR threshold ($p < 0.05$; panel A) and a decrease in their wave I amplitude (*$p < 0.001$; panel B) two weeks post-noise exposure. Values are mean ± SEM for the noise-exposed (n = 7) and control (n = 7) groups.*

2.3.2 Single-Unit Firing Rates & Neuron Classification

All rats included in this study experienced the same protocol for the electrophysiology experiment, which consisted of three recording penetrations, each with three successive recording depths. In control rats (n = 7), a total of 2614 waveform clusters were sorted, with 599 of these clusters being classified as single-units, of which 490 (82%) were found to be responsive to at least one stimulus modality. Similarly, 727 single-units were isolated in the noise-exposed rats (n = 7) from a total of 2721 waveform clusters, and 594 (82%) showed sensory responsiveness.

For control and noise-exposed rats, the relative proportion of the different classes of single neurons (i.e., unisensory, subthreshold multisensory and bimodal) were used to generate overall response profiles in each of the three cortical areas targeted along the recording penetrations: (1) the predominantly visual area, V2L-visual zone (1.25-2.0 mm); (2) the audiovisual area, V2L-multisensory zone (2.0-2.75 mm); and (3) the predominantly auditory area, AuD (2.75-3.5 mm). To that end, for each rat, the proportion of the various neuron types was calculated in each cortical area by first collapsing the findings across the three rostral-caudal penetrations (e.g., results for the V2L-visual zone were collapsed across 5.0, 5.5 and 6.0 mm caudal to bregma to generate a single measure of the proportion of neuron types found at 1.25-2.0 mm depth). Next, the group average response profile in each cortical area was determined to allow comparison between the control ($n = 7$) and noise-exposed rats ($n = 7$). A repeated-measures ANOVA was performed to investigate possible main effects and interactions between groups (controls; noise-exposed), neuron classification (visual; visual-integrating; bimodal, which consisted of both integrating and non-integrating subtypes; auditory-integrating; auditory) and cortical area (V2L-visual zone; V2L-multisensory zone; AuD). Because a significant interaction was found between neuron classification by group by cortical area ($F[8,96] = 3.8$, $p < 0.001$), additional statistical analyses (described below) were completed separately for the three cortical areas.

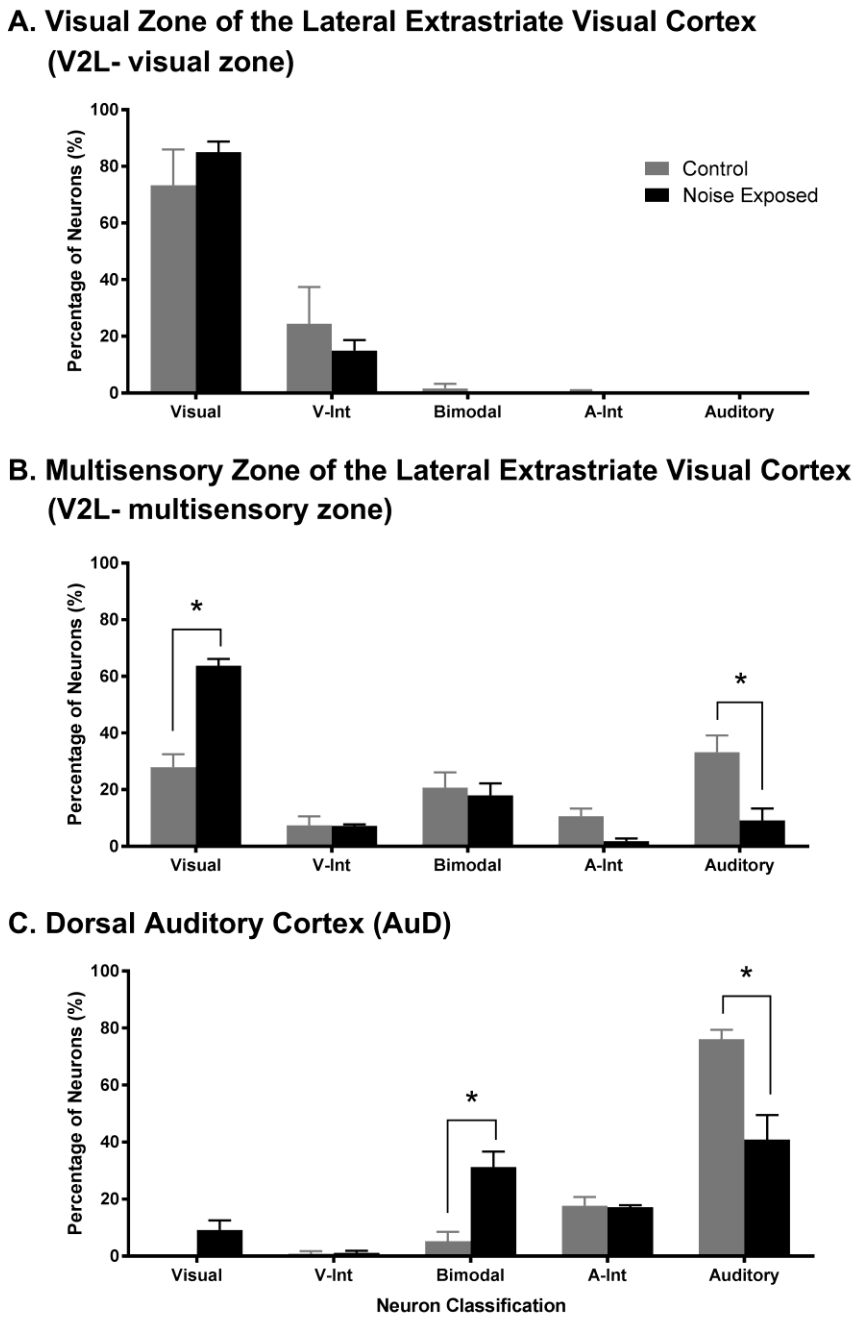

Figure 2.6. The proportion of unisensory and multisensory (bimodal and subthreshold) neurons in the V2L cortex and AuD cortex in normal hearing and noise-exposed rats.

Noise exposure had no effect on the proportion of neuron classes sampled in the predominantly visual area of the dorsomedial aspect of the lateral extrastriate visual

*cortex (V2L-visual zone; panel A). Conversely, in the audiovisual area of the V2L cortex (V2L-multisensory zone; panel B) as well as the AuD cortex (panel C), there was an increase in the proportion of unisensory visual neurons in noise-exposed rats compared to controls, and a concomitant decrease in neurons that only responded to auditory stimuli. Finally, compared to controls, noise-exposed rats showed a significant increase in the proportion of bimodal neurons in the AuD cortex (panel C). In panels A-C, the neuron classification of "bimodal" refers to the total proportion of neurons found which overtly responded to both auditory and visual stimuli, regardless of whether or not multisensory integration was observed. Values are mean ± SEM for the noise-exposed (n = 7) and control (n = 7) groups. Statistical comparisons based on repeated-measures ANOVAs and Bonferroni corrected post-hoc tests in which significant p-value adjusted to *p < 0.01 to account for the multiple comparisons.*

In the predominantly visual area, V2L-visual zone, noise exposure did not cause a change in the proportion of visual or multisensory neurons, as a repeated-measures ANOVA revealed that there was no interaction between group and neuron classification ($F[4,48] = 0.7$, $p = 0.632$). In both groups, the vast majority of neurons solely responded to visual stimulation (i.e., unisensory visual neurons: controls 73.4 ± 12.6% vs. noise-exposed 85.0 ± 3.7%, $p = 0.39$), with a smaller proportion of neurons demonstrating that their response to a visual stimulus was modulated by an auditory stimulus that was ineffective when presented alone (i.e., visual-integrating neurons: controls 24.5 ± 12.9% vs. noise-exposed 15.0 ± 3.7%, $p = 0.49$) (Fig. 2.6A). Despite a lack of sensory reorganization in the V2L-visual zone, the noise exposure did, however, cause a significant reduction in the maximum firing rate per trial of the unisensory visual neurons (controls 48.9 ± 3.3 Hz/trial vs. noise-exposed 34.7 ± 1.5 Hz/trial, $p < 0.001$, unpaired t-test; Fig. 2.7A left panel) and a similar trend for the visual-integrating neurons (controls 50.6 ± 11.2 Hz/trial vs. noise-exposed 31.5 ± 4.9 Hz/trial, $p = 0.09$, unpaired t-test; Fig. 2.7A right panel). Finally, in both control and noise-exposed rats, a nearly equal proportion of visual-integrating neurons showed response facilitation (controls 53.3%; noise-exposed 52.4%) when the effective visual

stimulus was combined with an auditory stimulus that failed to elicit an overt response when presented alone (Fig. 2.8A).

Unlike in the V2L-visual zone (described above), the proportion of neuron classes found in the audiovisual area of the lateral extrastriate visual cortex (V2L-multisensory zone) was affected by the noise exposure, as a repeated-measures ANOVA revealed a significant interaction between group and neuron classification ($F[4,48] = 28.3$, $p < 0.001$; Bonferroni-corrected post hoc tests were then used with significant p-value adjusted to $p < 0.01$ to account for multiple comparisons). Compared to control rats, the noise-exposed rats showed a significant increase in the proportion of unisensory visual neurons (controls 27.9 ± 4.5% vs. noise-exposed 63.7 ± 2.5%, $p < 0.001$). At the same time, there were significantly fewer neurons that were solely responsive to auditory stimuli (unisensory auditory: controls 33.2 ± 5.9% vs. noise-exposed 9.1 ± 4.2%, $p < 0.01$; Fig. 2.6B). This decrease in the proportion of unisensory auditory neurons was not likely due to the acoustic stimuli failing to be loud enough to elicit responses, given that both the absolute (90 dB SPL) and relative sound intensities (+30 dB SL; 65.0 ± 3.6 dB SPL) well-exceeded each noise-exposed rat's hearing threshold (e.g., click threshold was 35.0 ± 3.6 dB SPL following noise exposure). Despite the sensory reorganization that occurred in the V2L-multisensory zone, the maximum firing rates per trial did not differ between the control and noise-exposed rats for the unisensory visual neurons (control 40.1 ± 3.7 Hz/trial vs. noise-exposed 42.5 ± 2.7 Hz/trial, $p = 0.61$, unpaired t-test) or unisensory auditory neurons (control 33.0 ± 3.3 Hz/trial vs. noise-exposed 25.3 ± 4.6 Hz/trial, $p = 0.36$, unpaired t-test) (Fig. 2.7B left panel). Furthermore, noise exposure did not cause a change in the maximum firing rates per trial of visual-integrating neurons (control 36.6 ± 3.8 Hz/trial vs. noise-exposed 42.9 ± 4.9 Hz/trial, $p = 0.42$, unpaired t-test), auditory-integrating neurons (control 44.2 ± 6.5 Hz/trial vs. noise-exposed 32.9 ± 5.3 Hz/trial, $p = 0.38$, unpaired t-test) or bimodal neurons (control 50.0 ± 4.4 Hz/trial vs. noise-exposed 57.1 ± 5.0 Hz/trial, $p = 0.29$, unpaired t-test) (Fig. 2.7B right panel). Finally, noise exposure differentially affected the nature of multisensory integration observed in the various neuron classes sampled in the V2L-multisensory zone; visual-integrating and bimodal-integrating neurons were generally unaffected by the noise exposure, whereas the majority of auditory-integrating neurons transitioned from facilitation in controls (82.4%) to suppression in the noise-

exposed rats (100%) when the effective auditory stimulus was paired with a visual stimulus (Fig. 2.8B).

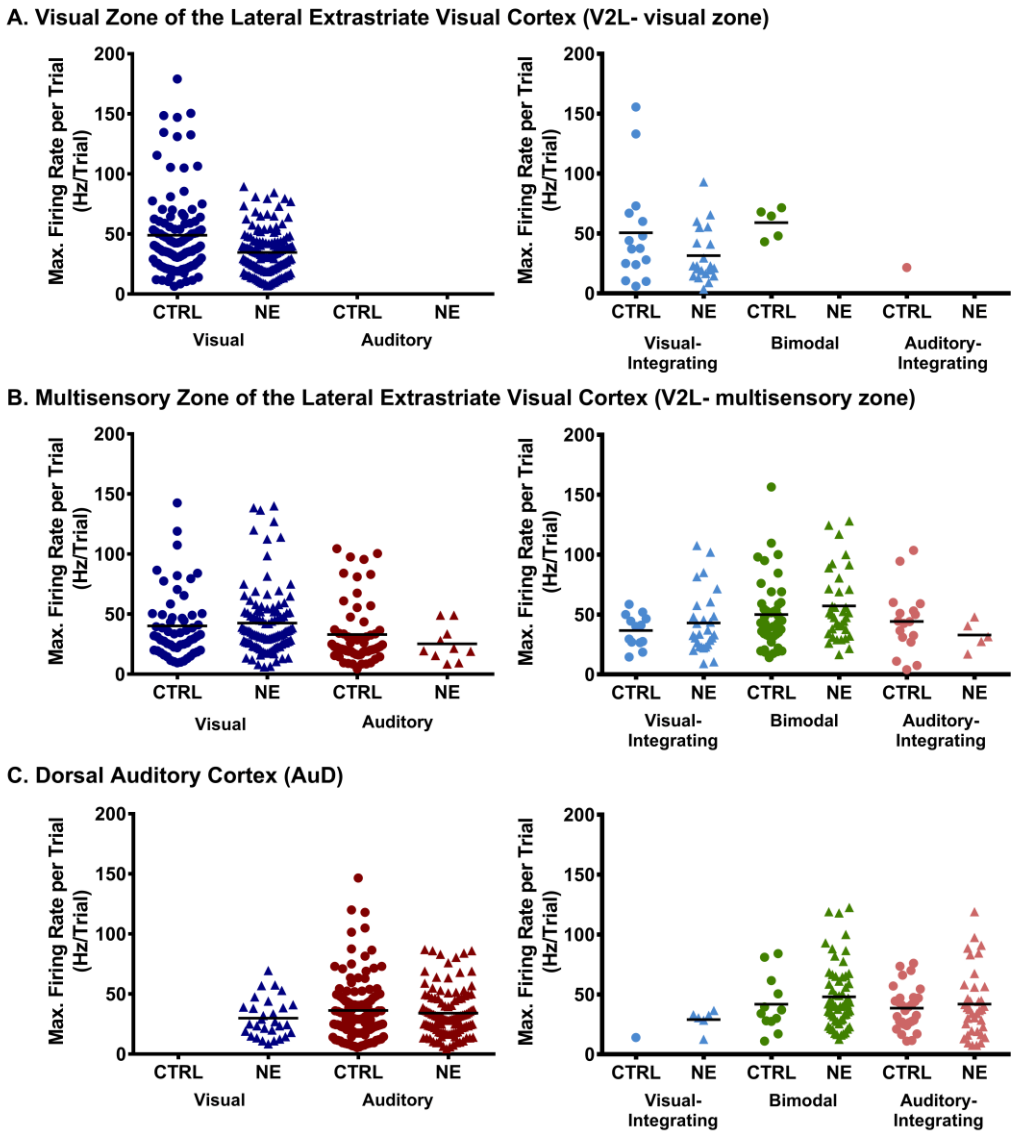

Figure 2.7. Maximum firing rates per trial of unisensory and multisensory (bimodal and subthreshold) neurons in the V2L cortex and AuD cortex of normal hearing and noise-exposed rats.

As shown in panel A, the maximum firing rates per trial of unisensory visual neurons (dark blue data points) were significantly greater in control (CTRL) versus noise-exposed (NE) rats in the dorsomedial aspect of the lateral extrastriate visual cortex (V2L-visual zone)

(control 48.9 ± 3.3 Hz/trial vs. noise-exposed 34.7 ± 1.5 Hz/trial, $p < 0.05$, unpaired t-test), and there was a similar trend for the visual-integrating neurons (pale blue data points: controls 50.6 ± 11.2 Hz/trial vs. noise-exposed 31.5 ± 4.9 Hz/trial, $p = 0.09$, unpaired t-test). In contrast, within the multisensory zone of the lateral extrastriate visual cortex (V2L-multisensory zone; panel B) as well as the AuD cortex (panel C), noise exposure did not affect the maximum firing rates of the unisensory or multisensory neurons. However, an increase in the number unisensory visual neurons was evident in the AuD cortex of the noise-exposed rats (panel C). In panels A-C, the neuron classification of "bimodal" refers to the total proportion of neurons found which overtly responded to both auditory and visual stimuli, regardless of whether or not multisensory integration was observed. In each plot, the mean maximum firing rate per trial is denoted by a black horizontal bar.

Noise exposure altered the proportion of neuron classes in the AuD cortex. A repeated-measures ANOVA with Bonferroni-corrected post hoc tests (significant p-value adjusted to $p < 0.01$ to account for multiple comparisons) revealed a considerable reduction in unisensory auditory neurons (controls 76.1 ± 3.3% vs. noise-exposed 40.9 ± 8.6%, $p < 0.01$), as well as a significant increase in the proportion of bimodal neurons (controls 5.3 ± 3.2% vs. noise- exposed 31.3 ± 5.4%, $p < 0.01$; Fig. 2.6C). Consistent with the findings in the V2L-multisensory zone (described above), noise exposure did not significantly affect the maximum firing rate per trial of unisensory auditory neurons (control 36.3 ± 2.2 Hz/trial vs. noise-exposed 34.0 ± 1.9 Hz/trial, $p = 0.43$, unpaired t-test), auditory-integrating neurons (control 38.5 ± 3.2 Hz/trial vs. noise-exposed 41.9 ± 4.6 Hz/trial, $p = 0.57$, unpaired t-test) or bimodal neurons (control 41.8 ± 6.7 Hz/trial vs. noise-exposed 48.0 ± 3.4 Hz/trial, $p = 0.45$, unpaired t-test) in the AuD cortex (Fig. 2.7C), despite the extensive sensory reorganization. Finally, of the bimodal neurons showing multisensory integration in the AuD cortex of noise-exposed rats, the vast majority (92.3%) demonstrated facilitation, in which the combination of auditory and visual stimuli elicited a response that was significantly greater than that of the most effective unisensory stimulus (Fig. 2.8C right panel).

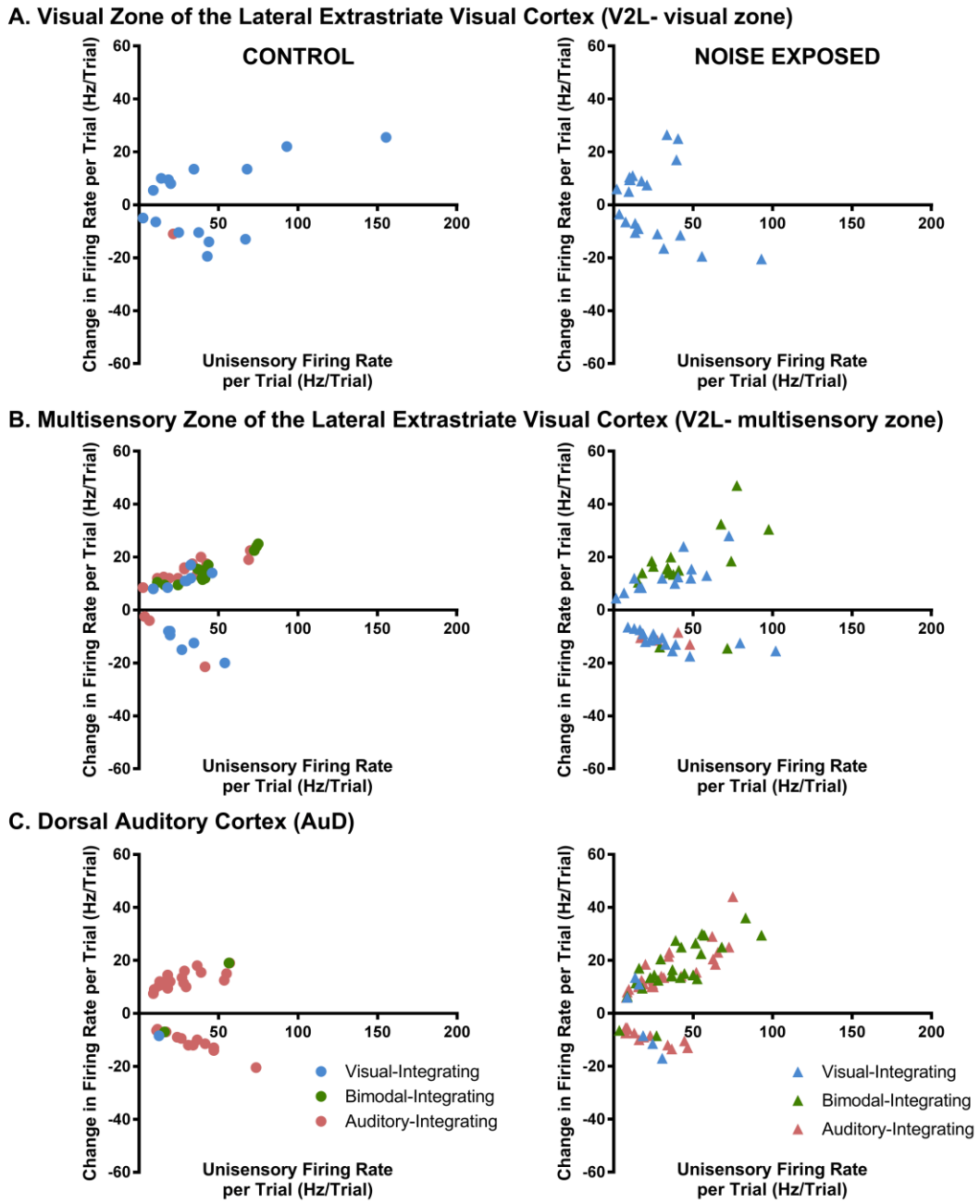

Figure 2.8. The effect of noise exposure on multisensory integration in bimodal-integrating and subthreshold multisensory neurons in the V2L cortex and AuD cortex.

For each neuron that was confirmed to exhibit multisensory integration (see Methods for details), its firing rate in the combined audiovisual stimuli condition was subtracted from its maximum firing rate elicited from the most effective unisensory stimulus. This change

in firing rate was plotted with respect to the unisensory firing rate, whereby values plotted above and below zero represent neurons that demonstrated response facilitation and suppression, respectively. The nature of multisensory integration was largely unaffected by noise exposure; however, in the AuD cortex of the noise-exposed rats (panel C), there was an increase in the number of bimodal-integrating neurons that demonstrated response facilitation during the combined presentation of the audiovisual stimuli (i.e., green triangles).

2.3.3 Multi-Unit Activity & Sensory Responsiveness

Of the total of 2015 waveform clusters sorted as multi-units in control rats, 2002 were found to be responsive to at least one stimulus modality. In the noise-exposed rats, a total of 2016 multi-units were sorted, of which 1994 showed sensory responsiveness. Separate from the aforementioned classification of single-units as either unisensory, subthreshold multisensory or bimodal, the sensory responsiveness of every single-unit and multi-unit cluster was determined for each rat, whereby the clusters were broadly categorized as either being responsive to auditory, visual or both auditory and visual stimuli (i.e., multisensory; see Fig. 2.4 for representative examples). After collapsing across the three rostral-caudal penetrations, the proportion of these three response types was calculated for each rat at every successive 0.25 mm along the recording penetrations from 1.25 to 3.5 mm, and the group averages were calculated for the control ($n = 7$) and noise-exposed rats ($n = 7$). Repeated-measures ANOVAs revealed a group by depth interaction for visual responsiveness ($F[8,108] = 8.3$, $p < 0.001$), auditory responsiveness ($F[8,108] = 11.0$, $p < 0.001$) and multisensory responsiveness ($F[8,108] = 7.8$, $p < 0.001$). As shown in Fig. 2.9, noise exposure caused approximately a 0.5 mm ventral shift in the overall mapping of sensory responsiveness spanning from the dorsomedial aspect of the V2L cortex to the AuD cortex. For example, approximately 50% of the single- and multi-unit clusters were responsive to both auditory and visual stimuli (i.e., multisensory) at 2.5 and 3.0 mm along the recording depth in the control and noise-exposed rats, respectively (Fig. 2.9B). Moreover, when the sensory responsiveness in noise-exposed rats was compared to control rats at 2.5 and 2.75 mm along the recording depth, there was a rightward (ventral) shift in

the curves that was indicative of an expansion of visual responsiveness (Fig. 2.9A) as well as a concomitant recession in auditory responsiveness (Fig. 2.9C) in the noise-exposed rats. Again, this reduced auditory responsiveness was not likely due to insufficient acoustic stimulation, as the sound intensity of the noise bursts were adjusted to be well-above each rat's hearing threshold.

2.4 Discussion

To our knowledge, the present study represents the first single-unit unit investigation into the effect of adult-onset partial hearing loss on crossmodal plasticity in higher-order cortical regions normally capable of integrating audiovisual information. Using extracellular electrophysiological techniques, neuronal activity was recorded under anesthesia from the dorsal auditory cortex (AuD) and lateral extrastriate visual cortex (V2L) of noise-exposed rats two weeks post-exposure, and the results compared to that of age-matched controls. Because the loudness of the auditory stimuli was adjusted to be +30 dB SPL above each rat's hearing threshold and a consistent stereotaxic approach was used in all animals, it was possible to map the overall effectiveness of the auditory and visual stimuli to elicit responses at locations spanning the neighbouring cortical areas in the noise-exposed rats versus controls. To summarize, we found that the cortical area showing the greatest relative degree of multisensory convergence transitioned ventrally, away from the audiovisual area, V2L, toward the predominantly auditory area, AuD, following partial hearing loss. Overall, the collective findings of the present study support the suggestion that crossmodal plasticity induced by adult-onset hearing impairment manifests in higher-order cortical areas as a transition in the functional border of the audiovisual cortex.

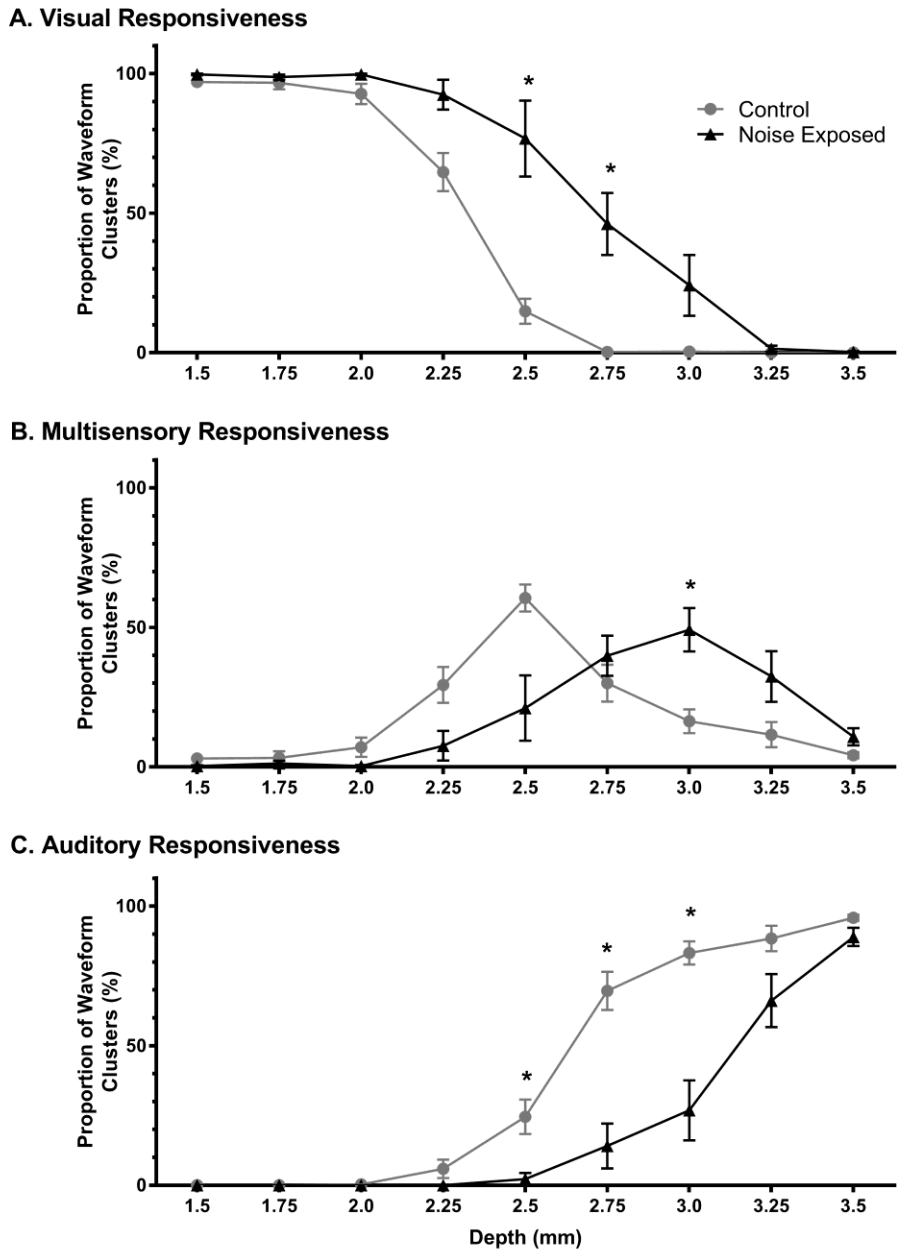

Figure 2.9. Sensory responsiveness in the V2L cortex and AuD cortex of normal hearing and noise-exposed rats.

Panels A-C, respectively, plot the group mean (±SEM) proportion of visual, multisensory and auditory responsive single- and multi-unit clusters across the V2L and AuD cortices in the control (n = 7) versus noise-exposed rats (n = 7). Consistent between the control (grey circles) and noise-exposed rats (black triangles), the neurons sampled more shallow in the penetration (e.g., 1.5 mm depth) showed a preferential responsiveness to visual

*stimuli, whereas deeper in the penetration (e.g., ~2.75 mm depth) the neurons were responsive to both visual and auditory stimulation, and finally at the deepest location (e.g., 3.5 mm depth) the neurons were preferentially responsive to auditory stimuli. Ultimately, noise exposure caused neurons throughout the penetration to be more responsive to visual stimulation and less responsive to auditory stimulation, resulting in approximately a 0.5 mm ventral shift in the overall mapping of sensory responsiveness across the V2L and AuD cortices. Statistical comparisons based on repeated-measures ANOVA and Bonferroni post-hoc tests in which significant p-value adjusted to *p < 0.0056 to account for the multiple comparisons.*

2.4.1 Audiovisual Processing in the Lateral Extrastriate Visual Cortex (V2L)

The V2L-multisensory zone of control rats contained a nearly equivalent proportion of unisensory visual, unisensory auditory and multisensory neurons (i.e., bimodal, visual-integrating and auditory-integrating neurons) (Fig. 2.6B); findings which further confirm that this region of the rat V2L cortex is capable of integrating audiovisual stimuli (Barth et al.,1995; Hirokawa et al., 2008; Toldi et al., 1986; Wallace et al., 2004; Xu et al., 2014). Moreover, consistent with previous reports (Wallace et al., 2004; Xu et al., 2014), the areal boundary of this audiovisual region spanned less than 1 mm in the dorsal-ventral direction (Figs. 2.9 and 2.10), and the majority of the constituent multisensory neurons showed an enhanced response when the auditory and visual stimuli were combined compared to that elicited by either stimulus presented alone (Fig. 2.8). Outside of this boundary, in the areas flanking the V2L-multisensory zone (i.e., V2L-visual zone, and AuD; see Fig. 2.1), the proportion of bimodal neurons dropped off considerably, whereas subthreshold multisensory neurons (i.e., visual-integrating and auditory-integrating) now constituted ~20% of the neurons sampled (Fig. 2.6). This transition in the classes of multisensory neurons encountered across the audiovisual cortex in the rat is similar to findings in the posterolateral lateral suprasylvian (PLLS) portion of the cat extrastriate visual cortex (Allman and Meredith, 2007).

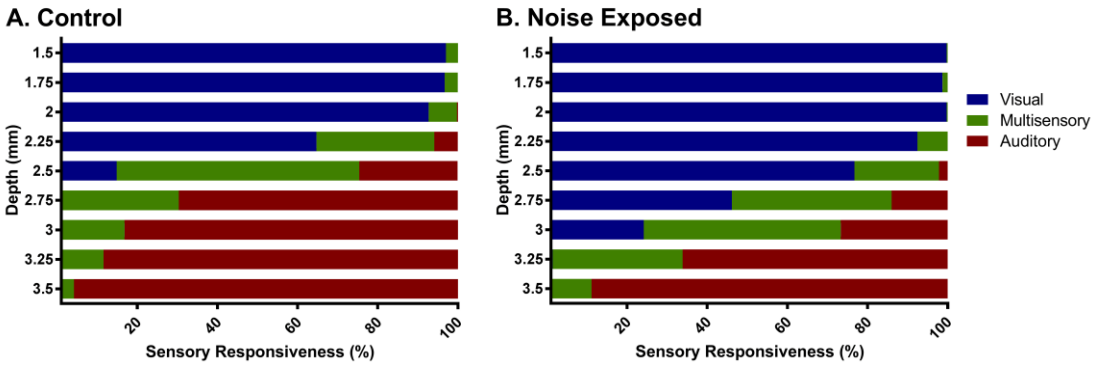

Figure 2.10. Ventral shift of sensory responsiveness across the V2L cortex and AuD cortex in noise-exposed rats.

For each rat, every single- and multi-unit cluster that was sorted was broadly categorized as being responsive to visual (blue), auditory (red) or both visual and auditory (i.e., multisensory; green) stimuli, and the proportion of these three response types was calculated at every successive 0.25 mm along the recording penetrations from 1.25 to 3.5 mm. For the control (n = 7) and noise-exposed rats (n = 7), a composite map was made of the mean proportion of response categories across the V2L and AuD cortices. Note, these composite maps present the same data included in Fig. 2.9; however, for each group, the visual, auditory and multisensory responsiveness results are collapsed into a single row instead of being partitioned into three separate graphs (i.e., panels A-C in Fig. 2.9). Compared to control rats (left panel), the noise-exposed rats showed a ventral expansion of visual responsiveness as well as a concomitant recession in auditory responsiveness across the V2L and AuD cortices; findings suggestive of a transition in the functional border of the audiovisual cortex.

2.4.2 Noise-Induced Crossmodal Plasticity

To date, the majority of studies on crossmodal plasticity following hearing loss have used congenitally deaf animals or ototoxic lesions in normal-hearing animals. In the present study, we used excessive exposure to loud noise to cause a predictable level of permanent hearing loss in adult rats, and investigated the nature and extent of cortical crossmodal

plasticity. Noise-induced hearing loss can result from a variety of cochlear pathologies, including mechanical damage to hair cell stereocilia, hair cell death caused by increased oxidative stress, as well as the loss of afferent nerve terminals in the cochlea and subsequent degeneration of the cochlear nerve (Henderson et al., 2006; Kujawa and Liberman, 2009; Rüttiger et al., 2013). Indeed, in the present study, we observed a 49.6% reduction in the wave I amplitude of the ABR in response to the suprathreshold 90 dB SPL click stimulus, which is indicative of damage to the auditory nerve fibers (Furman et al., 2013).

In both the V2L-multisensory zone and AuD cortices of noise-exposed rats, there was a relative increase in the proportion of neurons responsive to visual stimuli, and a concomitant decrease in neurons that were solely responsive to auditory stimuli despite accounting for each rat's hearing loss (Fig. 2.6B and 2.6C). The V2L-multisensory zone and AuD cortices differed, however, in how noise-induced hearing loss affected audiovisual processing; the total proportion of multisensory neurons (i.e., those classified as visual-integrating, auditory-integrating or bimodal) significantly decreased in the V2L-multisensory zone (control 38.8 ± 3.3% vs. noise-exposed 27.1 ± 3.4%, $p < 0.05$, unpaired t-test; Fig. 2.6B), yet dramatically increased in the AuD cortex (control 23.9 ± 3.3% vs. noise-exposed 49.8 ± 6.1%, $p < 0.01$, unpaired t-test; Fig. 2.6C). This doubling of the proportion of multisensory neurons in AuD was similar to the effect of crossmodal plasticity in the core auditory cortex of partially-deafened ferrets (Meredith et al., 2012). More specifically, both the core auditory cortex (Meredith et al., 2012) and AuD cortex (present study) of hearing-impaired animals experienced a dramatic increase in the proportion of bimodal neurons that overtly responded to both auditory and visual stimuli following adult-onset partial hearing loss, whereas the proportion of subthreshold multisensory neurons remained relatively unchanged (Fig. 2.6C). Recent studies using high-density EEG on adult humans with mild-moderate hearing loss also found decreased activation of the auditory cortex in response to auditory stimuli (Campbell and Sharma, 2013) as well as increased responsiveness to visual stimuli (Campbell and Sharma, 2014). Taken together, these studies on hearing-impaired humans and animal models confirm that partial hearing loss in adulthood is sufficient to induce crossmodal plasticity in the core- and higher-order auditory cortices.

2.4.3 Multisensory Integration Following Noise Exposure

Given the considerable increase in the proportion of neurons responsive to both auditory and visual stimuli in the AuD cortex of noise-exposed rats (Fig. 2.6C), it is important to also consider the nature and incidence of multisensory integration, as the combined presentation of two effective stimulus modalities can result in dramatic enhancement or depression of neural responses (Meredith and Stein, 1986). Over one third (42.6%) of the bimodal neurons in the reorganized AuD cortex of noise-exposed rats exhibited multisensory integration (up from 16.7% in controls), with the vast majority (92.3%) showing an enhanced response when the auditory and visual stimuli were presented in combination (Fig. 2.8C right panel). Within the V2L-multisensory zone, other than a trend for a decrease in the proportion of auditory-integrating neurons (Fig. 2.6B), the nature and extent of multisensory processing was mostly unaffected by partial hearing loss, as the maximal firing rates (Fig. 2.7B) and properties of multisensory integration (Fig. 2.8B) did not differ substantially between the noise-exposed rats and controls.

2.4.4 Transition of the Functional Border of the Audiovisual Cortex

In considering the seemingly differential effects observed in the V2L and AuD cortices following noise exposure, we further examined whether there was a progressive transition of sensory responsiveness across these neighbouring regions following partial hearing loss (Fig. 2.10). Because the orientation of the recording penetrations allowed for a systematic comparison between the groups, it was possible to observe a ventral shift in sensory responsiveness of approximately 0.5 mm in the noise-exposed rats (Fig. 2.9). For example, as shown in Fig. 2.9B, a nearly equivalent level of multisensory responsiveness (~50%) was found in the more ventrally-positioned AuD cortex (at 3.0 mm) in the noise-exposed rats as in the V2L cortex (at 2.5 mm) of controls. We suggest that this shift in sensory responsiveness represents a form of crossmodal plasticity, which is indicative of a transition of the functional border of the audiovisual cortex following adult-onset partial hearing loss. However, it should be noted that because we did not examine the cortical tissue using cytoarchitectonic analysis, we cannot rule out the possibility that the changes observed in the two weeks following noise exposure were instead due to a shift in the cytoarchitectonic borders of the neighbouring cortical areas rather than changes in the

responsiveness of neurons within the given cortical areas. Shifts in the structural location of borders between cortical areas have been reported in adult animals that were born deaf (Wong et al., 2013b) or those deafened early in life (Wong et al., 2013a).

In support of our suggestion of a functional transition in sensory responsiveness, Xu et al. (2014) demonstrated experience-dependent plasticity in the extrastriate visual cortex of normal hearing rats following the repetitive pairing of auditory and visual stimuli. Passively-exposing adult rats to audiovisual stimuli every 2 s for 12 hours/day for 2 months resulted in an expansion of the multisensory zone contained within V2L cortex (Xu et al., 2014). Moreover, consistent with the present results in the AuD cortex of hearing-impaired rats (Fig. 2.7C), the firing rates in response to auditory, visual or combined stimuli were unchanged following the audiovisual exposure paradigm, despite an increase in the incidence of multisensory neurons (Xu et al., 2014). Thus, altered sensory experience during adulthood, either through repetitive stimulation (Xu et al., 2014) or partial-deprivation (present study), causes the multisensory region of the V2L cortex to preferentially change its relative responsiveness to auditory and visual stimuli, without changing the firing rate properties of the constituent neurons. Interestingly, similar effects were seen in the AuD cortex in the present study, whereas opposing results were found in the predominantly visual area of the dorsomedial aspect of V2L (i.e., V2L-visual zone). Despite a lack of sensory reorganization in the V2L-visual zone, the maximum firing rates in response to the visual stimuli decreased in the noise-exposed rats (Fig. 2.7A). Collectively, these findings reveal that higher-order areas of neighbouring cortices demonstrate a complex pattern of crossmodal plasticity following partial hearing loss in adulthood.

2.4.5 Possible Mechanisms of Crossmodal Plasticity

What structural and/or physiological changes could account for the hearing loss-induced transition in sensory responsiveness across the cortical regions, as well as the variable effects on neuron firing rates? At present, the mechanisms underlying crossmodal plasticity have not been fully elucidated; however, a variety of neural and anatomical substrates have been proposed, albeit most often based on studies that investigated the primary sensory cortices following complete sensory loss. For example, it has been suggested that an

increase in multisensory convergence in subcortical loci could result in multimodal input being successively relayed to the deprived cortex via existing connections, ultimately manifesting as cortical crossmodal plasticity (Allman et al., 2009a; Laramée et al., 2011; Mezzera and López-Bendito, 2015). Separately, based on recent findings in visually-deprived mice, it was proposed that a loss of intracortical inhibition could permit existing intracortical crossmodal inputs to reactivate the deprived cortex (Nys et al., 2015). Given that the primary auditory cortex sends direct projections into V2L in normal-hearing rodents (Budinger et al., 2000; Laramée et al., 2011) and noise exposure impairs GABAergic neurotransmission in the primary auditory cortex (Yang et al., 2011), perhaps a loss of intracortical inhibition may have contributed to the noise-induced crossmodal plasticity observed in the present study.

Beyond possible changes in neural activity associated with existing connections, it is reasonable to consider whether sensory deprivation causes an increase in the density of projections from novel and/or existing sources which could provide additional crossmodal inputs into the deprived cortex (Rauschecker, 1995). Contrary to this suggestion, recent studies have shown a general lack of change in the relative proportion of intracortical or thalamocortical connections into various auditory cortices of animals with either partial (Meredith and Allman, 2012) or profound hearing loss (Allman et al., 2009a; Barone et al., 2013; Butler et al., 2016; Chabot et al., 2015; Clemo et al., 2014; Kok et al., 2014; Meredith et al., 2015; Wong et al., 2015), despite electrophysiological evidence of crossmodal plasticity in these models. That said, early-onset profound deafness in cats did cause an increase in dendritic spine density in the supragranular layers of the higher-order cortical area of the auditory field of the anterior ectosylvian sulcus (FAES), which the authors suggested could provide a synaptic basis for crossmodal plasticity if paired with an increase in terminal boutons (Clemo et al., 2014). Furthermore, a series of studies on visually-impaired mice have reported altered regulation of excitatory synapses in the supragranular layers in both the deprived and spared sensory cortices. This homeostatic plasticity, which allows neurons to stabilize their own activity in response to extended periods of increased/decreased input activity (Whitt et al., 2014), occurred after only a few days of visual deprivation, and was characterized by a scaling down of intracortical synapses in the supragranular layers in the spared primary cortices (somatosensory and auditory) (Goel et

al., 2006; He et al., 2012; Petrus et al., 2014), as well as an increased strength of lateral inputs to layer 2/3 neurons in primary visual (V1) cortex following a complete loss of vision (He et al., 2012). Consequently, it has been proposed that an up-scaling of these excitatory synapses could allow previously subthreshold crossmodal inputs to become strong enough to summate and reach the threshold to cause V1 neurons to respond with action potentials to auditory and/or tactile stimuli (Lee, 2012; Lee and Whitt, 2015). However, because these homeostatic changes in V1 only occurred under conditions of complete loss of vision (for review, see Whitt et al., 2014), it is uncertain whether partial hearing loss in adulthood would be sufficient to induce synaptic plasticity in either the primary auditory cortex and/ or higher-order cortical areas capable of normally integrating audiovisual information. Thus, future investigations are needed into the possible contributions of the aforementioned anatomical and neural substrates in the transition of sensory responsiveness that we observed in the neighbouring higher-order cortical areas following adult-onset hearing loss.

2.4.6 Behavioural Consequences of Partial Hearing Loss on Audiovisual Integration

Despite the prevalence of hearing impairment, a limited number of studies have investigated the functional implications of hearing loss-induced crossmodal plasticity on audiovisual integration. Contrary to the authors' predictions (Başkent and Bazo, 2011), older adults with moderate hearing loss showed similar temporal integration of audiovisual speech stimuli compared to younger normal hearing listeners when the subjects were asked to judge the simultaneity of auditory and visual sentence recordings. Consistent with these findings, audiovisual integration of speech stimuli was similar between older adults with mild-moderate hearing impairment compared to normal-hearing listeners of the same age (Tye- Murray et al., 2007). In contrast to these studies which used subject performance to assess audiovisual integration, when a comparison was made of the cortical evoked potentials elicited by watching and listening to speech stimuli, older adults with hearing loss showed degraded audiovisual integration compared to age-matched controls (Musacchia et al., 2009). Finally, Puschmann et al. (2014), used a crossmodal distractibility paradigm to evaluate the impact of distracting visual input on auditory processing, and

found that hearing-impaired subjects had poorer performance on an auditory task compared to normal-hearing controls, findings which were suggested to result from crossmodal plasticity in the auditory cortex.

To date, no studies have used animal models to investigate the effect of adult-onset partial hearing loss and the ensuing crossmodal plasticity on behavioural measures of audiovisual integration. Because the V2L cortex in rats is known to contribute to the improved reaction times to combined auditory and visual stimuli (Hirokawa et al., 2008), it is reasonable to predict that the transition in the functional border of the audiovisual cortex observed in the present study could lead to behavioural consequences in tasks requiring audiovisual processing. Ultimately, in addition to further identifying the behavioural implications of crossmodal plasticity on audiovisual integration, future studies on animal models could provide important insight into the lower limit of hearing loss necessary to induce crossmodal plasticity, as well as the time course of these cortical changes and the underlying anatomical and/or neural substrates. Such studies are expected to contribute to the continued refinement of our understanding of the adaptive versus maladaptive effects of crossmodal plasticity on auditory, visual and audiovisual processing (Heimler et al., 2014).

2.5 References

Agrawal Y, Platz EA, and Niparko JK (2008). Prevalence of hearing loss and differences by demographic characteristics among us adults: Data from the national health and nutrition examination survey, 1999-2004. *Arch. Intern. Med.* 168, 1522–1530.

Allman, B.L., and Meredith, M.A. (2007). Multisensory Processing in "Unimodal" Neurons: Cross-Modal Subthreshold Auditory Effects in Cat Extrastriate Visual Cortex. *J. Neurophysiol.* 98, 545–549.

Allman, B.L., Bittencourt-Navarrete, R.E., Keniston, L.P., Medina, A.E., Wang, M.Y., and Meredith, M.A. (2008a). Do Cross-Modal Projections Always Result in Multisensory Integration? *Cereb. Cortex* 18, 2066–2076.

Allman, B.L., Keniston, L.P., and Meredith, M.A. (2008b). Subthreshold auditory inputs to extrastriate visual neurons are responsive to parametric changes in stimulus quality: Sensory-specific versus non-specific coding. *Brain Res.* 1242, 95–101.

Allman, B.L., Keniston, L.P., and Meredith, M.A. (2009a). Adult deafness induces somatosensory conversion of ferret auditory cortex. *Proc. Natl. Acad. Sci.* 106, 5925–5930.

Allman, B.L., Keniston, L.P., and Meredith, M.A. (2009b). Not Just for Bimodal Neurons Anymore: The Contribution of Unimodal Neurons to Cortical Multisensory Processing. *Brain Topogr.* 21, 157–167.

Armstrong, R.A. (2014). When to use the Bonferroni correction. *Ophthalmic Physiol. Opt.* 34, 502–508.

Auer, E.T., Bernstein, L.E., Sungkarat, W., and Singh, M. (2007). Vibrotactile Activation of the Auditory Cortices in Deaf versus Hearing Adults. *Neuroreport* 18, 645–648.

Barone, P., Lacassagne, L., and Kral, A. (2013). Reorganization of the Connectivity of Cortical Field DZ in Congenitally Deaf Cat. *PLOS ONE* 8, e60093.

Barth, D.S., Goldberg, N., Brett, B., and Di, S. (1995). The spatiotemporal organization of auditory, visual, and auditory-visual evoked potentials in rat cortex. *Brain Res.* 678, 177–190.

Başkent, D., and Bazo, D. (2011). Audiovisual asynchrony detection and speech intelligibility in noise with moderate to severe sensorineural hearing impairment. *Ear Hear.* 32, 582–592.

Bavelier, D., Dye, M.W.G., and Hauser, P.C. (2006). Do deaf individuals see better? *Trends Cogn. Sci.* 10, 512–518.

Budinger, E., Heil, P., and Scheich, H. (2000). Functional organization of auditory cortex in the Mongolian gerbil (Meriones unguiculatus). III. Anatomical subdivisions and corticocortical connections. *Eur. J. Neurosci.* 12, 2425–2451.

Butler, B.E., Chabot, N., and Lomber, S.G. (2016). Quantifying and comparing the pattern of thalamic and cortical projections to the posterior auditory field in hearing and deaf cats. *J. Comp. Neurol.* 524:15, 3042-3063

Campbell, J., and Sharma, A. (2013). Compensatory changes in cortical resource allocation in adults with hearing loss. *Front. Syst. Neurosci*. 7, 71.

Campbell, J., and Sharma, A. (2014). Cross-Modal Re-Organization in Adults with Early Stage Hearing Loss. *PLOS ONE* 9, e90594.

Chabot, N., Butler, B.E., and Lomber, S.G. (2015). Differential modification of cortical and thalamic projections to cat primary auditory cortex following early- and late-onset deafness. *J. Comp. Neurol.* 523, 2297–2320.

Chen, Z., and Yuan, W. (2015). Central plasticity and dysfunction elicited by aural deprivation in the critical period. *Front. Neural Circuits* 9.

Clemo, H.R., Lomber, S.G., and Meredith, M.A. (2014). Synaptic Basis for Cross-modal Plasticity: Enhanced Supragranular Dendritic Spine Density in Anterior Ectosylvian Auditory Cortex of the Early Deaf Cat. *Cereb. Cortex*, bhu225.

Doucet, M.E., Bergeron, F., Lassonde, M., Ferron, P., and Lepore, F. (2006). Cross-modal reorganization and speech perception in cochlear implant users. *Brain* 129, 3376–3383.

Finney, E.M., Fine, I., and Dobkins, K.R. (2001). Visual stimuli activate auditory cortex in the deaf. *Nat. Neurosci*. 4, 1171–1173.

Finney, E.M., Clementz, Brett, A., Hickok, G., and Dobkins, K.R. (2003). Visual stimuli activate auditory cortex in deaf subjects: evidence from MEG. *Neuroreport* 14, 1425–1427.

Furman, A.C., Kujawa, S.G., and Liberman, M.C. (2013). Noise-induced cochlear neuropathy is selective for fibers with low spontaneous rates. *J. Neurophysiol*. 110, 577–586.

Goel, A., Jiang, B., Xu, L.W., Song, L., Kirkwood, A., and Lee, H.-K. (2006). Cross-modal regulation of synaptic AMPA receptors in primary sensory cortices by visual experience. *Nat. Neurosci.* 9, 1001–1003.

He, K., Petrus, E., Gammon, N., and Lee, H.-K. (2012). Distinct Sensory Requirements for Unimodal and Cross-Modal Homeostatic Synaptic Plasticity. *J. Neurosci*. 32, 8469–8474.

Heimler, B., Weisz, N., and Collignon, O. (2014). Revisiting the adaptive and maladaptive effects of crossmodal plasticity. *Neuroscience* 283, 44–63.

Henderson, D., Bielefeld, E.C., Harris, K.C., and Hu, B.H. (2006). The Role of Oxidative Stress in Noise-Induced Hearing Loss: *Ear Hear.* 27, 1–19.

Hirokawa, J., Bosch, M., Sakata, S., Sakurai, Y., and Yamamori, T. (2008). Functional role of the secondary visual cortex in multisensory facilitation in rats. *Neuroscience* 153, 1402–1417.

Hunt, D.L., Yamoah, E.N., and Krubitzer, L. (2006). Multisensory plasticity in congenitally deaf mice: How are cortical areas functionally specified? *Neuroscience* 139, 1507–1524.

Kok, M.A., Chabot, N., and Lomber, S.G. (2014). Cross-modal reorganization of cortical afferents to dorsal auditory cortex following early- and late-onset deafness. *J. Comp. Neurol.* 522, 654–675.

Kral, A., Schröder, J.-H., Klinke, R., and Engel, A.K. (2003). Absence of cross-modal reorganization in the primary auditory cortex of congenitally deaf cats. *Exp. Brain Res.* 153, 605–613.

Kujawa, S.G., and Liberman, M.C. (2009). Adding Insult to Injury: Cochlear Nerve Degeneration after “Temporary” Noise-Induced Hearing Loss. *J. Neurosci*. 29, 14077–14085.

Lambertz, N., Gizewski, E.R., de Greiff, A., and Forsting, M. (2005). Cross-modal plasticity in deaf subjects dependent on the extent of hearing loss. *Cogn. Brain Res*. 25, 884–890.

Laramée, M.E., Kurotani, T., Rockland, K.S., Bronchti, G., and Boire, D. (2011). Indirect pathway between the primary auditory and visual cortices through layer V pyramidal neurons in V2L in mouse and the effects of bilateral enucleation. *Eur. J. Neurosci*. 34, 65–78.

Lee, H.-K. (2012). Ca-permeable AMPA receptors in homeostatic synaptic plasticity. *Front. Mol. Neurosci.* 5, 17.

Lee, H.-K., and Whitt, J.L. (2015). Cross-modal synaptic plasticity in adult primary sensory cortices. *Curr. Opin. Neurobiol*. 35, 119–126.

Lin FR, Niparko JK, and Ferrucci L (2011). Hearing loss prevalence in the united states. *Arch. Intern. Med.* 171, 1851–1853.

Lomber, S.G., Meredith, M.A., and Kral, A. (2010). Cross-modal plasticity in specific auditory cortices underlies visual compensations in the deaf. *Nat. Neurosci*. 13, 1421–1427.

Meredith, M.A., and Allman, B.L. (2012). Early Hearing-Impairment Results in Crossmodal Reorganization of Ferret Core Auditory Cortex. *Neural Plast*. 2012, e601591.

Meredith, M.A., and Lomber, S.G. (2011). Somatosensory and visual crossmodal plasticity in the anterior auditory field of early-deaf cats. *Hear. Res*. 280, 38–47.

Meredith, M.A., and Stein, B.E. (1986). Visual, auditory, and somatosensory convergence on cells in superior colliculus results in multisensory integration. J. *Neurophysiol*. 56, 640–662.

Meredith, M.A., Keniston, L.P., and Allman, B.L. (2012). Multisensory dysfunction accompanies crossmodal plasticity following adult hearing impairment. *Neuroscience* 214, 136–148.

Meredith, M.A., Clemo, H.R., Corley, S.B., Chabot, N., and Lomber, S.G. (2015). Cortical and thalamic connectivity of the auditory anterior ectosylvian cortex of early-deaf cats: Implications for neural mechanisms of crossmodal plasticity. *Hear. Res.* 333, 25–36.

Mezzera, C., and López-Bendito, G. (2015). Cross-modal plasticity in sensory deprived animal models: From the thalamocortical development point of view. *J. Chem. Neuroanat.* 75, 32-40

Musacchia, G., Arum, L., Nicol, T., Garstecki, D., and Kraus, N. (2009). Audiovisual Deficits in Older Adults with Hearing Loss: Biological Evidence: *Ear Hear*. 30, 505–514.

Nicolelis, M.A.L., Dimitrov, D., Carmena, J.M., Crist, R., Lehew, G., Kralik, J.D., and Wise, S.P. (2003). Chronic, multisite, multielectrode recordings in macaque monkeys. *Proc. Natl. Acad. Sci.* 100, 11041–11046.

Nys, J., Smolders, K., Laramée, M.-E., Hofman, I., Hu, T.-T., and Arckens, L. (2015). Regional Specificity of GABAergic Regulation of Cross-Modal Plasticity in Mouse Visual Cortex after Unilateral Enucleation. *J. Neurosci*. 35, 11174–11189.

Pavani, F., and Roder, B. (2012). "Crossmodal plasticity as a consequence of sensory loss: insights from blindness and deafness." In *The New Handbook for Multisensory Processes*, eds. B. Stein (Cambridge, MA: MIT Press)737–759.

Paxinos, G., and Watson, C. (2007). The rat brain in stereotaxic coordinates (Burlington, MA: Elsevier Inc.).

Petrus, E., Isaiah, A., Jones, A.P., Li, D., Wang, H., Lee, H.-K., and Kanold, P.O. (2014). Crossmodal Induction of Thalamocortical Potentiation Leads to Enhanced Information Processing in the Auditory Cortex. *Neuron* 81, 664–673.

Polley, D.B., Read, H.L., Storace, D.A., and Merzenich, M.M. (2007). Multiparametric Auditory Receptive Field Organization Across Five Cortical Fields in the Albino Rat. *J. Neurophysiol*. 97, 3621–3638.

Popelar, J., Grecova, J., Rybalko, N., and Syka, J. (2008). Comparison of noise-induced changes of auditory brainstem and middle latency response amplitudes in rats. *Hear. Res.* 245, 82–91.

Puschmann, S., Sandmann, P., Bendixen, A., and Thiel, C.M. (2014). Age-related hearing loss increases cross-modal distractibility. *Hear. Res.* 316, 28–36.

Rauschecker, J.P. (1995). Compensatory plasticity and sensory substitution in the cerebral cortex. *Trends Neurosci.* 18, 36–43.

Rüttiger, L., Singer, W., Panford-Walsh, R., Matsumoto, M., Lee, S.C., Zuccotti, A., Zimmermann, U., Jaumann, M., Rohbock, K., Xiong, H., et al. (2013). The Reduced Cochlear Output and the Failure to Adapt the Central Auditory Response Causes Tinnitus in Noise Exposed Rats. *PLOS ONE* 8, e57247.

Stein, B.E., and Meredith, M.A. (1993). The merging of the senses (Cambridge, MA, US: The MIT Press).

Toldi, J., Fehér, O., and Wolff, J.R. (1986). Sensory interactive zones in the rat cerebral cortex. *Neuroscience* 18, 461–465.

Tye-Murray, N., Sommers, M., and Spehar, B. (2007). Audiovisual integration and lipreading of older adults with normal and impaired hearing. *Ear Hear.* 28, 656–668.

Vachon, P., Voss, P., Lassonde, M., Leroux, J.-M., Mensour, B., Beaudoin, G., Bourgouin, P., and Lepore, F. (2013). Reorganization of the auditory, visual and multimodal areas in early deaf individuals. *Neuroscience* 245, 50–60.

Wallace, M.T., Ramachandran, R., and Stein, B.E. (2004). A revised view of sensory cortical parcellation. *Proc. Natl. Acad.* 101, 2167–2172.

Whitt, J.L., Petrus, E., and Lee, H.-K. (2014). Experience-dependent homeostatic synaptic plasticity in neocortex. *Neuropharmacology* 78, 45–54.

Wong, C., Kuhne, D., Kral, A., and Lomber, S. (2013a). Duration of acoustic experience shapes development of auditory cortex cartography. In: Presented at the 43rd Annual Meeting of the Society for Neuroscience, San Diego, CA.

Wong, C., Chabot, N., Kok, M.A., and Lomber, S.G. (2013b). Modified Areal Cartography in Auditory Cortex Following Early- and Late-Onset Deafness. *Cereb. Cortex* 24, 1778–1792.

Wong, C., Chabot, N., Kok, M.A., and Lomber, S.G. (2015). Amplified somatosensory and visual cortical projections to a core auditory area, the anterior auditory field, following early- and late-onset deafness. *J. Comp. Neurol*. 523, 1925–1947.

Xu, J., Sun, X., Zhou, X., Zhang, J., and Yu, L. (2014). The cortical distribution of multisensory neurons was modulated by multisensory experience. *Neuroscience* 272, 1–9.

Yang, S., Weiner, B.D., Zhang, L.S., Cho, S.-J., and Bao, S. (2011). Homeostatic plasticity drives tinnitus perception in an animal model. *Proc. Natl. Acad. Sci*. 108, 14974–14979.

Chapter 3

3 Adult-Onset Hearing Impairment Induces Layer-Specific Cortical Reorganization: Evidence of Crossmodal Plasticity and Central Gain Enhancement [2]

3.1 Introduction

Hearing impairment is a highly prevalent neurological problem, affecting ~16% of adults in the USA (Agrawal et al., 2008; Lin et al., 2011). Furthermore, according to the Centers for Disease Control and Prevention, nearly 10 million Americans suffer from hearing loss related to excessive noise exposure, and each year ~22 million workers are exposed to noise levels that could lead to hearing impairment. Consistent with non-invasive studies on hearing-impaired individuals, preclinical research using animal models has revealed that noise-induced hearing loss causes considerable neural plasticity throughout the central auditory pathway. For example, the loss of sensory output from the damaged cochlea leads to a paradoxical increase in neural activity at the successive relay nuclei, ultimately manifesting as hyperactivity in the core auditory cortex (i.e., central gain enhancement) (Popelar et al., 1987, 1995, 2008; Salvi et al., 1990, 2000). Numerous studies have investigated the various cochlear insults that can lead to an increase in central gain, as well as the putative perceptual consequences (e.g., tinnitus? hyperacusis?) (for review, see Auerbach et al., 2014). At present, however, it remains unclear to what extent this deprivation-induced hyperactivity in the core auditory cortex is relayed to higher-order, multisensory areas of the brain that are tasked with integrating converging inputs from different sensory modalities (e.g., hearing and vision).

This issue of whether central gain enhancement in the auditory system disrupts audiovisual integration is particularly relevant given that hearing impairment not only affects how

---

[2] A version of this chapter is published as:

Schormans, A.L., Typlt, M., Allman, B.L. (2018) Adult-onset hearing impairment induces layer-specific cortical reorganization: evidence of crossmodal plasticity and central gain enhancement. *Cerebral Cortex*. 1-14

sound is processed but can also alter cortical responsiveness to non-auditory stimuli (i.e., crossmodal plasticity). It has long been suggested that the loss of one sense (e.g., hearing) allows for the invasion of the deprived cortical areas by the spared senses (e.g., vision) (Rauschecker, 1995). Although this suggestion is consistent with crossmodal plasticity observed in deaf humans (Finney et al., 2001, 2003; Doucet et al., 2006; Auer et al., 2007; Vachon et al., 2013) as well as early- and late-onset profound hearing loss in animal models (Kral et al., 2003; Hunt et al., 2006; Allman et al., 2009; Meredith and Lomber, 2011), it is reasonable to question whether it would be at odds with an increase in central gain that occurs in the core auditory cortex after moderate hearing loss. In such cases when some residual hearing is preserved, the core auditory cortex shows evidence of tonotopic reorganization, increased neuronal synchrony, and hyperactivity not quiescence (Komiya and Eggermont, 2000; Popescu and Polley, 2010; Engineer et al., 2011; Meredith and Keniston et al., 2012; Meredith and Allman et al., 2012; Salvi et al., 2000); factors which could alter its susceptibility to crossmodal plasticity. To date, numerous studies have separately examined the emergence of central gain enhancement or crossmodal plasticity, but no studies have determined whether these two phenomena compete or coexist in the neighbouring regions of auditory, visual and audiovisual cortices following partial hearing loss. This possibility of regional specificity is particularly relevant because it is known that not all areas of the auditory cortex show the same degree of crossmodal plasticity in profoundly deaf subjects (Kral et al., 2003; Lomber et al., 2010; Meredith et al., 2011).

Studies in both humans and animal models have shown that even a modest hearing impairment is sufficient to induce crossmodal plasticity. For example, visual and audiovisual-evoked potentials were altered in adults with mild-moderate hearing loss compared with age-matched controls (Musacchia et al., 2009; Campbell and Sharma, 2014), and these hearing-impaired subjects showed an increased responsiveness to visual stimuli in more temporal cortical regions (Campbell and Sharma, 2014). Consistent with these results, adult-onset hearing impairment increased visual processing in the core auditory cortex of ferrets (Meredith and Keniston et al., 2012) as well as the audiovisual cortex of rats (Schormans et al., 2017a). However, because these previous studies did not segregate their results according to the depth of the recording penetrations throughout the cortical mantle, it remains uncertain whether partial hearing loss differentially affects

sensory processing across the cortical layers within the higher-order sensory areas; findings that could provide important insight into the contributions of thalamocortical versus intracortical processing in the manifestation of central gain enhancement and crossmodal plasticity.

In the present study, we conducted the first investigation into how adult-onset hearing loss alters auditory, visual and audiovisual processing across the distinct layers of higher- order sensory cortices. In doing so, we sought to reveal the extent that deprivation-induced hyperactivity in the auditory pathway is relayed beyond the core auditory cortex, and thus, whether central gain enhancement competes or coexists with crossmodal plasticity in the audiovisual cortex following partial hearing loss in adulthood. Two weeks after loud noise exposure, adult rats were anesthetized, and extracellular electrophysiological recordings were performed in four neighbouring cortical regions: the primary visual cortex (V1), the multisensory zone of the lateral extrastriate visual cortex (V2L-Mz), the auditory zone of the lateral extrastriate visual cortex (V2L-Az), and the dorsal auditory cortex (AuD; a higher order auditory area). By inserting a 32-channel linear electrode array orthogonal to the pial surface, laminar processing was assessed in each cortical region in response to auditory, visual and combined audiovisual stimuli by sampling the local field potential (LFP) across the entire cortical thickness. Current-source density (CSD) analysis was then applied to these LFP data to determine the effect of partial hearing loss on central gain enhancement and crossmodal plasticity at the level of post-synaptic potentials. Ultimately, this novel approach allowed us to reveal that adult-onset hearing impairment causes a complex assortment of intramodal and crossmodal changes across the layers of neighbouring regions of the higher-order sensory cortices.

3.2 Methods

3.2.1 Animals

In total, 17 adult male Sprague-Dawley rats aged 110 ± 3 days (body mass: 421 ± 12.6 g); Charles River Laboratories Inc., Wilmington, MA) were used in this study, and were housed on a 12-hour light-dark cycle with food and water ad libitum. All experimental procedures were approved by the University of Western Ontario Animal Care and Use

Committee and were in accordance with the guidelines established by the Canadian Council of Animal Care.

3.2.2 Hearing Assessment

Consistent with an established protocol (Schormans et al., 2017a), hearing sensitivity was assessed with the auditory brainstem response (ABR), which was performed in a double-walled sound-attenuating chamber (MDL 6060 ENV, Whisper Room Inc, Knoxville, TN). Rats were anesthetized with ketamine (80 mg/kg; IP) and xylazine (5 mg/kg; IP), and subdermal electrodes (27 gauge; Rochester Electro-Medical, Lutz, FL) were positioned at the vertex, over the right mastoid and on the back. Throughout the hearing assessment procedure, body temperature was maintained at ~37 °C using a homeothermic heating pad (507220F; Harvard Apparatus, Kent, UK).

Auditory stimuli consisting of a click (0.1 ms) and 2 tones (4 kHz and 20 kHz; 5 ms duration and 1 ms rise/fall time) were generated using Tucker-Davis Technologies RZ6 processing module sampled at 100 kHz (TDT, Alachua, FL). The auditory stimuli were delivered by a speaker (MF1; TDT) positioned 10 cm from the animal's right ear while the left ear was occluded with a custom foam ear plug. All stimuli were presented 1000 times (21 times/s) at decreasing intensities from 90 to 10 dB sound pressure level (SPL). Near threshold, successive steps were decreased to 5 dB SPL, and each sound level was presented twice in order to best determine ABR threshold using the criteria of just noticeable deflection of the averaged electrical activity within the 10-ms time window (Popelar et al., 2008). Sound stimuli used for the ABR, noise exposure and electrophysiological recordings were calibrated with custom MATLAB software (The Mathworks, Natick, MA) using a ¼-inch microphone (2530; Larson Davis, Depew, NY) and preamplifier (2221; Larson Davis). The auditory-evoked activity was collected using a low-impedance headstage (RA4L1; TDT), then preamplified and digitized (RA16SD Medusa preamp; TDT) and sent to a RZ6 processing module via a fiber optic cable.

Rats in the control group (n = 8) underwent an ABR to assess their hearing levels, followed immediately by an *in vivo* extracellular electrophysiological recording experiment. Noise exposed rats (n = 9) underwent a baseline hearing assessment, followed by exposure to a

loud broadband noise (see below for details). Two weeks following the noise exposure, a final hearing assessment was performed, after which the same electrophysiological recording experiment was completed as in control rats.

3.2.3 Noise Exposure

Rats were bilaterally exposed to a broadband noise (0.8–20 kHz) for 2 hours at 120 dB SPL while under ketamine (80 mg/kg; IP) and xylazine (5 mg/kg; IP), and body temperature was maintained at ~37 °C using a homeothermic heating pad. This broadband noise exposure protocol was chosen because it was found to be effective at inducing a permanent threshold shift as assessed using the ABR as well as persistent changes in the auditory cortex (Popelar et al., 2008) and the audiovisual cortex (Schormans et al., 2017a). The broadband noise was generated with TDT software (RPvdsEx) and hardware (RZ6), and delivered by a super tweeter (T90A; Fostex, Tokyo, Japan) which was placed 10 cm in front of the rat.

3.2.4 Surgical Procedure

Following the final hearing assessment, each rat was maintained under ketamine/xylazine anesthesia, the foam earplug was removed from the left ear, and the animal was fixed in a stereotaxic frame with blunt ear bars. The absence of a pedal withdrawal reflex was an indication of anesthetic depth, and supplemental doses of ketamine/xylazine were administered IM as needed. A midline incision was made in the skin of the scalp, and the dorsal aspect of the skull was cleaned with a scalpel blade. The left temporalis muscle was reflected to provide access to the temporal bone overlying the auditory and audiovisual cortices. A stereotaxic manipulator was used to measure 6 mm caudal to bregma, which represents an approximate location of the lateral extrastriate visual cortex (V2L) (Wallace et al., 2004; Hirokawa et al., 2008; Schormans et al., 2017a; Xu et al., 2014), and a mark was made on the skull for later drilling. Additional marks were made on the temporal bone at 1, 2, and 3 mm ventral of the top of the skull (i.e., dorsal/ventral measurements were zeroed on the sagittal suture at 6 mm caudal to bregma; the most dorsal aspect of the skull). A stainless-steel screw was inserted in the left frontal bone to serve as an anchor for the headpost and an electrical ground. A craniotomy (2 × 5mm; 5–7 mm caudal to bregma)

was performed in the left temporal and parietal bone in order to expose the auditory, visual and audiovisual cortices. A headpost was fastened to the skull with dental acrylic on the right frontal bone, and the right ear bar was removed to allow free-field auditory stimulation of the right ear during the electrophysiological recordings in the contralateral cortex. The rat was held in position throughout the entire duration of the experiment within the stereotaxic frame using the left ear bar and the headpost.

3.2.5 Electrophysiological Recordings

At least four recording penetrations were performed in each animal. At each of the recording locations (described in detail below), a 32-channel linear electrode array was inserted perpendicular to the cortex through a small slit in the dura using a hydraulic microdrive (FHC; Bowdoin, ME). The array consisted of 32 iridium microelectrodes equally spaced 50 μm apart on a 50-μm-thick shank, spanning 1550 μm (A1x32-10mm-50-177-A32; NeuroNexus Technologies, Ann Arbor, MI). Prior to insertion in the cortex, the electrode array was coated in DiI cell-labeling solution (V22885; Molecular Probes, Inc., Eugene, OR) to allow for histological reconstruction of electrode penetrations. Initially, the electrode array was advanced into the cortex using a high-precision stereotaxic manipulator to penetrate the pia mater, and then withdrawn to the cortical surface. The hydraulic microdrive was then used to slowly advance the electrode array until it reached a depth of −1500 μm. For each cortical region, slight adjustments to depth were made based on a characteristic sharp negative peak of the LFP to the preferred stimulus (i.e., the unimodal stimulus that evoked the largest response) (typically −350 to −450 μm depth below the pial surface) (Stolzberg et al., 2012). Once at this depth (control: −396 ± 11 μm; noise exposed: −377 ± 13 μm), the electrode was allowed to settle in place for 45 minutes before electrophysiological recordings commenced. Electrophysiological signals were acquired using TDT System 3 (TDT, Alachua, FL), and LFP activity was continuously acquired (digitally resampled at approximately 1000 Hz) and bandpass filtered online at 1–300 Hz.

In all rats, recordings were completed within four brain regions: (1) the primary visual cortex (V1; corresponding to the 1 mm ventral of the marking on the skull using our measurements), (2) the multisensory zone of the lateral extrastriate visual cortex (V2LMz;

2 mm ventral); (3) the auditory zone of the lateral extrastriate visual cortex (V2L-Az; 2.5 mm ventral); and finally, (4) the dorsal auditory cortex (AuD; 3 mm ventral). Fig. 3.1 shows a schematic of the location for each of the four penetrations per animal from all of the electrophysiological experiments.

3.2.6 Sensory Stimulation

At each of the recording locations, a quantitative multisensory paradigm was performed, which included computer-triggered auditory and visual stimuli presented alone or in combination. Auditory stimuli consisted of noise bursts (1–32 kHz; 50 ms duration) from a speaker positioned 10 cm from the right pinna on a 30° angle to the right of midline. For each rat, the auditory stimulus was presented 40 dB above its click threshold (control: 68.3 ± 1.1 dB SPL; noise exposed: 82.5 ± 1.7 dB SPL). Visual stimuli consisted of light flashes (15 lux; 50ms duration) from an LED (diameter: 0.8 cm) positioned adjacent to the speaker (i.e., 10 cm from the right eye). The intensity of the visual stimulus was determined using a LED light meter (Model LT45, Extech Instruments, Nashua, NH). During the combined stimulus condition, the visual stimulus was presented 30 ms prior to the auditory stimulus. Consistent with previous studies (Allman and Meredith 2007; Allman et al. 2008; Meredith and Allman 2009, 2015), this timing offset maximized the potential for observing a multisensory interaction because it compensated for differences in latency for each modality and helped ensure that both stimuli arrived simultaneously within the temporal cortex. In total, the 3 stimuli conditions were presented in a randomized order, separated by an inter-stimulus interval of 3–5 s, and each condition was presented 50 times.

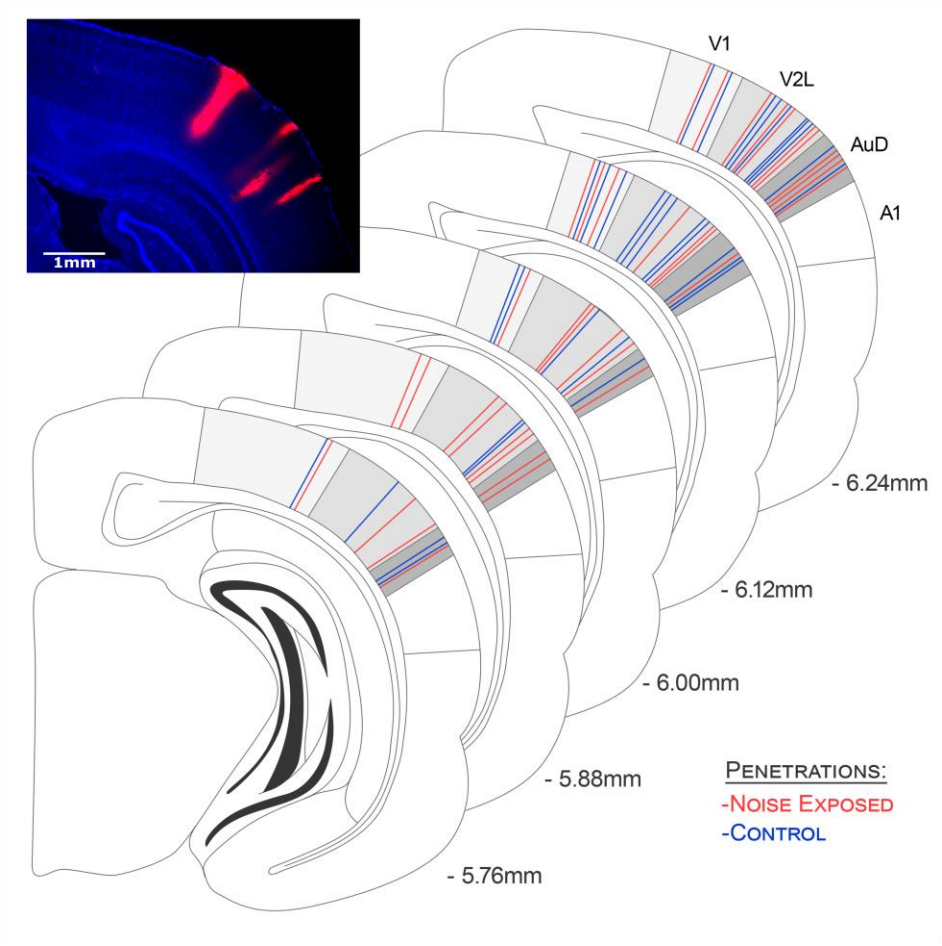

Figure 3.1. Electrode penetrations across all recording locations within V1, V2L and the AuD cortex.

The stained image shows a representative coronal section demonstrating the location of recording penetrations 6.0 mm caudal of bregma. Prior to being inserted into the cortex, the electrode was coated in DiI cell-labeling solution allowing for post-experiment histological reconstruction of the penetrations. Note that despite not being visible on this single section, it was confirmed in neighbouring rostral/caudal sections that all penetrations did indeed span the full distance of the cortical mantle. The schematic shows a reconstruction of all of the recording penetrations for control (blue; n = 32) and noise exposed (red; n = 36) experiments spanning 5.76–6.24 mm caudal of bregma. In accordance with Paxinos and Watson (2007), the most dorsal recording penetrations were located in the V1, whereas the most ventral recording penetrations were in the AuD. One penetration per rat was located in each of these predominantly unisensory areas. Two

penetrations per rat targeted the multisensory area, the lateral extrastriate visual cortex (V2L) (Schormans et al., 2017a); one penetration in the more dorsal-positioned, multisensory zone of the V2L (V2L-Mz), and the other in the auditory zone (V2L-Az).

3.2.7 Current Source Density Analysis

The CSD provides a measure of the total current density that enters or leaves the extracellular space through the cell membrane (Mitzdorf, 1985; Einevoll et al., 2013). A one-dimensional CSD analysis was applied to the mean LFPs recorded simultaneously across the entire cortical thickness using the following formula:

$$\mathrm{CSD} \approx -\frac{\Phi(z+n\Delta z)-2\,\Phi(z)+\,\Phi(z-n\Delta z)}{(n\Delta z)^2} \qquad (1)$$

where, Φ is the LFP, z is the spatial coordinate, Δz is the interelectrode spacing (Δz = 50 μm), and n is the differentiation grid (n = 4) (Nicholson and Freeman, 1975; Mitzdorf and Singer, 1977, 1980; Freeman and Singer, 1983; Mitzdorf, 1985). This CSD equation approximates the second derivative of the LFPs at each point in time across electrode sites, which is due to the transmembrane current sources or sinks. A 3-point Hamming filter was applied in order to smooth LFPs across channels before computing the CSD, as described by Stolzberg et al. (2012). In accordance with previous studies (Nicholson and Freeman, 1975; Mitzdorf and Singer, 1977, 1980; Freeman and Singer, 1983; Mitzdorf, 1985; Stolzberg et al., 2012), current sinks were positive in amplitude, and sources were negative.

CSD analysis reveals the net flow of ions into and out of the neural tissue; sinks represent the flow of positive ions into the neural tissue from the extracellular space, which corresponds to events such as active excitatory synaptic populations and axonal depolarization (Kral and Eggermont, 2007; Happel et al., 2010). Current sources are reflective of passive return currents, and are indicative of repolarization and possibly inhibition of the neighbouring tissue (Mitzdorf, 1985; Kral and Eggermont, 2007; Happel et al., 2010; Einevoll et al., 2013; Szymanski et al., 2009). In the present study, only CSD sinks were analyzed at each of the four recording locations and for each stimulus condition. Across all cortical regions, sinks were identified as being at least three standard deviations

(SDs) above the mean voltage measured during the 70 ms before either stimulus was presented. Within the majority of recording locations, prominent sinks were identified in the granular (−300 μm < depth ≥ −750 μm) and infragranular-upper layers (−750 μm < depth ≥ −1200 μm). Additional sinks of longer latency were observed in supragranular (depth ≥ −350 μm) and infragranular-lower layers (depth < −1200 μm) (Fig. 3.2A).

To assess changes across the cortical layers, CSD waveforms were extracted from the depth that demonstrated the highest amplitude within an individual sink (i.e., peak amplitude). For each of the four identified sinks, the peak amplitude was derived from a single depth in order to account for individual sink components that spanned various depths (e.g., extended beyond or were narrower than the space defined above). The peak amplitude was computed for all stimulus conditions. All calculations were performed using custom Matlab scripts.

3.2.8 Average Rectified CSD Analysis

To determine the overall strength of postsynaptic currents in each of the cortical areas, the average rectified CSD (AVREC) measure was applied to the CSD analysis (Schroeder et al., 1997, 2001; Happel et al., 2010; Stolzberg et al., 2012). Although rectification results in a loss of information about the direction of the transmembrane current flow, the AVREC waveform provides a measure of the temporal pattern of the overall strength of the postsynaptic currents (Givre et al., 1994; Schroeder et al., 1998; Happel et al., 2010). The AVREC was calculated by averaging the absolute values of the CSD across all channels (Eq. 2).

$$AVREC = \frac{\sum_{i=1}^{n} |CSD_i|(t)}{n} \tag{2}$$

where, CSD refers to Eq. 1, n refers to the number of channels, and t refers to the time point index. To complete a quantitative analysis of the AVREC, peak amplitude was calculated for all cortical areas and stimulus conditions within the first 200 ms from the onset of the visual stimulus.

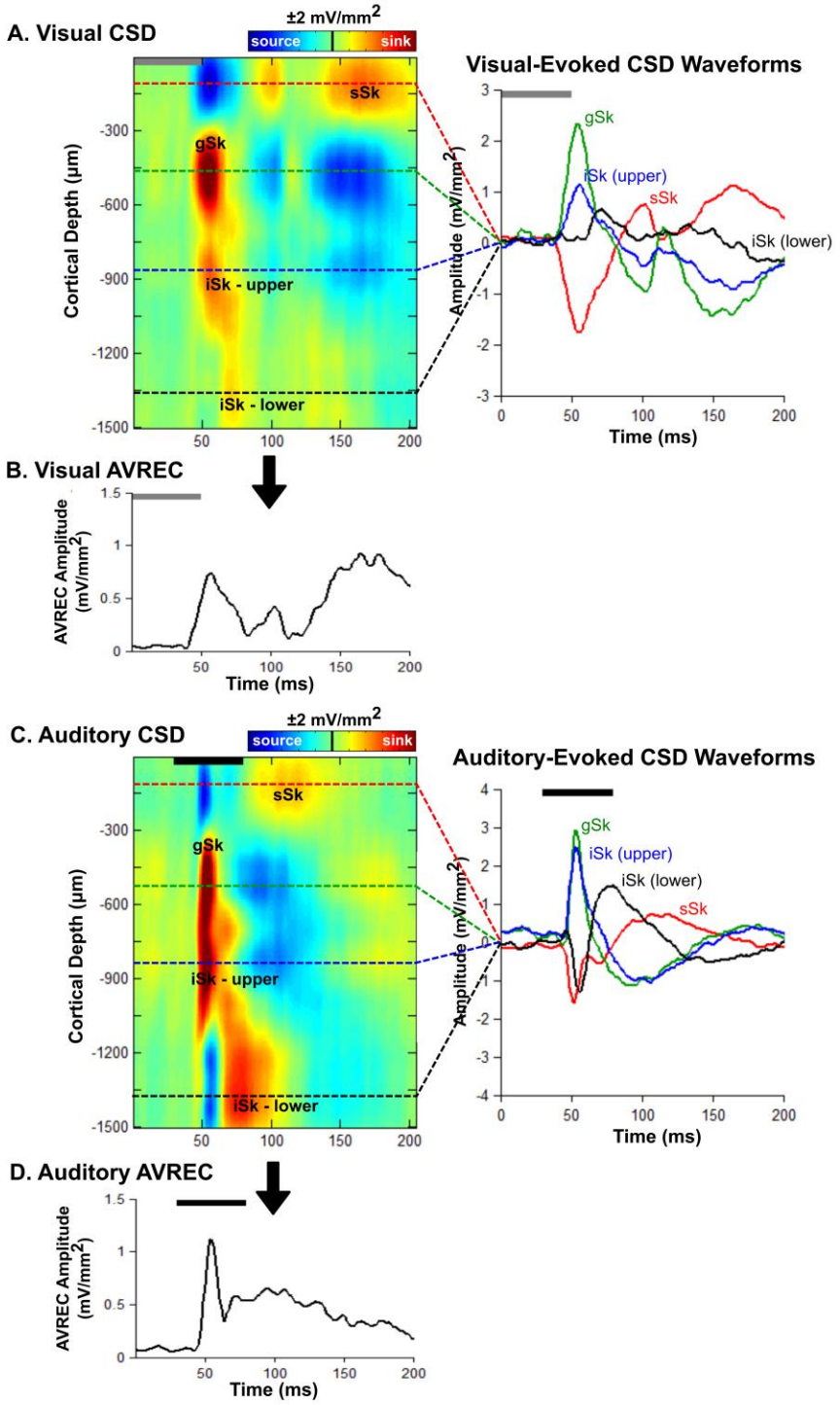

Figure 3.2. Visual- and auditory-evoked CSD profiles within the multisensory zone of the lateral extrastriate visual cortex (V2L-Mz).

(A) Representative CSD profile (left) and extracted CSD waveforms (right) from a control rat in response to a visual stimulus (50 ms LED flash at 15 lux, denoted by the grey bar).

Prominent current sinks (red) are reflective of a depolarization of neurons in the surrounding cortical region, whereas prominent current sources (blue) reflect a repolarization of neurons in the surrounding cortical regions. As shown in the CSD waveforms, the supragranular (sSk, red), granular (gSk, green), infragranular-upper (iSk upper, blue) and infragranular-lower (iSk lower, black) responses (sinks are positive, sources are negative) were extracted from the electrode showing the highest amplitude for each of the individual sinks (denoted by the dashed lines on the CSD images). (B) Average rectified current source density (AVREC) analysis derived from the CSD profiles in (A) in response to a visual stimulus. (C) Representative CSD profile (left) and extracted CSD waveforms (right) from a control rat in response to an auditory stimulus (50 ms noise burst at 40 dB above click threshold, denoted by the black bar). (D) Average rectified current source density (AVREC) analysis derived from the CSD profiles in (C) in response to an auditory stimulus.

3.2.9 Statistics

Statistical analyses were conducted on the data using various procedures, including repeated-measures analysis of variance (ANOVA), one-way ANOVA or paired/unpaired t-tests depending on the comparison of interest (see Results for details of each specific comparison). In several cases, statistical analyses commenced with a 3-way repeated-measures ANOVA, and following confirmation of significant interactions, subsequent 2-way repeated-measures ANOVAs were performed. All statistical comparisons used an alpha value of 0.05, and Bonferroni post hoc corrections were performed when appropriate. GraphPad Prism (GraphPad Software Inc.) and MATLAB (2012b; The Mathworks) were used for graphical display, and SPSS (Version 20, IBM Corporation) software was used for the various statistical analyses. Throughout the text and figures, data are presented as the mean values ± standard error of the mean (SEM).

3.2.10 Histology

At the completion of the electrophysiological experiment, the rats were injected with sodium pentobarbital (100 mg/kg; IP) in preparation for exsanguination via transcardial

perfusion of 0.1M phosphate buffer (PB), followed by 4% paraformaldehyde. Using a microtome (HM 430/34; Thermo Scientific, Waltham, MA), frozen sections (50 μm) were cut in the coronal plane and collected serially. The sections were mounted in fluorescent DAPI mounting medium (F6057 Fluoroshield™ with DAPI; Sigma, St. Louis, MO) and coverslipped. Because the recording electrode array was coated in fluorescent DiI cell-labeling solution prior to insertion into the cortex, it was possible to reconstruct the location and depth of the four recording penetrations in each rat (Fig. 3.1). Sections containing the recording penetrations were imaged with an Axio Vert A1 inverted microscope (Carl Zeiss Microscopy GmbH, Jena, Germany), and ZEN imaging software was used to reconstruct the location of each recording penetration.

3.3 Results

3.3.1 Noise-Induced Hearing Loss

To determine the effect of noise exposure on hearing sensitivity, the ABR threshold of the click, 4 and 20 kHz stimuli were compared at baseline versus two weeks post-noise in the noise exposed rats ($n = 9$). A two-way repeated-measures ANOVA ($F[1,8] = 24.9$, $p < 0.001$) with Bonferroni post hoc testing (adjusted p-value = 0.017) revealed that noise exposure caused a significant increase in the ABR threshold of the click (pre-noise 26.7 ± 1.2 dB SPL vs. post-noise 40.6 ± 1.6, $p < 0.001$), 4 kHz stimulus (pre-noise 22.8 ± 1.7 vs. post-noise 43.9 ± 3.2, $p < 0.001$), and 20 kHz stimulus (pre-noise 12.8 ± 1.7 vs. post-noise 36.7 ± 7.0, $p < 0.017$) (Fig. 3.3A). As expected at baseline, there was no difference in hearing sensitivity between the control and noise exposed rats for any of the stimuli (one-way ANOVA; $p > 0.05$) (Fig. 3.3A).

In addition to determining the ABR thresholds to the various stimuli, the amplitude of the first wave in response to the 90 dB SPL click stimulus was used to assess the level of damage to the cochlear hair cell afferents caused by the noise exposure (Kujawa and Liberman, 2009). When compared with baseline, the noise exposure resulted in a 55.6 ± 5.9% reduction of wave I amplitude measured two weeks later (pre-noise 1.67 ± 0.1 μV vs. post-noise 0.73 ± 0.09 μV, $p < 0.001$, paired t-test), whereas the baseline wave I

amplitude in the noise exposed rats was consistent with that of controls (1.5 ± 0.04 µV, p = 0.17, unpaired t-test) (Fig. 3.3B).

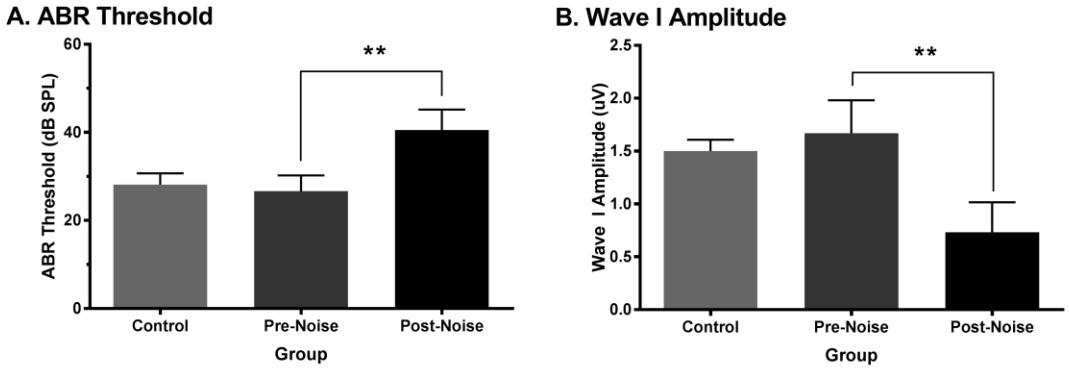

Figure 3.3. Assessment of the auditory brainstem response (ABR) to a click stimulus in control and noise exposed rats.

*ABR threshold (A) and amplitude of the first wave of the evoked response (B) to a click stimulus (0.1 ms) were assessed in control rats, as well as rats before (pre) and two weeks after (post) exposure to a loud broadband noise (0.8 – 20 kHz for two hours at 120 dB SPL). At baseline, the ABR click threshold and wave I amplitude did not differ between the control and noise exposed rats (p > 0.05). Compared to their pre-noise values, the rats in the noise exposure group showed a significant increase in their ABR threshold (**p < 0.001) and a decrease in their wave I amplitude (**p < 0.001) two weeks post-noise exposure. Values are mean ± SEM for the control (n = 8) and noise exposed (n = 9) groups.*

The sound intensity of the auditory stimulus (50 ms noise burst; 1–32 kHz) used in the electrophysiological experiments was adjusted for each rat to control for individual differences in hearing sensitivity. All rats were presented with an auditory stimulus that was 40 dB SPL above their ABR click threshold. Consequently, to account for their noise-induced hearing loss (Fig. 3.3A), the noise exposed rats were presented louder auditory stimulation than the controls during the electrophysiological experiment (noise exposed 81.3 ± 1.6 dB SPL vs. control 68.3 ± 0.9 dB SPL, p < 0.001, unpaired t-test).

3.3.2 Response Profile of Auditory, Visual and Audiovisual Cortices

The present study sought to characterize the effects of adult-onset hearing loss on laminar processing in auditory, visual and multisensory cortical areas. To that end, cortical plasticity throughout the distinct layers was investigated using analyses of the CSD sink amplitude as well as AVREC peak amplitude in response to auditory, visual and combined audiovisual stimuli. Guided by stereotaxic coordinates (Paxinos and Watson, 2007) and previous studies in the rat (Barth et al., 1995; Wallace et al., 2004; Hirokawa et al., 2008; Schormans et al., 2017a; Xu et al., 2014), 32-channel laminar recordings were performed in: (1) the primary visual cortex (V1); (2) the multisensory zone of the lateral extrastriate visual cortex (V2L-Mz); (3) the auditory zone of the lateral extrastriate visual cortex (V2L-Az); and (4) the dorsal auditory cortex (AuD) (Fig. 3.1).

In order to designate a given penetration to a particular cortical region for subsequent analysis, we relied on extensive pilot testing and stereotaxic consistency between experiments. In control rats, histological verification of each recording penetration was combined with an assessment of the response profile observed at that location to determine its designation. For example, in contrast to the V2L-Mz, the more ventral-positioned V2L-Az was more responsive to auditory than visual stimulation in control rats; findings which were consistent with our previous work using non-laminar recordings and high-density mapping (Schormans et al., 2017a). Furthermore, the V2L-Az in control rats could be differentiated from its neighbouring region, the AuD, because of consistent differences in the amplitude of the auditory-evoked AVREC (V2L-Az 2.2 ± 0.3 mV/mm^2 vs. AuD 1.5 ± 0.1 mV/mm^2). Finally, unlike in the AuD, recordings in the V2L-Az of control rats demonstrated mild visual activation observed in the AVREC peak amplitudes. Importantly, once the boundaries of the four cortical regions were established in the control rats, the recording penetrations reconstructed from the noise exposed rats could be designated according to their proximity to these boundaries. Ultimately, in control rats, V1 and AuD were considered predominantly unisensory areas, whereas the audiovisual cortex was comprised of two regions within the lateral extrastriate visual cortex (V2L-Mz and V2L-Az) (Schormans et al., 2017a).

3.3.3 Crossmodal Plasticity Occurred across Multiple Layers of the Higher-Order Sensory Cortices

Derived from the mean LFPs recorded simultaneously across the cortical thickness, the analysis of CSD sink amplitudes provided a measure of the current entering or leaving the neurons from the extracellular space through the cell membrane (Mitzdorf, 1985; Einevoll et al., 2013). For each cortical region, averaged CSD waveforms were computed in the two groups (control vs. noise exposed) within each individual sink (i.e., supragranular, granular, infragranular-upper, and infragranular-lower layers) in response to the visual stimulus. Given the number of factors included in the present study, statistical analysis of the visual-evoked CSD sink amplitudes began with a three-way repeated-measures ANOVA (group × cortical area × layer), which encompassed all of the data shown in Figure 3.4. As expected, this analysis yielded a significant interaction ($F[2.7,40.3] = 4.538$, $p < 0.01$). Due to the unique profile of each individual sink, subsequent statistical analyses were completed for each of the CSD sinks. Therefore, for each of the four panels in Figure 3.4 showing CSD sink amplitudes, a separate two-way repeated-measures ANOVA (group × cortical area) was performed with Bonferroni post hoc tests (adjusted p-value = 0.013).

Overall, we observed an increased level of postsynaptic activity in response to visual stimulation within multiple cortical regions and their distinct layers two weeks after noise exposure; findings consistent with crossmodal plasticity following partial hearing loss. Separate two-way repeated-measures ANOVAs of the CSD sink amplitudes revealed a significant interaction of group by cortical area in both the granular layer ($F[2.1,31.1] = 5.58$, $p < 0.01$) as well as the infragranular-upper layer ($F[2.0,29.6] = 4.989$, $p < 0.05$). Although the supragranular and infragranular-lower layers did not show a significant interaction between main effects, all cortical layers showed a main effect of area (supragranular: $F[1.8,24.1] = 80.7$, $p < 0.001$; granular: $F[2.1,31.1] = 56.8$, $p < 0.001$; infragranular-upper: $F[2.0,29.6] = 55.2$, $p < 0.001$; infragranular- lower: $F[1.6,24.1] = 43.6$, $p < 0.001$). As expected, visual-evoked CSD sink amplitudes within the primary visual cortex (V1) were not affected by noise-induced hearing loss in any cortical layer ($p > 0.05$). Conversely, noise-induced hearing loss caused a significant increase in visual-evoked CSD sink amplitudes within the supragranular ($p < 0.013$), granular ($p < 0.01$), and

infragranular-upper ($p < 0.01$) layers of the multisensory zone of V2L (V2L-Mz). Similarly, the neighbouring region of the V2L-Az, which predominantly responded to auditory stimuli in control rats, showed a noise-induced increase in visual-evoked CSD sink amplitude within the granular ($p < 0.01$) and infragranular-upper ($p < 0.05$) layers. Taken together, these results reveal for the first time that hearing loss-induced crossmodal plasticity was not restricted to a single layer of the higher order sensory cortices.

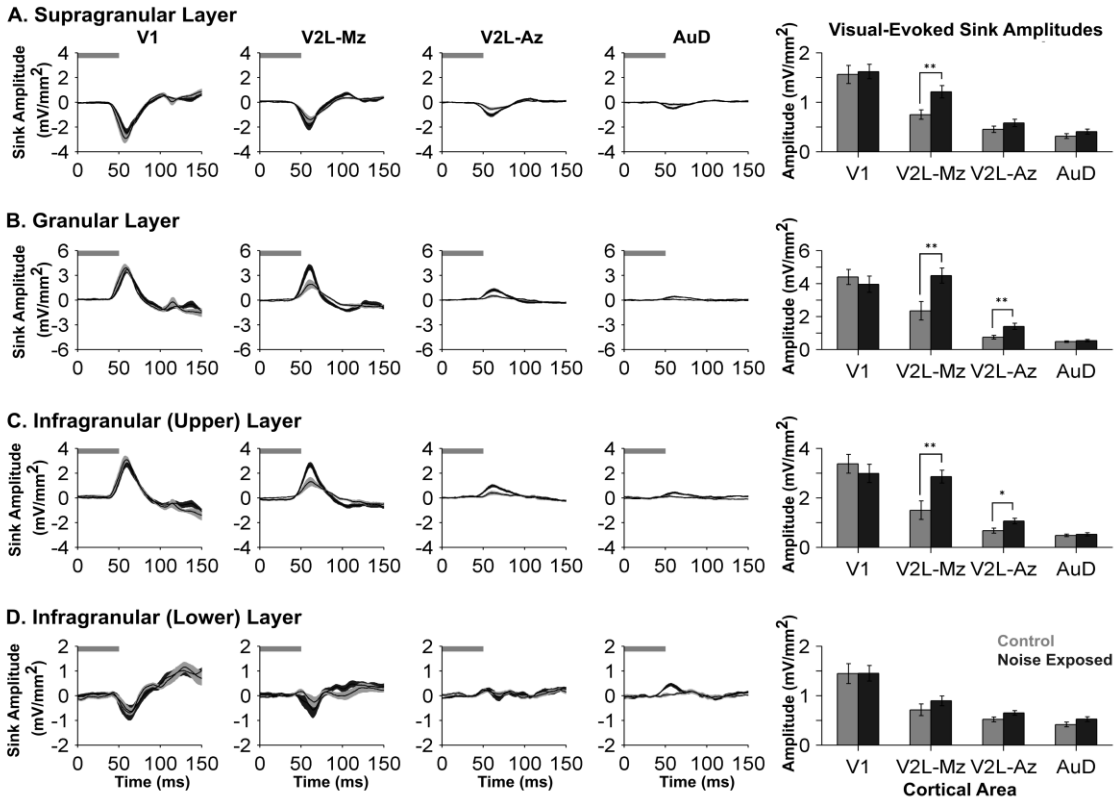

Figure 3.4. Increased visual responsiveness occurred across the cortical layers within higher-order sensory regions.

Averaged CSD waveforms from supragranular (A), granular (B), infragranular-upper (C), and infragranular-lower (D) layers within all recordings locations (i.e. V1, V2L-Mz, V2L-Az, and AuD; from left to right). Horizontal grey bar denotes the visual stimulus and the dark lines represent the group mean and shading represents the SEM for the noise exposed (dark grey; n = 9) and control (light grey; n = 8) groups. Note that in order to display the changes that occurred within each of the cortical layers, each y-ordinate is specific to the

*waveform profile for that layer. An analysis of sink amplitudes within each cortical layer (see bar graphs on the far right) shows a significant increase in visual responsiveness with the multisensory zone of V2L (V2L-Mz) across most cortical layers. This evidence of hearing loss-induced crossmodal plasticity was also present in the granular ($p < 0.01$) and the infragranular-upper layer ($p < 0.01$) of the auditory zone of V2L (V2L-Az). Values are mean ± SEM for the noise exposed ($n = 9$) and control ($n = 8$) groups. *$p < 0.05$; **$p < 0.013$*

3.3.4 Central Gain Enhancement was Layer-Specific and Did Not Extend Beyond the Auditory Cortex

Averaged CSD waveforms in response to auditory stimuli were also computed for the two groups within each of the four identified sinks (i.e., supragranular, granular, infragranular-upper, and infragranular-lower layers). Statistical analyses of the auditory-evoked CSD sink amplitudes began with a three-way repeated-measures ANOVA, which revealed a significant interaction ($F[2.7,40.4] = 10.9$, $p < 0.001$) of group by cortical area by layer (Fig. 3.5). Thus, subsequent analyses were completed for each of the four individual CSD sinks, whereby a separate two-way repeated-measures ANOVA (group × cortical area) was performed with Bonferroni post hoc tests (adjusted p-value = 0.013) for each of the four bar graphs presented in Figure 3.5.

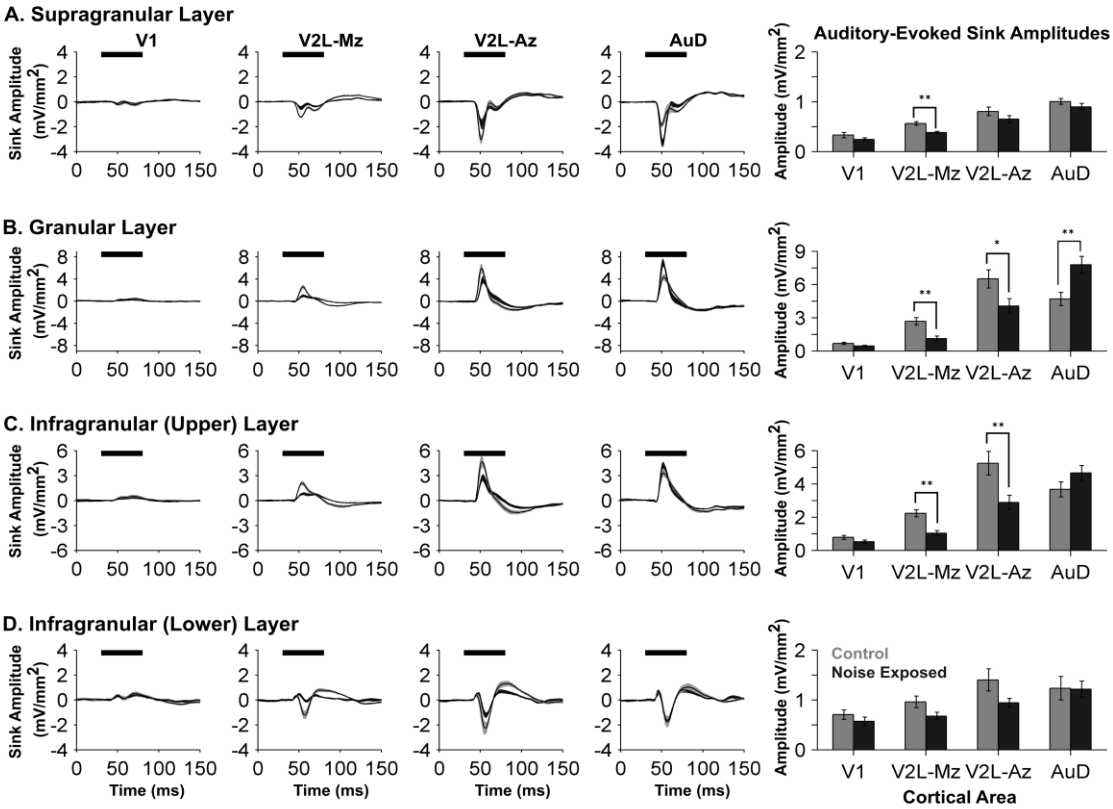

Figure 3.5. Noise-induced hearing loss caused region- and layer-specific plasticity in the auditory-evoked CSD profiles across auditory, visual and audiovisual cortices. *Averaged CSD waveforms from supragranular (A), granular (B), infragranular-upper (C), and infragranular-lower (D) layers within all recording locations (i.e. V1, V2L-Mz, V2L-Az, and AuD; from left to right). The horizontal black bar denotes the presentation of the auditory stimulus, and the dark lines represent the group mean and shading represents the SEM for the noise exposed (dark grey; n = 9) and control (light grey; n = 8) groups. Consistent with Figure 3.4, the y-ordinate is specific to the waveform profile for each cortical layer. An analysis of auditory-evoked sink amplitudes (see bar graphs on the far right) shows a decrease in sink amplitude within V2L-Mz and V2L-Az, despite adjusting for individual rat differences in hearing sensitivity. Whereas both sub-regions of V2L demonstrated crossmodal plasticity (i.e., increased visual responsiveness and a commensurate decrease in auditory), their neighbouring cortical region, AuD, showed a significant increase in auditory-evoked sink amplitude (p < 0.01), which was restricted to*

*the granular layer. Values are mean ± SEM for the noise exposed (n = 9) and control (n = 8) groups. *p < 0.05; **p < 0.013*

Auditory-evoked CSD sink amplitudes showed differential changes across the neighbouring cortical regions following noise exposure, as evidenced by significant interactions of group by cortical area in both the granular layer ($F[2.0,30.0] = 12.04$, $p < 0.001$) and infragranular-upper layer ($F[1.9,28.9] = 11.7$, $p < 0.001$) (Fig. 3.5; two-way repeated-measures ANOVAs). Furthermore, despite accounting for noise-induced hearing loss by adjusting the sound level of the auditory stimulus to be 40 dB above each rat's click threshold, the auditory-evoked CSD sink amplitudes were reduced across multiple layers in the audiovisual cortex of noise exposed rats. More specifically, within the multisensory zone of the V2L, noise exposure caused a significant decrease in the auditory-evoked CSD sink amplitude in the supragranular layer (control: 0.56 mV/mm^2 vs. noise exposed: 0.38 mV/mm^2, $p < 0.001$), granular layer (control: 2.68 mV/mm^2 vs. noise exposed: 1.11 mV/mm^2, $P < 0.001$), and infragranular-upper layer (control: 2.23 mV/mm^2 vs. noise exposed: 1.04 mV/mm^2, $p < 0.001$) (V2L-Mz; Fig. 3.5). Similarly, the auditory zone of the V2L showed a decrease in auditory-evoked CSD sink amplitude within the granular layer ($p = 0.034$) and infragranular-upper layer ($p < 0.01$) (V2L-Az; Fig. 3.5). A drastically different profile, however, emerged within the granular layer of the neighbouring auditory cortex, AuD (control: 4.69 mV/mm^2 vs. noise exposed: 7.77 mV/mm^2, $p < 0.01$; Fig. 3.5). To summarize, unlike the observed reduction in the net positive current entering the neurons in the granular layer of the audiovisual cortex (V2L-Az), the CSD sink amplitude in AuD increased following noise exposure; findings consistent with central gain enhancement in this higher order auditory area.

3.3.5 Noise Exposure Caused a Differential Effect on AVREC Peak Amplitude in the Auditory, Visual and Audiovisual Cortices

As a complement to the comparisons performed on individual CSD sinks, AVREC waveforms were computed for each of the four cortical regions in response to the separately presented auditory and visual stimuli. These results were then compared between groups

to provide an assessment of whether noise exposure changed the overall activation of postsynaptic currents in the different cortices (Fig. 3.6). An initial three-way repeated-measures ANOVA revealed a significant interaction of group by cortical area by stimulus ($F[3,45] = 10.6$, $p < 0.001$) for the AVREC peak amplitude. Consequently, for each of the unimodal stimulus conditions (i.e., visual, Fig. 3.6A; auditory, Fig. 3.6B), a separate two-way repeated measures ANOVA (group × cortical area) was performed with Bonferroni post hoc tests (adjusted p-value = 0.013).

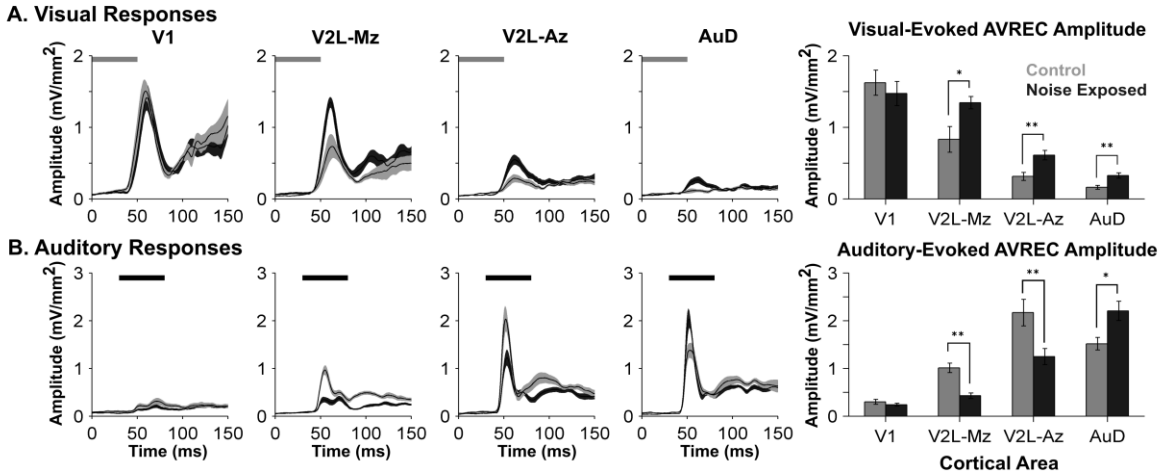

Figure 3.6. Neighbouring cortical regions were differentially affected by noise-induced hearing loss as measured by the stimulus-evoked AVREC peak amplitudes. *AVREC waveforms from V1, V2L-Mz and V2L-Az, AuD (from left to right) in response to a visual (A) and auditory (B) stimulus. In response to visual stimulation (A), noise exposed rats (dark grey) showed increased AVREC peak amplitudes within sub-regions of the multisensory cortex (V2L-Mz and V2L-Az) as well as the neighbouring dorsal auditory cortex (AuD). The horizontal grey and black bar denotes the presentation of the visual and auditory stimuli, respectively. In response to auditory stimulation (B), AVREC peak amplitudes were significantly reduced within the audiovisual cortex (V2L-Mz and V2L-Az) in noise exposed rats when compared to controls. Alternatively, noise exposed rats showed increased auditory-evoked activity within the dorsal auditory cortex (AuD). In the AVREC waveform plots, dark lines represent the group mean and shading represents the SEM for the noise exposed (dark grey; n = 9) and control (light grey; n = 8) groups. Values plotted*

*in the bar graphs on the far right are mean ± SEM for the noise exposed (n = 9) and control (n = 8) groups. *p < 0.05; **p < 0.013*

Consistent with the associated CSD profiles, noise exposure caused differential changes in the AVREC peak amplitude in the visual (V1), auditory (AuD) and audiovisual cortices (V2LMz; V2L-Az), whereby the nature and extent of this plasticity depended on the stimulus modality presented (Fig. 3.6). For example, in response to visual stimulation (Fig. 3.6A), an increase in AVREC peak amplitude was observed within the multisensory zone of V2L (V2L-Mz, $p = 0.018$), the auditory zone of V2L (V2L-Az; $p < 0.01$) and the dorsal auditory cortex (AuD; $p < 0.01$). There was no significant two-way interaction between the main effects of cortical area and group for visual-evoked AVREC peak amplitude ($F[1.8,27.2] = 3.35$, $p = 0.054$); however, there was a main effect of cortical area ($F[1.8,27.2] = 61.65$, $p < 0.001$). Thus, throughout the neighbouring regions of the higher order sensory cortices, noise exposure induced crossmodal plasticity which was characterized by an increase in the overall activation of postsynaptic currents in response to visual stimuli (Fig. 3.6A).

The effect of noise-induced hearing loss on the auditory-evoked AVREC peak amplitude was also examined in the four cortical regions (Fig. 3.6B). Despite accounting for each rat's hearing sensitivity, a two-way repeated measures ANOVA found a significant interaction of group by cortical area ($F[1.9,29.2] = 13.9$, $p < 0.001$) on the auditory-evoked AVREC peak amplitude. Furthermore, compared with the controls, post hoc testing revealed that the noise exposed rats had a significant decrease in AVREC peak amplitude in response to auditory stimulation within the audiovisual cortex (e.g., V2L-Mz $p < 0.001$; V2L-Az, $p < 0.013$). In stark contrast, the once-predominantly auditory region, AuD, showed a paradoxical increase (51 ± 17%) in its response to auditory stimulation following noise-induced hearing loss (AVREC peak amplitude: control: 1.52 mV/mm^2 vs. noise exposed: 2.21 mV/mm^2, $p = 0.014$; Fig. 3.6B); findings indicative of central gain enhancement. Collectively, these results further confirmed that noise-induced hearing loss

caused the neighbouring regions of the higher-order sensory cortices to experience differential plasticity at the level of postsynaptic potentials.

3.3.6 Audiovisual Responsiveness was Preserved Despite the Co-Existence of Central Gain Enhancement and Crossmodal Plasticity in Higher-Order Sensory Cortices

In addition to the separately presented auditory and visual cues, we delivered these stimuli in combination to the noise exposed rats and age-matched controls in order to determine if audiovisual responsiveness was affected by adult-onset hearing loss. To that end, we used the granular sink and AVREC peak amplitudes to assess whether the actual responses to audiovisual stimuli deviated from the linear summation of the two unisensory responses. Based on this established approach (Laurienti et al., 2005; Lippert et al., 2013; Stein et al., 2009), we expected that the predominantly unisensory areas (V1 and AuD) in control rats would show a near-linear relationship between the actual (i.e., measured) response to the combined audiovisual stimuli and the predicted response (i.e., the sum of the separately presented auditory and visual stimuli). Furthermore, it was expected that the audiovisual regions of the lateral extrastriate visual cortex (V2L-Mz and V2L-Az) would instead show a sublinear relationship because the measured response to the combined audiovisual stimuli would be less than the summation of the two unisensory conditions; a finding which would be consistent with recordings in the multisensory cortices of various species (Meredith and Allman et al., 2012; Foxworthy et al., 2013).

Within the predominantly unisensory areas of control rats, AuD showed a near-linear interaction in which the measured response within the granular sink to the combined audiovisual stimuli was nearly equivalent to that of the predicted (summed) response (94.5 ± 2.9% of predicted), whereas V1 demonstrated a modest sublinear audiovisual interaction within the granular sink (85.8 ± 3.9% of predicted; Fig. 3.7A). As shown in Figure 3.7B, AVREC analyses revealed a similar trend within these two predominantly unisensory cortical regions, with the majority of the data from the control rats clustering along the line of unity (i.e., measured = predicted). Also consistent with our expectations for control rats,

we observed that the multisensory zone of V2L (V2L-Mz) demonstrated the largest sublinear relationship, in which the measured response failed to approximate the predicted sum of the unisensory responses (granular sink: 78.6 ± 3.9% of predicted; AVREC peak amplitude: 75.1 ± 9.8% of predicted). Finally, the auditory zone of V2L (V2L-Az) of control rats showed a modest sublinear response (granular sink: 88.6 ± 3.7%; AVREC peak amplitude: 85.3 ± 2.7% of predicted).

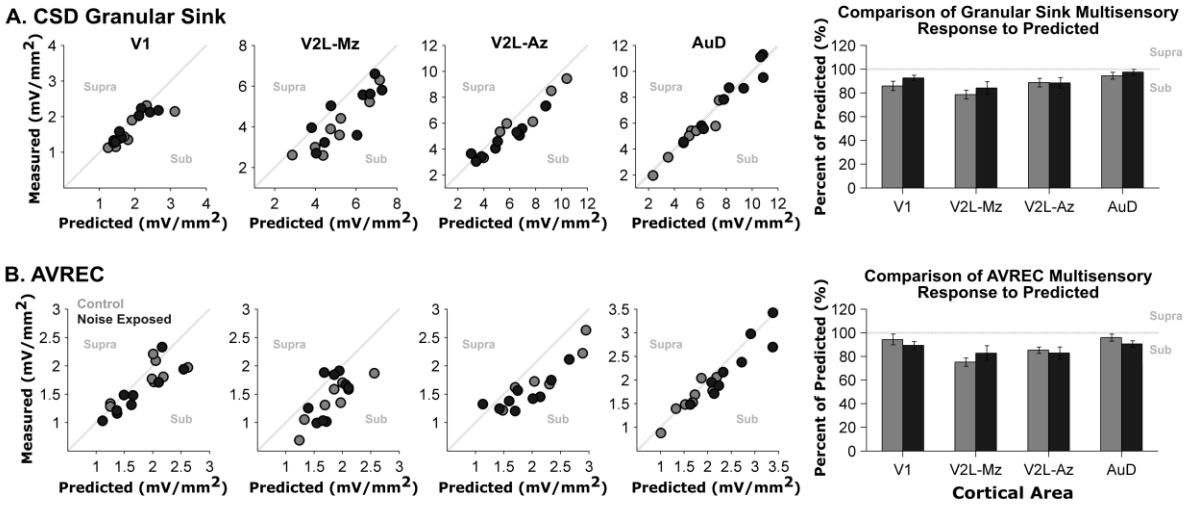

Figure 3.7. Audiovisual responsiveness was not affected by noise induced-hearing loss within the auditory, visual and audiovisual cortices.

Quantification of audiovisual responsiveness was completed for each experiment by determining to what degree the measured audiovisual response deviated from the predicted (summed) response. For each recording location, the measured audiovisual granular sink amplitudes (A) and AVREC peak amplitudes (B) are plotted with respect to their predicted (summed) amplitude for control (grey dots, n = 8) and noise exposed rats (dark grey dots; n = 9). Responses within the primary visual (V1; far left) and dorsal auditory cortex (AuD; far right scatter plot) predominantly fall near the line of unity, as a result of the measured amplitude to the combined audiovisual stimuli being equivocal to the predicted sum of the separately-presented auditory and visual stimuli. However, responses in the audiovisual cortex (V2L-Mz) were predominantly sub-linear (i.e., below the line of unity), because the

combined audiovisual response was smaller than the predicted sum. On each scatter plot, the words supra and sub describe the polarity of the response (i.e. responses that were greater- or lesser than the predicted sum were supra-additive or sub-additive, respectively). Overall, no significant differences were found between control and noise exposed groups for the granular sink or AVREC peak amplitudes across all recording locations.

Ultimately, to assess the effect of noise-induced hearing loss on audiovisual responsiveness, we compared whether the responses to audiovisual stimuli in the noise exposed rats deviated from the linear summation of the two unisensory responses to the same extent as was observed in the age-matched controls. Overall, a comparison of control versus noise exposed rats showed no significant difference between groups for the granular sink or AVREC peak amplitude for all cortical areas ($p > 0.05$). Furthermore, there was no significant interaction between the main effects of cortical area and group for both the granular sink ($F[3,45] = 0.341$, $p = 0.80$) and AVREC peak amplitude ($F[3,45] = 0.916$, $p = 0.44$). There was, however, a main effect of cortical area for both the granular sink ($F[3,45] = 5.074$, $p < 0.01$) and AVREC peak amplitude ($F[3,45] = 4.391$, $p < 0.01$); findings which (not surprisingly) indicated that the cortical areas did indeed show a differential response to audiovisual stimuli. Collectively, these results revealed that noise-induced hearing loss did no disrupt audiovisual responsiveness despite the co-existence of central gain enhancement and crossmodal plasticity within the higher-order sensory cortices.

3.4 Discussion

In the present study, we conducted the first investigation of altered laminar processing in the auditory, visual and audiovisual cortices following adult-onset hearing loss. More specifically, we compared the auditory and visually evoked postsynaptic activity in noise exposed rats versus age-matched controls to assess the cortical region- and layer-specificity of central gain enhancement and crossmodal plasticity; two phenomena that were known to occur following hearing impairment, but had never been studied concurrently. LFP

recordings and the subsequent CSD analyses revealed that central gain enhancement was restricted to the granular layer of the once-predominantly auditory area, AuD, whereas crossmodal plasticity—characterized by an increase in visual responsiveness—was evident across multiple layers of the audiovisual cortex (V2L) and extended into AuD. Surprisingly, despite these neighbouring cortical regions showing differing degrees of central gain enhancement and crossmodal plasticity, noise-induced hearing loss did not disrupt their overall responsiveness to combined audiovisual stimuli. Taken together, our results have shown for the first time that the plasticity induced by partial hearing loss manifests differentially across the layers of neighbouring regions of the higher order sensory cortices.

3.4.1 Cortical Region- and Layer-Specific Plasticity Following Partial Hearing Loss

Noise-induced hearing loss resulted in both region- and layer-specific plasticity in the auditory (AuD) and audiovisual cortices (V2L-Mz and V2L-Az). As predicted, central gain enhancement occurred in the higher order auditory area, AuD, characterized by an increase in synaptic input as measured by the AVREC peak amplitude (Fig. 3.6). This heightened auditory-evoked activity in the AuD was consistent with the increase in evoked potentials observed previously in the core auditory cortex following loud noise exposure in rats (Popelar et al., 1995, 2008). Interestingly, central gain enhancement was not present across all layers of the AuD, as only the granular layer showed a significant increase in CSD sink amplitude (Fig. 3.5B). Unexpectedly, there was no evidence of a noise-induced increase in auditory activation within the sub-regions of the audiovisual cortex (V2L-Mz and V2L-Az). In fact, across these cortical layers, partial hearing loss caused a significant decrease in auditory-evoked CSD sink amplitudes (Fig. 3.5). The restricted emergence of central gain enhancement in only the higher-order auditory cortex was surprising given that the audiovisual cortex in rodents (and other species) is known to receive extensive inputs from the auditory cortex (Budinger et al., 2000, 2006; Budinger and Scheich, 2009; Laramée et al., 2011). Based on this areal convergence, we had predicted that the hyperexcitability observed in the auditory cortex would be relayed to the directly connected audiovisual areas; however, this was not the case. Thus, our results provide the first direct evidence

that deprivation-induced central gain enhancement does not extend into the audiovisual cortex following partial hearing loss in adulthood.

Although the neighbouring regions of the auditory and audiovisual cortices experienced differential changes in their auditory responsiveness post-noise exposure (i.e., increased in AuD vs. decreased in V2L), both cortical areas experienced crossmodal plasticity, whereby the overall strength of the postsynaptic currents (AVREC) increased in response to visual stimulation (Fig. 3.6). Based on these LFP-derived results, it is reasonable to expect that this amplified visual input to V2L and AuD would facilitate an increase in neuronal spiking responses following partial hearing loss. Indeed, in our previous mapping study, we reported that an increased proportion of neurons in the AuD and V2L of noise exposed rats showed spiking responses to visual stimulation compared with age-matched controls (Schormans et al., 2017a).

We are unaware of any human studies that have investigated the coexistence of central gain enhancement and crossmodal plasticity; however, there have been recent reports of altered auditory and visual processing in hearing-impaired adults. For example, using functional magnetic resonance imaging (fMRI), Puschmann and Thiel (2017) found that the severity of hearing loss in adults was associated with an increase in the functional connectivity between the auditory cortex and the motion-sensitive visual area MT during audiovisual processing. Furthermore, in a series of studies using passively elicited EEG responses and current source localization procedures, Campbell and Sharma found that the temporal cortex of adults with mild-moderate hearing loss showed a reduced activation to speech sounds (2013) and an increased activation to visual stimuli (2014). Moreover, because this passive listening caused an increased activation of frontal cortical regions in these hearing-impaired adults, it was suggested that, in addition to crossmodal plasticity, a re-allocation of cortical resources had occurred such that frontal areas were now tasked with supporting non-attentive auditory processing (Campbell and Sharma, 2013). Ultimately, future studies will be needed to determine the long-term, functional consequences that follow the initial period of sensory reorganization observed in the present study. In addition to the suggestion to use longitudinal studies to track the progression of hearing loss-induced changes in audiovisual processing (Musacchia et al., 2009; Campbell and Sharma, 2014), it will also

be important to determine how the severity of hearing loss impacts the emergence and persistence of central gain enhancement and crossmodal plasticity in hearing-impaired adults.

3.4.2 Putative Mechanisms of Central Gain Enhancement and Crossmodal Plasticity

At present, the structural and/or physiological changes contributing to central gain enhancement and crossmodal plasticity have not been fully elucidated. Because we have shown that these phenomena can coexist following partial hearing loss, it is worth considering whether they share putative mechanisms. It has been proposed that central gain enhancement (Auerbach et al., 2014) and crossmodal plasticity (Nys et al., 2015) may arise from a loss of intracortical inhibition, which is perhaps not surprising given that noise exposure is known to alter the balance of excitation and inhibition in cortical circuits (Yang et al., 2011). In addition, it has long been suggested that an unmasking of inputs could lead to cortical crossmodal plasticity following sensory deprivation (Rauschecker, 1995), and it was recently proposed that central gain enhancement might represent an emergent property of altered network activity due to unmasked synaptic connections (Auerbach et al., 2014). Indeed, the upscaling of excitatory synapses via homeostatic plasticity mechanisms could increase the strength of previously subthreshold inputs following sensory deprivation (Lee, 2012; Lee and Whitt, 2015). That said, because the majority of studies investigating homeostatic mechanisms associated with crossmodal plasticity have used models of complete sensory loss (for review, see Whitt et al., 2014), future studies are needed to determine whether partial hearing loss is sufficient to cause crossmodal plasticity (and/or central gain enhancement) via synaptic scaling.

It is important to note that the mechanisms underlying central gain enhancement and crossmodal plasticity need not be constrained to intrinsic changes in the cortex. For example, cortical crossmodal plasticity could manifest from altered multisensory processing in subcortical areas that becomes effectively relayed to the impaired cortex (Allman et al., 2009; Laramée et al., 2011; Mezzera and López-Bendito, 2015). Interestingly, we observed that the changes induced by partial hearing loss were not restricted to processing within the supragranular/infragranular layers, as the granular CSD

sink amplitudes were also greatly affected (Fig. 3.5B). More specifically, within the audiovisual cortex (V2L-Mz and V2LAz), there was an increased response to visual stimulation, coupled with reduced input during auditory stimulation (Fig. 3.4B). At the same time, increased auditory activation was restricted to the granular layer; indicative of central gain enhancement within the neighbouring auditory area, AuD (Fig. 3.5B). Taken together, these results identify the potential contribution of thalamocortical projections to both central gain enhancement and cortical crossmodal plasticity following a modest hearing loss. Ultimately, because a previous study found that exposure to complete deafness for 6–8 days potentiated thalamocortical synapses in the primary visual cortex but not in the primary auditory cortex of mice (Petrus et al., 2014), future studies are warranted to explore the contribution of thalamocortical plasticity following partial hearing loss.

3.4.3 Audiovisual Processing and Partial Hearing Loss

In addition to revealing that noise-induced central gain enhancement and crossmodal plasticity were not mutually exclusive phenomena, we also investigated whether partial hearing loss affected the responsiveness of the higher order sensory cortices to combined audiovisual stimulation. Of the neighbouring cortical regions in control rats, the multisensory zone of the V2L (V2L-Mz) showed the largest degree of audiovisual processing as assessed by an established metric of additivity (see Methods; Laurienti et al., 2005; Lippert et al., 2013; Stein et al., 2009). As expected in control rats, we observed that the responsiveness of the V2L-Mz to the combined audiovisual stimulation failed to match the sum of the separately presented auditory and visual stimuli (i.e., there was a sublinear relationship; Fig. 3.7). At the same time, the AuD of control rats showed a near-linear relationship; findings which indicated that visual stimulation had a limited effect on auditory processing in this predominantly auditory area prior to hearing loss. Surprisingly, despite partial hearing loss causing both central gain enhancement and crossmodal plasticity, the relationships between the actual (measured) versus predicted (summed) responses were preserved in the neighbouring regions of their higher-order sensory cortices, such that the noise exposed rats showed the same degree of audiovisual additivity as the age-matched controls (Fig. 3.7). At this time, it is unclear how this preservation of

audiovisual responsiveness in the presence of layer-specific central gain enhancement and crossmodal plasticity, ultimately impacts audiovisual perception.

To date, only a few studies in humans have investigated how partial hearing loss affects audiovisual processing and multisensory integration, and the results suggest potential disparity between the subjects' behavioural performance versus the associated cortical activity. For example, during tasks requiring participant perceptual reporting, audiovisual integration of speech stimuli was similar between older adults with mild-moderate hearing impairment compared with normal-hearing listeners of the same age (Tye-Murray et al., 2007) or younger (Başkent and Bazo, 2011). In contrast, compared with age-matched controls, older adults with hearing loss showed degraded audiovisual integration as assessed with cortical evoked potentials elicited by watching and listening to speech stimuli (Musacchia et al., 2009).

Given that it is possible to train laboratory animals, including rodents, to perform complex audiovisual tasks (Sakata et al., 2004; Hirokawa et al., 2008; Gleiss and Kayser, 2012; Raposo et al., 2012; Siemann et al., 2015; Schormans et al., 2017b), we suggest that coupling electrophysiological recordings with behavioural studies could help to elucidate the effect of adult-onset hearing loss on audiovisual processing and perception. Using such models, it would be possible to determine the degree to which the adult brain is capable of compensating for hearing impairment, and by extension, the severity of hearing loss that ultimately results in a failure to accurately integrate audiovisual stimuli. Guided by the results of the present study, our future work will seek to uncover the perceptual implications of the complex assortment of the hearing loss-induced intramodal and crossmodal changes that occur across the layers of the higher order sensory cortices.

3.5 References

Agrawal, Y., Platz EA, and Niparko JK (2008). Prevalence of hearing loss and differences by demographic characteristics among us adults: Data from the national health and nutrition examination survey, 1999-2004. *Arch. Intern. Med*. 168, 1522–1530.

Allman, B.L., and Meredith, M.A. (2007). Multisensory Processing in "Unimodal" Neurons: Cross-Modal Subthreshold Auditory Effects in Cat Extrastriate Visual Cortex. *J. Neurophysiol.* 98, 545–549.

Allman, B.L., Bittencourt-Navarrete, R.E., Keniston, L.P., Medina, A.E., Wang, M.Y., and Meredith, M.A. (2008). Do Cross-Modal Projections Always Result in Multisensory Integration? *Cereb. Cortex* 18, 2066–2076.

Allman, B.L., Keniston, L.P., and Meredith, M.A. (2009). Adult deafness induces somatosensory conversion of ferret auditory cortex. *Proc. Natl. Acad. Sci.* 106, 5925–5930.

Auer, E.T., Bernstein, L.E., Sungkarat, W., and Singh, M. (2007). Vibrotactile Activation of the Auditory Cortices in Deaf versus Hearing Adults. *Neuroreport* 18, 645–648.

Auerbach, B.D., Rodrigues, P.V., and Salvi, R.J. (2014). Central gain control in tinnitus and hyperacusis. *Front. Neurol.* 5, 206.

Barth, D.S., Goldberg, N., Brett, B., and Di, S. (1995). The spatiotemporal organization of auditory, visual, and auditory-visual evoked potentials in rat cortex. *Brain Res.* 678, 177–190.

Başkent, D., and Bazo, D. (2011). Audiovisual asynchrony detection and speech intelligibility in noise with moderate to severe sensorineural hearing impairment. *Ear Hear.* 32, 582–592.

Budinger, E., and Scheich, H. (2009). Anatomical connections suitable for the direct processing of neuronal information of different modalities via the rodent primary auditory cortex. *Hear. Res.* 258, 16–27.

Budinger, E., Heil, P., and Scheich, H. (2000). Functional organization of auditory cortex in the Mongolian gerbil (Meriones unguiculatus). III. Anatomical subdivisions and corticocortical connections. *Eur. J. Neurosci.* 12, 2425–2451.

Budinger, E., Heil, P., Hess, A., and Scheich, H. (2006). Multisensory processing via early cortical stages: Connections of the primary auditory cortical field with other sensory systems. *Neuroscience* 143, 1065–1083.

Campbell, J., and Sharma, A. (2013). Compensatory changes in cortical resource allocation in adults with hearing loss. *Front. Syst. Neurosci*. 7, 71.

Campbell, J., and Sharma, A. (2014). Cross-Modal Re-Organization in Adults with Early Stage Hearing Loss. *PLOS ONE* 9, e90594.

Doucet, M.E., Bergeron, F., Lassonde, M., Ferron, P., and Lepore, F. (2006). Cross-modal reorganization and speech perception in cochlear implant users. *Brain* 129, 3376–3383.

Einevoll, G.T., Kayser, C., Logothetis, N.K., and Panzeri, S. (2013). Modelling and analysis of local field potentials for studying the function of cortical circuits. *Nat. Rev. Neurosci.* 14, 770–785.

Engineer, N.D., Riley, J.R., Seale, J.D., Vrana, W.A., Shetake, J.A., Sudanagunta, S.P., Borland, M.S., and Kilgard, M.P. (2011). Reversing pathological neural activity using targeted plasticity. *Nature* 470, 101.

Finney, E.M., Fine, I., and Dobkins, K.R. (2001). Visual stimuli activate auditory cortex in the deaf. *Nat. Neurosci.* 4, 1171–1173.

Finney, E.M., Clementz, Brett, A., Hickok, G., and Dobkins, K.R. (2003). Visual stimuli activate auditory cortex in deaf subjects: evidence from MEG. *Neuroreport* 14, 1425–1427.

Foxworthy, W.A., Allman, B.L., Keniston, L.P., and Meredith, M.A. (2013). Multisensory and unisensory neurons in ferret parietal cortex exhibit distinct functional properties. *Eur. J. Neurosci.* 37, 910–923.

Freeman, B., and Singer, W. (1983). Direct and indirect visual inputs to superficial layers of cat superior colliculus: a current source-density analysis of electrically evoked potentials. *J. Neurophysiol.* 49, 1075–1091.

Givre, S.J., Schroeder, C.E., and Arezzo, J.C. (1994). Contribution of extrastriate area V4 to the surface-recorded flash VEP in the awake macaque. *Vision Res.* 34, 415–428.

Gleiss, S., and Kayser, C. (2012). Audio-Visual Detection Benefits in the Rat. *PLOS ONE* 7, e45677.

Happel, M.F.K., Jeschke, M., and Ohl, F.W. (2010). Spectral integration in primary auditory cortex attributable to temporally precise convergence of thalamocortical and intracortical input. *J. Neurosci.* 30, 11114–11127.

Hirokawa, J., Bosch, M., Sakata, S., Sakurai, Y., and Yamamori, T. (2008). Functional role of the secondary visual cortex in multisensory facilitation in rats. *Neuroscience* 153, 1402–1417.

Hunt, D.L., Yamoah, E.N., and Krubitzer, L. (2006). Multisensory plasticity in congenitally deaf mice: How are cortical areas functionally specified? *Neuroscience* 139, 1507–1524.

Komiya, Hisashi, J.J.E. (2000). Spontaneous Firing Activity of Cortical Neurons in Adult Cats with Reorganized Tonotopic Map Following Pure-tone Trauma. *Acta Otolaryngol.* (Stockh.) 120, 750–756.

Kral, A., and Eggermont, J.J. (2007). What's to lose and what's to learn: Development under auditory deprivation, cochlear implants and limits of cortical plasticity. *Brain Res. Rev.* 56, 259–269.

Kral, A., Schröder, J.-H., Klinke, R., and Engel, A.K. (2003). Absence of cross-modal reorganization in the primary auditory cortex of congenitally deaf cats. *Exp. Brain Res.* 153, 605–613.

Kujawa, S.G., and Liberman, M.C. (2009). Adding Insult to Injury: Cochlear Nerve Degeneration after "Temporary" Noise-Induced Hearing Loss. *J. Neurosci.* 29, 14077–14085.

Laramée, M.E., Kurotani, T., Rockland, K.S., Bronchti, G., and Boire, D. (2011). Indirect pathway between the primary auditory and visual cortices through layer V pyramidal neurons in V2L in mouse and the effects of bilateral enucleation. *Eur. J. Neurosci.* 34, 65–78.

Laurienti, P.J., Perrault, T.J., Stanford, T.R., Wallace, M.T., and Stein, B.E. (2005). On the use of superadditivity as a metric for characterizing multisensory integration in functional neuroimaging studies. *Exp. Brain Res.* 166, 289–297.

Lee, H.-K. (2012). Ca-permeable AMPA receptors in homeostatic synaptic plasticity. *Front. Mol. Neurosci.* 5, 17.

Lee, H.-K., and Whitt, J.L. (2015). Cross-modal synaptic plasticity in adult primary sensory cortices. *Curr. Opin. Neurobiol*. 35, 119–126.

Lin, H.W., Furman, A.C., Kujawa, S.G., and Liberman, M.C. (2011). Primary Neural Degeneration in the Guinea Pig Cochlea After Reversible Noise-Induced Threshold Shift. *J. Assoc. Res. Otolaryngol.* 12, 605–616.

Lippert, M.T., Takagaki, K., Kayser, C., and Ohl, F.W. (2013). Asymmetric Multisensory Interactions of Visual and Somatosensory Responses in a Region of the Rat Parietal Cortex. *PLOS ONE* 8, e63631.

Lomber, S.G., Meredith, M.A., and Kral, A. (2010). Cross-modal plasticity in specific auditory cortices underlies visual compensations in the deaf. *Nat. Neurosci.* 13, 1421–1427.

Meredith, M.A., and Allman, B.L. (2009). Subthreshold multisensory processing in cat auditory cortex. *Neuroreport* 20, 126–131.

Meredith, M.A., and Allman, B.L. (2015). Single-unit analysis of somatosensory processing in the core auditory cortex of hearing ferrets. *Eur. J. Neurosci*. 41, 686–698.

Meredith, M.A., and Lomber, S.G. (2011). Somatosensory and visual crossmodal plasticity in the anterior auditory field of early-deaf cats. *Hear. Res*. 280, 38–47.

Meredith, M.A., Kryklywy, J., McMillan, A.J., Malhotra, S., Lum-Tai, R., and Lomber, S.G. (2011). Crossmodal reorganization in the early deaf switches sensory, but not behavioral roles of auditory cortex. *Proc. Natl. Acad. Sci.* 108, 8856–8861.

Meredith, M.A., Keniston, L.P., and Allman, B.L. (2012a). Multisensory dysfunction accompanies crossmodal plasticity following adult hearing impairment. *Neuroscience* 214, 136–148.

Meredith, M.A., Allman, B.L., Keniston, L.P., and Clemo, H.R. (2012b). "Are Bimodal Neurons the Same throughout the Brain?" In *The Neural Bases of Multisensory Processes*, eds. M.M. Murray, and M.T. Wallace, (Boca Raton, FL: CRC Press), 51-64

Mezzera, C., and López-Bendito, G. (2015). Cross-modal plasticity in sensory deprived animal models: From the thalamocortical development point of view. *J. Chem. Neuroanat.* 75, 32-40

Mitzdorf, U. (1985). Current source-density method and application in cat cerebral cortex: investigation of evoked potentials and EEG phenomena. *Physiol. Rev.* 65, 37–100.

Mitzdorf, U., and Singer, W. (1977). Laminar segregation of afferents to lateral geniculate nucleus of the cat: an analysis of current source density. *J. Neurophysiol.* 40, 1227–1244.

Mitzdorf, U., and Singer, W. (1980). Monocular activation of visual cortex in normal and monocularly deprived cats: an analysis of evoked potentials. *J. Physiol*. 304, 203–220.

Musacchia, G., Arum, L., Nicol, T., Garstecki, D., and Kraus, N. (2009). Audiovisual Deficits in Older Adults with Hearing Loss: Biological Evidence: *Ear Hear*. 30, 505–514.

Nicholson, C., and Freeman, J.A. (1975). Theory of current source-density analysis and determination of conductivity tensor for anuran cerebellum. *J. Neurophysiol*. 38, 356–368.

Nys, J., Smolders, K., Laramée, M.-E., Hofman, I., Hu, T.-T., and Arckens, L. (2015). Regional Specificity of GABAergic Regulation of Cross-Modal Plasticity in Mouse Visual Cortex after Unilateral Enucleation. *J. Neurosci*. 35, 11174–11189.

Paxinos, G., and Watson, C. (2007). The rat brain in stereotaxic coordinates (Burlington, MA: Elsevier Inc.).

Petrus, E., Isaiah, A., Jones, A.P., Li, D., Wang, H., Lee, H.-K., and Kanold, P.O. (2014). Crossmodal Induction of Thalamocortical Potentiation Leads to Enhanced Information Processing in the Auditory Cortex. *Neuron* 81, 664–673.

Popelar, J., Syka, J., and Berndt, H. (1987). Effect of noise on auditory evoked responses in awake guina pigs. *Hear. Res.* 26, 239–247.

Popelar, J., Hartmann, R., Syka, J., and Klinke, R. (1995). Middle latency responses to acoustical and electrical stimulation of the cochlea in cats. *Hear. Res.* 92, 63–77.

Popelar, J., Grecova, J., Rybalko, N., and Syka, J. (2008). Comparison of noise-induced changes of auditory brainstem and middle latency response amplitudes in rats. *Hear. Res.* 245, 82–91.

Popescu, M.V., and Polley, D.B. (2010). Monaural Deprivation Disrupts Development of Binaural Selectivity in Auditory Midbrain and Cortex. *Neuron* 65, 718–731.

Raposo, D., Sheppard, J.P., Schrater, P.R., and Churchland, A.K. (2012). Multisensory Decision-Making in Rats and Humans. *J. Neurosci.* 32, 3726–3735.

Rauschecker, J.P. (1995). Compensatory plasticity and sensory substitution in the cerebral cortex. *Trends Neurosci.* 18, 36–43.

Sakata, S., Yamamori, T., and Sakurai, Y. (2004). Behavioral studies of auditory-visual spatial recognition and integration in rats. *Exp. Brain Res.* 159, 409–417.

Salvi, R.J., Saunders, S.S., Gratton, M.A., Arehole, S., and Powers, N. (1990). Enhanced evoked response amplitudes in the inferior colliculus of the chinchilla following acoustic trauma. *Hear. Res.* 50, 245–257.

Salvi, R.J., Wang, J., and Ding, D. (2000). Auditory plasticity and hyperactivity following cochlear damage. *Hear. Res.* 147, 261–274.

Schormans, A.L., Typlt, M., and Allman, B.L. (2017a). Crossmodal plasticity in auditory, visual and multisensory cortical areas following noise-induced hearing loss in adulthood. *Hear. Res.* 343, 92–107.

Schormans, A.L., Scott, K.E., Vo, A.M.Q., Tyker, A., Typlt, M., Stolzberg, D., and Allman, B.L. (2017b). Audiovisual Temporal Processing and Synchrony Perception in the Rat. *Front. Behav. Neurosci.* 10.

Schroeder, C.E., Javitt, D.C., Steinschneider, M., Mehta, A.D., Givre, S.J., Jr, H.G.V., and Arezzo, J.C. (1997). N-methyl-d-aspartate enhancement of phasic responses in primate neocortex. *Exp. Brain Res.* 114, 271–278.

Schroeder, C.E., Mehta, A.D., and Givre, S.J. (1998). A spatiotemporal profile of visual system activation revealed by current source density analysis in the awake macaque. *Cereb. Cortex* N. Y. N 1991 8, 575–592.

Schroeder, C.E., Lindsley, R.W., Specht, C., Marcovici, A., Smiley, J.F., and Javitt, D.C. (2001). Somatosensory Input to Auditory Association Cortex in the Macaque Monkey. *J. Neurophysiol*. 85, 1322–1327.

Siemann, J.K., Muller, C.L., Bamberger, G., Allison, J.D., Veenstra-VanderWeele, J., and Wallace, M.T. (2015). A novel behavioral paradigm to assess multisensory processing in mice. *Front. Behav. Neurosci*. 8.

Stein, B.E., Stanford, T.R., Ramachandran, R., Perrault, T.J., and Rowland, B.A. (2009). Challenges in quantifying multisensory integration: alternative criteria, models, and inverse effectiveness. *Exp. Brain Res.* 198, 113.

Stolzberg, D., Chrostowski, M., Salvi, R.J., and Allman, B.L. (2012). Intracortical circuits amplify sound-evoked activity in primary auditory cortex following systemic injection of salicylate in the rat. *J. Neurophysiol.* 108, 200–214.

Szymanski, F.D., Garcia-Lazaro, J.A., and Schnupp, J.W.H. (2009). Current Source Density Profiles of Stimulus-Specific Adaptation in Rat Auditory Cortex. *J. Neurophysiol.* 102, 1483–1490.

Tye-Murray, N., Sommers, M., and Spehar, B. (2007). Audiovisual integration and lipreading of older adults with normal and impaired hearing. *Ear Hear.* 28, 656–668.

Vachon, P., Voss, P., Lassonde, M., Leroux, J.-M., Mensour, B., Beaudoin, G., Bourgouin, P., and Lepore, F. (2013). Reorganization of the auditory, visual and multimodal areas in early deaf individuals. *Neuroscience* 245, 50–60.

Wallace, M.T., Ramachandran, R., and Stein, B.E. (2004). A revised view of sensory cortical parcellation. *Proc. Natl. Acad. Sci.* 101, 2167–2172.

Whitt, J.L., Petrus, E., and Lee, H.-K. (2014). Experience-dependent homeostatic synaptic plasticity in neocortex. *Neuropharmacology* 78, 45–54.

Xu, J., Sun, X., Zhou, X., Zhang, J., and Yu, L. (2014). The cortical distribution of multisensory neurons was modulated by multisensory experience. *Neuroscience* 272, 1–9.

Yang, S., Weiner, B.D., Zhang, L.S., Cho, S.-J., and Bao, S. (2011). Homeostatic plasticity drives tinnitus perception in an animal model. *Proc. Natl. Acad. Sci*. 108, 14974–14979.

Chapter 4

4 Behavioural Plasticity of Audiovisual Perception: Rapid Recalibration of Temporal Sensitivity but not Perceptual Binding Following Adult-Onset Hearing Loss [3]

Prior to investigating the perceptual consequences of noise-induced hearing loss, we first needed to design and validate novel behavioural paradigms for rats that are capable of assessing their ability to perceive the relative timing of audiovisual stimuli (i.e., audiovisual perception). Consistent with psychophysical studies in humans, we found the rats are indeed capable of differentiating between auditory and visual stimuli presented at various timing offsets, reaching similar performance levels as those reported in humans (Appendix A) [4].

4.1 Introduction

In order to create a unified percept of objects or events within our external environment, our brain must be able to accurately integrate or bind stimuli from more than one sensory modality (e.g., hearing and vision). Decades of research in numerous species has confirmed that the successful integration of multisensory information is highly dependent upon the features of the unimodal stimuli presented, most notably their intensity and spatiotemporal alignment (King and Palmer, 1985; Meredith and Stein, 1986, 1996; Meredith et al., 1987; Miller et al., 2015; Perrault et al., 2005; Rowland and Stein, 2008; Stanford et al., 2005; Stein and Meredith, 1993). For example, in such cases when an auditory and visual stimulus occur within ~100 ms of each other, the stimuli can be perceived by the observer

---

[3] A version of this chapter is published as:

Schormans, A.L. and Allman, B.L. (2018) Behavioural plasticity of audiovisual perception: rapid recalibration of temporal sensitivity but no perceptual binding following adult-onset hearing loss. *Frontiers in Behavioral Neuroscience.* 12:256, 1-18

[4] This work was published as:

Schormans, A.L., Scott, KE, Vo, AMQ, Tyker, A, Typlt, M, Stolzberg, D, Allman, BL. (2017) Audiovisual Temporal Processing and Synchrony Perception in the Rat, *Frontiers in Behavioral Neuroscience*. 10:246, 1-18

as having occurred at the same moment in time even though the stimuli were physically asynchronous. Although this integration of closely-timed audiovisual stimuli can offer certain behavioural advantages, such as improved detection, identification and localization of objects in the environment (Diederich and Colonius, 2004; Gleiss and Kayser, 2012; Hershenson, 1962; Hirokawa et al., 2008; Raposo et al., 2012; Siemann et al., 2015), an overly broad window of temporal integration could be problematic, as information from truly separate events may not be correctly perceived as such (Basharat et al., 2018).

The ability to judge the timing of audiovisual stimuli has been well studied in humans using psychophysical testing (for review, see Keetels and Vroomen, 2012; van Eijk et al., 2008; Navarra et al., 2005a; Spence et al., 2001; Stekelenburg and Vroomen, 2007; Stevenson and Wallace, 2013; Vatakis and Spence, 2007; Vroomen and Keetels, 2010), and more recently in rats trained with appetitive operant conditioning (Schormans et al., 2017a). The two most widely used paradigms to assess audiovisual temporal acuity involve presenting the stimuli at varying stimulus onset asynchronies (SOAs), and requiring participants to judge which modality was presented first (i.e., temporal order judgment, TOJ), or whether the stimuli were presented at the same time or not (i.e., synchrony judgment, SJ). In addition to measuring overall performance during TOJ tasks, researchers often determine the actual timing of the audiovisual stimuli when the participant was most unsure of the temporal order (i.e., point of subjective simultaneity, PSS), as well as the smallest timing interval that could be detected reliably (i.e., just noticeable difference, JND) (Keetels and Vroomen, 2012; Vatakis et al., 2008a; Vroomen and Stekelenburg, 2011). In an SJ task such as the flash-beep paradigm, when participants are asked to judge whether or not the visual and auditory stimuli were presented synchronously or asynchronously, researchers can calculate the participant's temporal binding window (TBW); the epoch of time over which physically asynchronous stimuli are perceived as synchronous (for review, see Wallace and Stevenson, 2014). Thus, the TBW provides insight into the degree of temporal tolerance in which asynchronous audiovisual stimuli are likely to be integrated and perceptually bound (Krueger Fister et al., 2016).

Audiovisual temporal acuity normally undergoes fine-tuning throughout childhood and adolescence (Hillock et al., 2011; Hillock-Dunn and Wallace, 2012; Kaganovich, 2016;

Lewkowicz and Flom, 2014), making this perceptual ability susceptible to disruption in individuals with developmental disabilities, such as autism spectrum disorder (Bebko et al., 2006; Boer-Schellekens et al., 2013; Foss-Feig et al., 2010; Kwakye et al., 2011; Stevenson et al., 2014a, 2014b), dyslexia (Hairston et al., 2005; Wallace and Stevenson, 2014) and schizophrenia (Carroll et al., 2008; Foucher et al., 2007; Haß et al., 2017; Martin et al., 2013; Stekelenburg et al., 2013; Stevenson et al., 2017). In such cases, atypical audiovisual temporal acuity often manifests as an increased length of time over which audiovisual stimuli are perceptually bound (i.e., the TBW is wider). Later in life, the ability to accurately perceive the timing of audiovisual stimuli can also be affected, whereby older participants typically show impairments in their perception of temporal order as well as their ability to judge simultaneity (Basharat et al., 2018; Bedard and Barnett-Cowan, 2016; Chan et al., 2014a, 2014b; Setti et al., 2011). Overall, it is clear that the ability to integrate and perceptually bind audiovisual stimuli can vary widely across individuals, as well as shift throughout one's lifespan. What remains unknown, however, is how adult-onset hearing loss, separate from aging, affects audiovisual temporal acuity. This is an important topic given the prevalence of hearing impairment in younger individuals, often caused by excessive exposure to loud noise at work or during recreational activities. For example, ~12% of children and young adults in the U.S. suffer from noise-induced hearing threshold shifts (Lin et al., 2011), and it is estimated that 22 million U.S. workers are exposed to hazardous noise each year (Tak et al., 2009).

It would be reasonable to predict that moderate hearing loss—which reduces one's sensitivity to environmental sounds—could distort audiovisual temporal acuity due to the fact that varying the intensity (effectiveness) of auditory and/or visual stimuli is known to alter perceptual judgments in normal-hearing participants (Boenke et al., 2009; Krueger Fister et al., 2016; Neumann and Niepel, 2004; Neumann et al., 1992; Smith, 1933). That said, it is well-established that the perceptual binding of audiovisual stimuli is highly-adaptive to experience, as evidenced from research on participants who were passively exposed to asynchronous audiovisual stimuli (Fujisaki et al., 2004; Navarra et al., 2005; Vatakis et al., 2007, 2008b), as well as those actively engaged in perceptual training (De Niear et al., 2016, 2018; Powers et al., 2009). Thus, an alternative prediction could be that individuals who experience adult-onset hearing loss may show limited changes to their

audiovisual temporal acuity, owed to a recalibration of their perceptual ability as they adapt to their permanent hearing impairment.

In the present study, we used a rat model to investigate, for the first time, the nature and extent that audiovisual temporal acuity is affected by adult-onset hearing loss, with specific focus on the time-course of perceptual changes following loud noise exposure. Using appetitive operant conditioning, separate groups of rats were trained to either determine the temporal order of audiovisual stimuli (TOJ task), or differentiate whether audiovisual stimuli were presented synchronously or not (SJ task). In the first experimental series, psychophysical testing was completed for both behavioural tasks in which the intensity of the auditory stimulus was modulated, while the intensity of the visual stimulus was held constant. In the second experimental series, rats trained on the TOJ and SJ tasks were exposed to a loud noise known to cause permanent hearing loss (Schormans et al., 2017b, 2018), and their behavioural performance and associated metrics (e.g., PSS and JND) were monitored for the next three weeks. Ultimately, the first experimental series served to confirm that audiovisual temporal acuity in normal-hearing rats, like in humans, is influenced by sound intensity, as well as to provide additional context when interpreting any noise-induced changes in perceptual judgment caused by a permanent loss of auditory sensitivity.

4.2 Methods

Overall, the present study included two experimental series: (1) to investigate how modulating sound intensity affects performance on either the TOJ task (Experiment 1A) or SJ task (Experiment 1B), and (2) to determine whether noise-induced hearing loss affected the perception of simultaneity (Experiment 2A; TOJ task) or synchrony (Experiment 2B; SJ task). A total of 31 adult male Sprague-Dawley rats (Charles River Laboratories Inc., Wilmington, MA) were used in the present study: Experiment 1A (n = 10); Experiment 1B (n = 10); Experiment 2A (n = 9; one which was also used in Experiment 1A); Experiment 2B (n = 9; six of which were also used in Experiment 1B). All behavioural procedures were approved by the University of Western Ontario Animal Care and Use Committee and were in accordance with the guidelines established by the Canadian Council of Animal Care.

4.2.1 Behavioural Apparatus and Sensory Stimuli

Behavioural training and testing were performed in a standard modular test chamber (ENV-008CT; Med Associates Inc., St. Albans, VT) that was housed within a sound-attenuating box (29” W by 23.5” H by 23.5” D; Med Associates Inc., St. Albans, VT). The front wall of the behavioural chamber was equipped with a center nose poke, a left feeder trough and a right feeder trough that were each fitted with an infrared (IR) detector (see Figure 4.1B), whereas the back wall was equipped with a house light that illuminated the test chamber. Real-time processing hardware (RZ6 and BH-32, Tucker Davis Technologies, Alachua, FL) were interfaced with the test chamber. Custom behavioural protocols running in Matlab (EPsych Toolbox, dstolz.github.io/epsych/) monitored the nose poke responses, and controlled the presentation of the auditory and visual stimuli, as well as the positive reinforcement (i.e., sucrose pellet delivery) and punishment (i.e., turning off the house light and an inability to commence the next trial).

The visual stimulus was a 50 ms light flash (27 lux) from an LED (ENV-229M; Med Associates Inc.) located above the center nose poke. The intensity of the visual stimulus was determined using a LED light meter (Model LT45, Extech Instruments, Nashua, NH). The auditory stimulus was a 50 ms noise burst (1-32 kHz) from a speaker (FT28D, Fostex, Tokyo) mounted on the ceiling of the behavioural chamber near the front wall (see Fig. 4.1B). Consistent with Schormans et al., (2017a), rats were trained on the behavioural tasks using a 75 dB sound pressure level (SPL) auditory stimulus. The auditory stimulus was calibrated using custom Matlab software with a ¼-inch microphone (2530, Larson Davis) and preamplifier (2221; Larson Davis).

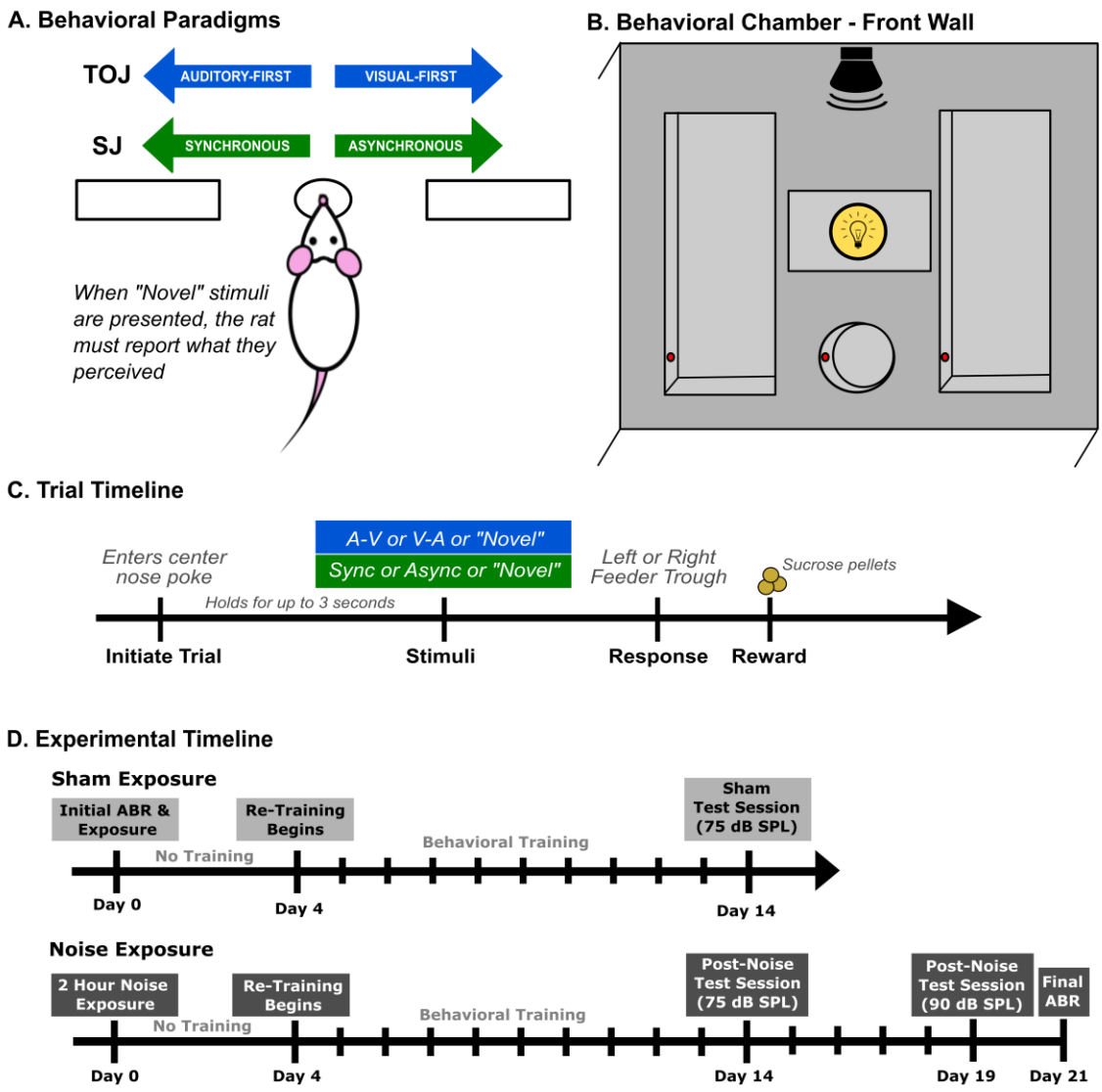

Figure 4.1. Rat audiovisual behavioural tasks and chamber set up.

Rats were trained on either an audiovisual temporal order judgment (TOJ) task or a synchrony judgment (SJ) task. (A) Overview of both behavioural tasks. Through a series of stages, rats were trained using a two-alternative forced choice paradigm, where they were required to choose the right or left feeder trough depending on the stimulus condition presented. For example, in the TOJ task, rats were trained to discriminate between auditory-first and visual-first trials, where the rats respond to the left feeder trough when an auditory-first stimulus condition is presented and the right feeder trough when a visual-first stimulus condition is presented. (B) Schematic of the front wall of the behavioural chamber used for both tasks. The front wall of the chamber consists of a left and right

feeder trough and a center nose poke, all outfitted with infra-red (IR) detectors (represented by the red circles within the feeders and nose poke) used for response detection and trial initiation, respectively. The auditory stimulus was delivered from a speaker located above the center nose poke from above the chamber and the visual stimulus was presented from the LED located immediately above the center nose poke. (C) Representative timeline of a single trial for rats trained on either the audiovisual TOJ or SJ task. (D) The experimental timeline for the second experimental series consisting of two different test sessions completed after sham or noise exposure.

4.2.2 Overview of Behavioural Training Procedures for the TOJ and SJ Tasks

Using appetitive operant conditioning, rats were trained on either an audiovisual TOJ task or an audiovisual SJ task which were both designed as two-alternative forced-choice (2AFC) paradigms. In the TOJ task, rats were trained to differentiate the temporal order of auditory and visual stimuli, whereas rats trained on the SJ task learned to differentiate between trials when the visual and auditory stimuli were presented synchronously or when the visual stimulus preceded the auditory stimulus. For both behavioural tasks, rats began training at 70 days old (body mass: 281 ± 4.7 g), and were trained 6 days a week. All experimental testing took place when the rats were between 6 and 11 months of age.

Prior to commencing behavioural training, rats were weighed daily and maintained on a food restricted diet until they neared 85% of their free-feeding body mass. During the first few training sessions, unprompted nose pokes into the center port (which were detected by the IR beam; red circles in Fig. 4.1B) resulted in the presentation of an audiovisual stimulus condition, and the delivery of a 45 mg sucrose pellet (Bio-Serv, Frenchtown, NJ) to the feeder associated with the stimulus condition (i.e., TOJ task: auditory-first = left trough, visual-first = right trough; SJ task: synchronous = left trough, asynchronous = right trough; Fig. 4.1A). Furthermore, rats were positively reinforced with a second pellet if they went to the correct feeder trough following the stimulus presentation (as monitored with the IR

detector; Fig. 4.1B). The second pellet was delivered in order to help the rats associate a given feeder trough with a specific audiovisual stimulus condition.

After three consecutive training sessions, the initial pellet reinforcement was eliminated, and now the delivery of a pellet was contingent on the rats selecting the correct feeder trough in response to a given stimulus condition. At this stage of the training procedure, the stimulus onset asynchrony (SOA) was maintained at 400 ms. More specifically, in the TOJ task, rats were required to differentiate between “visual-first” and “auditory-first” conditions, where the timing between stimuli presented was 400 ms (i.e., the auditory stimulus was presented 400 ms prior to the visual stimulus and vice versa). Similarly, in the SJ task, rats were required to differentiate between synchronous (i.e., 0 ms SOA) and asynchronous audiovisual stimuli in which the visual stimulus preceded the auditory stimulus by 400 ms. Throughout all stages of the behavioural training procedure, sessions consisted of 30-min of daily training, where correct feeder trough responses were reinforced with a sucrose pellet, and incorrect responses resulted in the house light turning off for up to 15 s, during which time a new trial could not be initiated (Fig. 4.1C). Consistent with previous investigations, the daily amount of food provided was adjusted so that each rat’s body mass increased with age, while providing enough motivation for it to complete ~200 trials in a session (Schormans et al., 2017a; Stolzberg et al., 2013).

In order for rats to move on to the next training stage, they were required to correctly discriminate between the two audiovisual stimulus conditions (i.e., TOJ task: auditory-first vs. visual-first; SJ task: synchronous vs. asynchronous) with >75% accuracy. Once this performance criterion was achieved for three consecutive days, the SOA timing was reduced to 300 ms for both stimulus conditions in the TOJ task, as well as the asynchronous stimulus condition in the SJ task. Consistent with the previous stage, rats trained for 30 min/day until the criterion of 75% correct was achieved for both stimulus conditions. Rats progressed to the final stage of training once they reached the 75% performance criterion in five consecutive days. During this final training stage, the SOA was reduced to 200 ms for both stimulus conditions in the TOJ task, as well as the asynchronous stimulus condition in the SJ task. The second stimulus condition in the SJ task (i.e., synchronous audiovisual stimuli) did not change throughout the training stages. As described in further detail below,

each rat was considered ready to progress to experimental test days once it had achieved >80% accuracy for five consecutive days on the final training stage.

4.2.3 Experiment 1- Modulation of Sound Intensity

4.2.3.1 Experiment 1A- TOJ Task Performance and Analysis

Once rats (n = 10) had successfully completed all stages of behavioural training for the TOJ task, experimental test sessions were introduced in which novel SOAs were presented to determine each rat's audiovisual temporal order perception. Three different experimental tests were performed in each rat that differed in the intensity of the auditory stimulus (i.e., 60, 75 or 90 dB SPL). Experimental tests were randomized in order to counterbalance the potential influence of training duration. For each of the tests completed, seven SOAs were randomly delivered (i.e., 0, ±40, ±100 and ±200 ms); however, to reduce the potential of developing a side bias, 70% of the trials were the same as the training stimuli (i.e., TOJ task: ± 200 ms SOA). The remaining 30% of trials consisted of the random presentation of the novel SOAs (0, ±40, ±100 ms). A sucrose pellet was delivered following each novel SOA regardless of whether a correct or incorrect response was made. In contrast, the trained stimulus conditions were positively reinforced for correct responses with sucrose pellets, and punished for incorrect responses with a 15-s timeout. Within a given test session, rats performed a minimum of 10 trials at each of the novel SOAs (mean of 13 ± 0.3 trials) to ensure that they had experienced a sufficient number of trials to accurately determine their ability to judge the relative timing of audiovisual stimuli (Schormans et al., 2017a).

To assess the effect of sound intensity on audiovisual temporal order perception, multiple metrics were extracted from each of the experimental test sessions. For all seven SOAs, performance was measured as the proportion of trials in which the rat perceived the stimuli as visual-first (i.e., responded to the right feeder trough, Fig. 4.1A). Test sessions were repeated if the trained stimuli (i.e. ± 200 ms) did not reach the criterion of 70% correct or if a strong side bias formed. Consistent with Vatakis et al. (2007b), a psychophysical profile at each sound intensity was generated for each rat by plotting straight lines between each of the neighbouring SOAs tested, and the associated slope and intercept values were

calculated. Using these values, the point of subjective simultaneity (PSS) was calculated by determining the SOA at which 50% of the responses were perceived as visual-first. In addition, the just noticeable difference (JND) was determined by taking the difference between the SOAs at which 25% and 75% of the responses were perceived as visual-first, and then dividing by two (Vroomen and Stekelenburg, 2011). The PSS and JND were calculated for each of the test sessions, and averaged across rats within a given sound intensity (i.e., 60, 75 and 90 dB SPL).

4.2.3.2 Experiment 1B- SJ Task Performance and Analysis

Once rats trained on the SJ task (n = 10) had successfully reached the final criterion (i.e., >80% correct on synchronous [0 ms SOA] and asynchronous [200 ms SOA] conditions for five consecutive days), experimental test sessions were completed that differed in the intensity of the auditory stimulus (i.e., 60, 75 or 90 dB SPL). Consistent with the TOJ task, experimental tests were randomized in order to counterbalance the potential influence of training duration. Test sessions consisted of the random presentation of five SOAs (i.e., the visual stimulus preceded the auditory stimulus by 0, 10, 40, 100 or 200 ms). On each of the test sessions, the trained stimulus conditions (i.e., 0 ms and 200 ms SOAs) made up 70% of the trials presented, and these trials continued to be reinforced with sucrose pellets for correct responses and punished with 15-s timeouts for incorrect responses. The remaining 30% of the trials were equally divided among the novel SOAs (i.e., 10, 40, and 100 ms SOAs), and were reinforced with a sucrose pellet regardless of whether a correct or incorrect response was made. Within a given test session, rats were presented a minimum of 18 trials at each of the novel SOAs (mean of 25 ± 0.5 trials); a suitable number of trials from which it was possible to accurately determine each rat's perception of synchrony (Schormans et al., 2017a).

Ultimately, to assess the effect of sound intensity on audiovisual synchrony judgments, various metrics were extracted from each of the experimental test sessions. For all five SOAs, performance was measured as the proportion of trials in which the rat perceived the stimuli as synchronous (i.e., they responded to the left feeder trough, Fig. 4.1A). Test sessions were repeated if the trained stimuli (i.e., 0 ms and 200 ms SOAs) did not reach the criterion of 70% correct or if a strong side bias formed. For each rat and a given sound

intensity, a psychophysical profile was generated by plotting straight lines between each of the neighbouring SOAs tested, and the associated slope and intercept values were tabulated. Using these calculated values, two audiovisual asynchrony thresholds (50% and 70%) were extracted in order to evaluate the perceptual consequences of sound intensity on the audiovisual SJ task. Thresholds of 50% and 70% were extracted as they are common values used to determine the TBW in humans (Başkent and Bazo, 2011; Eg et al., 2015; Kaganovich, 2016; Stevenson and Wallace, 2013).

4.2.4 Experiment 2- Noise Exposure and Audiovisual Temporal Acuity

To determine how hearing loss affects audiovisual temporal acuity, rats that were trained on the TOJ task (n = 9; Experiment 2A) or SJ task (n = 9; Experiment 2B) underwent a sham and loud noise exposure, after which their behavioural performance during subsequent training and testing sessions were monitored for the next three weeks. As outlined in the experimental timeline (Fig. 4.1D), once the rats had reached the training performance criterion, their baseline hearing sensitivity was assessed with an auditory brainstem response (ABR) prior to the 2-hour sham exposure (Day 0). After a 3-day hiatus, rats returned to performing training sessions for 10 days, followed by a test session on Day 14 (see Fig. 4.1D). Once the training and testing sessions were completed following the sham exposure, all rats underwent a 2-hour noise exposure. Consistent with the sham exposure procedure, behavioural performance was monitored for three weeks following the noise exposure. In addition to the test session completed on Day 14, noise-exposed rats also performed a final test session on Day 19 during which time the intensity of the auditory stimulus was increased from the standard 75 dB SPL to 90 dB SPL. A final ABR was performed three weeks after the noise exposure (Day 21) to assess the level of permanent hearing loss. Because all trained rats first underwent a sham exposure (see Fig. 4.1D), this allowed for a within-subject control of the possible effects of anesthesia and/or time delay before returning to the behavioural sessions post-noise exposure.

4.2.4.1 Hearing Assessment

Hearing sensitivity before and after noise exposure were assessed using an ABR, which was performed in a double-walled sound-attenuating chamber. Rats were anesthetized with ketamine (80 mg/kg; IP) and xylazine (5 mg/kg; IP), and subdermal electrodes were positioned at the vertex, over the right mastoid process and on the back. Throughout the procedure, body temperature was maintained at ~37°C using a homeothermic heating pad (507220F; Harvard Apparatus, Kent, UK). Auditory stimuli consisted of a click (0.1 ms) and two tones (4 kHz and 20 kHz; 5 ms duration and 1 ms rise/fall time) which were generated using a Tucker-Davis Technologies (TDT, Alachua, FL) RZ6 processing module at 100 kHz sampling rate. Stimuli were delivered from a magnetic speaker (MF1; TDT) positioned 10 cm from the animal's right ear. The left ear was occluded with a custom foam earplug. Each of the stimuli were presented 1000 times (21 times/second) at decreasing intensities from 90 to 10 dB SPL in 10 dB SPL steps. Near threshold, successive steps were decreased to 5 dB SPL, and each level was presented twice in order to best determine ABR threshold using the criteria of just noticeable deflection of the averaged electrical activity within the 10 ms window (Popelar et al., 2008; Schormans et al., 2017b). The auditory evoked activity was collected using a low impedance headstage (RA4L1; TDT), preamplified and digitized (RA16SD Medusa preamp; TDT), and sent to a RZ6 processing module via a fiber optic cable. The signal was filtered (300 – 3000 Hz) and averaged using BioSig software (TDT). Sound stimuli for the ABR and noise exposure were calibrated with custom Matlab software (The Mathworks, Natick, MA) using a ¼-inch microphone (2530; Larson Davis, Depew, NY) and preamplifier (2221; Larson Davis).

4.2.4.2 Noise Exposure

Rats were anesthetized with ketamine (80 mg/kg; IP) and xylazine (5 mg/kg: IP), and placed on a homeothermic heating pad to maintain body temperature at ~37°C. Noise exposure consisted of a calibrated broadband noise (0.8 – 20 kHz) delivered bilaterally at 120 dB SPL for two hours. The broadband noise was generated with TDT software and hardware (RPvdsEx; RZ6 module), and delivered by a super tweeter (T90A; Fostex, Tokyo, Japan) which was placed 10 cm in front of the rat. This noise exposure protocol was chosen as it is known to cause persistent changes at the level of the auditory cortex

(Popelar et al., 2008) as well as to induce crossmodal plasticity within higher-order sensory cortices (Schormans et al., 2017b).

4.2.4.3 Behavioural Testing and Performance Post-Noise Exposure

Consistent with the experimental parameters described above, the sham/noise-exposed rats performed test sessions that included both the novel and training SOAs for audiovisual stimuli during the TOJ task (i.e., 0, ±40, ±100 and ±200 ms; Experiment 2A) and SJ task (i.e., visual preceding auditory by 0, 10, 40, 100 or 200 ms; Experiment 2B). Ultimately, for both the TOJ and SJ tasks, the effect of noise-induced hearing loss on audiovisual temporal acuity was determined by comparing the sham versus noise exposure performance for the SOAs on the training sessions of Day 4 to 13, as well as the audiovisual psychophysical curves generated on Day 14 (i.e., 75 dB SPL) and Day 19 (i.e., 90 dB SPL). Furthermore, the PSS and JND were calculated for rats that performed the TOJ task, and the results were compared between the sham and noise exposure conditions. Based on performance during the SJ task, it was possible to determine the effect of noise-induced hearing loss on the temporal window of integration by comparing the audiovisual asynchrony thresholds (50% and 70%) in rats post-sham versus post-noise exposure.

4.2.5 Statistics and Data Presentation

The statistical analyses performed in the present study included one- and two-way repeated-measures analysis of variance (rmANOVA), and paired samples t-tests, depending on the comparison of interest (see Results section for the details of each specific comparison). If Mauchly's test of sphericity was violated within the repeated-measures ANOVA, the Greenhouse-Geisser correction was used. SPSS software (version 25, IBM Corporation, Armonk, NY) was used for statistical analyses, and GraphPad Prism (GraphPad Software Inc., La Jolla, CA) was used to plot the results. Data are presented as the mean values ± standard error of the mean (SEM).

4.3 Results

4.3.1 Experiment 1A- Modulation of Sound Intensity Shifted the Perception of Simultaneity during the TOJ Task

The effect of sound intensity on audiovisual temporal order perception was examined during the TOJ task using three testing conditions which differed in the intensity of the auditory stimulus presented (i.e., 60, 75 and 90 dB SPL). For each test session, the proportion of trials that were perceived as visual-first were determined for all SOAs ranging from -200 ms (i.e., auditory-first) to +200 ms (i.e., visual-first). Overall, a two-way rmANOVA revealed a significant interaction of sound intensity by SOA ($F[3.8,34.3] = 6.0$, $p < 0.01$). To examine this interaction, post hoc paired samples t-tests were completed between the test sessions at 75 dB SPL and 60 or 90 dB SPL. As shown in Figure 4.2A, when performance was compared across all SOAs for 75 and 60 dB SPL testing conditions, a significantly higher proportion of trials were perceived as "visual-first" when the 60 dB SPL auditory stimulus was delivered 200 ms before the visual stimulus ($p < 0.007$). Although additional comparisons did not reach statistical significance once corrected for multiple comparisons (Bonferroni-adjusted p-value of 0.007), trends persisted at an SOA of -40 ms and 0 ms (see Table 4.1 for detailed statistics), in which the 60 dB SPL auditory stimulus was more likely to be perceived as visual-first (Fig. 4.2A). Contrary to the results observed during the 60 dB SPL test session, as the sound intensity increased from 75 to 90 dB SPL, the majority of SOAs tested were predominantly perceived as auditory-first. More specifically, there was a significant decrease in the proportion of trials perceived as visual-first at SOAs of -200, 0, and 40 ms ($p < 0.007$; Fig. 4.2A), demonstrating that the 90 dB SPL testing session influenced perception on both sides of simultaneity, whereas the 60 dB SPL session only affected auditory-first SOAs. Although additional comparisons did not reach statistical significance, the aforementioned results persisted as trends for the -100 ms SOA (see Table 4.1), in which the 90 dB SPL auditory stimulus was more likely to be perceived as auditory-first (Fig. 4.2A). Taken together, these results demonstrate that sound intensity influenced the perception of audiovisual stimuli at various SOAs, with louder stimuli having the largest effect on judgments of audiovisual temporal order.

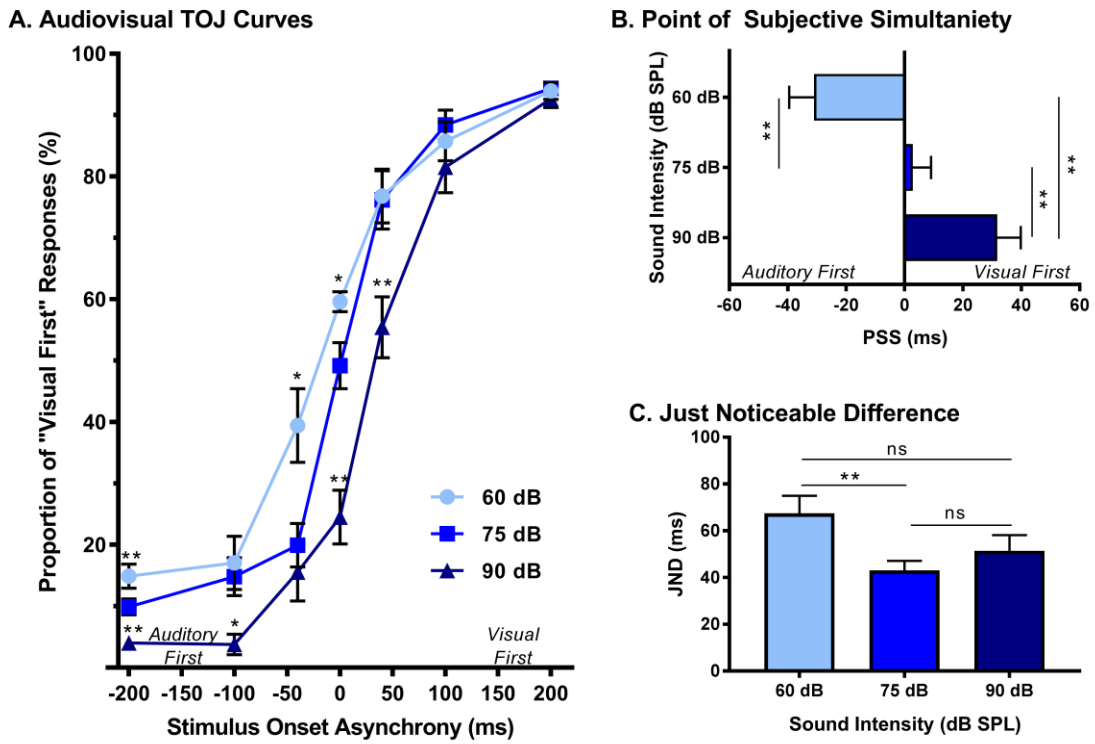

Figure 4.2. Effect of sound intensity on audiovisual temporal order perception.

*(A) Behavioural performance was plotted as the proportion of responses the rat perceived as "visual-first" (i.e., right feeder trough) for test days completed at 60 dB, 75 dB and 90 dB SPL. A right-ward shift in the TOJ curve was observed as the intensity of the auditory stimulus increased. For example, at 0 ms SOA there was an increase in "visual-first" responses at 60 dB SPL when compared to 75 dB SPL (*p < 0.01), and a significant decrease in "visual-first" responses at 90 dB SPL when compared to 75 dB SPL (**p < 0.001). (B) The point of subjective simultaneity (PSS) and (C) the just noticeable difference (JND) were derived from the TOJ task. For PSS, a significant difference was observed between all sound intensities (**p < 0.001), demonstrating a right-ward shift from "auditory-first" responses to "visual-first" responses as the sound intensity increased. For JND, a significance difference was only observed at the lowest sound intensity (i.e., 60 dB SPL), resulting in an increased window of integration (**p < 0.01). Results are displayed as mean ± SEM, n = 10.*

In addition to the analyses completed on the TOJ psychophysical curves, the point of subjective simultaneity (PSS) and just noticeable difference (JND) were calculated and compared across the three sound intensity testing conditions. As expected based on the TOJ psychophysical curves, a one-way rmANOVA revealed that sound intensity influenced the perception of audiovisual simultaneity (i.e., PSS; $F[2,18] = 36.7$, $p < 0.001$). Consistent with our previous study (Schormans et al., 2017a), during the 75 dB SPL testing condition, the PSS was centered around an SOA of 0 ms (PSS = 2.7 ± 6.3 ms; Fig. 4.2B). However, when the intensity of the auditory stimulus was decreased, the PSS also decreased ($p < 0.001$), such that the auditory stimulus needed to be presented well before the visual stimulus in order for the stimulus pair to be perceived as simultaneous (Fig. 4.2B). The opposite pattern occurred when the intensity of the auditory stimulus was 90 dB SPL, as the PSS was significantly increased ($p < 0.001$). Interestingly, although the rats' PSS was greatly affected by the intensity of the auditory stimulus, their ability to accurately discriminate the temporal order of the audiovisual stimuli (i.e., JND) was less affected (one-way rmANOVA, $F[2,18] = 5.0$, $p < 0.05$). For example, whereas the testing condition with the 60 dB SPL auditory stimulus showed a significant increase in JND compared to 75 dB SPL, no other differences were observed (Fig. 4.2C). Overall, these collective results demonstrate that sound intensity influenced the rats' perception of simultaneity, but did not appreciably affect their sensitivity to reliably detect differences in the timing of the stimuli.

4.3.2 Experiment 2A- Rapid Recalibration of Audiovisual Temporal Order Perception following Hearing Loss

The effect of noise exposure on hearing sensitivity was assessed for rats trained on the TOJ task (n = 9) by comparing their ABR thresholds for the 4 kHz, 20 kHz and click stimuli pre- and post-noise exposure. A two-way rmANOVA (time x stimulus type) revealed a significant interaction of time by stimulus type ($F[2,16] = 7.26$, $p < 0.01$). Overall, noise exposure increased ABR thresholds across all stimuli with the 20 kHz tone showing the greatest threshold shift (pre-noise: 20.6 ± 1.3 dB SPL vs. post-noise: 53.9 ± 5.2 dB SPL) compared to the 4 kHz tone (pre-noise: 28.9 ± 1.4 dB SPL vs. post-noise: 53.9 ± 4.6 dB SPL), and click stimulus (pre-noise: 26.1 ± 0.7 dB SPL vs. post-noise: 46.1 ± 3.2 dB SPL).

Table 4.1. Effect of auditory intensity and hearing loss on audiovisual temporal perception at all stimulus onset asynchronies when compared to 75 dB SPL testing sessions

Experiment		SOA (ms)	t-score	p-value
Exp. 1A	Decreased Sound Intensity (75 dB vs. 60 dB SPL)	-200	4.29	2.02×10^{-3}
		-100	0.69	n.s.
		-40	3.29	9.37×10^{-3}
		0	3.30	9.20×10^{-3}
		40	-0.20	n.s.
		100	-0.87	n.s.
		200	-0.34	n.s.
Exp. 1A	Increased Sound Intensity (75 dB vs. 90 dB SPL)	-200	-5.05	6.95×10^{-4}
		-100	-3.04	1.40×10^{-2}
		-40	-1.40	n.s.
		0	-5.28	5.08×10^{-4}
		40	-4.21	2.28×10^{-3}
		100	-1.72	n.s.
		200	-1.37	n.s.
Exp. 2A	Increased Sound Intensity (Post-Noise: 75 dB vs. 90 dB SPL)	-200	3.09	1.49×10^{-2}
		-100	0.61	n.s.
		-40	3.75	5.64×10^{-3}
		0	3.09	1.49×10^{-2}
		40	4.18	3.07×10^{-3}
		100	-0.01	n.s.
		200	-0.36	n.s.

n.s. = not significant

Following a three-day hiatus, rats that were trained on the TOJ task returned to the behavioural chamber for daily training sessions. As described above, training sessions consisted of the random presentation of auditory- or visual-first stimuli at an SOA of ±200 ms. To determine the effect of hearing loss on judgments of audiovisual temporal order, performance on trials made up of auditory-first stimuli were analyzed pre- and post-exposure. A two-way rmANOVA (exposure x time) for auditory-first stimuli revealed a significant interaction of exposure by time ($F[1,8] = 8.6$, $p < 0.05$). As can be seen in Figure 4.3A, a comparison of performance pre- and post-exposure showed a decrease in performance on auditory-first trials following noise exposure ($p < 0.05$; Fig. 4.3A). Next, we investigated if there was a relationship between TOJ task performance and the degree of hearing loss. A Pearson correlational analysis revealed a significant relationship between

final click thresholds and auditory-first performance three days following noise exposure ($r = -0.84$, $p < 0.01$), such that higher hearing thresholds (i.e., greater degree of hearing loss) resulted in the larger impairments in auditory-first performance (Fig. 4.3B). Not surprisingly, following the sham exposure, there was no difference in performance on auditory-first trials ($p = 0.80$; Fig. 4.3A). In addition to the first training session, performance was monitored over a total of 10 days post-exposure, at which point the first experimental test session was completed (i.e., post-exposure test at 75 dB SPL). A two-way rmANOVA revealed a significant interaction of exposure by training session ($F[2.7,21.4] = 4.0$, $p < 0.05$), and post hoc paired samples t-tests demonstrated a slight decrease in auditory-first performance during the first two training sessions (i.e., Day 4 and 5; $p < 0.05$). Following the second training session (i.e., Day 5), performance returned to normal (i.e., equivalent to post-sham exposure performance, $p > 0.05$), indicating the auditory-first performance rapidly re-calibrated following adult-onset hearing loss (Fig. 4.3C).

To further explore the effect of noise exposure on judgments of audiovisual temporal order, performance on visual-first trials was analyzed pre- and post-exposure. A two-way rmANOVA (exposure x time) revealed a significant interaction of exposure by time ($F[1,8] = 7.7$, $p < 0.05$). Similar to the results during the auditory-first performance, there was a significant decrease in performance on visual-first trials following noise exposure ($p < 0.01$; Fig. 4.3D). As expected, no difference was observed following the sham exposure ($p = 0.13$). Contrary to the auditory-first performance (Fig. 4.3B), there was no significant relationship between final click thresholds and visual-first performance three days following noise exposure (Pearson correlational analysis; $r = -0.01$, $p = 0.76$; Fig. 4.3E). Moreover, visual-first performance showed no impairments over the course of the 10 days post-exposure, as there was no effect of training session ($F[3.4,27.5] = 2.3$, $p = 0.09$) and no interaction of training session by exposure ($F[3.8,30.5] = 1.1$, $p = 0.38$) (Fig. 4.3F). Taken together, these results demonstrate that hearing loss predominantly influenced performance on trials when the auditory stimulus was presented before the visual stimulus.

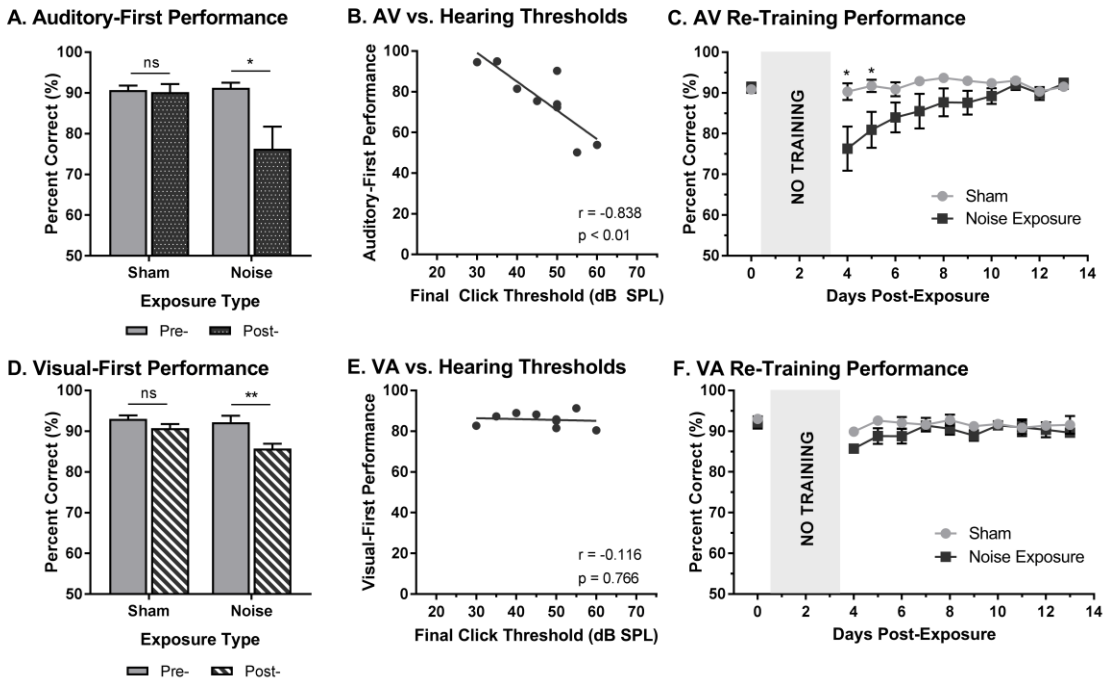

Figure 4.3. Altered auditory- and visual-first performance during TOJ training sessions following noise exposure.

*(A) Auditory-first performance and (D) visual-first performance pre- and three days post-exposure to a loud noise or sham. Following noise exposure there was a slight decrease in auditory-first performance (*p < 0.05), as well as a significant decrease in visual-first performance (** p < 0.02). Solid bars represent pre-exposure performance, and patterned bars represent post-exposure performance. Correlation results for (B) auditory-first performance and (E) visual-first performance as a function of final hearing sensitivity (i.e., click thresholds). Grey circles represent the individual data for each rat post-noise exposure. The solid line represents the linear regression line, and the Pearson correlation results along with the significance levels are displayed in the bottom of the panel. Behavioural performance on (C) auditory-first trials and (F) visual-first trials were monitored for 10 days post-exposure. A decrease in performance on auditory-first trials was observed following noise exposure during the first two training sessions (*p < 0.05). Results are displayed as mean ± SEM, n = 9.*

4.3.3 Experiment 2A- Audiovisual Temporal Order Perception in Noise-Exposed Rats Remained Sensitive to Sound Intensity Modulation

To examine the effect of noise-induced hearing loss on audiovisual temporal perception, experimental tests were completed two weeks following sham exposure and noise exposure. Consistent with Experiment 1A, for each test session, the proportion of trials that were perceived as visual-first were calculated for all SOAs. A two-way rmANOVA (exposure x SOA) revealed a main effect of SOA ($F[2.3,18.1] = 190.5$, $p < 0.001$) and no effect of exposure ($F[1,8] = 0.25$, $p = 0.634$), as well as no interaction of exposure by time ($F[6,48] = 0.43$, $p = 0.859$). Thus, despite an initial difficulty in differentiating the temporal order of audiovisual stimuli in the first few days following noise exposure (Fig. 4.3A and 4.3C), the ability to accurately judge the temporal order of audiovisual stimuli returned to pre-exposure performance levels in rats with permanent hearing loss (Fig. 4.4A).

To determine whether audiovisual temporal perception continued to be sensitive to changes in sound intensity following hearing loss, an additional experimental test session was conducted in which the intensity of the auditory stimulus was increased to 90 dB SPL. A two-way rmANOVA revealed a significant interaction of sound intensity by SOA ($F[6,48] = 5.7$, $p < 0.001$). As shown in Figure 4.4B, when performance was compared across all SOAs at 75 and 90 dB SPL post-noise testing conditions, a significantly higher proportion of trials were perceived as “auditory-first” when the 90 dB SPL auditory stimulus was delivered at an SOA of -40 ms and 40 ms ($p < 0.007$). Although additional comparisons did not reach statistical significance once corrected for multiple comparisons, trends persisted at an SOA of -200 ms and 0 ms, in which the 90 dB SPL auditory stimulus was more likely to be perceived as auditory-first (see Table 4.1). Thus, adult-onset hearing loss does not seem to impair audiovisual temporal perception, as the behavioural performance of the noise-exposed rats remained sensitive to modulation of the intensity of the auditory stimulus.

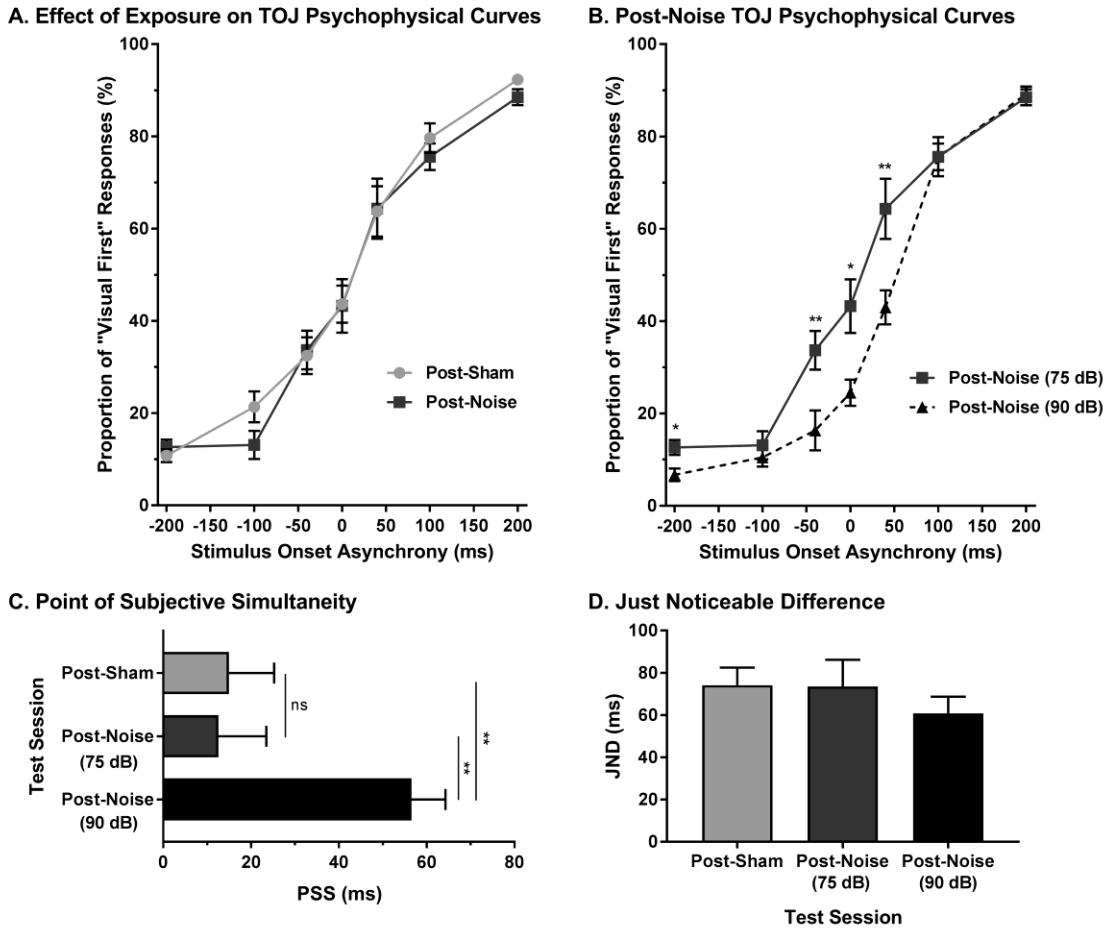

Figure 4.4. Preserved audiovisual temporal perception following adult-onset hearing loss.

(A) Test sessions at 75 dB SPL were completed two weeks following exposure to a loud noise (i.e., post-noise) or quiet (i.e., post-sham). (B) An additional test session was completed at 90 dB SPL (i.e., post-noise [90 dB SPL]) and compared to the test session at 75 dB SPL (i.e., post-noise [75 dB SPL]), in order to determine if temporal perception remained sensitive to sound intensity. For all test sessions, performance was plotted as the proportion of trials that the rats perceived as "visual-first" (i.e., responded to the right feeder trough). (C) The point of subjective simultaneity (PSS) and (D) the just noticeable difference (JND) were derived from each of the test sessions. Results are displayed as mean ± SEM, n = 9.

Finally, to further examine the effect of hearing loss on judgments of audiovisual temporal order, PSS and JND were analyzed and compared across all experimental test sessions. Overall, we found that the PSS was indeed influenced by the experimental test session (one-way rmANOVA; $F[2,16] = 8.9$, $p < 0.01$). Consistent with the results in the TOJ curves, PSS did not change following noise exposure ($p = 0.87$). However, when the sound intensity was increased from 75 to 90 dB SPL, the PSS of the noise-exposed rats significantly increased ($p < 0.01$; Fig. 4.4C); results which were consistent with those observed in rats with normal hearing (Experiment 1A; Fig. 4.2A). As can be seen in Figure 4.4D, JND did not differ across the various experimental test sessions (one-way rmANOVA; $F[2,16] = 1.3$, $p = 0.302$). Overall, these results demonstrate that adult-onset hearing loss did not alter the perception of audiovisual simultaneity or temporal sensitivity as assessed with the TOJ task.

4.3.4 Experiment 1B- Modulation of Sound Intensity Altered the Detection of Asynchronous Stimulus during the SJ Task

The effect of sound intensity on audiovisual synchrony perception was investigated during the SJ task using three testing conditions which differed in the intensity of the auditory stimulus presented (i.e., 60, 75 and 90 dB SPL). For each testing condition, the proportion of trials that were perceived as synchronous were determined for all SOAs ranging from 0 ms (i.e., synchronous) to 200 ms (i.e., asynchronous). Overall, a two-way rmANOVA revealed a significant interaction of sound intensity by SOA ($F[8,72] = 8.1$, $p < 0.001$). To further investigate this interaction, post hoc paired samples t-tests were completed between the test sessions at 75 dB SPL and 60 or 90 dB SPL. As shown in Figure 4.5A, a comparison of performance across the various SOAs for the 75 and 60 dB SPL testing conditions revealed that the rats perceived a significantly lower proportion of trials as synchronous when the 60 dB SPL auditory stimulus was delivered 40 ms before the visual stimulus ($p < 0.001$). Consistent with the nature of these differences observed at 60 dB SPL, when the auditory stimulus intensity was increased from 75 to 90 dB SPL, there was a significant increase in the proportion of trials at an SOA of 40 ms that the rats perceived as synchronous ($p < 0.008$; see Table 4.2 for detailed statistics). Given that there were no performance differences when the visual stimulus preceded the various auditory stimuli by

100 or 200 ms (Fig. 4.3A), the collective results show that modulation of sound intensity had the greatest effect on audiovisual synchrony perception when the pair of stimuli were presented relatively close together in time (0-100 ms).

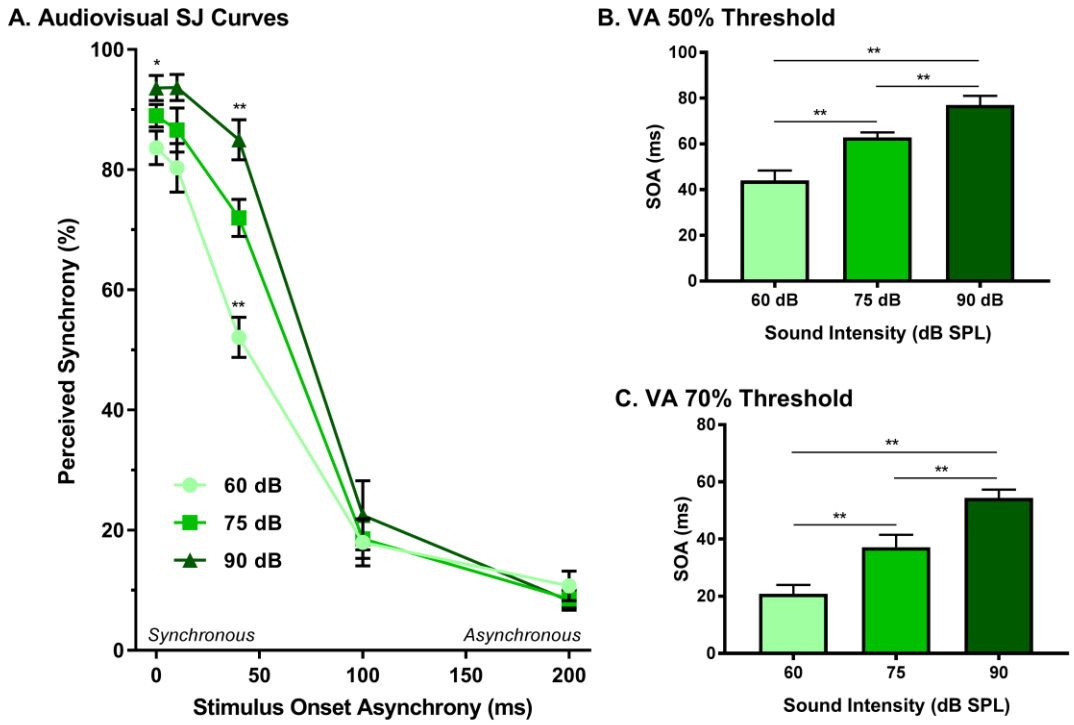

Figure 4.5. Effect of sound intensity on audiovisual synchrony perception as measured during an SJ task.

*(A) Behavioural performance was plotted as the proportion of trials the rat perceived as "synchronous" (i.e., left feeder trough) for tests completed at 60 dB, 75 dB, and 90 dB SPL. A significant difference was observed at both 60 dB SPL (52.1 ± 3.3%) and 90 dB SPL (85.0 ± 3.3%) when compared to 75 dB SPL (69.0 ± 1.7%; **p < 0.01), indicating that as sound intensity increased, the rate of perceived synchrony also increased when the SOA was less than 100 ms. The (B) 50% threshold and (C) 70% threshold were derived from the SJ task. Consistent with the SJ curves, both thresholds showed a significant increase as the intensity of the auditory stimulus increased (**p < 0.01). Results are displayed as mean ± SEM, n = 10.*

In addition to analyzing the role of sound intensity modulation on the SJ psychophysical curves, the 50% and 70% audiovisual asynchrony thresholds were extracted and compared across all sound intensities, as these thresholds represent criteria used previously to determine the temporal binding window (TBW) (Stevenson and Wallace, 2013). A one-way rmANOVA revealed a significant main effect of sound intensity for the 50% threshold ($F[2,18] = 44.2$, $p < 0.001$), whereby the rats' threshold significantly increased ($p < 0.001$) in accordance with the intensity of the auditory stimulus (Fig. 4.5B). Similarly, a significant main effect was also observed at the 70% threshold (one-way rmANOVA; $F[1.2,11.0] = 30.1$, $p < 0.001$), such that when the auditory stimulus intensity increased from 60 to 90 dB SPL, there was a significant widening of the right-sided temporal binding window (Fig. 4.5C). Thus, these collective results indicate that the louder the sound intensity during a flash-beep SJ task, the longer the time interval that was needed between the visual and auditory stimuli for the rats to correctly judge that the stimulus pair was indeed asynchronous.

4.3.5 Experiment 2B- Persistent Impairments in the Ability to Judge the Synchrony of Audiovisual Stimuli following Adult-Onset Hearing Loss

Alterations in hearing sensitivity were assessed pre- and post-exposure for the rats trained on the SJ task ($n = 9$) by comparing their ABR thresholds for the 4 kHz, 20 kHz and click stimuli. As expected, a two-way rmANOVA revealed a significant interaction of time by stimulus type ($F[2,16] = 11.2$, $p < 0.01$). Moreover, Bonferroni-corrected post hoc t-tests revealed that noise exposure caused a significant increase in the ABR threshold of the click (pre-noise: 26.7 ± 0.8 dB SPL vs. post-noise: 54.4 ± 3.7 dB SPL, $p < 0.001$), 4 kHz (pre-noise: 28.3 ± 1.2 dB SPL vs. post-noise: 61.7 ± 3.3 dB SPL, $p < 0.001$), and 20kHz tone (pre-noise: 23.3 ± 0.8 dB SPL vs. post-noise: 63.9 ± 4.5 dB SPL, $p < 0.001$).

Table 4.2. Effect of auditory intensity and hearing loss on audiovisual synchrony perception at all stimulus onset asynchronies when compared to 75 dB SPL testing sessions

Experiment		SOA (ms)	t-score	p-value
Exp. 1B	Decreased Sound Intensity (75 dB vs. 60 dB SPL)	0	-1.97	n.s.
		10	-1.89	n.s.
		40	-4.81	9.63×10^{-4}
		1000	-0.20	n.s.
		200	0.87	n.s.
Exp. 1B	Increased Sound Intensity (75 dB vs. 90 dB SPL)	0	2.43	3.78×10^{-2}
		10	2.10	n.s.
		40	4.36	1.82×10^{-3}
		1000	1.41	n.s.
		200	-0.20	n.s.
Exp. 2B	Post-Exposure at 75 dB SPL (Post-Sham vs. Post-Noise)	0	0.89	n.s.
		10	2.53	3.53×10^{-2}
		40	-1.31	n.s.
		1000	-3.99	4.03×10^{-3}
		200	-2.57	3.33×10^{-2}
Exp. 2B	Increased Sound Intensity (Post-Noise: 75 dB vs. 90 dB SPL)	0	-1.63	n.s.
		10	-2.16	n.s.
		40	-4.65	1.64×10^{-3}
		1000	0.26	n.s.
		200	1.05	n.s.

n.s. = not significant

Rats that were trained on the SJ task returned to daily behavioural training sessions three days following exposure to a loud noise or sham. Training sessions consisted of the random presentation of synchronous (i.e., 0 ms SOA) and asynchronous (i.e., 200 ms SOA) audiovisual stimuli. To examine the effect of hearing loss on the ability to accurately perceive the synchrony of audiovisual stimuli, performance on trials made up of synchronous and asynchronous stimuli were analyzed pre- and post-exposure. For synchronous stimuli, a two-way rmANOVA revealed a significant interaction of exposure by time ($F[1,8] = 15.0$, $p < 0.01$). As can be seen in Figure 4.6A, exposure to the loud noise caused a significant decrease in performance on synchronous trials ($p < 0.01$). As expected, there was no change in performance on synchronous trials following the sham exposure ($p = 0.762$). Next, we examined the rats' performance on synchronous trials following noise exposure to determine if this performance correlated with final hearing thresholds. Indeed,

a Pearson correlational analysis revealed a significant negative relationship between final click thresholds and synchronous performance three days following noise exposure ($r = -0.857$, $p < 0.01$; Fig. 4.6B). Therefore, the perceptual ability of noise-exposed rats to judge the synchrony of the audiovisual stimuli was dependent on their level of hearing impairment; a higher proportion of trials were perceived to be asynchronous if the rats had a greater degree of hearing impairment.

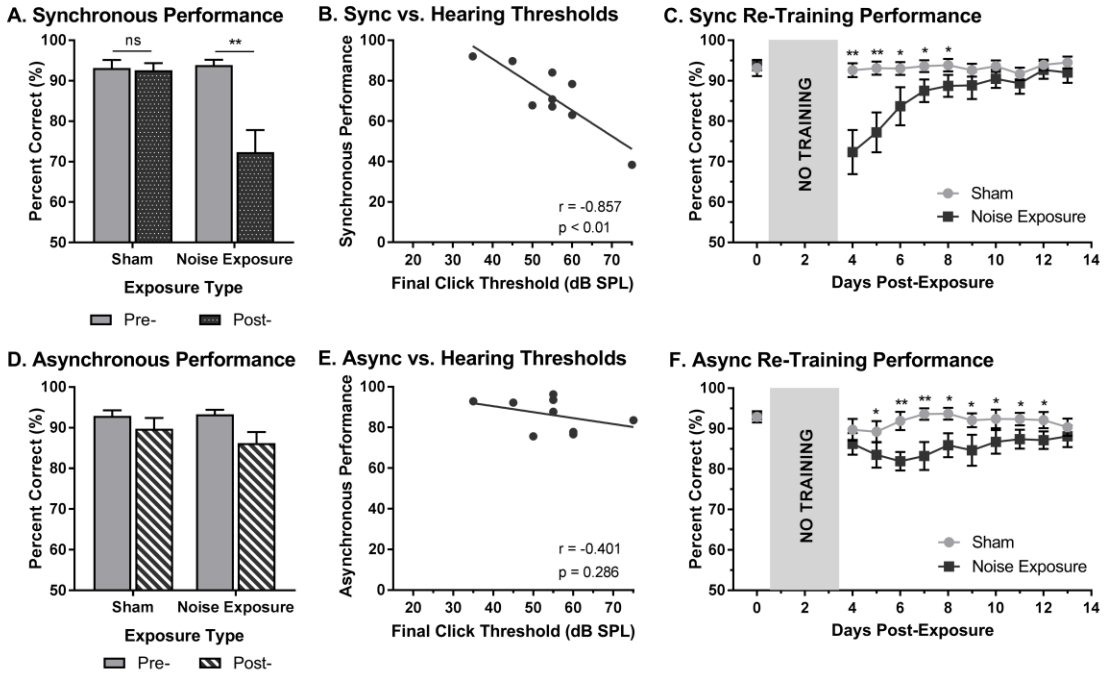

Figure 4.6. Hearing loss impaired performances during SJ training sessions.
*Performance on (A) synchronous and (D) asynchronous trials was compared pre- and three days post- exposure to a loud noise or sham. Following noise exposure, a significant decrease in performance on synchronous trials was observed (**p < 0.02). No difference was observed on asynchronous trials. Solid bars represent pre-exposure performance and patterned bars represent post-exposure performance. Correlation results for (B) synchrony performance and (E) asynchrony performance were plotted as a function of final hearing sensitivity (i.e., click thresholds). Grey circles represent the individual data for each rat post-noise exposure. The solid line represents the linear regression line, and the Pearson correlation results along with the significance levels are displayed in the bottom of the panel. Behavioural performance on (C) synchronous and (F) asynchronous trials were*

*monitored for ten days following sham and noise exposure. Performance on synchronous trials returned to typical performance within 5 days, whereas performance on asynchronous trials remained consistently impaired across the majority of the training days (*p < 0.05, **p < 0.004). Results are displayed as mean ± SEM, n = 9.*

Beyond assessing performance in the first training session following the noise exposure, synchrony perception was also monitored for 10 days, after which the first experimental test session was completed (i.e., post-exposure test at 75 dB SPL). A two-way rmANOVA revealed a significant interaction of exposure by training session ($F[3.2,25.6] = 7.9$, $p < 0.001$). As shown in Figure 4.6C, a significant decrease in performance occurred during the first two training sessions (i.e., Day 4 and 5). While no other training sessions reached statistical significance once corrected for multiple comparisons (Bonferroni-adjusted p-value of 0.004), trends persisted on days 6 through 8 ($p < 0.05$), in which synchronous trials were more likely to be perceived as asynchronous. However, following the fifth training session (i.e., Day 8), performance returned to normal (i.e., equivalent to post-sham exposure performance, $p > 0.05$), suggesting that the ability to detect synchronous stimuli eventually recovered after noise exposure.

To further examine the effect of hearing loss on judgments of synchrony, performance on asynchronous trials during the first training session was also examined pre- and post-exposure. Surprisingly, a two-way rmANOVA only revealed a main effect for exposure ($F[1,8] = 6.6$, $p < 0.05$); there was no effect of time ($F[1,8] = 2.6$, $p = 0.15$) and no significant interaction of exposure by time ($F[1,8] = 1.3$, $p = 0.28$). Therefore, contrary to synchronous trials (i.e., 0 ms SOA), the ability to categorize asynchronous trials (i.e., 200 ms SOA) was not influenced by exposure to a loud noise or sham (Fig. 4.6D). Consistent with the analyses described above, asynchronous performance and final hearing thresholds were examined in order to determine if performance was dependent upon hearing sensitivity. A Pearson correlation analysis revealed no significant relationship between performance on asynchronous trials and final click thresholds ($r = -0.4$, $p = 0.286$). While performance on the first training session was relatively maintained (see Fig. 4.6D),

performance across the 10 training sessions prior to the first experimental test session was consistently impaired (Fig. 4.6F). A two-way rmANOVA revealed a significant interaction of exposure by training session ($F[3.8,30.3] = 3.5$, $p < 0.05$). A further examination of this interaction demonstrated significant impairments in performance on Day 6 and 7 ($p < 0.004$) as well as slight impairments on Day 5 and 8 through 13 ($p < 0.05$). Therefore, hearing loss caused persistent impairments in asynchrony detection, such that a greater proportion of trials were perceived as synchronous; findings which could ultimately relate to an impaired perceptual binding of audiovisual stimuli.

4.3.6 Experiment 2B- Impairments in Asynchrony Detection Resulted in Altered Perceptual Binding of Audiovisual Stimuli following Hearing Loss

To explore the consequences of adult-onset hearing loss on audiovisual synchrony perception, rats trained on the SJ task were tested two weeks following exposure to a loud noise. For each test session, the rate of perceived synchrony was calculated as the proportion of trials that were perceived as synchronous for all SOAs ranging from 0 ms (i.e., synchronous) to 200 ms (i.e., asynchronous). A two-way rmANOVA revealed a significant interaction of exposure (i.e., post-sham vs. post-noise) by SOA ($F[2.1,16.6] = 6.9$, $p < 0.01$). To further examine this interaction, post hoc paired samples t-tests completed between the two post-exposure test sessions (i.e., post-sham vs. post-noise) revealed that rats reported a significantly higher proportion of trials as synchronous following noise exposure when the visual stimulus was delivered 100 ms before the auditory stimulus ($p < 0.01$; Fig. 4.7A). Although additional comparisons did not reach statistical significance once corrected for multiple comparisons, modest changes were observed at an SOA of 10 ms and 200 ms (see Table 4.2 for detailed statistics). Overall, these results demonstrate that adult-onset hearing loss impairs synchrony perception, such that truly asynchronous audiovisual stimuli were more likely to be perceived as synchronous.

To determine whether sound intensity was still capable of influencing synchrony perception following adult-onset noise-induced hearing loss, an additional test session was completed in which the intensity of the auditory stimulus was increased from 75 dB to 90

dB SPL. As predicted, a two-way rmANOVA revealed a significant interaction of sound intensity (i.e., 75 dB vs. 90 dB SPL post-noise) by SOA ($F[1.6,13.0] = 4.3$, $p < 0.05$). Similar to the differences observed in normal-hearing rats in Experiment 1B, when the intensity of the auditory stimulus was increased from 75 dB to 90 dB SPL, noise-exposed rats showed a significant increase in the proportion of trials perceived as synchronous at an SOA of 40 ms (Fig. 4.7B). Thus, audiovisual synchrony perception remained sensitive to changes in the intensity of the auditory stimulus, despite these same rats showing an impaired ability to detect asynchronous stimuli.

In addition to the analyses completed on the SJ psychophysical curves following hearing loss, the 50% and 70% audiovisual asynchrony thresholds were compared across all test sessions. Separate one-way rmANOVAs revealed a significant effect of test session for the 50% threshold ($F[2,16] = 14.3$, $p < 0.001$) and the 70% threshold ($F[2,16] = 12.4$, $p < 0.01$). As shown in Figure 4.7C, the 50% asynchrony threshold significantly increased following noise exposure ($p < 0.01$); findings indicative of a greater degree of temporal tolerance which could result in a broadened TBW. While the 70% threshold did not significantly increase following a noise exposure, a trend towards an increase in threshold was observed ($p = 0.08$; Fig. 4.7D). Overall, despite this increase in the epoch of time over which the audiovisual stimuli appeared to be perceptually bound, the noise-exposed rats remained sensitive to changes in the intensity of the auditory stimulus; i.e., when the intensity of the auditory stimulus was increased, there was a significant increase in the 70% threshold ($p < 0.01$), as well as a trend towards an increase in the 50% threshold ($p = 0.051$). Thus, the collective results demonstrate that adult-onset hearing loss alters the perception of audiovisual synchrony.

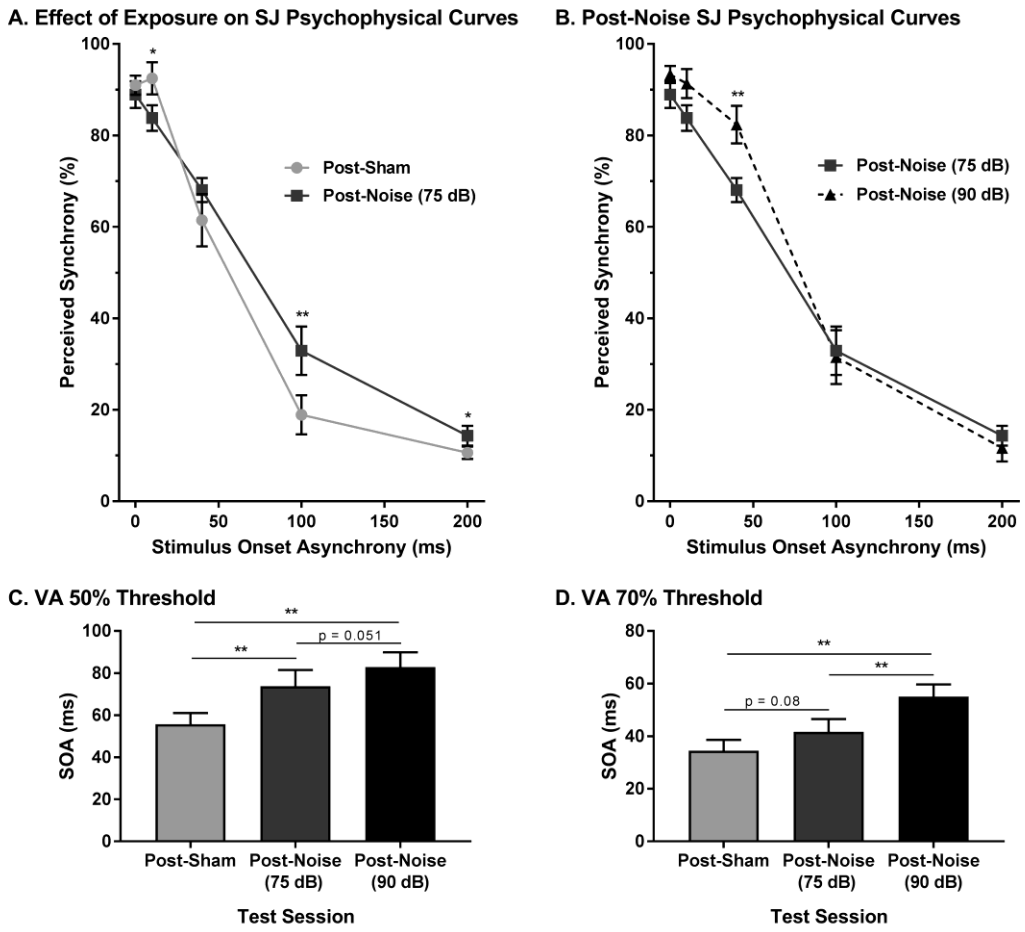

Figure 4.7. Impaired audiovisual synchrony perception following adult-onset hearing loss.

*(A) Experimental test sessions for the SJ task at 75 dB SPL were completed two weeks following exposure to a loud noise (i.e., post-noise) or quiet (post-sham). (B) An additional test session was completed at 90 dB SPL (i.e., post-noise [90 dB SPL]) and compared to the test session at 75 dB SPL (i.e., post-noise [75 dB SPL]), in order to determine if synchrony perception remained sensitive to sound intensity. For all test sessions, performance was plotted as the proportion of trials that the rats perceived as "synchronous" (i.e., responded to the left feeder trough). The (C) 50% threshold and (D) 70% threshold were derived from all SJ test sessions. Two weeks following noise exposure, there was a significant increase in the 50% threshold (**$p < 0.017$), and a modest increase in the 70% threshold ($p = 0.08$), indicative of a wider window of perceptual binding. Results are displayed as mean ± SEM, $n = 9$.*

4.4 Discussion

To our knowledge, the present study represents the first comprehensive investigation into the degree to which audiovisual temporal acuity is influenced by adult-onset hearing loss, with a specific focus on the time-course of perceptual changes following loud noise exposure. Using operant conditioning, rats were trained and tested on either a TOJ task in which they reported the relative timing of audiovisual stimuli presented at various SOAs, or an SJ task in which they reported whether audiovisual stimuli were presented at the same moment in time or at different times. Ultimately, adult-onset hearing loss caused a differential effect on audiovisual temporal acuity depending on whether perception was assessed with the TOJ or SJ task. For example, performance on the TOJ task revealed that the perception of temporal order rapidly recalibrated following noise exposure, resulting in a preservation of temporal sensitivity. In contrast, noise-exposed rats showed a persistent impairment in their ability to detect asynchronous audiovisual stimuli during the SJ task, resulting in a greater tolerance of asynchronous stimuli which could manifest as a widening of their TBW. Taken together, these results provide important insight into the nature and extent of behavioural plasticity of audiovisual perception following adult-onset hearing loss.

4.4.1 Stimulus Intensity Predicts Audiovisual Temporal Acuity

Prior to conducting our studies into the effect of adult-onset hearing loss on audiovisual temporal acuity, psychophysical testing was completed in normal-hearing rats for both the TOJ and SJ tasks in which the intensity of the auditory stimulus was modulated, while the intensity of the visual stimulus was held constant. Overall, the results of this first series of experiments demonstrated that sound intensity predicted audiovisual perception, such that when a lower-intensity sound was presented the rats were biased to perceive the audiovisual stimuli as asynchronous (SJ task), or as though the visual stimulus was presented first (TOJ task). As discussed below, these results are consistent with previous studies on humans that assessed PSS during TOJ tasks (Boenke et al., 2009; Neumann and Niepel, 2004; Neumann et al., 1992; Smith, 1933). For example, Boenke and colleagues (2009) found that increasing the intensity of the visual stimulus during a TOJ task caused the participants' perception of simultaneity (i.e., PSS) to decrease; findings consistent to

when we lowered the intensity of the auditory stimulus in the present study. Indeed, we found that when the sound intensity was lowered, the PSS was more likely to be perceived as “auditory-first” and conversely, when the sound intensity was increased, the PSS shifted to being perceived as “visual-first” (Fig. 4.2B). Collectively, the results in humans and rats confirm that when the auditory or visual stimulus intensity is modulated, a predicable perceptual shift occurs regarding which stimulus modality was thought to have been presented first.

Previous studies that screened for synchrony perception using SJ tasks have demonstrated differential results when the intensity of both stimuli were modulated, perhaps due to different task parameters. For example, Smith (1933) observed minimal effects of stimulus intensity on participants’ perceptual judgment when presenting audiovisual stimuli on both sides of simultaneity. However, when Krueger Fister et al. (2016) presented stimuli only on the right-side of simultaneity (i.e., a flash-beep task with visual-first asynchronies), they observed that pairing weak auditory and visual stimuli resulted in a decreased ability to accurately perceive when the stimuli were asynchronous. Interestingly, using the same task parameters as Krueger Fister and colleagues (2016), we found that decreasing the intensity of only the auditory stimulus increased the proportion of trials reported as asynchronous, indicating that the rats exhibited an improvement in asynchrony detection during the SJ task. Thus, it appears that decreasing the intensity of both modalities increases the temporal offsets over which perceptual binding occurs (i.e., TBW widens), yet decreasing the intensity of only the auditory stimulus, potentially narrows the TBW. While the degree of temporal tolerance appears to move in opposite directions depending on whether the intensity of both modalities or a single modality are modulated, these collective results are in accordance with perceptual latencies. For example, stimuli that are of lower intensity tend to occur at a greater distance from the individual and thus result in greater temporal differences between the respective sensory receptors. Therefore, it has been postulated that the brain must compensate for lower stimulus intensities by providing a greater degree of tolerance, allowing for stimuli to be perceptually bound (Krueger Fister et al., 2016). However, when only a single stimulus is modulated, the intensity disparity between the two stimuli could result in a lower degree of temporal integration as the brain may be less likely to bind the stimuli because they are more likely perceived as two separate

events. As the present study and that of Krueger Fister and colleagues (2016) used an SJ task that only presented stimuli on the right-side of simultaneity, further studies will be needed to determine how alterations in stimulus intensity influence the entire temporal window of integration. Ultimately, the collective results of the first experimental series complement our understanding of the factors that influence audiovisual temporal acuity, and may offer important considerations when interpreting TOJ and SJ task performance of participants with altered hearing sensitivity (e.g., those with hearing loss, or individuals who experience hyper-sensitivity to sounds).

4.4.2 Hearing Loss and Audiovisual Temporal Acuity

Given that hearing loss reduces one's sensitivity to environmental sounds, and we and others have shown that varying the intensity of an auditory stimulus alters perceptual judgments in normal-hearing participants, we reasoned that noise-induced hearing loss in adulthood may impact audiovisual temporal acuity. Interestingly, we found that 2-3 weeks after noise exposure, rats with permanent hearing loss maintained their ability to judge the temporal order of the audiovisual stimuli, as PSS was unchanged, and their temporal sensitivity was preserved (i.e., JND was consistent). To our knowledge, this is the first investigation of the effect of hearing loss on audiovisual temporal perception as assessed with a TOJ task. That said, Başkent and Bazo (2011) used an SJ task to study individuals with a hearing impairment, and found that their level of perceptual binding (as assessed via the TBW) was similar to normal-hearing participants; findings that disagree with the persistent impairment in asynchrony detection ability observed in the present study. However, these conflicting results could arise due to experimental differences, including the age of the participants used in each of the experimental groups, the duration of hearing loss (2-3 weeks in rats vs. 6-28 years in humans), as well as the absolute/relative intensity of the auditory stimuli used in the SJ tasks (75 or 90 dB SPL in rats vs. adjusted to compensate for sensation level in each hearing-impaired participant). The presentation of auditory stimuli at sensation level (i.e., adjusted based on the degree of hearing loss in each participant) is a particularly important experimental difference, as stimulus intensity is known to have a significant influence on audiovisual perception. Thus, future studies in

subjects with hearing-impairments should include psychophysical testing at both an absolute auditory intensity as well as at sensation level.

In considering the differential effects of hearing loss on the TOJ and SJ task performance observed in the present study, it is worth noting that previous research on normal-hearing participants has also shown disparate results between the two tasks. These differences in task performance are thought to arise partially from participant response biases and experimental methodology (García-Pérez and Alcalá-Quintana, 2012; Vatakis and Spence, 2007; Vatakis et al., 2008b; Vroomen and Keetels, 2010), or alternatively, because the TOJ and SJ task rely on distinct perceptual processes (Kostaki and Vatakis, 2018). Indeed, Zampini et al. (2003) suggested that the TOJ task performance may reflect processes related to temporal discrimination, whereas SJ tasks may be more related to temporal binding mechanisms. Examining our results under this proposed framework, it seems that temporal order perception is preserved, whereas the perceptual binding of stimuli is impaired following adult-onset hearing loss. Interestingly, a previous study found the opposite relationship in older participants (with corrected-to-normal hearing), who showed more difficulty in discriminating the temporal order of the auditory and visual stimuli, but their TBW during the SJ task was not different from younger adults (Bedard and Barnett-Cowan, 2016).

4.4.3 Behavioural Plasticity of Audiovisual Temporal Acuity following Adult-Onset Hearing Loss

Although we observed no effect of hearing loss on the TOJ task performance 2-3 weeks post-noise exposure, when the rats first resumed training on the task three days after noise exposure, they did show an impaired ability to accurately judge the temporal order of audiovisual stimuli when the auditory stimulus was presented before the visual stimulus. Moreover, this impairment on “auditory-first” trials was related to their level of hearing loss, such that the rats with the greatest hearing loss performed the poorest on the “auditory-first” trials. It was during the next 10 days of training that we observed a progressive shift in the rats’ perception of temporal order toward pre-noise exposure performance. Similar findings were observed for rats’ performing the SJ task, in which their ability to detect synchronous audiovisual stimuli was initially impaired in relation to the level of hearing

loss, but this ability recovered progressively over the next 10 days. Overall, the daily exposure to the training stimuli pairings (e.g., TOJ task: ±200 ms SOA; SJ task: 0 and 200 ms SOA) may have resulted in the rats re-learning the association between the stimuli pairings within their new perceptual state (i.e., impaired hearing sensitivity from hearing loss), which ultimately led to a perceptual recalibration of audiovisual perception. Support for this suggestion comes from previous studies on normal-hearing participants which found that engagement in perceptual training paradigms that included trial-by-trial feedback (like in the present study) led to an improved ability to detect asynchronous audiovisual stimuli, thus resulting in a narrower temporal window of integration (De Niear et al., 2016, 2018; Powers et al., 2009). Future studies are needed to determine whether exposure to training stimuli is necessary for the preservation of audiovisual perception.

At this time, it remains uncertain why the perception of audiovisual temporal order fully recovered post-noise exposure, whereas there was a persistent impairment in the rats' ability to detect asynchronous audiovisual stimuli during the SJ task. Given that aspects of the SJ task performance (i.e., synchrony detection) did indeed recover, it is reasonable to question whether it would just have required a longer duration (>3 weeks) for asynchrony detection and perceptual binding to also fully recalibrate following permanent hearing loss. In support of this possibility, Başkent and Bazo (2011) observed that participants with a relatively short duration of deafness had wider TBWs, which could suggest that, following auditory deprivation, synchrony perception may improve over time. Ultimately, based on the differential rates of recalibration post-noise exposure of the aforementioned features of audiovisual temporal acuity (e.g., PSS and JND from the TOJ task; synchrony/asynchrony detection and TBW from the SJ task), our collective results provide additional support for the suggestion that different perceptual processes likely underlie TOJ and SJ task performance.

4.5 References

Basharat, A., Adams, M.S., Staines, W.R., and Barnett-Cowan, M. (2018). Simultaneity and Temporal Order Judgments Are Coded Differently and Change With Age: An Event-Related Potential Study. *Front. Integr. Neurosci.* 12.

Başkent, D., and Bazo, D. (2011). Audiovisual asynchrony detection and speech intelligibility in noise with moderate to severe sensorineural hearing impairment. *Ear Hear.* 32, 582–592.

Bebko, J.M., Weiss, J.A., Demark, J.L., and Gomez, P. (2006). Discrimination of temporal synchrony in intermodal events by children with autism and children with developmental disabilities without autism. *J. Child Psychol. Psychiatry* 47, 88–98.

Bedard, G., and Barnett-Cowan, M. (2016). Impaired timing of audiovisual events in the elderly. *Exp. Brain Res*. 234, 331–340.

Boenke, L.T., Deliano, M., and Ohl, F.W. (2009). Stimulus duration influences perceived simultaneity in audiovisual temporal-order judgment. *Exp. Brain Res.* 198, 233–244.

Boer-Schellekens, L.D., Eussen, M., and Vroomen, J. (2013). Diminished sensitivity of audiovisual temporal order in autism spectrum disorder. *Front. Integr. Neurosci*. 7.

Carroll, C.A., Boggs, J., O'Donnell, B.F., Shekhar, A., and Hetrick, W.P. (2008). Temporal processing dysfunction in schizophrenia. *Brain Cogn.* 67, 150–161.

Chan, Y.M., Pianta, M.J., and McKendrick, A.M. (2014a). Older age results in difficulties separating auditory and visual signals in time. *J. Vis.* 14, 13–13.

Chan, Y.M., Pianta, M.J., and McKendrick, A.M. (2014b). Reduced audiovisual recalibration in the elderly. *Front. Aging Neurosci.* 6.

De Niear, M.A., Koo, B., and Wallace, M.T. (2016). Multisensory perceptual learning is dependent upon task difficulty. *Exp. Brain Res.* 234, 3269–3277.

De Niear, M.A., Gupta, P.B., Baum, S.H., and Wallace, M.T. (2018). Perceptual training enhances temporal acuity for multisensory speech. *Neurobiol. Learn. Mem*. 147, 9–17.

Diederich, A., and Colonius, H. (2004). Bimodal and trimodal multisensory enhancement: Effects of stimulus onset and intensity on reaction time. *Percept. Psychophys*. 66, 1388–1404.

Eg, R., Behne, D., and Griwodz, C. (2015). Audiovisual temporal integration in reverberant environments. *Speech Commun*. 66, 91–106.

van Eijk, R.L.J., Kohlrausch, A., Juola, J.F., and Par, S. van de (2008). Audiovisual synchrony and temporal order judgments: Effects of experimental method and stimulus type. *Percept. Psychophys*. 70, 955–968.

Foss-Feig, J.H., Kwakye, L.D., Cascio, C.J., Burnette, C.P., Kadivar, H., Stone, W.L., and Wallace, M.T. (2010). An extended multisensory temporal binding window in autism spectrum disorders. *Exp. Brain Res*. 203, 381–389.

Foucher, J.R., Lacambre, M., Pham, B.-T., Giersch, A., and Elliott, M.A. (2007). Low time resolution in schizophrenia: Lengthened windows of simultaneity for visual, auditory and bimodal stimuli. *Schizophr. Res.* 97, 118–127.

Fujisaki, W., Shimojo, S., Kashino, M., and Nishida, S. (2004). Recalibration of audiovisual simultaneity. *Nat. Neurosci*. 7, 773–778.

García-Pérez, M.A., and Alcalá-Quintana, R. (2012). On the discrepant results in synchrony judgment and temporal-order judgment tasks: a quantitative model. *Psychon. Bull.* Rev. 19, 820–846.

Gleiss, S., and Kayser, C. (2012). Audio-Visual Detection Benefits in the Rat. *PLOS ONE* 7, e45677.

Hairston, W.D., Burdette, J.H., Flowers, D.L., Wood, F.B., and Wallace, M.T. (2005). Altered temporal profile of visual–auditory multisensory interactions in dyslexia. *Exp. Brain Res.* 166, 474–480.

Haß, K., Sinke, C., Reese, T., Roy, M., Wiswede, D., Dillo, W., Oranje, B., and Szycik, G.R. (2017). Enlarged temporal integration window in schizophrenia indicated by the double-flash illusion. *Cognit. Neuropsychiatry* 22, 145–158.

Hershenson, M. (1962). Reaction time as a measure of intersensory facilitation. *J. Exp. Psychol*. 63, 289–293.

Hillock, A.R., Powers, A.R., and Wallace, M.T. (2011). Binding of sights and sounds: Age-related changes in multisensory temporal processing. *Neuropsychologia* 49, 461–467.

Hillock-Dunn, A., and Wallace, M.T. (2012). Developmental changes in the multisensory temporal binding window persist into adolescence. *Dev. Sci*. 15, 688–696.

Hirokawa, J., Bosch, M., Sakata, S., Sakurai, Y., and Yamamori, T. (2008). Functional role of the secondary visual cortex in multisensory facilitation in rats. *Neuroscience* 153, 1402–1417.

Kaganovich, N. (2016). Development of Sensitivity to Audiovisual Temporal Asynchrony during Mid-Childhood. *Dev. Psychol*. 52, 232–241.

Keetels, M., and Vroomen, J. (2012). “Perception of Synchrony between the Senses” In *The Neural Bases of Multisensory Processes*, eds M.M. Murray and M.T. Wallace (Boca Raton, FL: CRC Press/Taylor & Francis), 147-178.

King, A.J., and Palmer, A.R. (1985). Integration of visual and auditory information in bimodal neurons in the guinea-pig superior colliculus. *Exp. Brain Res*. 60, 492–500.

Kostaki, M., and Vatakis, A. (2018). “Temporal Order and Synchrony Judgments: A Primer for Students”. In *Timing and Time Perception: Procedures, Measures, and Applications*, eds. A. Vatakis, F. Balci, M. Di Luca, and A. Correa, (Leiden, Netherlands: Koninklijke Brill), 233-262

Krueger Fister, J., Stevenson, R.A., Nidiffer, A.R., Barnett, Z.P., and Wallace, M.T. (2016). Stimulus intensity modulates multisensory temporal processing. *Neuropsychologia* 88, 92–100.

Kwakye, L.D., Foss-Feig, J.H., Cascio, C.J., Stone, W.L., and Wallace, M.T. (2011). Altered Auditory and Multisensory Temporal Processing in Autism Spectrum Disorders. *Front. Integr. Neurosci.* 4.

Lewkowicz, D.J., and Flom, R. (2014). The Audiovisual Temporal Binding Window Narrows in Early Childhood. *Child Dev*. 85, 685–694.

Lin, F., Niparko, J., and Ferrucci, L. (2011). Hearing loss prevalence in the united states. *Arch. Intern. Med.* 171, 1851–1853.

Martin, B., Giersch, A., Huron, C., and van Wassenhove, V. (2013). Temporal event structure and timing in schizophrenia: Preserved binding in a longer “now.” *Neuropsychologia* 51, 358–371.

Meredith, M.A., and Stein, B.E. (1986). Visual, auditory, and somatosensory convergence on cells in superior colliculus results in multisensory integration. *J. Neurophysiol*. 56, 640–662.

Meredith, M.A., and Stein, B.E. (1996). Spatial determinants of multisensory integration in cat superior colliculus neurons. *J. Neurophysiol.* 75, 1843–1857.

Meredith, M.A., Nemitz, J.W., and Stein, B.E. (1987). Determinants of multisensory integration in superior colliculus neurons. I. Temporal factors. *J. Neurosci*. 7, 3215–3229.

Miller, R.L., Pluta, S.R., Stein, B.E., and Rowland, B.A. (2015). Relative Unisensory Strength and Timing Predict Their Multisensory Product. *J. Neurosci*. 35, 5213–5220.

Navarra, J., Vatakis, A., Zampini, M., Soto-Faraco, S., Humphreys, W., and Spence, C. (2005). Exposure to asynchronous audiovisual speech extends the temporal window for audiovisual integration. *Cogn. Brain Res.* 25, 499–507.

Neumann, O., and Niepel, M. (2004). “Timing of “Perception” and Perception of “Time”,” In *Psychophysics Beyond Senstion: Laws and Invariants of Human Cognition*, eds C. Kaerbach, E. Schroger and H. Muller (Mahwah, NJ: Lawrence Erlbaum Associates), 245-269

Neumann, O., Koch, R., Niepel, M., and Tappe, T. (1992). Reaction time and temporal serial judgment: corroboration or dissociation? *Z. Exp. Angew. Psychol*. 39, 621–645.

Perrault, T.J., Vaughan, J.W., Stein, B.E., and Wallace, M.T. (2005). Superior Colliculus Neurons Use Distinct Operational Modes in the Integration of Multisensory Stimuli. *J. Neurophysiol.* 93, 2575–2586.

Popelar, J., Grecova, J., Rybalko, N., and Syka, J. (2008). Comparison of noise-induced changes of auditory brainstem and middle latency response amplitudes in rats. *Hear. Res*. 245, 82–91.

Powers, A.R., Hillock, A.R., and Wallace, M.T. (2009). Perceptual Training Narrows the Temporal Window of Multisensory Binding. *J. Neurosci*. 29, 12265–12274.

Raposo, D., Sheppard, J.P., Schrater, P.R., and Churchland, A.K. (2012). Multisensory Decision-Making in Rats and Humans. *J. Neurosci*. 32, 3726–3735.

Rowland, B.A., and Stein, B.E. (2008). Temporal Profiles of Response Enhancement in Multisensory Integration. *Front. Neurosci.* 2, 218–224.

Schormans, A.L., Scott, K.E., Vo, A.M.Q., Tyker, A., Typlt, M., Stolzberg, D., and Allman, B.L. (2017a). Audiovisual Temporal Processing and Synchrony Perception in the Rat. *Front. Behav. Neurosci*. 10.

Schormans, A.L., Typlt, M., and Allman, B.L. (2017b). Crossmodal plasticity in auditory, visual and multisensory cortical areas following noise-induced hearing loss in adulthood. *Hear. Res*. 343, 92–107.

Schormans, A.L., Typlt, M., and Allman, B.L. (2018). Adult-Onset Hearing Impairment Induces Layer-Specific Cortical Reorganization: Evidence of Crossmodal Plasticity and Central Gain Enhancement. *Cereb. Cortex*, bhy067

Setti, A., Finnigan, S., Sobolewski, R., McLaren, L., Robertson, I.H., Reilly, R.B., Anne Kenny, R., and Newell, F.N. (2011). Audiovisual temporal discrimination is less efficient with aging: an event-related potential study. *NeuroReport* 22, 554.

Siemann, J.K., Muller, C.L., Bamberger, G., Allison, J.D., Veenstra-VanderWeele, J., and Wallace, M.T. (2015). A novel behavioral paradigm to assess multisensory processing in mice. *Front. Behav. Neurosci*. 8.

Smith, W.F. (1933). The relative quickness of visual and auditory perception. *J. Exp. Psychol.* 16, 239–257.

Spence, C., Shore, D.I., and Klein, R.M. (2001). Multisensory prior entry. *J. Exp. Psychol. Gen.* 130, 799–832.

Stanford, T.R., Quessy, S., and Stein, B.E. (2005). Evaluating the Operations Underlying Multisensory Integration in the Cat Superior Colliculus. *J. Neurosci*. 25, 6499–6508.

Stein, B.E., and Meredith, M.A. (1993). The merging of the senses (Cambridge, MA, US: The MIT Press).

Stekelenburg, J.J., and Vroomen, J. (2007). Neural Correlates of Multisensory Integration of Ecologically Valid Audiovisual Events. *J. Cogn. Neurosci*. 19, 1964–1973.

Stekelenburg, J.J., Maes, J.P., Van Gool, A.R., Sitskoorn, M., and Vroomen, J. (2013). Deficient multisensory integration in schizophrenia: An event-related potential study. *Schizophr. Res*. 147, 253–261.

Stevenson, R.A., and Wallace, M.T. (2013). Multisensory temporal integration: task and stimulus dependencies. *Exp. Brain Res*. 227, 249–261.

Stevenson, R.A., Siemann, J.K., Schneider, B.C., Eberly, H.E., Woynaroski, T.G., Camarata, S.M., and Wallace, M.T. (2014a). Multisensory temporal integration in autism spectrum disorders. *J. Neurosci.* 34, 691–697.

Stevenson, R.A., Segers, M., Ferber, S., Barense, M.D., and Wallace, M.T. (2014b). The impact of multisensory integration deficits on speech perception in children with autism spectrum disorders. *Front. Psychol.* 5, 379.

Stevenson, R.A., Park, S., Cochran, C., McIntosh, L.G., Noel, J.-P., Barense, M.D., Ferber, S., and Wallace, M.T. (2017). The associations between multisensory temporal processing and symptoms of schizophrenia. *Schizophr. Res.* 179, 97–103.

Stolzberg, D., Hayes, S.H., Kashanian, N., Radziwon, K., Salvi, R.J., and Allman, B.L. (2013). A novel behavioral assay for the assessment of acute tinnitus in rats optimized for simultaneous recording of oscillatory neural activity. *J. Neurosci. Methods* 219, 224–232.

Tak, S., Davis, R.R., and Calvert, G.M. (2009). Exposure to hazardous workplace noise and use of hearing protection devices among US workers—NHANES, 1999–2004. *Am. J. Ind. Med.* 52, 358–371.

Vatakis, A., and Spence, C. (2007). Crossmodal binding: evaluating the "unity assumption" using audiovisual speech stimuli. *Percept. Psychophys*. 69, 744–756.

Vatakis, A., Bayliss, L., Zampini, M., and Spence, C. (2007). The influence of synchronous audiovisual distractors on audiovisual temporal order judgments. *Percept. Psychophys*. 69, 298–309.

Vatakis, A., Ghazanfar, A.A., and Spence, C. (2008a). Facilitation of multisensory integration by the “unity effect” reveals that speech is special. *J. Vis*. 8, 14.1-11.

Vatakis, A., Navarra, J., Soto-Faraco, S., and Spence, C. (2008b). Audiovisual temporal adaptation of speech: temporal order versus simultaneity judgments. *Exp. Brain Res.* 185, 521–529.

Vroomen, J., and Keetels, M. (2010). Perception of intersensory synchrony: A tutorial review. *Atten. Percept. Psychophys*. 72, 871–884.

Vroomen, J., and Stekelenburg, J.J. (2011). Perception of intersensory synchrony in audiovisual speech: Not that special. *Cognition* 118, 75–83.

Wallace, M.T., and Stevenson, R.A. (2014). The construct of the multisensory temporal binding window and its dysregulation in developmental disabilities. *Neuropsychologia* 64, 105–123.

Zampini, M., Shore, D.I., and Spence, C. (2003). Audiovisual temporal order judgments. *Exp. Brain Res*. 152, 198–210.

Chapter 5

5 Compensatory Plasticity in the Lateral Extrastriate Visual Cortex Preserves Audiovisual Temporal Processing Following Adult-Onset Hearing Loss [5]

5.1 Introduction

Following sensory deprivation, such as vision or hearing loss, the brain has the capacity to undergo extensive reorganization, which is often characterized by an increased responsiveness of neurons in the deprived sensory cortex to the spared senses (i.e., crossmodal plasticity) (for review see, Merabet and Pascual-Leone, 2010). For example, in conditions of profound hearing loss, the "deafened" auditory cortex has shown increased activity to visual and/or tactile stimuli, as measured using neuroimaging in humans as well as invasive electrophysiological recordings in animal models (Auer et al., 2007; Doucet et al., 2006; Frasnelli et al., 2011; Lambertz et al., 2005; Meredith and Lomber, 2011). In addition to these neurophysiological changes, behavioural studies have also identified that deafness in early life can lead to improved performance on tasks that emphasize the processing of peripheral visual stimuli or visual motion (Bavelier et al., 2000; Dye et al., 2007; Lomber et al., 2010; Neville and Lawson, 1987; Stevens and Neville, 2006).

Despite the high prevalence of *partial* hearing impairments in society (~1 out of 5 adults) (Agrawal et al., 2008; Feder et al., 2015), appreciably less is known about the nature and extent of crossmodal plasticity that occurs in individuals who retain some level of residual auditory processing, compared to cases of profound hearing loss. That said, recent studies have confirmed that crossmodal plasticity does occur following mild-moderate hearing loss, albeit to a lesser degree than in deaf subjects. Interestingly, not only does the auditory cortex show increased visual and tactile responses following adult-onset hearing

---

[5] A version of this chapter has been accepted for publication as:

Schormans, A.L. and Allman, B.L. (2019) Compensatory plasticity in the lateral extrastriate visual cortex preserves audiovisual temporal processing following noise-induced hearing loss. *Neural Plasticity*. [In Press]

impairment in humans (Campbell and Sharma, 2013, 2014; Cardon and Sharma, 2018) and ferrets (Meredith et al., 2012), but our recent work in rats exposed to loud noise found a differential effect in how auditory and visual stimuli were processed in the auditory cortex versus the multisensory cortex (Schormans et al., 2017a, 2018). More specifically, despite accounting for each rat's elevated hearing threshold two weeks post-noise exposure, we observed a decrease in the proportion of neurons in the multisensory cortex that could be activated by auditory stimuli, as well as an increased responsiveness to visual stimuli in both the auditory and multisensory cortices (Schormans et al., 2017a, 2018). Consequently, following noise exposure, the cortical area now showing the greatest relative degree of multisensory convergence transitioned beyond the audiovisual cortex into a neighbouring auditory region; findings which led to the suggestion that crossmodal plasticity induced by adult-onset hearing impairment can manifest in higher-order areas as a transition in the functional border of the audiovisual cortex.

In normal-hearing subjects, there is clear evidence of several behavioural advantages afforded by the brain's natural ability to integrate auditory and visual information, including improved detection, localization and identification of the stimuli. In addition, psychophysical testing has revealed that auditory and visual stimuli presented within ~100 ms offset from each other can be bound into a unified percept, with subjects showing difficulty accurately judging whether the auditory or visual stimulus was presented first. Ultimately, because neuroimaging studies in humans have shown that synchronized activity in the multisensory cortex underlies audiovisual temporal acuity (Balz et al., 2016), it is reasonable to question how partial hearing impairment, and its ensuing crossmodal plasticity, could disrupt one's perception of the relative timing of audiovisual stimuli, and ultimately the binding of these multisensory cues into a unified percept. Of the few reports available, however, it appears that audiovisual synchrony perception is largely preserved in hearing-impaired subjects (Başkent and Bazo, 2011; Butera et al., 2018; Hay-McCutcheon et al., 2009), provided that potential confounding factors, such as aging, are addressed. Moreover, we recently reported that adult rats with a moderate hearing loss experienced a rapid recalibration of their ability to accurately judge the order of audiovisual stimuli, with temporal perception being restored two weeks following the loud noise exposure (Schormans and Allman, 2018). This inconsistency between the extent of

crossmodal plasticity reported previously and the apparent lack of behavioural consequences raises an important question: how is the brain able to maintain (or re-establish) temporally-precise audiovisual integration and perception in the presence of extensive sensory reorganization in the cortical regions thought to subserve such behavioural tasks?

To date, no studies have investigated whether changes in the temporal precision of audiovisual processing occurs at the neuronal level following adult-onset hearing loss, or if these crossmodal effects differ across the neighbouring regions of the multisensory cortex that normally integrate audiovisual stimuli. Thus, in the present study, we used *in vivo* extracellular electrophysiological recordings in anesthetized rats to investigate how crossmodal plasticity induced by moderate hearing loss alters audiovisual temporal processing across the distinct layers of higher-order sensory cortices. To do so, adult rats were exposed to loud noise exposure, and two weeks later extracellular electrophysiological recordings were performed within two neighbouring regions of the lateral extrastriate visual cortex (V2L); a multisensory area known to be responsive to audiovisual stimuli (V2L-multisensory zone), and a more predominantly-auditory area (V2L-auditory zone). More specifically, a 32-channel linear electrode array was inserted perpendicular to the cortical surface, and laminar processing was examined within each cortical region in response to combined audiovisual stimuli at various stimulus onset asynchronies (SOAs). To examine the layer-specific effects of crossmodal plasticity at the level of postsynaptic potentials, a current source density (CSD) analysis was applied to the local field potential (LFP) data. Based on our earlier work which suggested that moderate hearing loss caused an expansion of the functional boundary of the audiovisual cortex into the neighbouring auditory regions, we predicted that the auditory zone of the V2L cortex would not only become more responsive to visual stimuli post-noise exposure, but it would also inherit the capacity to process audiovisual stimuli with the temporal precision and specificity that was previously restricted to the audiovisual cortex in normal-hearing rats; electrophysiological results that could provide the neurophysiological basis for the preservation/restoration of audiovisual temporal perception following adult-onset hearing loss.

5.2 Methods

The present study included two experimental series; each using a separate group of adult male Sprague-Dawley rats (n = 34 total; Charles River Laboratories, Inc., Wilmington, MA). Prior to examining the cortical consequences of noise-induced crossmodal plasticity, we conducted Experiment 1 to first confirm that the V2L cortex does indeed play an important role in audiovisual temporal acuity, by pharmacologically silencing the region in rats (n = 16) trained to perform perceptual judgment tasks. In Experiment 2, we then performed electrophysiological recordings in anesthetized rats (n = 18) to examine the effect of noise-induced crossmodal plasticity on audiovisual temporal processing within two regions of the V2L cortex. All experiments were approved by the University of Western Ontario Animal Care and Use Committee, and were conducted in accordance with the guideline established by the Canadian Council of Animal Care.

5.2.1 Experiment 1: Role of V2L in Audiovisual Temporal Acuity

5.2.1.1 Audiovisual Behavioural Tasks – TOJ & SJ

Using appetitive operant conditioning, rats were trained on a two-alternative forced-choice paradigm that assessed their ability to perform audiovisual temporal order judgments (TOJ; n = 8) or synchrony judgments (SJ; n = 8). In the TOJ task, rats were trained to differentiate the temporal order of auditory and visual stimuli, whereas rats trained on the SJ task learned to differentiate between trials when the auditory and visual stimuli were presented synchronously or when the visual stimulus preceded the auditory stimulus (i.e., asynchronous). For both tasks, behavioural training began at 70 days old (body mass: 284 ± 7.0g), and the rats were trained 6 days a week. All experimental testing took place when the rats were between 8 and 9 months of age.

Behavioural training and testing were conducted in a standard modular test chamber (ENV-008CT; Med Associates Inc., St. Albans, VT) that was housed within a sound-attenuating box (29” W by 23.5” H by 23.5” D; Med Associates Inc., St. Albans, VT). The front wall of the behavioural chamber included a nose poke as well as a left and right feeder trough, each fitted with an infrared detector to monitor the rat’s performance. The test chamber was illuminated by a house light on the back wall. Real-time processing hardware (RZ6

and BH-32, Tucker Davis Technologies, Alachua, FL) were interfaced with the test chamber. Custom behavioural protocols running in Matlab (EPsych Toolbox, dstolz.github.io/epsych/) monitored nose poke responses, and controlled the presentation of the auditory and visual stimuli, as well as the positive reinforcement (i.e., sucrose pellet delivery) and punishment (i.e., turning off the house light and an inability to commence the next trial).

The auditory stimulus was a 50 ms noise burst (75 dB SPL; 1-32 kHz) presented from a speaker (FT28D, Fostex, Tokyo) mounted on the ceiling of the behavioural chamber near the front wall. The intensity of the auditory stimulus was calibrated using custom Matlab software with a ¼-inch microphone (2530, Larson Davis) and preamplifier (2221; Larson Davis). The visual stimulus was a 50 ms light flash (27 lux) from an LED (ENV-229M; Med Associates Inc.) located above the center nose poke. An LED light meter (Model LT45, Extech Instruments, Nashua, NH) was used to determine the intensity of the visual stimulus.

5.2.1.2 Behavioural Training for the TOJ and SJ Tasks

Prior to commencing behavioural training, rats were weighed daily and maintained on a food restricted diet until they neared 85% of their free-feeding body mass. Over the course of several stages of training, rats learned to associate a given audiovisual stimulus condition with a specific feeder (i.e., TOJ task: auditory-first = left trough, visual-first = right trough; SJ task: synchronous = left trough, asynchronous = right trough; Fig. 5.1A). Once rats successfully reached the final stage of training, they were able to accurately discriminate between auditory and visual stimuli presented at an SOA of ±200 ms for the TOJ task, and synchronous (i.e., 0 ms SOA) versus asynchronous audiovisual stimuli (i.e. 200 ms SOA) in the SJ task. Throughout all stages of the behavioural training procedure, correct feeder trough responses were reinforced with a sucrose pellet, and incorrect responses resulted in the house light turning off for up to 15 s, during which time a new trial could not be initiated. A full description of the behavioural training procedure can be found in our earlier publication (Schormans et al., 2017b).

5.2.1.3 Surgery and Cannulation

Once rats had successfully completed all stages of behavioural training, they were prepared for chronic implantation of bilateral guide cannulae into the V2L cortex, as this would ultimately allow for the local micro-infusion of artificial cerebrospinal fluid (aCSF) or muscimol prior to behavioural test sessions. In preparation for surgery, the rats were anesthetized with isoflurane (induction: 4%; maintenance: 2%), and body temperature was maintained at 37°C using a homeothermic heating pad (507220F; Harvard Apparatus). A subcutaneous injection of meloxicam (1mg/kg) was administered before surgery and as needed post-surgery for pain management. Once a surgical plane of anesthesia was achieved, rats were placed in a stereotaxic frame with blunt ear bars, and a midline incision was made in the scalp, and the dorsal aspect of the skull was cleaned with a scalpel blade. In an effort to improve post-surgical recovery, we elected to have the guide cannulae enter into the cortex on a dorsal-medial-to-ventral-lateral approach, as this left the temporalis muscles intact. After small burr holes were drilled in the skull, stainless-steel guide cannulae (26-gauge, 3 mm in length) were bilaterally implanted to target the V2L cortex using the following coordinates: 6mm caudal to Bregma, 5.6mm lateral to the midline; 10° angle (Fig. 5.1B). These guide cannulae were secured to the skull using dental cement and bone screws as anchors. Stylets were placed into the guide cannulae to prevent their blockage. Finally, the skin surrounding the surgical implant was sutured, and rats were allowed to recover for one week prior to undergoing experimental test sessions that included micro-infusions.

5.2.1.4 Micro-Infusions and Behavioural Testing of the TOJ and SJ Tasks

The rats returned to daily behavioural training after they had fully recovered from surgery, and once their performance again achieved >80% accuracy, experimental test sessions were introduced in which novel SOAs were presented (described below). Ultimately, each rat performed two experimental test sessions following the local micro-infusion of either aCSF, which served as the control condition, or muscimol, a potent agonist of GABA-A receptors, which was used to silence the neuronal activity within the V2L cortex.

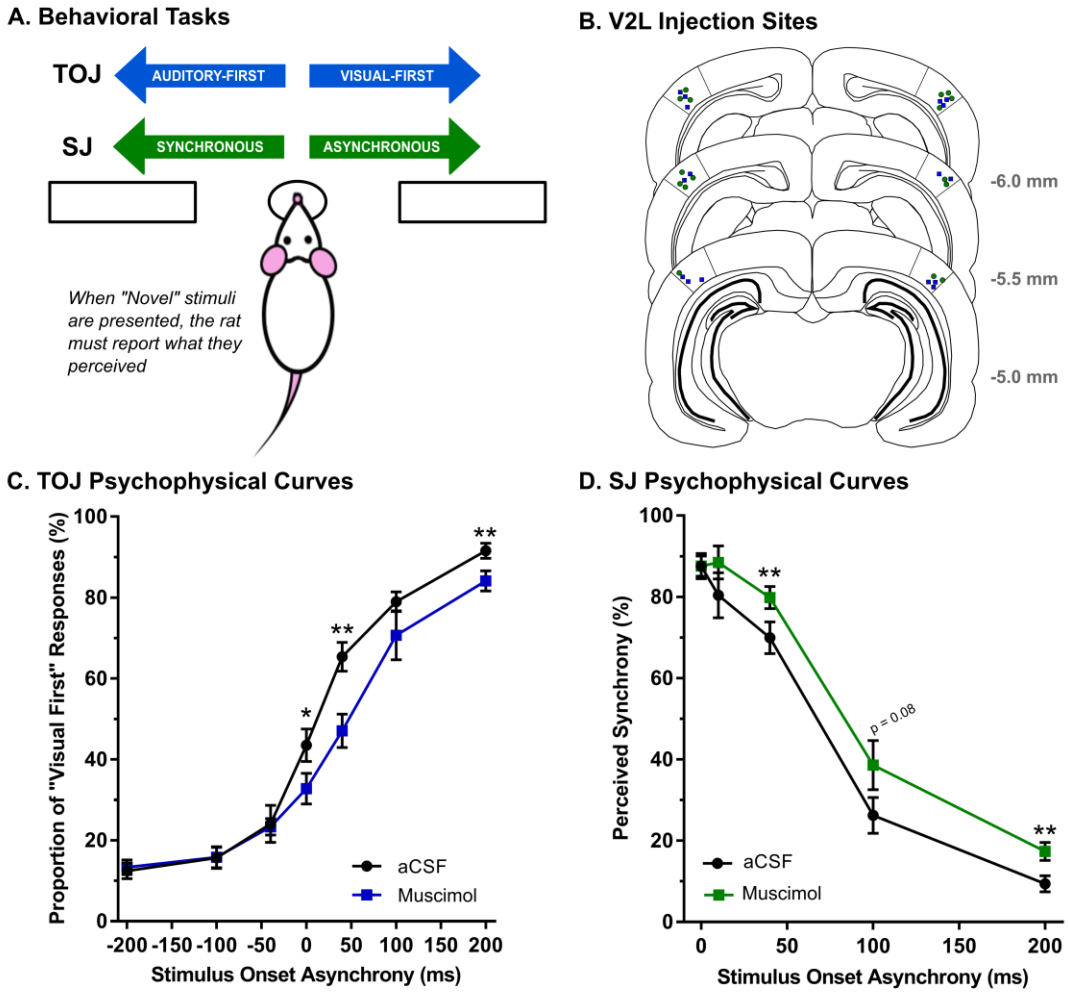

Figure 5.1. Pharmacological silencing of the V2L cortex disrupts audiovisual temporal acuity in rats.

(A) An overview of both the TOJ task and SJ task that were used to screen rats for their audiovisual temporal acuity. Across several stages, rats were trained to select the right or left feeder trough depending on the stimulus condition presented (i.e., TOJ task: auditory-first = left trough, visual-first = right trough; SJ task: synchronous = left trough, asynchronous = right trough). (B) Schematic of the location of the drug infusion cannulae reconstructed from histological sections for each of the rats trained on the TOJ (blue squares) or the SJ task (green circles). (C) Behavioural performance on the TOJ task was plotted as the proportion of trials perceived as visual-first for test sessions completed following the infusion of aCSF (black circles) and muscimol (blue squares). Overall there

*was a rightward shift in the TOJ psychometric curve when muscimol was infused into the V2L cortex, with a significant decrease in trials perceived as visual-first at SOAs of 40 and 200 ms (**p < 0.007), as well as a modest decrease at an SOA of 0 ms (*p < 0.05). (D) For the SJ task, behavioural performance was plotted as the proportion of trials perceived as synchronous for test sessions completed following an infusion of aCSF (black circles) or muscimol (blue squares). Following an infusion of muscimol, a greater proportion of SJ trials were perceived as synchronous at SOAs of 40 and 200 ms (**p < 0.01), and a trend towards an increase was observed at an SOA of 100 ms (p = 0.08). Results are displayed as mean ± SEM for the rats trained to perform the TOJ (n = 8) and SJ (n = 8) tasks.*

Micro-injections were performed in awake animals using infusion cannulae that extended 1.2 mm beyond the length of the chronically-implanted guide cannulae. On a testing day, a given rat received a bilateral infusion of either aCSF (0.5 µL/side) or muscimol (4 mM; 0.5 µL/side) into its V2L cortex before beginning the TOJ or SJ test session. Both sides of the brain were infused simultaneously using a micro-infusion pump and Hamilton syringes paired to the infusion cannula via Teflon tubing. Infusions were made over 2 minutes (0.25 µL/min), and the infusion cannulae were then left in place for an additional 2 minutes to allow adequate diffusion of the drug into the V2L cortex.

During the TOJ test sessions, 7 SOAs were randomly delivered (i.e., 0, ±40, ±100 and ±200 ms), and rats performed a minimum of 10 trials at each of the novel SOAs. For the SJ test sessions, 5 SOAs were randomly delivered (i.e., 0, 10, 40, 100 and 200 ms), and rats were presented with at least 18 trials at each of the novel SOAs. For both behavioural tasks, 70% of the trials presented consisted of training stimuli (i.e., TOJ task: ±200 ms SOA; SJ task: 0 and 200 ms SOA), while the remaining 30% of trials was made up of the random presentation of the novel SOAs. This distribution of trials has been previously shown to reduce the potential of developing a side-bias (Schormans et al., 2017b). Furthermore, the trained stimulus conditions continued to be positively reinforced for correct responses with sucrose pellets and punished for incorrect responses with a 15-s timeout, whereas a sucrose

pellet was delivered following each novel SOA regardless of whether a correct or incorrect response was made.

For each of the TOJ test sessions, performance across all 7 SOAs was measured as the proportion of trials in which the rat perceived the stimuli as visual-first (i.e., it responded to the right feeder trough, Fig. 5.1A). Consistent with human testing, a psychophysical profile was generated for each rat by plotting straight lines between each of the neighbouring SOAs, and the associated slope and intercept values were calculated (Vatakis et al., 2007). Using these values, the point of subjective simultaneity (PSS) and just noticeable difference (JND) were calculated for each of the test sessions (Schormans and Allman, 2018; Schormans et al., 2017b; Vroomen and Stekelenburg, 2011). For each of the SJ test sessions, performance for all 5 SOAs was measured as the proportion of trials in which the rat perceived the stimuli as synchronous (i.e., responded to the left feeder trough, Fig. 5.1A). Similar to the TOJ task, a psychophysical profile was generated for each rat by plotting straight lines between each of the neighbouring SOAs tested, and the associated slope and intercept values were tabulated (Schormans and Allman, 2018; Schormans et al., 2017b). Using these values, two audiovisual asynchrony thresholds (50% and 70%) were extracted, as these are common values used to determine the temporal binding window (TBW) in humans (Başkent and Bazo, 2011; Eg et al., 2015; Kaganovich, 2016; Stevenson and Wallace, 2013).

5.2.2 Experiment 2: Electrophysiological Investigation of Audiovisual Temporal Processing following Noise-Induced Hearing loss

5.2.2.1 Hearing Assessment

In a separate group of rats (n = 18) from those that performed the aforementioned behavioural testing, hearing sensitivity was assessed using the auditory brainstem response (ABR), which was carried out in a double-walled sound-attenuating chamber (MDL 6060 ENV, Whisper Room Inc., Knoxville, TN). Consistent with Schormans et al. (Schormans et al., 2017a), rats were anesthetized with ketamine (80 mg/kg; IP) and xylazine (5 mg/kg; IP), and subdermal electrodes (27 gauge; Rochester Electro-Medical, Lutz, FL) were positioned at the vertex, over the right mastoid and on the back. Body temperature was

maintained at ~37°C using a homeothermic heating pad (507220F; Harvard Apparatus, Kent, UK). Auditory stimuli consisted of a click (0.1 ms) and two tones (4 kHz and 20 kHz; 5 ms duration and 1 ms rise/fall time) which were generated using a Tucker-Davis Technologies RZ6 processing module sampled at 100 kHz (TDT, Alachua, FL). Auditory-evoked activity was collected using a low impedance headstage (RA4LI; TDT), preamplified and digitized (RA16SD Medusa preamp; TDT), and sent to a RZ6 processing module via a fiber optic cable. Stimulus delivery and threshold detection were performed in accordance with an established protocol (Schormans et al., 2017a, 2018). The sound stimuli used in the ABR testing, as well as the subsequent noise exposure and electrophysiological recordings, were calibrated using custom MATLAB software (The Mathworks, Natick, MA) using a ¼-inch microphone (2530; Larson Davis, Depew, NY) and preamplifier (2221; Larson Davis).

Prior to the *in vivo* extracellular electrophysiological recordings, rats in the control group (n = 8) underwent an ABR to assess their hearing sensitivity, while rats in the noise exposed group (n = 10) underwent a baseline hearing assessment, followed by exposure to a broadband noise (see below for details). Two weeks following the noise exposure, a final hearing assessment was performed, after which the same electrophysiological recordings were completed as those in control rats. Electrophysiological recordings were completed two weeks following the noise exposure, as previous studies have demonstrated extensive region- and layer-specific plasticity across the higher-order sensory cortices at this time post-noise exposure (Schormans et al., 2018).

5.2.2.2 Noise Exposure

Under ketamine (80 mg/kg; IP) and xylazine (5 mg/kg; IP) anesthesia, rats were bilaterally exposed to a broadband noise (0.8 – 20 kHz) for two hours at 120 dB SPL, and body temperature was maintained at ~37°C using a homeothermic heating pad. This noise exposure was selected because it has been shown to be effective at inducing changes in the auditory cortex (Popelar et al., 2008) and higher-order, multisensory cortices (Schormans et al., 2017a). The broadband noise was generated with TDT software (RPvdsEx) and hardware (RZ6) and delivered by a super tweeter (T90A; Fostex, Tokyo, Japan) which was placed 10 cm in front of the rat.

5.2.2.3 Surgical Procedure

Following the final hearing assessment, each rat was maintained under ketamine/xylazine anesthesia and fixed in a stereotaxic frame with blunt ear bars. Anesthetic depth was assessed by the absence of a pedal withdrawal reflex, and supplemental doses of ketamine/xylazine were administered IM as needed. An incision was made along the midline of the skull and the dorsal aspect of the skull was cleaned with a scalpel blade. The left temporalis muscle was reflected and removed using a blunt dissection technique in order to provide access to the temporal bone overlying the left auditory and multisensory cortices. A stereotaxic micromanipulator was used to make a mark on the skull 6 mm caudal of Bregma, which represents the approximate stereotaxic coordinates of the lateral extrastriate visual cortex (V2L) (Hirokawa et al., 2008; Schormans et al., 2017a; Wallace et al., 2004; Xu et al., 2014). Additional marks were made on the temporal bone at 1, 2, and 3 mm ventral of the top of the skull for later drilling. A small hole was hand drilled and a stainless-steel screw was inserted in the left frontal bone to serve as an anchor for the headpost and electrical ground. In order to provide free-field sound stimulation, a headpost was fastened to the skull with dental acrylic. Once the dental cement had hardened, a craniotomy (2 x 5 mm; 5-7 mm caudal to Bregma) was made in the left temporal and parietal bone to expose the multisensory cortex. Subsequently, the right ear bar was removed to allow free-field auditory stimulation of the right ear during electrophysiological recordings in the contralateral cortex. The rat was held in position throughout the duration of the experiment within the stereotaxic frame using the left ear bar and the headpost.

5.2.2.4 Electrophysiological Recordings and Stimulation Parameters

In each animal, two recording penetrations were performed which encompassed the majority of the audiovisual cortex. At each of the recording locations (described in detail below), a small slit was made in the dura, and a 32-channel linear electrode array was slowly inserted perpendicular to the cortical surface (Fig. 5.2B) using a hydraulic microdrive (FHC, Bowdoin, ME). The array consisted of 32 iridium microelectrodes equally-spaced 50 µm apart on a 50-µm-thick shank (model: A1x32-10mm-50-177-A32; NeuroNexus Technologies, Ann Arbor, MI). Initially, the electrode array was rapidly

advanced into the cortex using a high-precision stereotaxic manipulator in order to penetrate the pia mater, and then withdrawn to the cortical surface. Subsequently, the hydraulic microdrive was used to slowly advance the electrode array until a depth of -1500 µm was reached. Slight adjustments were made based on a characteristic sharp negative peak of the local field potential to auditory or visual stimuli (typically -350 to -450 µm depth below the pial surface) (Stolzberg et al., 2012). Once the appropriate depth was reached, the electrode array was allowed to settle in place for at least 45 minutes before beginning the electrophysiological recordings. Neural signals were acquired using TDT System 3 (TDT, Alachua, FL), and the local field potential (LFP) activity was continuously acquired (digitally resampled at 1000 Hz and bandpass filtered online at 1 – 300 Hz).

In each rat, laminar recordings were completed in two brain regions: (1) the multisensory zone of the lateral extrastriate visual cortex (V2L-Mz; corresponding to the 2 mm ventral mark made on the skull using our measurements), and (2) the auditory zone of the lateral extrastriate visual cortex (V2L-Az; 2.5 mm ventral). Consistent with previous studies demonstrating that higher-order sensory cortices occur at the intersection of the primary sensor cortices (Wallace et al., 2004), the V2L-Mz is located ventral to the primary visual cortex (V1) (otherwise termed ‘lateral’) and its neighbouring region, the V2L-Az, is found dorsal to the primary auditory cortex. Figure 5.2A shows a schematic of the relative position of these zones in the V2L cortex, as well as the location for each of the penetrations from all electrophysiological experiments.

At each of the recording locations, auditory, visual and combined audiovisual stimuli were presented using a TDT RZ6 processing module (100 kHz sampling rate) and custom Matlab software. Auditory stimuli consisted of 50 ms noise bursts (1-32 kHz) from a speaker (MF1, TDT) positioned 10 cm from the right pinna on a 30° angle from midline. The intensity of the auditory stimulus was customized for each rat, such that it was presented 40 dB above the rat’s click threshold (control: 68.1 ± 0.9 dB SPL; noise exposed: 80.6 ± 1.4 dB SPL) as determined by the preceding hearing assessment. Visual stimuli consisted of 50 ms light flashes (15 lux; 50 ms duration) from an LED positioned adjacent to the speaker (i.e., 10 cm from the right eye). The intensity of the visual stimulus was determined using a LED light meter (Model LT45, Extech Instruments, Nashua, NH). The

combined audiovisual stimuli were presented at various stimulus onset asynchronies (SOAs) in which the visual stimulus was presented 50, 40, 30, 20, 10, and 0 ms before the auditory stimulus. In total 6 stimuli conditions were presented in a randomized order, separated by an inter-stimulus interval of 3 – 5 s, and each condition was presented 50 times.

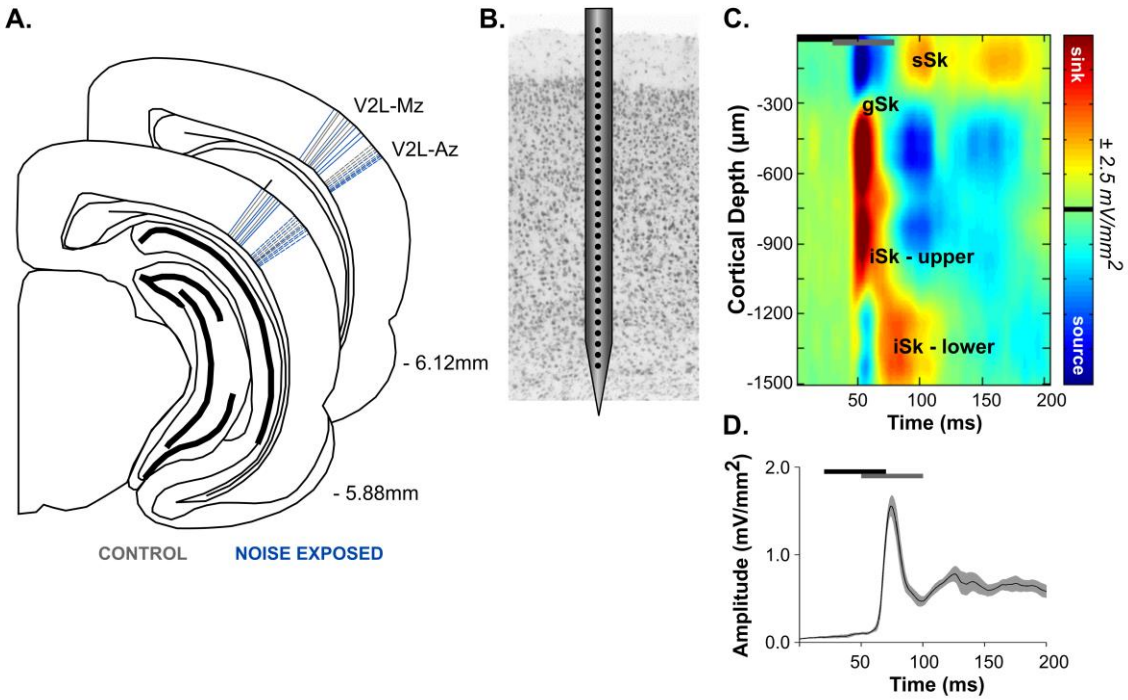

Figure 5.2. Recording site reconstruction, and audiovisual-evoked CSD analysis in the multisensory zone of the V2L cortex (V2L-Mz).

(A) The schematic shows a reconstruction of all recording penetrations in normal-hearing control rats (grey; n = 16) and noise exposed rats (blue; n = 20). In each rat, two penetrations were performed in the lateral extrastriate visual cortex; one in the multisensory zone of V2L (V2L-Mz), and the other in the more ventral-positioned, auditory zone of V2L (V2L-Az). (B) A representation of a 32-channel linear electrode array spanning the entire cortical thickness within the V2L-Mz. (C) Representative CSD profile in a control rat in response to audiovisual stimuli presented at an SOA of 30 ms. Prominent current sinks (red) are reflective of a depolarization of neurons in the surrounding cortical region, whereas prominent current sources (blue) reflect a repolarization of neurons in the

surrounding cortical regions. The black horizontal bar denotes the presentation of the visual stimulus (50 ms LED flash at 15 lux) and the grey horizontal bar shows the timing of the auditory stimulus (50 ms noise burst at 40 dB sensation level (SL)). (D) Average rectified current source density (AVREC) analysis derived from the CSD profiles in (C) in response to the combined audiovisual stimulus.

5.2.2.5 Current Source Density (CSD) Analysis:

The CSD analysis provides a spatial profile of ionic flow and a measure of the total current density that enters or leaves the extracellular matrix through the cell membrane (Einevoll et al., 2013; Mitzdorf, 1985). A one-dimensional CSD analysis was applied to the mean LFPs recorded simultaneously across the entire cortical thickness using the formula (Eq. 1):

$$CSD \approx -\frac{\Phi(z+n\Delta z)-2\,\Phi(z)+\,\Phi(z-n\Delta z)}{(n\Delta z)^2} \qquad (1)$$

where Φ is the LFP, z is the spatial coordinate, Δz is the inter-electrode spacing (Δz = 50 µm), and n is the differentiation grid (n = 4) (Freeman and Singer, 1983; Mitzdorf, 1985; Mitzdorf and Singer, 1977; Nicholson and Freeman, 1975). The CSD equation approximates the second spatial derivative of the LFPs at each time point across electrode sites. A 3-point Hamming filter was applied in order to smooth LFPs across channels before computing the CSD, as described by Stolzberg et al. (2012). Consistent with previous studies (Freeman and Singer, 1983; Mitzdorf, 1985; Mitzdorf and Singer, 1977, 1980; Nicholson and Freeman, 1975; Stolzberg et al., 2012), current sinks were positive in amplitude and sources were negative.

The CSD analysis reveals the flow of ions into and out of the neural tissue across the cortical thickness. Current sinks represent the flow of positive ions into the neural tissue from the extracellular space, which is reflective of events such as active excitatory synaptic populations and axonal depolarization (Happel et al., 2010; Kral and Eggermont, 2007). Current sources represent passive return currents, which corresponds to repolarization and possibly inhibition of the neighbouring tissue (Einevoll et al., 2013; Happel et al., 2010;

Kral and Eggermont, 2007; Mitzdorf, 1985; Szymanski et al., 2009). For each of the recording locations and each of the stimulus combinations, only CSD sinks were analyzed. Current sinks were identified as being at least three standard deviations above the mean voltage measured during the 50 ms before the first stimulus was presented. Within both recording locations, prominent sinks were identified in the granular (-300 µm < depth ≥ -750 µm) and infragranular-upper layers (-750 < depth ≥ -1200 µm). Additional sinks were observed in the supragranular (depth ≥ -350 µm) and infragranular-lower layers (depth < -1200 µm) (see Fig. 5.2C for reference).

Consistent with Schormans et al. (2018), CSD waveforms were extracted from the depth that demonstrated the largest amplitude within an individual sink (i.e., peak amplitude; see Fig. 5.3). For each of the identified sinks, the peak amplitude was derived from a single depth in order to account for individual sink components that spanned various depths (e.g., extended beyond or were narrower than the space defined above). Using the same method, peak latency was also derived for each of the four identified sinks. The peak amplitude and latency was calculated for all stimulus combinations. All calculations were performed using custom Matlab scripts.

5.2.2.6 Average Rectified CSD Analysis

To examine the overall strength of postsynaptic currents in each of the cortical areas, the average rectified CSD (AVREC) measure was applied to the CSD analysis (Happel et al., 2010; Schroeder et al., 1997, 2001; Stolzberg et al., 2012). While rectification of the CSD results in a loss of information about the direction of the transmembrane current flow, the AVREC waveform provides information about the temporal pattern of the overall strength of the postsynaptic currents (Givre et al., 1994; Happel et al., 2010; Schroeder et al., 1998). The AVREC was calculated by averaging the absolute values of the CSD across all channels (Eq. 2).

$$AVREC = \frac{\sum_{i=1}^{n} |CSD_i|(t)}{n} \tag{2}$$

where CSD refers to Eq. 1, n refers to the number of channels, and t refers to the time point index. To quantitatively analyze the AVREC waveforms for each cortical region, peak

amplitude and latency were calculated for each stimulus combination within the first 200 ms from the onset of the visual stimulus (Fig. 5.2D).

5.2.2.7 Data Analysis

Multisensory interactions were quantified by comparing the response of the combined audiovisual stimulus to that of the unimodal stimulus that evoked the largest response in each experiment (King and Palmer, 1985; Meredith et al., 1987). The magnitude of the response interaction was calculated using the formula (Eq. 3).

$$Response\ Interaction\ (\%) = \frac{(MS - UNI_{max})}{UNI_{max}} \times 100 \qquad (3)$$

where *MS* is the amplitude to the combined audiovisual stimulus and *UNImax* is the amplitude from the unimodal stimulus that evoked the largest amplitude. To analyze the temporal response profile across the various SOAs, the magnitude of the response interaction was calculated for each SOA, and then averaged across experiments within each group and cortical region for both the granular sink and the AVREC amplitudes.

5.2.3 Histology

At the conclusion of both of the experimental series, the rats were injected with sodium pentobarbital (100 mg/kg; IP) in preparation for exsanguination via transcardial perfusion with 4% paraformaldehyde. Brains were serially sectioned (50 µm) using a microtome (HM 430/34; Thermo Scientific, Waltham, MA). To verify that the cannulae tips were correctly located within the V2L cortex from the behavioural experiments, the coronal sections were mounted and stained with thionin. To reconstruct the location of each of the recording penetrations following the electrophysiological recordings, the coronal sections were mounted in fluorescent DAPI mounting medium (F6057 FluoroshieldTM with DAPI; Sigma, St. Louis, MO) and cover slipped. Ultimately, fluorescent and brightfield images were obtained using an Axio Vert A1 inverted microscope (Carl Zeiss Microscopy GmbH, Jena, Germany), and ZEN imaging software.

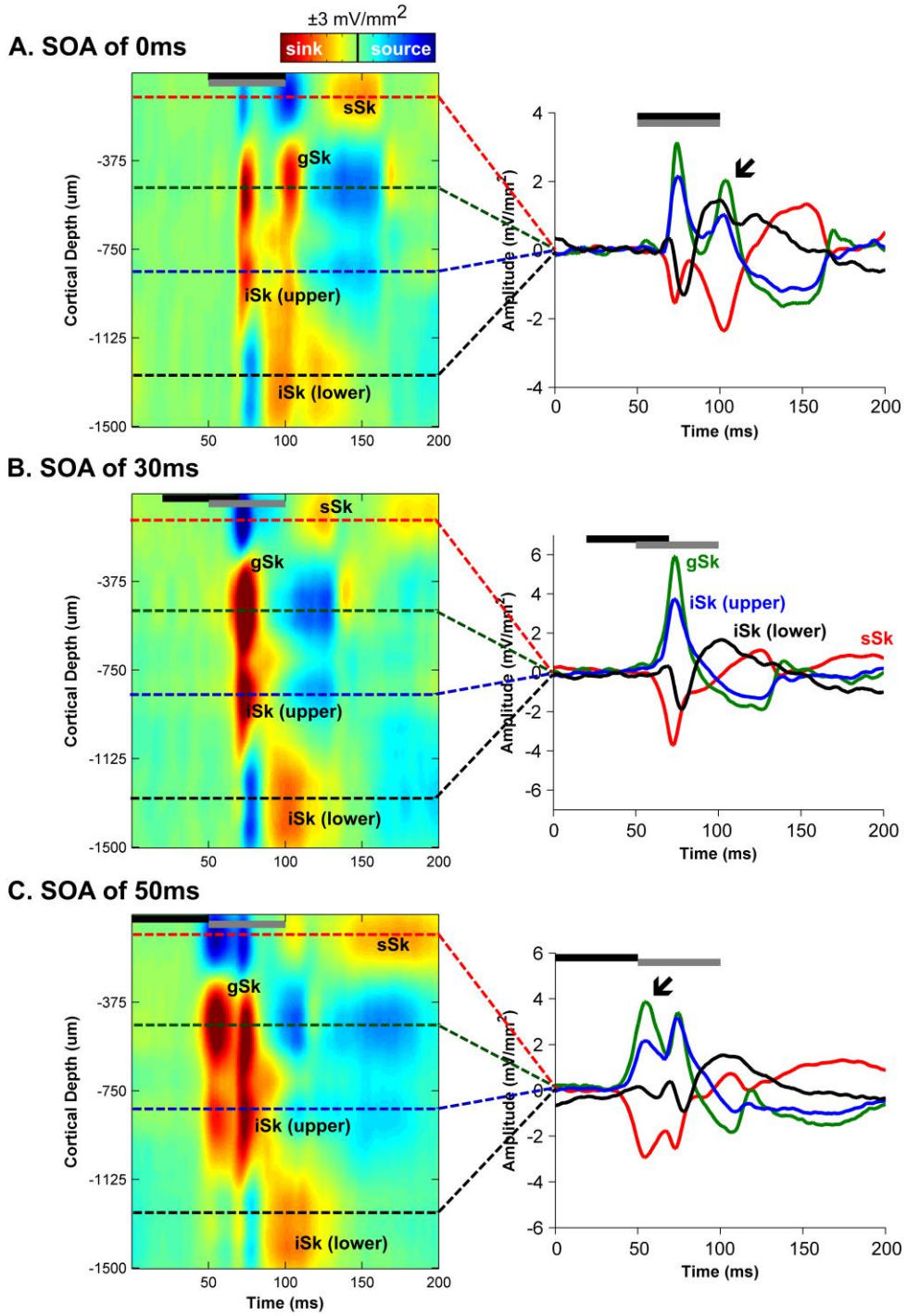

Figure 5.3. Audiovisual-evoked CSD profiles within the multisensory zone of the V2L cortex in response to 3 different SOAs.

Representative CSD profiles (left) and extracted CSD waveforms (right) at an SOA of (A) 0 ms, (B) 30ms, and (C) 50 ms in response to a combined audiovisual stimulus. CSD

waveforms were extracted from the electrode showing the largest amplitude from each of the individual sinks (denoted by the dashed lines on the CSD images for the supragranular (sSk, red), granular (gSk, green), infragranular-upper (iSk upper, blue) and infragranular-lower (iSk lower, black) responses; sinks are positive, whereas sources are negative. In each of the plots, the horizontal black bar denotes the presentation of the visual stimulus (50 ms LED flash at 15 lux) and the grey horizontal bar shows the timing of the auditory stimulus (50 ms noise burst at 40 dB sensation level (SL)). The black arrow within the CSD waveforms on panels (A) and (C) show the location of the visual response, demonstrating that the visual response changes from occurring second at an SOA of 0 ms, to occurring first at an SOA of 50 ms.

5.2.4 Statistics

Statistical analyses were conducted on the data using various procedures, including repeated-measures analysis of variance (ANOVA), one-way ANOVA or paired/unpaired t-tests depending on the comparison of interest. All statistical comparisons used an alpha value of 0.05, and Bonferroni post hoc corrections were performed when appropriate. GraphPad Prism (GraphPad Software Inc.,) and MATLAB (2012b; The Mathworks) were used for graphical display, and SPSS (Version 25, IBM Corporation) software was used for the various statistical analyses. Throughout the text and figures, data are presented as the mean values ± standard error of the mean (SEM).

5.3 Results

5.3.1 Inactivation of the V2L Cortex Shifted the Perception of Simultaneity and Perceived Synchrony

In Experiment 1, we investigated the contribution of the V2L cortex to (1) the perception of simultaneity during a TOJ task, and (2) synchrony perception during an SJ task, by locally infusing the GABA-A receptor agonist, muscimol, prior to behavioural testing, and ultimately comparing the performance results to those following the control condition (i.e., aCSF infusion). During the TOJ test sessions, the proportion of trials that were perceived as visual-first were determined for all 7 SOAs, ranging from -200 ms (i.e., auditory-first)

to +200 ms (i.e., visual-first). A two-way repeated-measures ANOVA revealed a significant interaction of infusion by SOA ($F[4.5,31.3] = 2.8$, $p < 0.05$). To further investigate this interaction, post hoc paired samples t-tests were completed between the test sessions. As shown in Figure 5.1C, following the local micro-infusion of muscimol into the V2L cortex, a significantly greater proportion of trials were perceived as visual-first at an SOA of 40 and 200 ms ($p < 0.007$), indicating that the V2L cortex plays a role in audiovisual temporal perception. Moreover, the point of subjective simultaneity (PSS), which is described as the timing at which participants are most unsure of the temporal order of the audiovisual stimuli, significantly increased following the inactivation of the V2L cortex (aCSF: 9.2 ± 6.1 ms vs. Muscimol: 55.1 ± 12.5 ms; $p < 0.01$; paired samples t-test). Analysis of the just noticeable difference (JND) data, demonstrated that inactivating the audiovisual cortex did not impair the ability to accurately detect the audiovisual stimuli (aCSF: 69.7 ± 9.8 ms vs. Muscimol: 82.0 ± 12.6 ms; $p = 0.45$). These data reveal that the inactivation of the V2L cortex via muscimol shifted the perception of simultaneity, but did not affect temporal sensitivity during the TOJ task. Thus, the V2L cortex appears to play an important role in perceiving the relative timing of the audiovisual stimuli, but does not influence the ability to detect subtle timing differences between the stimuli.

During the SJ test sessions, the proportion of trials that were perceived as synchronous (i.e., the rat responded to the right feeder trough) were determined for all 5 SOAs ranging from 0 ms (i.e. synchronous) to 200 ms (i.e., asynchronous; visual stimulus presented 200 ms before the auditory stimulus). Overall, a two-way repeated-measures ANOVA revealed main effects of infusion and SOA ($F[1,7] = 11.1$, $p < 0.05$; $F[1.5,10.3] = 98.8$, $p < 0.001$; respectively), but no significant interaction of infusion by SOA ($F[4,28] = 85.4$, $p = 0.13$). Follow-up paired samples t-tests demonstrated that a larger proportion of trials were perceived as synchronous at an SOA of 40 and 200 ms ($p < 0.01$; Fig. 5.1D) following the inactivation of the V2L cortex. Although no additional comparisons reached statistical significance, trends were observed at an SOA of 10 ($p = 0.09$) and 100 ms ($p = 0.08$). In addition to the analyses completed on the SJ psychophysical curves, the 50% and 70% audiovisual asynchrony thresholds were examined. Consistent with the results observed on the SJ psychophysical curves, there was a significant increase in the 50% (aCSF: 67.8 ± 5.1 ms vs. 91.4 ± 8.6 ms; $p < 0.05$) and 70% (aCSF: 31.2 ± 5.6 ms vs. 55.7 ± 4.5 ms; p <

0.05) audiovisual asynchrony thresholds. These results reveal that inactivation of the V2L cortex impairs synchrony perception, such that physically asynchronous stimuli were more likely to be perceived as synchronous.

The collective results of Experiment 1 show for the first time that the V2L cortex is directly involved in the perceived timing of audiovisual stimuli. Moreover, the fact that these results confirm the importance of the V2L cortex in TOJ task performance was interesting given that our previous studies on hearing-impaired rats showed a preservation of audiovisual temporal perception despite extensive crossmodal reorganization in the V2L cortex in the weeks following noise-induced hearing loss. In considering this apparent paradox, we conducted Experiment 2 in which in vivo electrophysiological recordings were performed in noise-exposed rats to determine how their V2L cortex alters its responsiveness to audiovisual stimuli at varying SOAs, so as to ultimately preserve audiovisual temporal perception following hearing impairment.

5.3.2 Noise-Induced Hearing Loss

Consistent with Schormans et al. (2017a, 2018), crossmodal plasticity was induced by exposing rats to a broadband noise at 120 dB SPL for two hours. To ensure that rats had a partial hearing loss, ABR thresholds were compared at baseline versus two weeks post-noise in the noise exposed rats ($n = 10$). A two-way repeated-measures ANOVA revealed a significant difference in ABR thresholds two weeks post-noise exposure ($F[1,9] = 30.3$, $p < 0.001$). Bonferroni post hoc correction testing (adjusted p-value = 0.017) revealed a significant increase in the ABR threshold of the click (pre-noise: 27 ± 1.1 dB SPL vs. post-noise: 39.5 ± 1.4 dB SPL; $p < 0.001$), 4 kHz (pre-noise: 24 ± 1.5 dB SPL vs. post-noise: 44.5 ± 2.9 dB SPL; $p < 0.001$) and 20 kHz stimulus (pre-noise: 12.5 ± 1.5 dB SPL vs. post-noise: 34.5 ± 6.3 dB SPL; $p < 0.05$). Prior to noise exposure, there were no differences in hearing sensitivity between the control and noise exposed rats for any of the stimuli (one-way ANOVA; $p > 0.05$). In addition to examining ABR thresholds, the amplitude of the first wave of the ABR was used to assess the level of damage to the auditory nerve afferents caused by the noise exposure (Kujawa and Liberman, 2009). As expected, two weeks following the noise exposure, there was a significant reduction (56.5 ± 5.7 %) in wave 1 amplitude (pre-noise: 1.7 ± 0.08 uV vs. post-noise: 0.7 ± 0.09 uV; $p < 0.001$).

For all electrophysiological experiments, the intensity of the auditory stimulus (50 ms noise burst; 1-32 kHz) was adjusted for each rat in order to control for potential differences in hearing sensitivity among rats. To account for each rat's noise-induced hearing loss, the auditory stimulus was presented 40 dB SPL above its click threshold. As such, the auditory stimulus that was presented during the electrophysiological experiments to the noise exposed rats was greater in comparison to the controls (noise exposed: 80.0 ± 1.4 dB SPL vs. control: 68.1 ± 0.9 dB SPL, $p < 0.001$, independent samples t-test).

5.3.3 Crossmodal Plasticity Increases Audiovisual Responsiveness within the Multisensory Zone of the V2L Cortex across a Range of SOAs

Using the analysis of CSD sink amplitudes, we investigated whether noise-induced crossmodal plasticity within the multisensory zone of the lateral extrastriate visual cortex (V2L-Mz) altered audiovisual temporal processing across the cortical layers. Within the V2L-Mz—a region previously shown to exhibit increased visual responsiveness following exposure to a loud noise (Schormans et al., 2018)—the averaged CSD waveforms were computed for both groups. Waveforms were generated for each individual sink (i.e., supragranular, granular, infragranular-upper and infragranular-lower layers) in response to audiovisual stimuli presented at 6 SOAs (i.e., the visual stimulus preceded the auditory stimulus by 0, 10, 20, 30, 40, 50 ms). Due to the large number of factors in the present study, a three-way repeated-measures ANOVA (layer x SOA x group) was performed on audiovisual-evoked CSD amplitudes within the multisensory zone of V2L (Fig. 5.4), which ultimately revealed a significant interaction ($F[7.9,127.0] = 3.1$, $p < 0.01$). Due to the unique characteristics of each cortical sink, subsequent statistical analyses were completed for individual CSD sinks. Therefore, a separate two-way repeated-measures ANOVAs (SOA x group) were performed with Bonferroni-corrected post hoc tests (adjusted p-value = 0.008) for each of the CSD sinks.

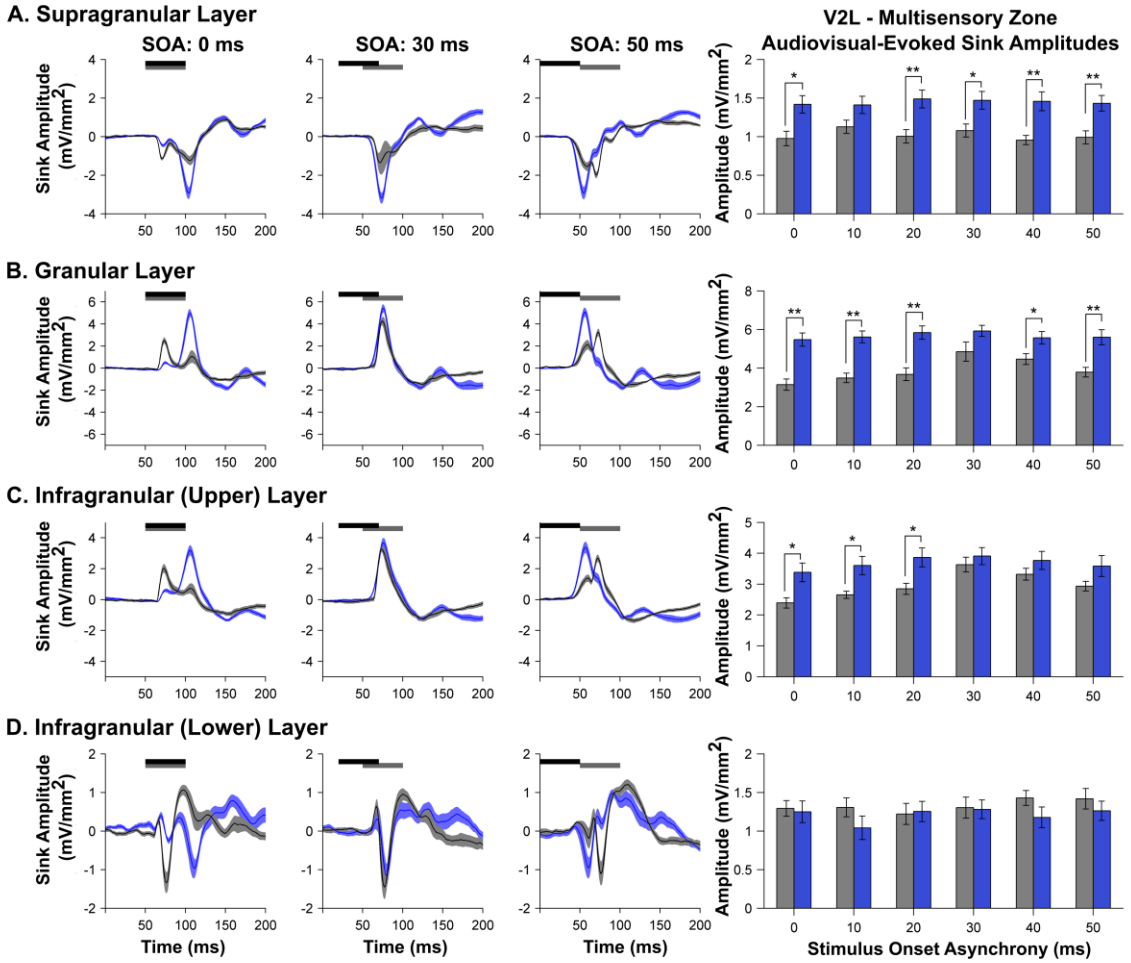

Figure 5.4. A loss of the characteristic audiovisual temporal profile was observed across the majority of layers of the multisensory zone of the V2L cortex in noise exposed rats.

Averaged CSD waveforms from the (A) supragranular, (B) granular, (C) infragranular-upper and (D) infragranular-lower layers within the V2L-Mz in response to audiovisual stimuli presented at an SOA of 0, 30 and 50 ms. The black horizontal bar denotes the presentation of the visual stimulus, and the grey horizontal bar shows the timing of the auditory stimulus. The dark lines represent the group mean and the shading represents the SEM for the noise exposed rats (blue; n = 10) and age-matched controls (light grey; n = 8). An analysis of audiovisual-evoked sink amplitudes within each cortical layer (see bar graphs on the far right) shows an increase in responsiveness across most of the cortical

*layers in the noise exposed rats. Values are displayed as mean ± SEM. *p < 0.05; **p < 0.008.*

As shown in Figure 5.4, there was an overall increase in audiovisual-evoked sink amplitudes across multiple SOAs and cortical layers two weeks following noise exposure. Separate two-way repeated-measures ANOVAs revealed a significant interaction of SOA by group in the supragranular layer ($F[5,80] = 2.6$, $p < 0.05$) as well as the granular layer ($F[5,80] = 3.6$, $p < 0.01$). Although both of the infragranular layers did not show a significant interaction, the upper infragranular layer revealed a main effect of SOA ($F[5,80] = 7.3$, $p < 0.001$). Within the supragranular and granular layers, noise-induced hearing loss increased the level of postsynaptic activity in response to audiovisual stimulation across a range of SOAs (Fig. 5.4A, 5.4B). Within the upper-infragranular layer, there was a modest increase in audiovisual-evoked sink amplitudes only at SOAs less than 30 ms. Taken together, these results demonstrate that crossmodal plasticity alters audiovisual temporal processing within the multisensory zone of V2L, such that this cortical region demonstrates increased responsiveness to audiovisual stimuli across a range of SOAs.

In addition to examining the effects of noise-induced hearing loss within distinct cortical layers, AVREC waveforms were computed in order to provide additional information about the temporal pattern of the overall strength of the postsynaptic currents (Givre et al., 1994; Happel et al., 2010; Schroeder et al., 1998). AVREC peak amplitude and latency were computed for each group in response to each of the presented SOAs. A two-way repeated-measures ANOVA revealed a significant interaction of SOA by group ($F[5,80] = 9.3$, $p < 0.001$) for AVREC peak amplitude (Fig. 5.5). Similar to the results observed in the upper infragranular layer, there was a significant increase in the AVREC peak amplitude at SOAs less than 30 ms ($p < 0.008$). As can be seen in Figure 5.5B, SOAs from 30 to 50 ms showed no difference in peak amplitude. In order to further examine the effect of noise-induced crossmodal plasticity, AVREC peak latency was analyzed within the multisensory zone of the V2L cortex. A two-way repeated-measures ANOVA revealed a significant interaction of SOA by group for AVREC peak latency ($F[1.6,25.7] = 19.25$, $p < 0.001$).

Although there was only a difference in peak amplitude at SOAs less than 30 ms, significant differences in peak latency were observed across multiple SOAs (Fig. 5.5C). More specifically, there was a significant increase in latency at an SOA of 10 ms ($p < 0.008$) as well as a modest increase at a SOA of 0 ms ($p < 0.05$). Furthermore, a significant decrease in peak latency was observed at SOAs greater than 30 ms (i.e., 40 and 50 ms SOA; $p < 0.008$). This differential response profile, whereby AVREC peak latency increases or decreases on either side of 30 ms SOA is consistent with the profile observed in the primary visual cortex (unpublished results from our lab). Overall, the collective results from the multisensory zone of the V2L cortex demonstrated that noise-induced crossmodal plasticity resulted in significant changes in audiovisual temporal processing across the layers of this cortical region, and ultimately altered the relative timing of sensory responses after adult-onset hearing loss.

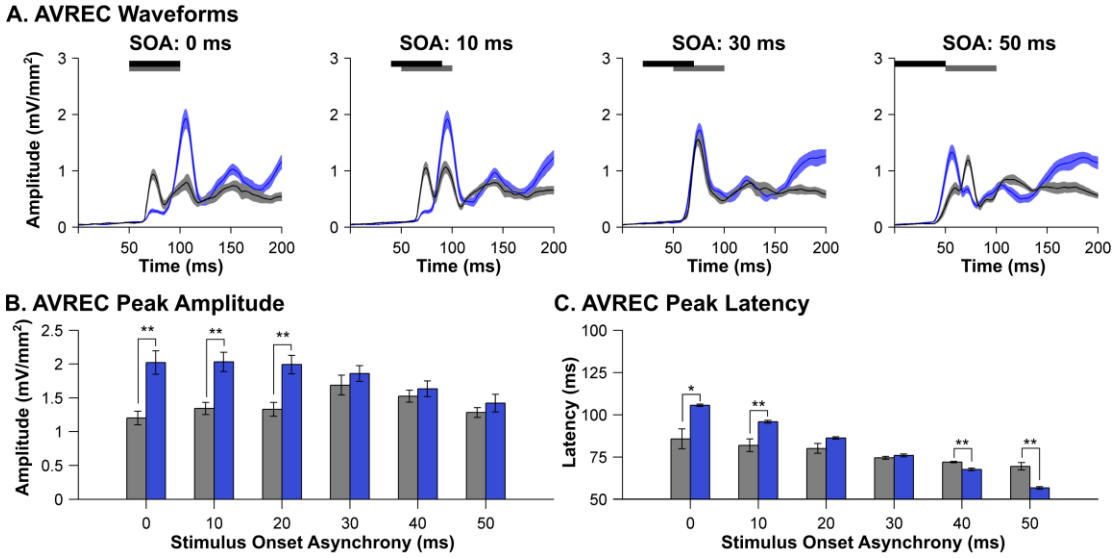

Figure 5.5. Noise-induced hearing loss enhanced the audiovisual-evoked AVREC amplitudes at select SOAs within the multisensory zone of the V2L cortex.

(A) AVREC waveforms in response to audiovisual stimuli presented at and SOA of 0, 10, 30 and 50 ms (from left to right) for noise exposed rats (blue; n = 10) and age-matched controls (light grey; n = 8). The horizontal black and grey bars denote the presentation of the visual and auditory stimuli, respectively. (B) Audiovisual-evoked AVREC amplitudes were significantly increased in the noise exposed rats when the timing between the stimuli

*was less than 30 ms. (C) AVREC peak latency showed differential effects between the groups, which were dependent on the SOA. In comparison to the controls, the noise exposed rats showed a significant increase in peak latency at SOAs less than 20 ms, whereas they showed a significant decrease in peak latency at SOAs greater than 30 ms. Values are displayed as mean ± SEM for the noise exposed (n = 10) and control (n = 8) groups. *p < 0.05; **p < 0.008.*

5.3.4 Audiovisual Responsiveness within the Auditory Zone of the V2L Cortex following Adult-Onset Hearing Loss

Similar to V2L-Mz, it has been previously demonstrated that there is increased visual responsiveness within the auditory zone of the V2L cortex following noise-induced hearing loss (Schormans et al., 2018). Therefore, using the same techniques as described above, we sought to investigate whether crossmodal plasticity influenced audiovisual temporal processing across the cortical layers within a once predominantly auditory-responsive region. For each cortical layer, average CSD waveforms were computed in the two groups (control vs. noise exposure) in response to the audiovisual stimuli at multiple SOAs. A three-way repeated-measures ANOVA of audiovisual-evoked CSD sink amplitudes, revealed a main effect of cortical layer ($F[1.6,25.2] = 72.8$, $p < 0.001$). Due to the unique profile of each individual sink, subsequent statistical analyses were performed independently for each sink. Ultimately, for each of the panels in Figure 5.6, a separate two-way repeated-measures ANOVA (SOA x group) was performed with Bonferroni-corrected post hoc tests (adjusted p-value = 0.008) for each of the CSD sinks.

While the multisensory zone of V2L demonstrated an overall increase in CSD sink amplitude, an opposite pattern emerged in the more ventrally located auditory zone of the V2L cortex (V2L-Az). As shown in Figure 5.6, there was a general decrease in level of postsynaptic activity in response to audiovisual stimulation across a range of SOAs. Separate two-way repeated-measures ANOVAs revealed minimal differences across all of the cortical layers, as only the upper infragranular layer demonstrated a main effect of group ($F[1,16] = 6.1$, $p < 0.05$). Follow-up Bonferroni post hoc t-tests showed a modest decrease in audiovisual-evoked amplitudes across a range of SOAs ($p < 0.05$; Fig. 5.6C).

Overall, these results demonstrate that the multisensory zone of the V2L shows the largest crossmodal effects following noise-induced hearing loss, whereas the V2L-Az cortex showed modest changes in the opposite direction.

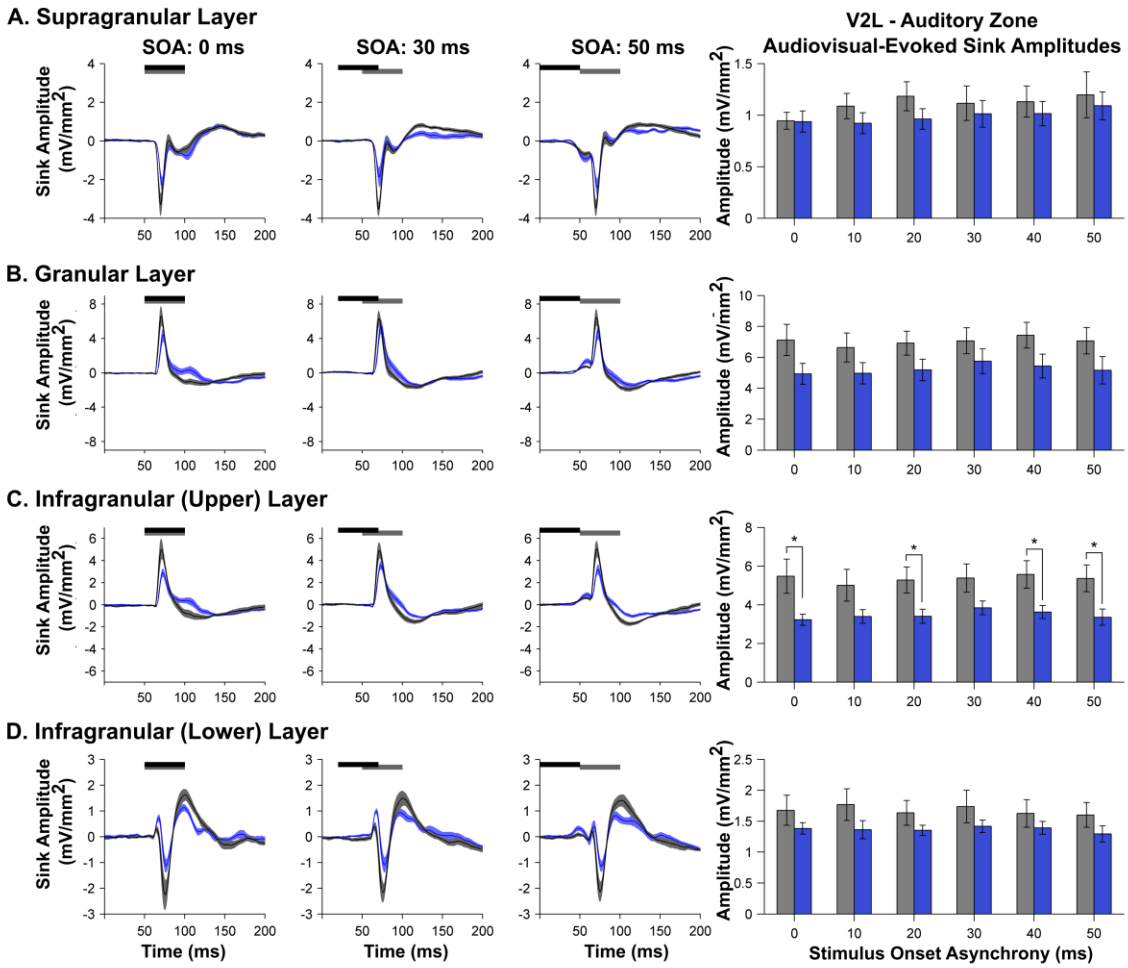

Figure 5.6. A decrease in audiovisual-evoked CSD amplitudes was generally observed within the auditory zone of the V2L cortex in noise exposed rats.

Averaged CSD waveforms from the (A) supragranular, (B) granular, (C) infragranular-upper and (D) infragranular-lower layers within the auditory zone of V2L cortex in response to audiovisual stimuli presented at an SOA of 0, 30 and 50 ms. The black horizontal bar denotes the presentation of the visual stimulus, and the grey horizontal bar shows the timing of the auditory stimulus. The dark lines represent the group mean, and the shading represents the SEM for the noise exposed rats (blue; n = 10) and the age-

*matched controls (light grey; n = 8). Unlike the V2L-Mz cortex, which showed an extensive increase in the audiovisual-evoked sink amplitudes across the majority of its layers following noise-induced hearing loss (Figure 5.4), the auditory zone of V2L (V2L-Az) showed only a modest decrease in audiovisual responsiveness which was mostly restricted to the upper-infragranular layer (*p < 0.05). Values are displayed as mean ± SEM.*

To further examine the consequences of a partial hearing loss on the auditory zone of the V2L cortex, the overall strength of the postsynaptic currents was examined by computing AVREC waveforms for each of the groups. To do so, AVREC peak amplitude and latency were extracted from the waveforms in response to audiovisual stimuli across a range of SOAs. Overall, a two-way repeated-measures ANOVA revealed a main effect of group ($F[1,16] = 4.9$, $p < 0.05$) as well as a trend towards a main effect for SOA ($F[5,80] = 2.0$, $p = 0.08$). Consistent with CSD sink amplitudes within V2L-Az, there was a general decrease in AVREC peak amplitude across multiple SOAs ($p < 0.05$; Fig. 5.7B). Contrary to the multisensory zone of V2L (Fig. 5.5C), the auditory zone showed no differences in peak latency ($p > 0.05$; Fig. 5.7C). Therefore, despite the increased visual responsiveness observed within V2L-Az two weeks after noise-induced hearing loss, the audiovisual temporal response profile within this region was relatively maintained.

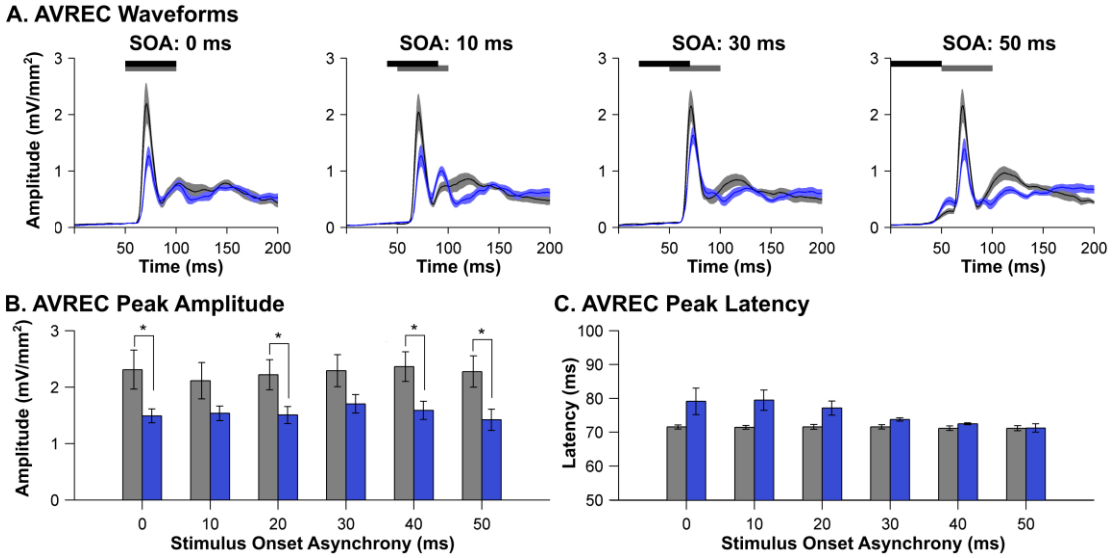

Figure 5.7. Audiovisual-evoked AVREC amplitude and latency within the auditory zone of the V2L cortex following noise-induced hearing loss.

*(A) Audiovisual-evoked AVREC waveforms within the auditory zone of the V2L cortex at SOAs of 0, 10, 30, and 50 ms (from left to right) for noise exposed rats (blue; n = 10) and age-matched controls (light grey; n = 8). The horizontal black and grey bars denote the presentation of the visual and auditory stimuli, respectively. (B) An overall decrease in AVREC peak amplitude was observed across multiple SOAs within the auditory zone of V2L (*p < 0.05). (C) No differences in AVREC peak latency were observed. Values are displayed as mean ± SEM*

5.3.5 A Shift in the Temporal Profile following Noise-Induced Crossmodal Plasticity

To further examine changes in audiovisual processing following noise-induced hearing loss, the magnitude of response interaction was calculated for the granular sink and AVREC peak amplitudes by comparing audiovisual-evoked amplitudes to the unimodal stimulus that produced the largest amplitude. More specifically, the magnitude of response interaction for both the granular sink data and AVREC data were calculated for each group at all temporal offsets ranging from 0 ms (synchronous) to 50 ms (visual leading) within

both V2L-Mz and V2L-Az. Consistent with the neuronal response profile observed in the superior colliculus (King and Palmer, 1985; Meredith et al., 1987) and the V2L cortex (Schormans et al., 2017b) in normal-hearing animals, we expected that peak amplitudes within the multisensory zone of the V2L cortex would show the same temporal sensitivity whereby the greatest response interaction would occur when the visual stimulus preceded the auditory stimulus at an SOA of 20 to 40 ms.

For the granular sink data set, an initial three-way repeated-measures ANOVA found a significant interaction of area by SOA by group ($F[5,80] = 8.44$, $p < 0.001$), and thus, we further examined each of these interactions in order to reveal the specific differences between the groups, as well as the temporal profiles within each of the groups. As shown in Figure 5.8, the response interactions in the granular layer of the multisensory zone as well as the auditory zone of the V2L cortex showed drastic differences between the noise exposed rats and the controls. Within the V2L-Mz, a significant interaction of SOA by group was observed ($F[5,80] = 7.02$, $p < 0.001$), yet post hoc t-tests failed to show significant differences between the groups at any of the SOAs presented (Fig. 5.8A). In contrast, within the V2L-Az, a two-way repeated-measures ANOVA revealed a significant interaction of SOA by group ($F[5,80] = 3.82$, $p < 0.01$), and post hoc t-tests found a difference between groups at 30 ms SOA ($p = 0.013$) in which the noise exposed rats demonstrated an increased response interaction compared to the controls (Fig. 5.8D). Next, to examine how the timing of the audiovisual stimuli influenced the response interaction in the granular layer of both groups, separate one-way repeated-measures ANOVAs were performed in the noise exposed and control rats. As expected, the multisensory zone of V2L of control rats demonstrated a main effect of SOA ($F[5,35] = 13.91$, $p < 0.001$) and these rats showed a significant increase in the magnitude of the response interaction at SOAs of 30, 40 and 50 ms when compared to an SOA of 0 ms (paired samples t-test; $p < 0.01$; Fig. 5.8B). In contrast, there was no main effect of SOA in the multisensory zone of the V2L cortex of noise exposed rats ($F[5,45] = 0.70$, $p = 0.624$). Furthermore, the opposite pattern emerged in the auditory zone of V2L, where there was no effect of stimulus timing in controls [one-way rmANOVA; ($F[5,35] = 0.90$, $p = 0.493$)], but in the noise exposed rats there was a significant increase in the magnitude of the response interaction at an SOA of 30 ms ($p < 0.01$) and a modest increase at an SOA of 40 ms ($p = 0.011$). These findings

highlight that the typical temporal profile observed in the granular layer of the multisensory zone of the V2L cortex in normal-hearing rats was now evident in the more-ventrally located auditory zone in the noise exposed rats.

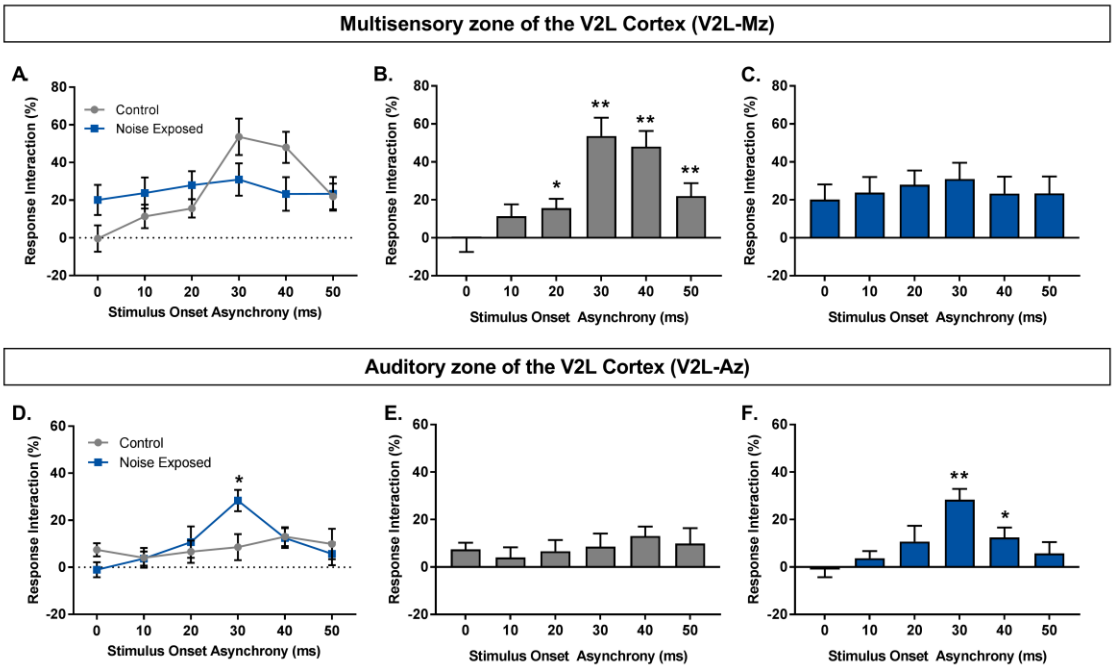

Figure 5.8. The magnitude of the multisensory response interactions varied across the regions of the V2L cortex before- and after noise exposure.

*To assess how hearing loss affected the sensitivity of neurons in the multisensory- and auditory zones of the V2L cortex to the relative timing of the auditory and visual stimuli, the magnitude of the multisensory response interaction was calculated by comparing the amplitude of the granular sink in response to the combined audiovisual stimulus to that of the separately-presented unimodal stimulus that evoked the largest response. Overall, a differential effect was observed in the between noise exposed rats (n = 10) and control rats (n = 8) within the (A) V2L-Mz and the (D) V2L-Az, with a significant difference between groups at 30 ms SOA (*p < 0.05). (B-F) Bar graphs show the change in the multisensory response interaction at each SOA within each group. In controls rats, only the neurons in the V2L-Mz showed multisensory interactions that were sensitive to the relative timing of the auditory and visual stimuli (compare panels B and E). In contrast, only the neurons in the V2L-Az showed a newfound temporal sensitivity after the noise-induced hearing loss*

*(compare panels C and F). Following two-way repeated measures ANOVAs, paired samples t-tests were completed between each SOA and 0 ms (synchrony) to investigate the temporal profile within each cortical region (*p < 0.05; **p < 0.01). Values are displayed as mean ± SEM.*

Additional support for a functional transition in the cortical region showing the greatest degree of audiovisual response interaction was evident from analyses of the AVREC data collected from the multisensory- and auditory zones of the V2L cortex in noise exposed rats versus controls. As shown in Figure 5.9, the influence of the SOA on the degree of response interaction in the multisensory zone of the V2L cortex was evident in the control rats [Fig. 5.9A; ($F[5,35] = 8.51$, $p < 0.001$)] but not in the noise exposed rats (Fig. 5.9B), as they failed to show a preferred response interaction when the visual stimulus preceded the auditory stimulus by 30 ms compared to when they were presented simultaneously (0 ms SOA). That said, the auditory zone of the V2L cortex of the noise exposed rats, unlike the controls, now showed evidence of temporal sensitivity in the magnitude of the response interaction [Fig. 5.9D; ($F[5,45] = 7.72$, $p < 0.001$)]. Interestingly, when paired samples t-tests were completed between each SOA and 0 ms (synchrony), a consistent profile emerged between the V2L-Mz in controls (Fig. 5.9A) and the V2L-Az in the noise exposed rats (Fig. 5.9D), in which both regions showed a significant increase in the magnitude of the response interaction of the AVREC at SOAs of 30 ms ($p < 0.05$) and 40 ms ($p < 0.01$). Thus, these collective results are consistent with a functional transition in the cortical region showing the greatest degree of audiovisual temporal sensitivity following adult-onset hearing loss (Fig. 5.9E vs. 5.9F).

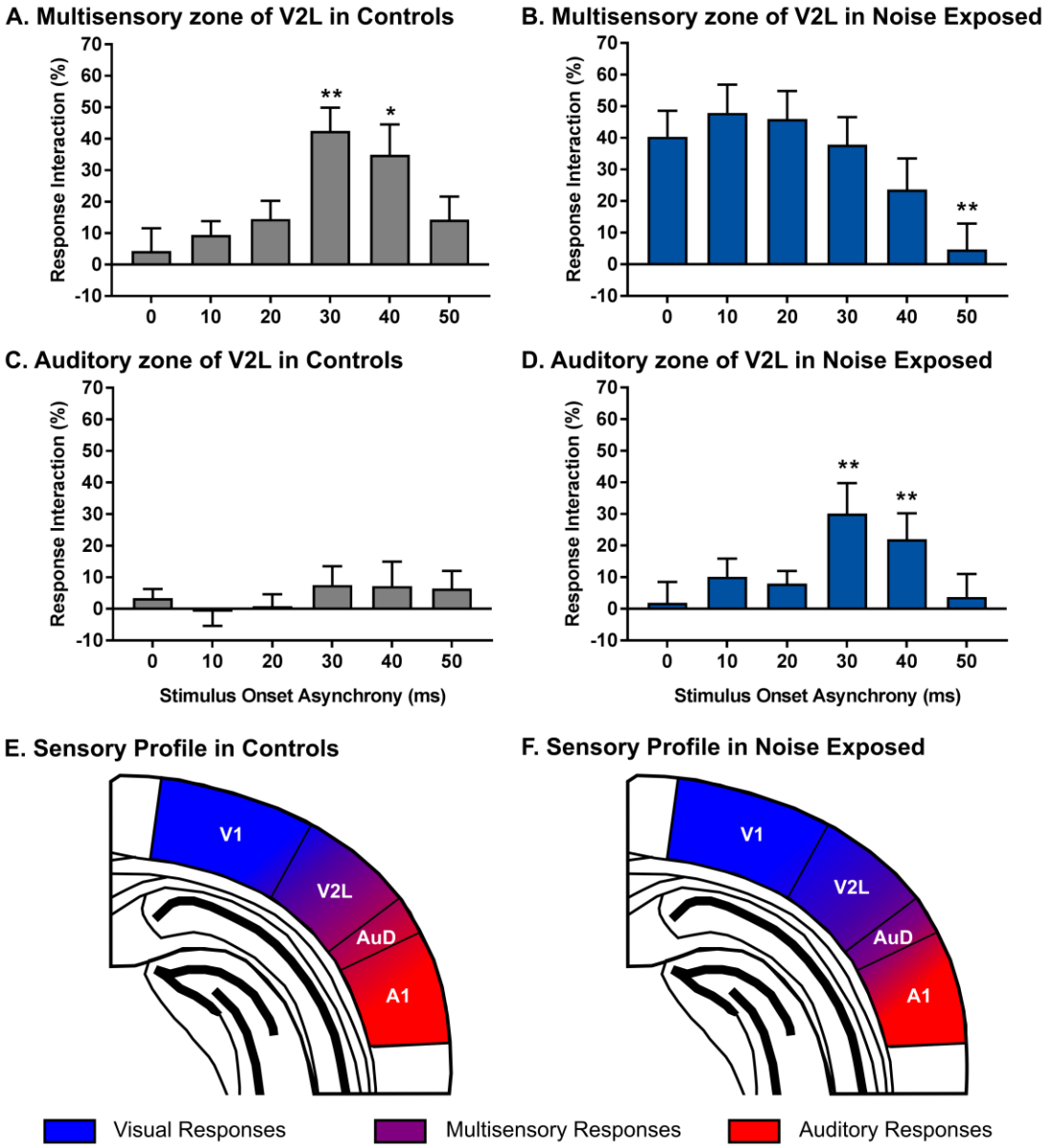

Figure 5.9. Compensatory plasticity in the auditory zone of the V2L cortex preserved audiovisual temporal processing following moderate hearing loss.

Using the AVREC amplitude as a measure of the overall strength of postsynaptic currents in a given cortical region, the magnitude of the multisensory response interactions was then calculated at each SOA to determine how noise-induced hearing loss affected the sensitivity of neurons in the multisensory- and auditory zones of the V2L cortex to the relative timing of the auditory and visual stimuli. Ultimately, the temporal profile observed

*in the V2L-Mz of control rats (A), in which there was a significant increase in the magnitude of the multisensory response interaction at an SOA of 30 and 40 ms, was consistent with the temporal profile that emerged within the V2L-Az of noise exposed rats (D). Following two-way repeated-measures ANOVAs, paired samples t-tests were completed between each SOA and 0 ms (synchrony) to investigate the temporal profile within each cortical region (*p < 0.05; **p < 0.01). Values are displayed as mean ± SEM. (E and F) As schematized, it appears that noise exposure did not result in a loss of temporally-precise audiovisual processing, but instead caused a functional transition in the cortical region displaying this temporal sensitivity; findings which are suggestive of compensatory plasticity having occurred following moderate hearing loss.*

5.4 Discussion

Following moderate hearing loss, neurons in the auditory cortex as well as the higher-order audiovisual cortex maintain a residual capacity for sound processing, while also now demonstrating crossmodal plasticity, a phenomenon characterized by an increased responsiveness to visual stimuli (Campbell and Sharma, 2014; Meredith et al., 2012). Interestingly, despite this sensory reorganization, behavioural studies on hearing-impaired humans and rats have reported that audiovisual temporal acuity—the perceptual ability to accurately judge the relative timing of auditory and visual stimuli—is largely unaffected (Başkent and Bazo, 2011; Schormans and Allman, 2018). To investigate the potential neurophysiological basis of how audiovisual temporal acuity may be preserved in the presence of hearing loss-induced crossmodal plasticity, we exposed adult rats to a loud noise, and two weeks later performed *in vivo* electrophysiological recordings across the distinct layers of neighbouring regions of the audiovisual cortex (i.e., the lateral extrastriate visual area, V2L) to ultimately assess the nature and extent of changes in audiovisual temporal processing at the level of post-synaptic potentials. In particular, we sought to determine whether the increased visual responsiveness of neurons in a once-predominantly auditory area was also accompanied by a newfound capacity to temporally-integrate auditory and visual information similar to that of the audiovisual cortex in normal-hearing

rats; electrophysiological results that could provide the neural substrate for the preservation of audiovisual temporal perception following adult-onset hearing loss.

5.4.1 The Role of the V2L Cortex in Audiovisual Temporal Processing and Perception

Previous studies on normal-hearing rats have reported that the V2L cortex, which is wedged between the primary visual cortex (V1) and the dorsal auditory cortex (AuD), shows several hallmarks of cortical multisensory processing consistent with other mammals (Barth et al., 1995; Hirokawa et al., 2008; Schormans et al., 2017b; Toldi et al., 1986; Wallace et al., 2004; Xu et al., 2014). For example, within the V2L cortex, there exists a diverse population of sensory-responsive neurons, some of which show robust spiking responses to both auditory and visual stimuli (i.e., bimodal neurons), and others that only overtly respond to a single modality yet this response can be modulated by the other seemingly-ineffective modality (i.e., subthreshold multisensory neurons) (Schormans et al., 2017a). Moreover, in normal-hearing rats, the cortical region that has the greatest proportion of bimodal neurons (i.e., the V2L multisensory zone, V2L-Mz) is relatively small (~500 µm span from dorsal-to-ventral), whereas the areas flanking the V2L-Mz, such as the auditory- or visual zones of the V2L cortex (V2L-Az; V2L-Vz), have a reduced capacity for multisensory processing (Schormans et al., 2017a; Wallace et al., 2004). To further investigate the multisensory profile of the V2L cortex, in the present study we simultaneously recorded the LFP activity across the distinct layers of V2L-Mz and V2L-Az in response to separate- versus combined auditory and visual stimulation at various temporal offsets. As expected, the subsequent CSD analyses revealed that neurons in the V2L-Mz showed the greatest multisensory response interaction when the visual stimulus preceded the auditory stimulus by ~30-40 ms (Fig. 5.8B; 5.9A), whereas the neurons in the V2L-Az, did not show any preferential multisensory effects upon manipulation of the relative timing of the auditory and visual stimuli (Fig. 5.8E; 5.9C). Thus, in normal-hearing rats, audiovisual temporal processing appeared to be restricted to a discrete region of the higher-order multisensory cortex (Fig. 5.9E).

Based on these electrophysiological findings, it would be reasonable to suspect that the V2L cortex plays a role in perceptual tasks that require audiovisual temporal acuity, such

as those in which the rats must judge the temporal order of auditory and visual stimuli (TOJ task), or whether the auditory and visual stimuli were presented synchronously or not (SJ task). To investigate this possibility, we chronically-implanted cannulae into the V2L cortex of normal-hearing rats that had been trained to perform the TOJ or SJ task, and then micro-infused muscimol (or aCSF) prior to behavioural testing to determine the effect of pharmacological silencing of the V2L cortex on audiovisual temporal acuity. Ultimately, this novel experimental series revealed that the inactivation of the V2L cortex caused (1) a shift in the perception of simultaneity during the TOJ task, such that the light flash now had to be presented much earlier before the noise burst for the two stimuli to be perceived as having occurred simultaneously, and (2) caused a lengthened epoch of time over which the physically asynchronous auditory and visual stimuli were perceived to have occurred at the same moment in time (i.e., the temporal binding window increased on the right side of physical synchrony) (Fig. 5.1). Taken together, these findings confirm that the V2L cortex contributes to audiovisual temporal acuity, and ultimately prompted us to wonder what happens at the neuronal level to audiovisual temporal processing in the V2L cortex following noise-induced hearing loss that allows for audiovisual temporal perception to be preserved in the presence of crossmodal plasticity.

5.4.2 Effects of Hearing Loss on Audiovisual Temporal Processing

Our previous studies on noise exposed rats found a significant reduction in the auditory-evoked activity in the V2L-Mz (despite increasing the noise burst intensity to control for their elevated hearing thresholds), and a concomitant increase in visual responsiveness in the neighbouring region, V2L-Az (Schormans et al., 2017a, 2018). Consequently, in the present study we predicted that, in addition to showing increased multisensory convergence post-noise exposure, neurons in the V2L-Az would also be able to process audiovisual stimuli with the temporal selectivity that was previously restricted to the V2L-Mz in normal-hearing rats. In support of this prediction, we found a differential effect of hearing loss-induced crossmodal plasticity in the neighbouring regions of the V2L cortex, whereby the typical temporal profile observed in the granular layer of the V2L-Mz in normal-hearing rats (i.e., an increased multisensory response interaction when the visual stimulus preceded the auditory stimulus by ~30 ms; Fig. 5.8B) was now only present in the more-

ventrally located V2L-Az in the noise exposed rats (Fig. 5.8F). Thus, we have shown for the first time that hearing loss-induced crossmodal plasticity does not result in a loss of temporally-precise audiovisual processing, but instead there appears to be a functional transition in the cortical region displaying this temporal sensitivity (schematized in Fig. 5.9E vs. 5.9F).

At present, the cellular mechanisms underlying the functional shift in multisensory convergence across the neighbouring cortical regions remains elusive. With respect to hearing loss-induced crossmodal plasticity in general, it has been postulated that cortical reorganization may emerge via (1) altered multisensory processing in subcortical loci that ultimately manifests as cortical plasticity (Allman et al., 2009); (2) a loss of local cortical inhibition (Yang et al., 2012); (3) altered dendritic spine density in the deprived cortical region (Clemo et al., 2014); and/or (4) a complex assortment of homeostatic plasticity associated with the upward- and downward-scaling of intracortical and thalamocortical excitatory synapses in the deprived and spared cortices (Lee and Whitt, 2015; Petrus et al., 2014, 2015; Whitt et al., 2014). Clearly, future studies are needed to resolve which, if any, of the aforementioned mechanisms contribute to the transition in the functional boundary of the audiovisual cortex following moderate hearing loss in adulthood. We suspect, however, that this functional transition of the audiovisual cortex would not likely be due to an anatomical shift in the territorial borders of the respective cortices because no significant differences in the cytoarchitectonic borders or cortical connectivity were found within the sensory cortices of congenitally deaf cats (Berger et al., 2017; Meredith et al., 2017; Barone et al., 2013); a much more extreme model of sensory deprivation than the moderate hearing impairment induced in the present study.

5.4.3 Compensatory Plasticity following Hearing Loss

To date, the vast majority of studies that have investigated the behavioural consequences of hearing loss-induced crossmodal plasticity have focused on humans and laboratory animals with profound hearing loss. Given the improved processing of peripheral visual stimuli and visual motion (Bavelier et al., 2000; Dye et al., 2007; Lomber et al., 2010; Neville and Lawson, 1987; Stevens and Neville, 2006) commonly reported in these deaf subjects, the underlying neurophysiological changes have been described as

"compensatory" in nature. To our knowledge, the present study provides the first evidence of compensatory plasticity at the neuronal level following moderate hearing loss, characterized by a transition in the functional boundary of the audiovisual cortex that ultimately preserved the temporal sensitivity of multisensory processing post-noise exposure. Based on these neurophysiological results, it is reasonable to postulate that this compensatory plasticity ultimately contributes to the preservation of audiovisual temporal acuity previously reported in humans and rats with hearing impairment (Başkent and Bazo, 2011; Schormans and Allman, 2018).

5.4.4 Conclusions

The present study aimed to advance our understanding of the nature and extent of sensory reorganization that occurs following moderate hearing loss in adulthood, with an emphasis on how this highly-prevalent form of sensory deprivation impacts audiovisual temporal processing at the neuronal level. Using a rat model of noise exposure and layer-specific electrophysiological recordings of postsynaptic potentials in neighbouring regions within the lateral extrastriate visual (V2L) cortex, we have shown for the first time that adult-onset hearing loss does not result in a loss of temporally-precise audiovisual processing, but rather a shift in the cortical region displaying this capacity for temporal sensitivity. Indeed, although the neurons in multisensory zone of the V2L cortex of noise exposed rats no longer showed the canonical enhancement of multisensory responses when the visual stimulus preceded the auditory stimulus by ~30 ms, this temporal profile emerged in the neighbouring cortical region, the once-predominantly auditory zone of the V2L. Future studies are needed to uncover the cellular mechanisms associated with this compensatory plasticity, and whether the transition in the functional boundary of the audiovisual cortex is indeed the neural substrate for the preservation of audiovisual temporal perception reported in hearing-impaired subjects.

5.5 References

Agrawal, Y., Platz EA, and Niparko JK (2008). Prevalence of hearing loss and differences by demographic characteristics among us adults: Data from the national health and nutrition examination survey, 1999-2004. *Arch. Intern. Med.* 168, 1522–1530.

Allman, B.L., Keniston, L.P., and Meredith, M.A. (2009). Adult deafness induces somatosensory conversion of ferret auditory cortex. *Proc. Natl. Acad. Sci.* 106, 5925–5930.

Auer, E.T., Bernstein, L.E., Sungkarat, W., and Singh, M. (2007). Vibrotactile Activation of the Auditory Cortices in Deaf versus Hearing Adults. *Neuroreport* 18, 645–648.

Balz, J., Keil, J., Roa Romero, Y., Mekle, R., Schubert, F., Aydin, S., Ittermann, B., Gallinat, J., and Senkowski, D. (2016). GABA concentration in superior temporal sulcus predicts gamma power and perception in the sound-induced flash illusion. *NeuroImage* 125, 724–730.

Barone, P., Lacassagne, L., and Kral, A. (2013) Reorganization of the connectivity of cortical field DZ in congenitally deaf cats. *PLOS ONE*. 8, e60093.

Barth, D.S., Goldberg, N., Brett, B., and Di, S. (1995). The spatiotemporal organization of auditory, visual, and auditory-visual evoked potentials in rat cortex. *Brain Res*. 678, 177–190.

Başkent, D., and Bazo, D. (2011). Audiovisual asynchrony detection and speech intelligibility in noise with moderate to severe sensorineural hearing impairment. *Ear Hear.* 32, 582–592.

Bavelier, D., Tomann, A., Hutton, C., Mitchell, T., Corina, D., Liu, G., and Neville, H. (2000). Visual attention to the periphery is enhanced in congenitally deaf individuals. *J. Neurosci.* 20, RC931-6.

Berger, C., Kühne, D., Scheper, V., and Kral, A. (2017). Congenital deafness affects deep layers in primary and secondary auditory cortex. *J. Comp. Neurol.* 525, 3110–3125.

Butera, I.M., Stevenson, R.A., Mangus, B.D., Woynaroski, T.G., Gifford, R.H., and Wallace, M.T. (2018). Audiovisual Temporal Processing in Postlingually Deafened Adults with Cochlear Implants. *Sci. Rep.* 8, 11345.

Campbell, J., and Sharma, A. (2013). Compensatory changes in cortical resource allocation in adults with hearing loss. *Front. Syst. Neurosci.* 7, 71.

Campbell, J., and Sharma, A. (2014). Cross-Modal Re-Organization in Adults with Early Stage Hearing Loss. *PLOS ONE* 9, e90594.

Cardon, G., and Sharma, A. (2018). Somatosensory Cross-Modal Reorganization in Adults With Age-Related, Early-Stage Hearing Loss. *Front. Hum. Neurosci*. 12.

Clemo, H.R., Lomber, S.G., and Meredith, M.A. (2014). Synaptic Basis for Cross-modal Plasticity: Enhanced Supragranular Dendritic Spine Density in Anterior Ectosylvian Auditory Cortex of the Early Deaf Cat. *Cereb. Cortex*, bhu225.

Doucet, M.E., Bergeron, F., Lassonde, M., Ferron, P., and Lepore, F. (2006). Cross-modal reorganization and speech perception in cochlear implant users. *Brain* 129, 3376–3383.

Dye, M.W.G., Baril, D.E., and Bavelier, D. (2007). Which aspects of visual attention are changed by deafness? The case of the Attentional Network Test. *Neuropsychologia* 45, 1801–1811.

Eg, R., Behne, D., and Griwodz, C. (2015). Audiovisual temporal integration in reverberant environments. *Speech Commun*. 66, 91–106.

Einevoll, G.T., Kayser, C., Logothetis, N.K., and Panzeri, S. (2013). Modelling and analysis of local field potentials for studying the function of cortical circuits. *Nat. Rev. Neurosci. Lond.* 14, 770–785.

Feder, K., Michaud, D., Ramage-Morin, P., McNamee, J., and Beauregard, Y. (2015). Prevalence of hearing loss among Canadians aged 20 to 79: audiometric results from the 2012/2013 Canadian Health Measures Survery. *Stat. Can*. 26, 18–25.

Frasnelli, J., Collignon, O., Voss, P., and Lepore, F. (2011). Chapter 15 - Crossmodal plasticity in sensory loss. In *Progress in Brain Research*, eds. A.M. Green, C.E. Chapman, J.F. Kalaska, and F. Lepore, (Amsterdam, Netherlands: Elsevier), 233–249.

Freeman, B., and Singer, W. (1983). Direct and indirect visual inputs to superficial layers of cat superior colliculus: a current source-density analysis of electrically evoked potentials. *J. Neurophysiol.* 49, 1075–1091.

Givre, S.J., Schroeder, C.E., and Arezzo, J.C. (1994). Contribution of extrastriate area V4 to the surface-recorded flash VEP in the awake macaque. *Vision Res.* 34, 415–428.

Happel, M.F.K., Jeschke, M., and Ohl, F.W. (2010). Spectral Integration in Primary Auditory Cortex Attributable to Temporally Precise Convergence of Thalamocortical and Intracortical Input. *J. Neurosci.* 30, 11114–11127.

Hay-McCutcheon, M.J., Pisoni, D.B., and Hunt, K.K. (2009). Audiovisual Asynchrony Detection and Speech Perception in Hearing-Impaired Listeners with Cochlear Implants: A Preliminary Analysis. *Int. J. Audiol.* 48, 321–333.

Hirokawa, J., Bosch, M., Sakata, S., Sakurai, Y., and Yamamori, T. (2008). Functional role of the secondary visual cortex in multisensory facilitation in rats. *Neuroscience* 153, 1402–1417.

Kaganovich, N. (2016). Development of Sensitivity to Audiovisual Temporal Asynchrony during Mid-Childhood. *Dev. Psychol*. 52, 232–241.

King, A.J., and Palmer, A.R. (1985). Integration of visual and auditory information in bimodal neurones in the guinea-pig superior colliculus. *Exp. Brain Res.* 60, 492–500.

Kral, A., and Eggermont, J.J. (2007). What's to lose and what's to learn: Development under auditory deprivation, cochlear implants and limits of cortical plasticity. *Brain Res. Rev.* 56, 259–269.

Kujawa, S.G., and Liberman, M.C. (2009). Adding Insult to Injury: Cochlear Nerve Degeneration after "Temporary" Noise-Induced Hearing Loss. *J. Neurosci.* 29, 14077–14085.

Lambertz, N., Gizewski, E.R., de Greiff, A., and Forsting, M. (2005). Cross-modal plasticity in deaf subjects dependent on the extent of hearing loss. *Cogn. Brain Res.* 25, 884–890.

Lee, H.-K., and Whitt, J.L. (2015). Cross-modal synaptic plasticity in adult primary sensory cortices. *Curr. Opin. Neurobiol*. 35, 119–126.

Lomber, S.G., Meredith, M.A., and Kral, A. (2010). Cross-modal plasticity in specific auditory cortices underlies visual compensations in the deaf. *Nat. Neurosci*. 13, 1421–1427.

Merabet, L.B., and Pascual-Leone, A. (2010). Neural reorganization following sensory loss: the opportunity of change. *Nat. Rev. Neurosci*. 11, 44–52.

Meredith, M.A., and Lomber, S.G. (2011). Somatosensory and visual crossmodal plasticity in the anterior auditory field of early-deaf cats. *Hear. Res*. 280, 38–47.

Meredith, M.A., Nemitz, J.W., and Stein, B.E. (1987). Determinants of multisensory integration in superior colliculus neurons. I. Temporal factors. *J. Neurosci*. 7, 3215–3229.

Meredith, M.A., Keniston, L.P., and Allman, B.L. (2012). Multisensory dysfunction accompanies crossmodal plasticity following adult hearing impairment. *Neuroscience* 214, 136–148.

Meredith, M.A., Clemo, H.R., and Lomber, S.G. (2017). Is territorial expansion a mechanism for crossmodal plasticity? *Eur. J. Neurosci.* 45, 1165–1176.

Mitzdorf, U. (1985). Current source-density method and application in cat cerebral cortex: investigation of evoked potentials and EEG phenomena. *Physiol. Rev.* 65, 37–100.

Mitzdorf, U., and Singer, W. (1977). Laminar segregation of afferents to lateral geniculate nucleus of the cat: an analysis of current source density. *J. Neurophysiol.* 40, 1227–1244.

Mitzdorf, U., and Singer, W. (1980). Monocular activation of visual cortex in normal and monocularly deprived cats: an analysis of evoked potentials. *J. Physiol*. 304, 203–220.

Neville, H.J., and Lawson, D. (1987). Attention to central and peripheral visual space in a movement detection task: an event-related potential and behavioral study. II. Congenitally deaf adults. *Brain Res*. 405, 268–283.

Nicholson, C., and Freeman, J.A. (1975). Theory of current source-density analysis and determination of conductivity tensor for anuran cerebellum. *J. Neurophysiol*. 38, 356–368.

Petrus, E., Isaiah, A., Jones, A.P., Li, D., Wang, H., Lee, H.-K., and Kanold, P.O. (2014). Crossmodal Induction of Thalamocortical Potentiation Leads to Enhanced Information Processing in the Auditory Cortex. *Neuron* 81, 664–673.

Petrus, E., Rodriguez, G., Patterson, R., Connor, B., Kanold, P.O., and Lee, H.-K. (2015). Vision Loss Shifts the Balance of Feedforward and Intracortical Circuits in Opposite Directions in Mouse Primary Auditory and Visual Cortices. *J. Neurosci*. 35, 8790–8801.

Popelar, J., Grecova, J., Rybalko, N., and Syka, J. (2008). Comparison of noise-induced changes of auditory brainstem and middle latency response amplitudes in rats. *Hear. Res.* 245, 82–91.

Schormans, A.L., and Allman, B.L. (2018). Behavioral Plasticity of Audiovisual Perception: Rapid Recalibration of Temporal Sensitivity but Not Perceptual Binding Following Adult-Onset Hearing Loss. *Front. Behav. Neurosci*. 12.

Schormans, A.L., Typlt, M., and Allman, B.L. (2017a). Crossmodal plasticity in auditory, visual and multisensory cortical areas following noise-induced hearing loss in adulthood. *Hear. Res.* 343, 92–107.

Schormans, A.L., Scott, K.E., Vo, A.M.Q., Tyker, A., Typlt, M., Stolzberg, D., and Allman, B.L. (2017b). Audiovisual Temporal Processing and Synchrony Perception in the Rat. *Front. Behav. Neurosci*. 10.

Schormans, A.L., Typlt, M., and Allman, B.L. (2018). Adult-Onset Hearing Impairment Induces Layer-Specific Cortical Reorganization: Evidence of Crossmodal Plasticity and Central Gain Enhancement. *Cereb. Cortex*, bhy067

Schroeder, C.E., Javitt, D.C., Steinschneider, M., Mehta, A.D., Givre, S.J., Jr, H.G.V., and Arezzo, J.C. (1997). N-methyl-d-aspartate enhancement of phasic responses in primate neocortex. *Exp. Brain Res.* 114, 271–278.

Schroeder, C.E., Mehta, A.D., and Givre, S.J. (1998). A spatiotemporal profile of visual system activation revealed by current source density analysis in the awake macaque. *Cereb. Cortex* 8, 575–592.

Schroeder, C.E., Lindsley, R.W., Specht, C., Marcovici, A., Smiley, J.F., and Javitt, D.C. (2001). Somatosensory Input to Auditory Association Cortex in the Macaque Monkey. *J. Neurophysiol.* 85, 1322–1327.

Stevens, C., and Neville, H. (2006). Neuroplasticity as a double-edged sword: deaf enhancements and dyslexic deficits in motion processing. *J. Cogn. Neurosci*. 18, 701–714.

Stevenson, R.A., and Wallace, M.T. (2013). Multisensory temporal integration: task and stimulus dependencies. *Exp. Brain Res.* 227, 249–261.

Stolzberg, D., Chrostowski, M., Salvi, R.J., and Allman, B.L. (2012). Intracortical circuits amplify sound-evokes activity in primary auditory cortex following systemic injection of salicylate in the rat. *J. Neurophysiol.* 108, 200–214.

Szymanski, F.D., Garcia-Lazaro, J.A., and Schnupp, J.W.H. (2009). Current Source Density Profiles of Stimulus-Specific Adaptation in Rat Auditory Cortex. *J. Neurophysiol.* 102, 1483–1490.

Toldi, J., Fehér, O., and Wolff, J.R. (1986). Sensory interactive zones in the rat cerebral cortex. *Neuroscience* 18, 461–465.

Vatakis, A., Bayliss, L., Zampini, M., and Spence, C. (2007). The influence of synchronous audiovisual distractors on audiovisual temporal order judgments. *Percept. Psychophys.* 69, 298–309.

Vroomen, J., and Stekelenburg, J.J. (2011). Perception of intersensory synchrony in audiovisual speech: Not that special. *Cognition* 118, 75–83.

Wallace, M.T., Ramachandran, R., and Stein, B.E. (2004). A revised view of sensory cortical parcellation. *Proc. Natl. Acad. Sci.* 101, 2167–2172.

Whitt, J.L., Petrus, E., and Lee, H.-K. (2014). Experience-dependent homeostatic synaptic plasticity in neocortex. *Neuropharmacology* 78, 45–54.

Xu, J., Sun, X., Zhou, X., Zhang, J., and Yu, L. (2014). The cortical distribution of multisensory neurons was modulated by multisensory experience. *Neuroscience* 272, 1–9.

Yang, S., Su, W., and Bao, S. (2012). Long-term, but not transient, threshold shifts alter the morphology and increase the excitability of cortical pyramidal neurons. *J. Neurophysiol.* 108, 1567–1574.

Chapter 6

6 Noise-Induced Crossmodal Plasticity within the Audiovisual Cortex: Layer-Specific Enhancement and Rapid Manifestation of Visual-Evoked Activity

6.1 Introduction

Experience plays a vital role in the successful development of our sensory systems. Consequently, a loss of one of the sensory modalities (e.g., deafness) can result in extensive reorganization at the neuronal level, as well as enhanced behavioural performance that involves the spared senses (e.g., improved peripheral visual processing in the deaf) (for review see Bavelier and Neville, 2002; Frasnelli et al., 2011; Merabet and Pascual-Leone, 2010). Overall, this sensory reorganization is referred to as crossmodal plasticity, which is often characterized by an increase in the responsiveness of neurons in the deprived cortical regions to the spared sensory modalities. With respect to hearing impairment, crossmodal plasticity has been predominantly studied following a profound loss of auditory input early in life (Auer et al., 2007; Frasnelli et al., 2011; Lambertz et al., 2005). That said, recent reports in humans and animal models have begun to describe the nature and extent of crossmodal plasticity induced by partial hearing impairments in adulthood. Unlike in conditions of complete deafness, subjects with partial lesion in their cochleae still maintain some residual auditory processing in addition to the emergence of crossmodal plasticity. For example, auditory stimulation in hearing-impaired adults showed decreased activation in temporal cortical areas, as well as increased activation in response to visual and tactile stimulation (Campbell and Sharma, 2013, 2014; Cardon and Sharma, 2018). Furthermore, single-unit recordings of partially-deafened ferrets revealed an increase in the proportion of neurons in the core auditory cortex that respond to both auditory and non-auditory stimuli (i.e., multisensory neurons) (Meredith et al., 2012).

It is important to note that hearing loss-induced crossmodal plasticity is not restricted to regions of the deprived auditory cortex. Indeed, using a rat model of loud noise exposure, we found an increased proportion of neurons in the higher-order, audiovisual cortex (i.e., the lateral extrastriate visual cortex, V2L) that were overtly responsive to visual stimulation

two weeks after moderate hearing loss occurred (Schormans et al., 2017a). In addition to this remapping of sensory organization post-noise exposure, a follow-up study revealed that noise-induced plasticity in the V2L cortex manifested as layer-specific changes in visual-evoked activity. At present, however, the cellular mechanisms underlying the distinct laminar effects of crossmodal plasticity remain unresolved. Furthermore, it is unknown whether this crossmodal plasticity observed in cortical microcircuits manifests solely from intrinsic changes in the cortex itself, or whether partial hearing impairment leads to increased visual responsiveness via a combination of altered intracortical processing as well as thalamocortical plasticity. To our knowledge, no previous studies have investigated if hearing loss-induced crossmodal plasticity occurs at subcortical loci, nor have studies revealed the time-course by which crossmodal plasticity emerges following adult-onset hearing loss.

In the present study, we conducted the first investigation of the thalamocortical contributions to noise-induced crossmodal plasticity within higher-order sensory cortices. By using a previously-established, pharmacological silencing technique to separate the intracortical from the thalamocortical components of stimulus-induced excitation within the cortex (Happel et al., 2010, 2014; Lippert et al., 2013), we examined alterations in thalamocortical processing following noise-induced hearing loss within the audiovisual cortex of the rat (Experiment 1). To do so, adult rats were exposed to loud noise and two weeks later, laminar extracellular electrophysiological recordings were performed in the multisensory zone of the lateral extrastriate visual cortex (V2L-Mz) in response to auditory, visual and combined audiovisual stimulation. A current source density (CSD) analysis was applied to the mean local field potential (LFP) data before and after pharmacological silencing with muscimol, in an effort to reveal the extent that adult-onset hearing loss causes a layer-specific enhancement of thalamocortical processing within V2L-Mz cortex. In addition to examining the thalamocortical contributions to crossmodal plasticity, we also sought to investigate the working hypothesis that the characteristic increase in visual responsiveness observed following partial hearing loss occurs, at least in part, because of pre-existing connections becoming unmasked via the auditory deprivation. To that end, we used an epidural electrode array that spanned the higher-order sensory cortices, and compared the visual-evoked LFP responses before- and immediately after loud noise

exposure in the same adult rats (Experiment 2). Overall, we predicted that hearing loss-induced crossmodal plasticity would manifest in the audiovisual cortex from a combination of both thalamocortical and intracortical effects, and that this increased responsiveness to visual stimulation would emerge rapidly following hearing loss, characteristic of an unmasking of pre-existing inputs.

6.2 Methods

6.2.1 Animals

The present study included two experimental series that each used a separate group of adult male Sprague-Dawley rats (n = 24; Charles River Laboratories Inc., Wilmington, MA). All experimental procedures were approved by the University of Western Ontario Animal Care and Use Committee and were conducted in accordance with the guidelines established by the Canadian Council of Animal Care.

6.2.2 Hearing Assessment & Noise Exposure

Consistent across both series of experiments, hearing sensitivity was assessed using the auditory brainstem response (ABR), which was performed in a double-walled sound attenuating chamber (MDL 6060 ENV, Whisper Room Inc., Knoxville, TN). ABR recordings were completed as previously described by Schormans et al. (2017a). Briefly, rats were anesthetized with ketamine (80 mg/kg) and xylazine (5 mg/kg), and subdermal electrodes (27G; Rochester Electro-Medical, Lutz, FL) were positioned at the vertex, over the right mastoid and on the back. Auditory stimuli consisted of a click (0.1 ms) and two tones (4 kHz and 20 kHz) and were generated using Tucker-Davis Technologies RZ6 processing modulate sampled at 100 kHz (TDT, Alachua, FL). Auditory evoked activity was collected using a low impedance headstage (RA4LI; TDT), preamplified and digitized (RA16SD Medusa preamp; TDT) and sent to a RZ6 processing module via a fiber optic cable. Delivery of the stimuli and detection of ABR thresholds was performed in accordance with Schormans et al. (2017a). Throughout the entire procedure, body temperature was maintained at ~37°C using a homeothermic heating pad (507220F; Harvard Apparatus, Kent, UK). Sound stimuli for the ABR, noise exposure and electrophysiological recordings were calibrated using custom MATLAB software (The

Mathworks, Natick, MA) using a ¼-inch microphone (2530; Larson Davis, Depew, NY) and preamplifier (2221; Larson Davis).

Rats were bilaterally exposed to a broadband noise (0.8 – 20 kHz) for two hours at 120 dB SPL, while under ketamine (80 mg/kg; IP) and xylazine (5 mg/kg; IP) anesthesia. The broadband noise was generated with TDT software (RPvdsEx) and hardware (RZ6), and delivered by a super tweeter (T90A, Fostex, Tokyo, Japan) which was placed 10 cm in front of the rat. Consistent with the ABR procedure, body temperature was maintained at ~37°C using a homeothermic heating pad (Harvard Apparatus).

6.2.3 Experiment 1: Thalamocortical Contributions to Noise-Induced Crossmodal Plasticity

In the first experimental series, rats in the control group (n = 7) underwent an ABR to assess their hearing sensitivity, followed immediately by an *in vivo* extracellular electrophysiological recording. Rats in the noise exposed group (n = 8) underwent a baseline hearing assessment, followed by exposure to a loud noise. A final hearing assessment was completed two weeks following the noise exposure, after which the same electrophysiological recording experiment was completed as that of control rats.

6.2.3.1 Surgical Procedure

Following the final hearing assessment, each rat was maintained under ketamine/xylazine anesthesia, and the animal was fixed in a stereotaxic frame with blunt ear bars. The absence of a pedal reflex was used as an indication of anesthetic depth, and supplemental doses of ketamine/xylazine were administered IM as needed. A midline incision was made in the scalp, and the left temporalis muscle was ultimately reflected in order to provide access to the temporal bone overlying the audiovisual cortex. A stereotaxic manipulator was used to measure 6 mm caudal to bregma and 2 mm ventral of the top of the skull, which represents the approximate location of the lateral extrastriate visual cortex (V2L) (Hirokawa et al., 2008; Schormans et al., 2017a, 2018; Wallace et al., 2004; Xu et al., 2014), and marks were made on the skull for later drilling. A stainless-steel screw was inserted in the left frontal bone to serve as both an anchor for the headpost and an electrical ground. A craniotomy (2 x 5mm; 5-7mm caudal to bregma) was performed in the left temporal bone to expose the

audiovisual cortex. To allow for free-field auditory stimulation during the electrophysiological recordings, a headpost was fastened to the skull with dental acrylic on the right frontal bone. The rat was held in place throughout the entire duration of the experiment within the stereotaxic frame using the left ear bar and the headpost.

6.2.3.2 Electrophysiological Recordings

In each rat, extracellular electrophysiological recordings were completed in the multisensory zone of the lateral extrastriate visual cortex (V2L-Mz; corresponding to the 2 mm ventral of the top of the skull using our measurements). Consistent with Schormans et al. (2018), a 32-channel linear electrode array was inserted perpendicular to the cortical surface through a small slit in the dura using a hydraulic microdrive (FHC; Bowdoin, ME). The linear array consisted of 32 iridium microelectrodes equally spaced 50 µm apart on a 50 µm thick shank (A1x32-10mm-50-177-A32; NeuroNexus Technologies, Ann Arbor, MI). To allow for histological reconstruction of electrode penetrations, the electrode array was coated in DiI cell-labelling solution (V22885; Molecular Probes Inc., Eugene, OR) prior to the electrode being inserted into the cortex. The electrode was advanced into the cortex using a high-precision stereotaxic manipulator to penetrate the pia mater, and then withdrawn to the cortical surface. The electrode array was then slowly advanced into the cortex until it reached a depth of -1500 µm. Slight adjustments to depth were made based on a characteristic sharp negative peak of the LFP to the preferred stimulus (i.e., the unimodal stimulus that evoked the largest response) (Schormans et al., 2018; Stolzberg et al., 2012). Once at the correct depth, the electrode array was allowed to settle in place for at least 60 minutes before electrophysiological recordings commenced. Neural signals were acquired using TDT System 3 (TDT, Alachua, FL), and LFP activity was continuously acquired (digitally resampled at approximately 1000 Hz) and bandpass filtered online at 1-300 Hz.

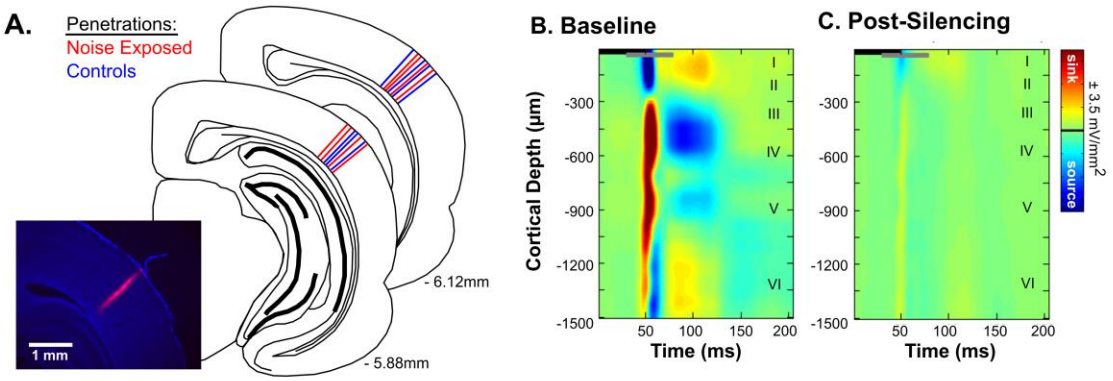

Figure 6.1. Electrophysiological recordings within the multisensory zone of the V2L cortex (V2L-Mz).

(A) Electrode penetrations within the V2L-Mz cortex of control (n = 7) and noise exposed (n = 8) rats. The stained image shows a representative coronal section demonstrating the location of the recording penetrations 6.0 mm caudal of Bregma. Representative CSD profile within the V2L-Mz cortex in response to audiovisual stimulation before (B) and after pharmacological silencing (C). Prominent current sinks (red) are reflective of depolarization of neurons in the surrounding cortical area, whereas prominent current sources (blue) reflect a repolarization of neurons in the surrounding cortical regions. The black horizontal bar denotes the presentation of the visual stimulus and the grey horizontal bar denotes the presentation of the auditory stimulus.

6.2.3.3 Stimulation Paradigm

A quantitative multisensory paradigm was presented before and after pharmacologically silencing local cortical activity within the V2L cortex. Stimuli consisted of computer-triggered auditory and visual stimuli presented alone or in combination using a RZ6 processing module (TDT; 100 kHz sampling rate) and custom Matlab software. Auditory stimuli were noise bursts (1-32 kHz; 50 ms duration) presented from a magnetic speaker (MF1; TDT) positioned 10 cm from the base of the right pinna on a 30° angle from midline in the contralateral space. For each rat, auditory stimuli were presented at two sound levels: 90 dB SPL and 40 dB above its click threshold (i.e., + 40 dB; as determined by the

preceding click ABR). In the control group, the sound intensity of the + 40 dB auditory stimulus was 67.9 ± 1.0 dB SPL, whereas it was 77.5 ± 2.3 dB SPL in the noise exposed group. The visual stimuli consisted of light flashes (15 and 82 lux; 50 ms duration) from an LED positioned adjacent to the speaker. For both experiments, the intensity of the visual stimulus was determined using an LED light meter (Model LT45, Extech Instruments, Nashua, NH). In the combined audiovisual stimuli conditions (i.e., low: +40 dB SPL and 15 lux; high: 90 dB SPL and 81 lux), the visual stimuli were presented 30 ms prior to the auditory stimuli to compensate for differences in modality latencies. This timing offset has been shown to maximize the potential for observing multisensory interactions and ensures that both stimuli arrive simultaneously within the temporal cortex (Allman and Meredith, 2007; Allman et al., 2008; Meredith and Allman, 2009, 2015). In total six stimuli conditions were presented in random order, which were separated by an inter-stimulus interval of 3-5 s, and each of the conditions was presented 50 times.

6.2.3.4 Pharmacological Silencing of Local Cortical Activity

To examine the effects of crossmodal plasticity arising from cortical afferents, such as the thalamocortical inputs, the local postsynaptic activity was silenced by the application of muscimol (GABA agonist). Muscimol prevents local neuronal spiking by inhibiting all postsynaptic cells expressing GABA receptors (Lippert et al., 2013). However, muscimol alone has been shown to potentially activate GABA-B receptors (Yamauchi et al., 2000), that could generate thalamocortical EPSPs that are smaller in amplitude, which could be attributed to presynaptic inhibition. Therefore, consistent with previous studies (Happel et al., 2010, 2014; Lippert et al., 2013), an established method was adopted to effectively block the non-specific effects of muscimol on GABA-B receptors which was developed by Yamauchi et al. (2000) (also see Liu et al., 2007). More specifically, the selective GABA-B receptor antagonist SCH50911 (6 mM, 20 µl; Sigma) was applied in combination with muscimol (4 mM, 20 µl; Sigma). Previous studies have demonstrated that this combination still effectively reduces the number of action potentials by >95% (Happel et al., 2010; Liu et al., 2007). Once baseline electrophysiological recordings were completed, the solution was topically applied to the cortical surface within the craniotomy window. Following the

topical application, the drugs were allowed diffuse into the brain for 1 hour, which ensured that all spontaneous electrical activity had ceased.

6.2.3.5 Current Source Density (CSD) Analysis

Using the simultaneously recorded LFPs across the entire cortical thickness; a one-dimensional CSD profile was calculated from the second spatial derivative of the LFP (Freeman and Singer, 1983; Mitzdorf, 1985; Mitzdorf and Singer, 1977; Nicholson and Freeman, 1975) (Eq.1):

$$CSD \approx -\frac{\Phi(z+n\Delta z)-2\,\Phi(\mathrm{z})+\,\Phi(\mathrm{z}-\mathrm{n}\Delta\mathrm{z})}{(n\Delta z)^2} \quad (1)$$

where Φ is the LFP, z is the spatial coordinate, Δz is the inter-electrode spacing (Δz = 50 µm), and n is the differentiation grid (n = 4). A 3-point Hamming filter was applied in order to smooth LFPs across channels before computing the CSD, as described by Stolzberg et al. (2012). Consistent with previous studies (Freeman and Singer, 1983; Mitzdorf, 1985; Mitzdorf and Singer, 1977, 1980; Nicholson and Freeman, 1975; Stolzberg et al., 2012), current sinks were positive in amplitude and sources were negative.

The CSD analysis provides a spatial profile of the flow of ions and serves as a measure of the total current density that enters or leaves the extracellular matrix through the cell membrane (Einevoll et al., 2013; Mitzdorf, 1985). Current sinks are representative of the flow of positive ions into the neural tissue from the extracellular matrix, which is reflective of active excitatory synaptic populations and axonal depolarization (Happel et al., 2010; Kral and Eggermont, 2007). Current sources represent passive return currents, which corresponds to repolarization and possibly inhibition of the neighbouring tissue (Einevoll et al., 2013; Happel et al., 2010; Kral and Eggermont, 2007; Mitzdorf, 1985; Szymanski et al., 2009). Consistent with Schormans et al. (2018), current sinks were identified as being at least two standard deviations above the mean voltage measures during the 70 ms before the presentation of the stimuli. Within the V2L-Mz, prominent sinks were identified in the granular (-300 µm < depth ≥ -750 µm) and infragranular-upper layers (-750 < depth ≥ -1200 µm). Additional sinks were observed in the supragranular (depth ≥ -350 µm) and infragranular-lower layers (depth < -1200 µm) (see Fig. 6.1B).

Using the procedure previously described by Schormans et al. (2018), CSD waveforms were extracted from the depth that demonstrated the largest amplitude within an individual sink (i.e., peak amplitude). For each of the identified sinks, the peak amplitude was derived from a single depth in order to account for individual sink components that spanned various depths (e.g., extended beyond or were narrower than the space defined above). All calculations were performed using custom Matlab scripts.

6.2.3.6 Average Rectified CSD (AVREC) Analysis

The average rectified CSD (AVREC) measure was applied to the CSD analysis, in order to examine the overall strength of postsynaptic currents within the audiovisual cortex (Happel et al., 2010; Schroeder et al., 1997, 2001; Stolzberg et al., 2012). Although rectification of the CSD results in a loss of information about the direction of the transmembrane flow, the AVREC waveform provides useful information about the temporal pattern of the overall strength of the postsynaptic currents (Givre et al., 1994; Happel et al., 2010; Schroeder et al., 1998). The AVREC was calculated by averaging the absolute values of the CSD across all channels (Eq. 2).

$$\mathrm{AVREC} = \frac{\sum_{i=1}^{n} |\mathrm{CSD_i}|(t)}{n} \tag{2}$$

where, CSD refers to Eq. 1, n refers to the number of channels and t refers to the time point index. To examine the overall strength of the postsynaptic currents before and after pharmacological silencing, AVREC waveforms were generated for each stimulus condition and peak amplitude was calculated within the first 100 ms from the onset of the visual stimulus.

6.2.3.7 Histology

At end of each electrophysiological experiment, the rats were injected with sodium pentobarbital (100 mg/kg; IP) in preparation for exsanguination via transcardial perfusion of 0.9% saline, followed by 4% paraformaldehyde. Using a microtome (HM 430/34; Thermo Scientific, Waltham, MA), frozen sections were cut (50 µm) in the coronal plane and were mounted in fluorescent DAPI mounting medium (F6057 FluoroshieldTM with DAPI; Sigma, St. Louis, MO) and coverslipped. Sections containing the recording

penetrations were imaged with an Axio Vert A1 inverted microscope (Carl Zeiss Microscopy GmbH, Jena, Germany) and ZEN imaging software was used to reconstruct the location of each penetration. Figure 6.1A shows a schematic of the location of the penetration for each animal from all electrophysiological experiments.

6.2.4 Experiment 2: Onset of Crossmodal Plasticity

In the second experimental series, rats (n = 9) that were chronically implanted with a 16-channel electrocorticography (ECoG) electrode underwent electrophysiological recordings before and immediately after exposure to quiet (n = 3) or a loud noise (n = 6). In both groups hearing assessments were completed before and immediately after exposure, as well as at the end of the recording session.

6.2.4.1 Surgical Procedure and Electrode Implantation

Rats were anaesthetized with isoflurane (induction: 4%; maintenance: 2%), and body temperature was maintained at 37°C using a homeothermic hearing pad (507220F; Harvard Apparatus) throughout the duration of the procedure. For pain management, a subcutaneous injection of meloxicam (1 mg/kg) was administered before the surgery and post-surgery as needed. Once a surgical plane of anesthesia had been achieved, blunt ear bars and a snout mask were used in order to secure the head in the stereotaxic frame. A midline incision was made in the scalp, and the dorsal aspect of the skull was cleaned with a scalpel blade. To provide access to the left multisensory cortex, the left temporalis muscle was reflected and removed using a blunt dissection technique. A stereotaxic micromanipulator was used to make marks on the skull at 5 mm and 7 mm caudal of Bregma, which represents the approximate rostral-caudal borders of the lateral extrastriate visual cortex (V2L) (Hirokawa et al., 2008; Schormans et al., 2017a; Wallace et al., 2004; Xu et al., 2014). An additional mark was made on the temporal bone at 2 mm ventral of the top of the skull for later drilling. A craniotomy (2.5 mm x 4 mm) was made in the left temporal and parietal bone to expose the multisensory cortex. Finally, a small hole was hand drilled and a stainless-steel screw was fastened in the occipital bone to serve as a reference and electrical ground.

The ECoG array consisted of 16 electrode sites organized in a 4 x 4 grid covering a surface area of ~2 mm^2 (model: E16-500-2-200-Z16; NeuroNexus Technologies). The electrode sites (200 µm) were spaced 500 µm apart on a 20 µm thin polyimide film. Using a stereotaxic micromanipulator the electrode was centered at 6 mm caudal of Bregma and 2 mm ventral of the top of the skull, which represents the location of the audiovisual cortex (i.e., V2L cortex) (see Fig. 6.2B). Once the electrode was correctly positioned, a silicon sealant (Kwik-Cast; World Precision Instruments, Inc. Sarasota, FL), was used to fill the craniotomy and protect the cortical surface and electrode from dental acrylic. Once the sealant was dry, dental acrylic was used to secure the electrode to the skull. The skin surrounding the surgical implant was sutured, and the rats were allowed to recover for several days prior to undergoing electrophysiological recordings.

6.2.4.2 Electrophysiological Recordings

Following a complete surgical recovery, rats were again anaesthetized with ketamine (80 mg/kg; IP) and xylazine (5 mg/kg; IP), and body temperature was maintained at ~37°C using a homeothermic heating pad (Harvard Apparatus). Consistent with the previous experiment, anesthetic depth was assessed by the absence of a pedal reflex, and supplemental doses of ketamine/xylazine were administered IM as needed. To assess changes in hearing sensitivity, ABR click thresholds were examined pre-exposure, immediately post-exposure, and at the end of the experiment (as described above). In each rat, electrophysiological recordings were completed prior to the exposure (i.e., pre-exposure) as well as immediately post-exposure (i.e., post-exposure).

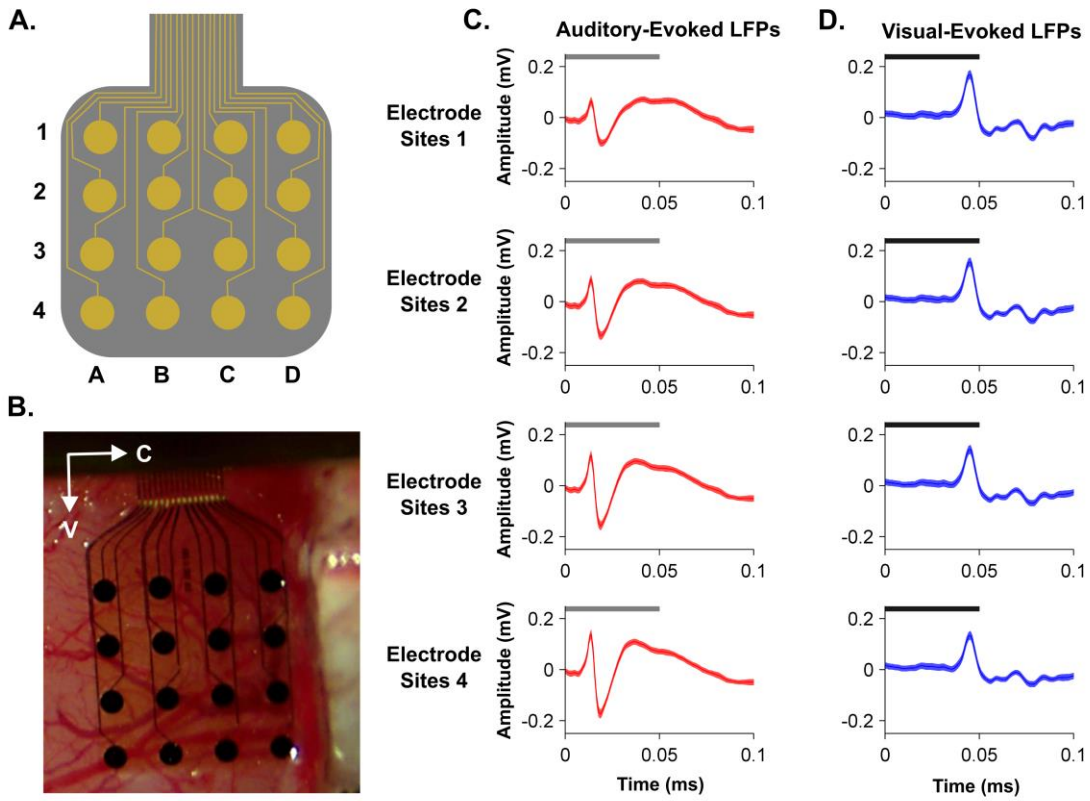

Figure 6.2. Recordings from an ECoG electrode positioned over the V2L cortex of the rat.

(A) Schematic of the ECoG electrode array. (B) Image of an ECoG grid positioned over the higher-order sensory cortex of the rat. (C) Representative LFP activity across the four collapsed electrode sites in response to auditory stimulation (50 ms noise burst at 90 dB SPL, denoted by the grey bar). (D) Representative LFP activity across the four collapsed electrode sites in response to visual stimulation (50 ms noise burst at 73 lux, denoted by the black bar). Due to consistency between LFP activity across the rostral-caudal axis, LFP responses were averaged across the ECoG columns (i.e., A, B, C, and D), generating four response profiles across the dorsal-ventral axis, identified as electrode sites 1 through 4.

Because the animals were implanted with the ECoG electrodes prior to the electrophysiological recordings, a custom recording setup was used which allowed for bilateral free-field acoustic stimulation. Consistent with Experiment 1, recordings were performed in a double-walled sound attenuating chamber (MDL 6060 ENV, Whisper Room Inc.). Neural signals were digitized at the headstage (ZD32; TDT) and amplified using the PZ5 NeuroDigitizer (TDT), and then sent to a RZ2 processing module via a fiber optic cable. Local field potential (LFP) activity was continuously acquired and digitally resampled at 1000 Hz and bandpass filtered online at 1 – 300 Hz.

6.2.4.3 Sensory Stimulation Paradigm

At each time point (i.e., pre- and post-exposure), computer-trigger auditory and visual stimuli were presented using a TDT RZ6 processing module (100 kHz sampling rate) and custom Matlab software. Auditory stimuli consisted of 50 ms noise bursts (1-32 kHz) from a speaker (MF1, TDT) positioned 10 cm from the right pinna. Visual stimuli consisted of 50 ms light flashes from a LED positioned 10 cm from the right eye on a 30° angle from midline. For each rat, auditory and visual stimuli were presented at 3 different intensities. More specifically, the auditory stimuli were presented at 50 dB, 70 dB, and 90 dB SPL, and the visual stimuli were presented at 3, 33, and 73 lux. All stimuli were presented in a randomized order, separated by an inter-stimulus interval of 3 – 5 s, and each condition was presented 50 times.

6.2.4.4 Analysis of Local Field Potentials

For each of the completed recordings and stimuli, mean LFPs were calculated by averaging across the 50 trials. The level of background activity was determined by averaging over all amplitude values within a 50 ms pre-stimulus time window. To allow for a comparison between measurements, this background level of activity was subtracted from the mean LFP (Konerding et al., 2018; Moeller et al., 2010). Similar to Konerding et al. (2018), peak-to-peak amplitude of the LFP was analyzed from 0-100 ms after the onset of the auditory stimulus. In response to visual stimulation, peak amplitude of the LFP was analyzed from 0-150 ms after stimulus onset. In addition to LFP amplitudes, peak latency was calculated within the same time windows described above.

6.2.5 Statistics and Data Presentation

Depending on the comparison of interest, a variety of statistical analyses were performed in the present study, including repeated-measures analysis of variance (ANOVA), one-way ANOVA or paired/unpaired t-tests depending on the comparison of interest (see Results for details on each specific comparison). If Mauchly's test of sphericity was violated within the repeated-measures ANOVA, the Greenhouse-Geisser correction was used. The level of significance was set to 5%. When performing multiple comparisons following an ANOVA, the Bonferroni post hoc correction was used, and the adjusted p-values are cited accordingly in the text and figure legends. GraphPad Prism (GraphPad Software Inc., La Jolla, CA) and MATLAB (2012b; The Mathworks) were used for graphical display, and SPSS (Version 25, IBM Corporation) software was used for the various statistical analyses. Throughout the text and figures, data are presented as the mean values ± standard error of the mean (SEM).

6.3 Results

6.3.1 Experiment 1: Thalamocortical Contributions to Noise-Induced Crossmodal Plasticity

6.3.1.1 Hearing Sensitivity Two Weeks Following Noise Exposure

A loss in hearing sensitivity was confirmed by comparing ABR thresholds at baseline versus two weeks post-noise in rats exposed to a broadband noise at 120 dB SPL for two hours. A two-way repeated-measures ANOVA revealed an effect of time (i.e., pre- versus post-noise) on ABR thresholds ($F[1,7] = 34.77$, $p < 0.001$). Consistent with previous studies (Schormans et al., 2017a, 2018), post hoc paired samples t-tests revealed a significant increase in the ABR threshold of the click (pre-noise: 26.9 ± 0.9 dB SPL vs. post-noise: 37.5 ± 2.3 dB SPL; $p < 0.01$), 4 kHz (pre-noise: 24.4 ± 1.5 dB SPL vs. post-noise: 41.3 ± 2.5 dB SPL; $p < 0.001$) and 20 kHz stimulus (pre-noise: 15.6 ± 2.2 dB SPL vs. post-noise: 32.5 ± 5.9 dB SPL; $p < 0.05$). As expected, there were no differences in hearing sensitivity between the control and noise exposed rats for any of the stimuli at baseline (one-way ANOVA; $p > 0.05$). Furthermore, to assess the degree of damage at the level of the cochlear hair cell afferents caused by the noise exposure, the amplitude of the

first wave of the ABR was assessed (Kujawa and Liberman, 2009). Two weeks following the noise exposure, there was a 43.1 ± 5.6 % reduction in wave 1 amplitude (pre-noise: 1.5 ± 0.08 uV vs. post-noise: 0.8 ± 0.1 uV; $p < 0.001$).

6.3.1.2 Preserved Auditory Input Following Crossmodal Plasticity

Using CSD analyses in the multisensory zone of the lateral extrastriate visual cortex of anesthetized rats (V2L-Mz; n = 15), we investigated the thalamocortical contributions of noise-induced crossmodal plasticity in response to auditory, visual and combined audiovisual stimuli. Within the V2L-Mz of normal hearing rats, audiovisual stimuli evoked a typical profile of current sinks across layers with initial input in the granular and upper-infragranular layers following by supragranular and lower-infragranular layers (see Fig. 6.1B), consistent with the activation pattern observed in local cortical microcircuits (Happel et al., 2010; Sakata and Harris, 2009; Schroeder et al., 1998; Stolzberg et al., 2012). To examine the potential thalamocortical contributions of crossmodal plasticity within the audiovisual cortex, the local cortical microcircuit was pharmacologically silenced using muscimol in noise exposed rats and age-matched controls (see Fig. 6.1C). Because thalamocortical projections are predominantly restricted to the granular layer and the infragranular layers (Burkhalter, 2016; Olsen and Witter, 2016), and due to the unique characteristics of these cortical sinks, all statistical analyses were within these two cortical layers.

Within the granular layer, a three-way repeated-measures ANOVA (stimulus intensity x time x group) revealed a main effects of stimulus intensity ($F[1,13] = 22.5$, $p < 0.001$), time ($F[1,13] = 58.7$, $p < 0.001$), and group ($F[1,13] = 5.8$, $p < 0.05$). Due to the main effect of stimulus intensity, separate two-way repeated measures ANOVAs were then completed for each stimulus intensity (i.e., + 40 dB SPL and 90 dB SPL). For both the low and high auditory stimuli, separate two-way repeated-measures ANOVAs revealed a significant interaction of time by group ($F[1,13] = 5.1$, $p < 0.05$; $F[1,13] = 5.5$, $p < 0.05$, respectively). Consistent with previous studies (Schormans et al., 2018), noise-induced hearing loss resulted in a decrease in auditory-evoked granular sink amplitudes at baseline in response to both sound intensities ($p < 0.05$; Fig. 6.3C). Interestingly, following cortical inactivation there were no significant differences between the control and noise exposed rats at the low

(control: 0.46 ± 0.09 vs. noise-exposed: 0.25 ± 0.05 mV, $p = 0.07$) or high sound intensities (control: 0.62 ± 0.16 vs. noise-exposed: 0.34 ± 0.09 mV, $p = 0.14$). To further examine changes in auditory-evoked input within the granular layer, the degree of change (i.e., percent decrease) was calculated for each group and stimulus intensity. As can be seen in Figure 6.3D, the percent decrease following cortical inactivation is consistent between the control and noise exposed rats within the granular layer (two-way repeated measures ANOVA, $F[1,13] = 0.04$, $p = 0.847$). Therefore, there was no change in auditory-evoked thalamocortical inputs within the granular layer following noise-induced hearing loss.

A similar trend occurred within the upper-infragranular layer, as a three-way repeated-measures ANOVA revealed main effects of stimulus intensity ($F[1,13] = 20.9$, $p < 0.001$), time ($F[1,13] = 83.2$, $p < 0.001$), and group ($F[1,13] = 6.2$, $p < 0.05$). Consistent with the granular layer, separate two-way repeated measures ANOVAs for the low and high auditory stimuli, revealed significant interactions of time by group ($F[1,13] = 4.9$, $p < 0.05$; $F[1,13] = 8.6$, $p < 0.05$). As can been in Figure 6.3E, there was a decrease in auditory-evoked sink amplitude at baseline for both stimulus intensities ($p < 0.05$). However, no differences were observed between the control and noise exposed groups following pharmacological silencing ($p > 0.05$). Furthermore, there was no difference in the degree of change within the upper-infragranular layer in response to the low (control: 82.75 ± 2.18 vs. noise-exposed: 78.16 ± 2.67 %, $p = 0.21$) or high (control: 81.90 ± 1.82 vs. noise-exposed: 77.15 ± 2.11 %, $p = 0.12$; Fig. 6.3F) auditory stimuli. Taken together, these collective results demonstrate that there is no change in auditory-evoked thalamocortical input following noise-induced hearing loss.

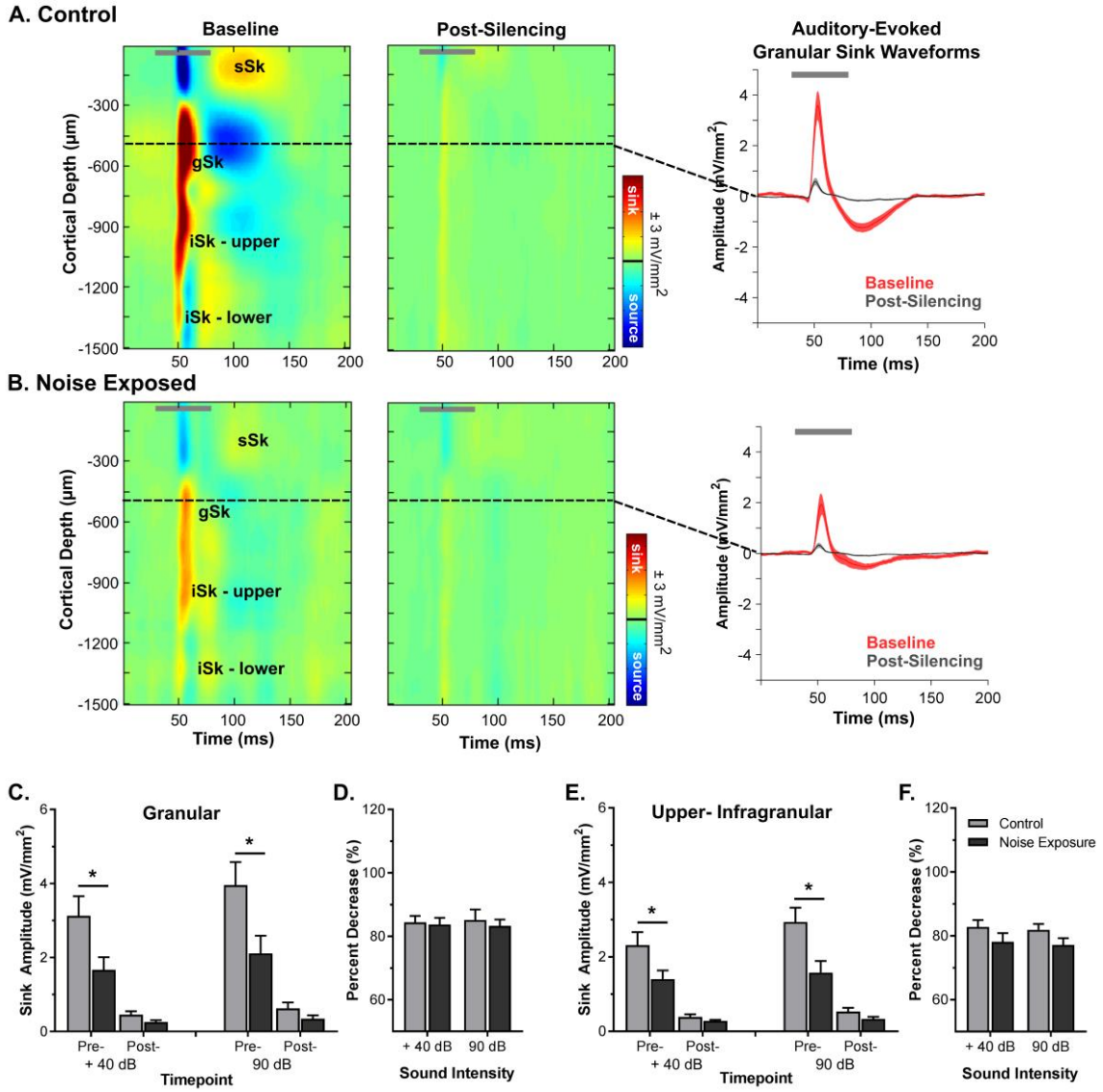

Figure 6.3. Auditory-evoked sink amplitudes following cortical silencing in control and noise-exposed rats.

*Representative CSD profiles and extracted CSD waveforms pre- (i.e., baseline) and post-silencing within the V2L cortex in response to auditory stimulus (50 ms noise burst at 90 dB SPL, denoted by the grey bar from a control (A) and noise exposed (B) rat. (C) Granular sink amplitudes in response to auditory stimulation at +40 dB and 90 dB SPL pre- and post-silencing of control and noise exposed rats. A decrease in auditory-evoked granular sink amplitudes were observed pre-silencing (*p < 0.05) (D) No difference in the degree of change (i.e., percent decrease) was observed within the granular layer at both sound*

intensities ($p > 0.05$). Similar to granular sink amplitudes, (E) upper-infragranular sink amplitudes in response to auditory stimulation at +40 dB and 90 dB SPL showed a decrease only prior to pharmacological silencing ($p < 0.05$). Furthermore, (F) no difference in the degree of change was observed within the upper-infragranular layer at both sound intensities ($p > 0.05$). Values are mean ± SEM for the noise exposed ($n = 8$) and control ($n = 7$) groups. *$p < 0.05$*

6.3.1.3 Enhanced Visual Input following Noise-Induced Crossmodal Plasticity within the V2L Cortex

To investigate whether crossmodal plasticity alters thalamocortical processing within higher-order sensory cortices, visual-evoked sink amplitudes were examined following cortical inactivation within the granular and upper-infragranular layers. A three-way repeated-measures ANOVA for granular sink amplitudes, revealed main effects of stimulus intensity ($F[1,13] = 10.6$, $p < 0.01$), time ($F[1,13] = 60.8$, $p < 0.001$), and group ($F[1,13] = 12.5$, $p < 0.01$). Because there was a significant effect of stimulus intensity, separate two-way repeated measures ANOVAs we completed for each of the visual intensities (i.e., 15 lux and 81 lux). For low and high visual stimuli, separate two-way repeated-measures ANOVAs revealed a significant interaction of time by group ($F[1,13] = 8.2$, $p < 0.05$; $F[1,13] = 6.4$, $p < 0.05$, respectively). As expected based on previous studies, there was a significant increase in visual-evoked granular sink amplitudes following noise-induced hearing loss before pharmacological silencing for both stimulus intensities ($p < 0.01$; Fig. 6.4C). Interestingly, there was also a significant increase in visual-evoked amplitudes in the noise exposed rats following cortical inactivation at the low (control: 0.13 ± 0.06 vs. noise-exposed: 0.95 ± 0.26 mV; $p < 0.05$) and high (control: 0.20 ± 0.07 vs. noise-exposed: 1.3 ± 0.22 mV, $p < 0.01$) stimulus intensities (see Fig. 6.4B, 6.4C). To further examine the increased visual input within the granular layer, the percent decrease was calculated for both groups and stimulus intensities. A two-way repeated-measures ANOVA revealed a main effect of stimulus intensity ($F[1,13] = 4.7$, $p < 0.05$) and a main effect of group ($F([1,13] = 14.8$, $p < 0.01$). As can be seen in Figure 6.4D, follow-up post hoc tests showed a significant decrease in the degree of change following

pharmacological silencing ($p < 0.05$), indicative of an increase in visual-evoked thalamocortical input. Furthermore, the high visual stimulus (i.e., 81 lux) demonstrated the greatest amount of residual input following cortical inactivation (77.1 ± 3.01 % decrease) when compared to normal-hearing controls (92.9 ± 2.1 % decrease; see Figure 6.4D). Overall, these data demonstrate that noise-induced crossmodal plasticity results in an increase in visual-evoked activity, suggestive of an enhancement of thalamocortical plasticity within the granular layer.

Within the upper-infragranular layer, a three-way repeated-measures ANOVA revealed main effects of stimulus intensity ($F[1,13] = 12.9$, $p < 0.01$), time ($F[1,13] = 72.0$, $p < 0.001$), and group ($F[1,13] = 9.0$, $p < 0.05$). Similar to the granular layer, separate two-way repeated-measures ANOVAs for low and high stimulus intensities revealed a significant interaction of time by group ($F[1,13] = 6.9$, $p < 0.05$; $F[1,13] = 6.2$, $p < 0.05$, respectively). As can be seen in Figure 6.4E, a similar trend was observed in the upper-infragranular layer, where there was an increase in visual-evoked sink amplitude before ($p < 0.02$) and after pharmacological silencing ($p < 0.05$). However, despite the slight increase in visual input within the upper-infragranular layer, there were no differences between control and noise exposed rats when percent decrease was examined (two-way repeated-measures ANOVA, $F[1,13] = 1.3$, $p = 0.275$). Further support for this observation can be seen in Figure 6.4F, where the degree of change following cortical inactivation was consistent at both stimulus intensities and between groups (e.g., at the low intensity percent decrease was 93.2 ± 1.5% in controls and 91.9 ± 1.4 % in noise exposed rats). Therefore, the increased visual input following cortical inactivation is restricted to the granular layer following noise-induced hearing loss.

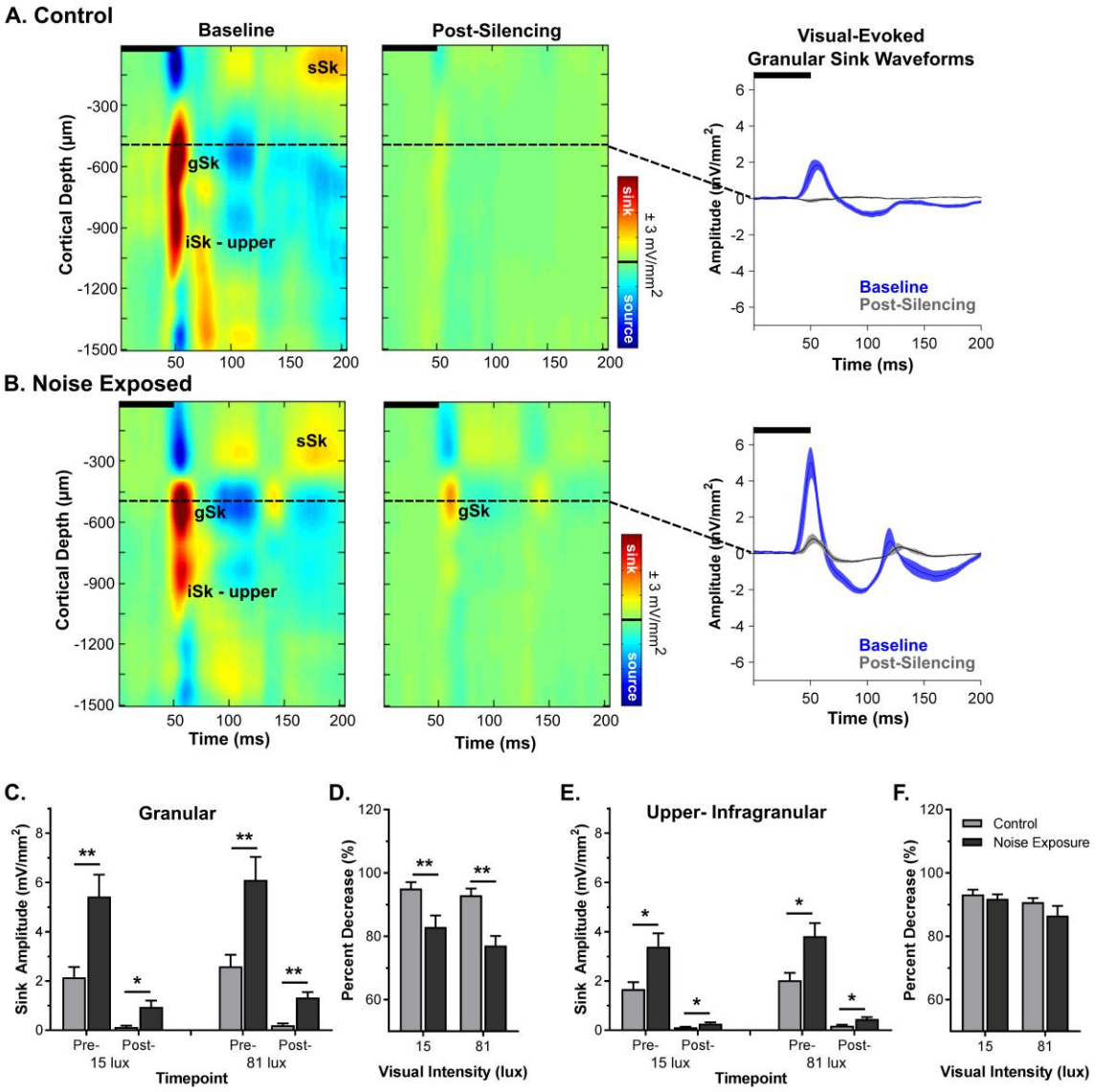

Figure 6.4. Visual-evoked sink amplitudes following cortical silencing in control and noise-exposed rats

Representative CSD profiles and extracted CSD waveforms pre- (i.e., baseline) and post-silencing within the V2L cortex in response to a visual stimulus (50 ms LED flash at 81 lux denoted by the black bar from a control (A) and noise exposed (B) rat. (C) Within the granular layer there was a significant increase in sink amplitudes in response to both visual stimuli (i.e., 15 and 81 lux) pre- ($p < 0.013$) and post-silencing ($p < 0.05$) in the noise exposed rats. (D) There was a significant decrease in the degree of change (i.e., percent decrease) within the granular layer at both visual intensities ($p < 0.05$). (E) Within

*the upper-infragranular layer, there is an increase in visual-evoked sink amplitude pre- and post-silencing in the noise exposed rats ($p < 0.05$). However, (F) there was no difference in the degree of change between control and noise exposed rats at both intensities ($p > 0.05$). Values are mean ± SEM for the noise exposed ($n = 8$) and control ($n = 7$) groups. *$p < 0.05$, **$p < 0.013$*

6.3.1.4 Loss of Audiovisual Response Interactions following Cortical Inactivation

Due to the layer-specific enhancement of visual input in the noise exposed rats following cortical inactivation, we sought to investigate whether a similar trend was observed in response to combined auditory and visual stimulation specifically within the granular layer. A three-way repeated-measures ANOVA for audiovisual-evoked sink amplitudes within the granular layer revealed main effects of stimulus intensity ($F[1,13] = 47.03$, $p < 0.001$) and time ($F[1,13] = 109.74$, $p < 0.001$). Separate two-way repeated-measures ANOVAs for the low and high audiovisual stimuli revealed no significant interactions of time by group ($F[1,13] = 0.9$, $p = 0.36$; $F[1,13] = 1.04$, $p = 0.33$, respectively). Thus, in contrast to visual stimulation, there are no differences between control and noise exposed groups in response to audiovisual stimuli at either stimulus intensity (Fig. 6.5A).

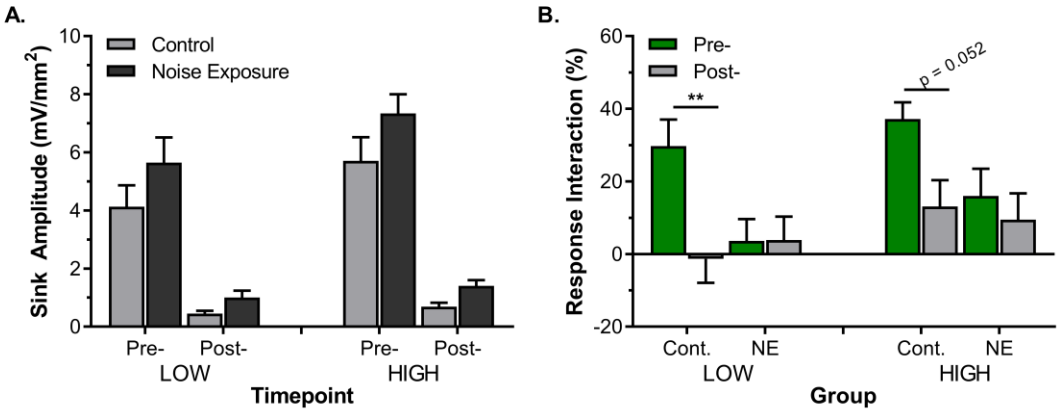

Figure 6.5. Preservation of audiovisual-evoked responses following pharmacological silencing following noise-induced hearing loss.

*(A) Granular sink amplitudes of control and noise exposed rats in response to combined audiovisual stimuli at two different stimulus intensities (i.e., low: +40 dB SPL and 15 lux; high: 90 dB SPL and 81 lux) pre- and post-pharmacological silencing. No significant differences were observed between the control and noise exposed rats ($p > 0.05$). (B) The magnitude of the response interaction (i.e., change in multisensory responsiveness in comparison to the unimodal stimulus that evoked the greatest response) was calculated for both groups before and after pharmacological silencing. The magnitude of the response interaction was significantly decreased in controls following pharmacological silencing in response to the low audiovisual stimuli ($p < 0.01$). No other significant differences were observed. Values are mean ± SEM for the noise exposed ($n = 8$) and control ($n = 7$) groups. *$p < 0.05$, **$p < 0.01$*

In addition to analyzing audiovisual-evoked sink amplitudes, the strength of the response interaction was examined before and after pharmacological silencing in both the control and noise exposed groups. Because there was a significant effect of stimulus intensity ($F[1,13] = 7.2$, $p < 0.05$; three-way repeated-measures ANOVA), separate two-way repeated-measures ANOVAs were conducted for the low and high audiovisual stimuli. Interestingly, a significant interaction of time by group was only observed for the low

audiovisual stimuli ($F[1,13] = 6.9$, $p < 0.05$). In the multisensory zone of V2L in controls, there was a significant decrease in the strength of the response interaction following pharmacological silencing in response to the low audiovisual stimuli (pre: 29.7 ± 7.4 % vs. post: -1.3 ± 6.6 %, $p < 0.01$), indicating that this region is responsible for enhancing neuronal activity in response to audiovisual stimuli (Fig. 6.5B). Although no other significant differences were observed, a similar trend was observed in response to the high audiovisual stimuli. In contrast to the responses observed in the controls, the multisensory zone of V2L in noise exposed rats demonstrated no change in the strength of the response interaction ($p > 0.05$), which was already reduced in the noise exposed group prior to pharmacological silencing. Surprisingly, the strength of the response interaction after cortical inactivation of controls was similar to that of the noise exposed rats, prior to inactivation, indicating that the noise exposed rats lost the ability to modulate audiovisual activity within this cortical region; findings consistent with our previous results (Chapter 5).

6.3.1.5 Overall Strength of Postsynaptic Inputs Maintained Following Noise Exposure

In addition to examining the layer-specific effects of noise-induced crossmodal plasticity, we also investigated changes in the overall strength of postsynaptic currents within the audiovisual cortex following pharmacological silencing. To do so, audiovisual-evoked AVREC amplitudes were compared before and after cortical inactivation, and the percent decrease was calculated for each of the groups and stimulus intensities (Fig. 6.6). A two-way repeated-measures ANOVA revealed no interaction of stimulus intensity by group ($F[1,13] = 1.60$, $p = 0.229$) and no effect of stimulus intensity ($F[1,13] = 0.59$, $p = 0.455$). As can be seen in Figure 6.6C, there were no differences between the control and noise exposed groups at the low (control: 77.7 ± 3.6% vs. noise-exposed: 79.8 ± 2.2%) or high (control: 78.3 ± 2.8 vs. noise-exposed: 77.3 ± 2.5%) stimulus intensities. Overall, these results demonstrate that the multisensory zone of the V2L cortex receives ~ 22% of its input from long-range afferents such as thalamocortical inputs, which do not change

following noise-induced hearing loss, indicating that this region adapts to a partial loss of sensory input by altering the strength of the auditory and visual inputs.

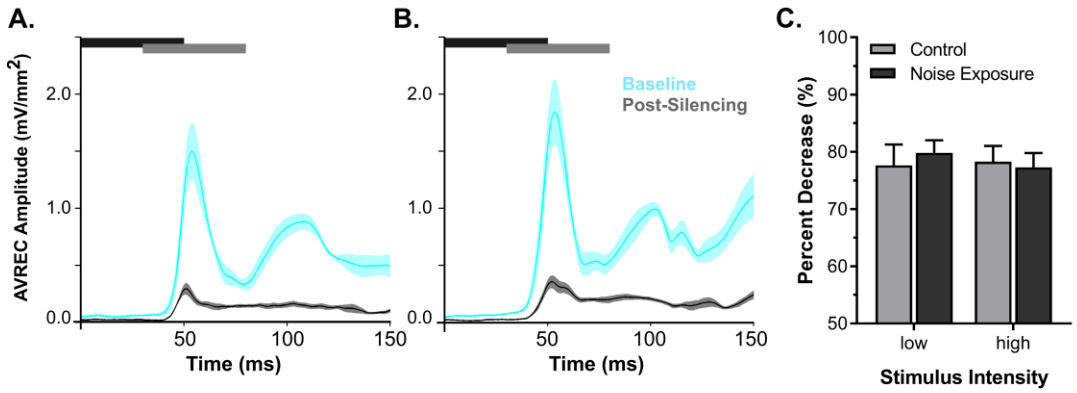

Figure 6.6. Total strength of audiovisual-evoked postsynaptic input preserved following adult-onset hearing loss.

(A) AVREC waveforms from control (left) and noise exposed (right) rats in response to combined audiovisual stimulation (i.e., 90 dB SPL and 81 lux). (B) Audiovisual-evoked AVREC amplitudes demonstrated no difference in the degree of change (i.e., percent decrease) between the control and noise exposed groups in response to the low (i.e., +40 dB SPL and 15 lux) and high (i.e., 90 dB SPL and 81 lux) stimuli. In the AVERC waveforms, dark lines represented the group mean and shading represents the SEM for the baseline (light blue) and post-silencing (light grey) recordings. Values are mean ± SEM for the noise exposed (n = 8) and control (n = 7) groups.

6.3.2 Experiment 2: Onset of Crossmodal Plasticity

6.3.2.1 Cortical-Evoked Responses across the Audiovisual Cortex

To explore alterations in cortical activity following noise-induced hearing loss, auditory and visual-evoked responses were analyzed across all 16 electrode sites. Based on preliminary studies, the magnitude of the evoked responses demonstrated electrode site-specific effects, whereby auditory responses were strongest on the most ventral sites, whereas visual responses were strongest on the most dorsal electrode sites. To investigate

this further, auditory and visual-evoked responses were averaged across the rostral-caudal axis generating four electrode sites organized from most dorsal to ventral (i.e., sites 1, 2, 3, and 4; see Fig. 6.2) and the responses were statistically analyzed. Consistent with our preliminary observations, a one-way repeated-measures ANOVA revealed a significant effect of auditory-evoked LFP amplitudes ($F[1.0,8.1] = 8.1$, $p < 0.05$) and a significant effect of visual-evoked LFP amplitudes ($F[1.0,8.1] = 5.3$, $p < 0.05$). Therefore, all further analyses were completed across the four averaged electrode sites (see Fig. 6.2C, 6.2D for representative examples), allowing for the comparison of amplitudes across the most dorsal and ventral portions of the V2L cortex.

6.3.2.2 Loss of Hearing Sensitivity Following Noise Exposure

To assess changes in hearing sensitivity, ABR thresholds in response to a click stimulus were compared before exposure, immediately after exposure and at the end of the recording session (~3 hours post-exposure). In rats exposed to the loud broadband noise at 120 dB SPL for two hours, a one-way repeated-measures ANOVA revealed a significant effect of time (i.e., pre-, post-, and final) on ABR click thresholds. Bonferroni- corrected post hoc t-tests demonstrated a significant increase in click threshold immediately following the noise exposure (pre-noise: 30.0 ± 1.3 dB SPL vs. post-noise: 70.8 ± 3.0 dB SPL, $p < 0.001$). Interesting, click thresholds measured at the end of the experimental procedure (i.e., final) showed a slight decrease (final: 65.8 ± 2.4 dB SPL, $p = 0.041$) when compared to the threshold assessed immediately following the noise exposure. As expected, there were no differences in hearing sensitivity when rats were exposed to quiet for two hours in the sham condition ($F[2,4] = 1.0$, $p = 0.44$). Furthermore, there were no significant differences between baseline hearing sensitivity of sham and noise exposed rats ($p > 0.05$; independent samples t-test).

In addition to changes in hearing thresholds, cortical auditory-evoked amplitudes were examined before and after noise-induced hearing loss. For each of the four electrode sites, peak-to-peak amplitudes were calculated across three different sound intensities (i.e., 50, 70, and 90 dB SPL). Consistent across all electrode sites, a two-way repeated-measures ANOVA revealed a significant effect of time (see Table 6.1 for detail statistical values). For the second series of electrode sites (i.e., electrode sites 2) which would represent the

approximate location of V2L-Mz, a two-way repeated-measures ANOVA revealed a main effect of sound intensity and a trend towards an effect of stimulus intensity (see Table 6.1, section 1.2a). As can be seen in Figure 6.7B, there was a decrease in P2P amplitude across all intensities (e.g., 50 dB SPL: pre: 0.053 ± 0.01 vs. post: 0.018 ± 0.003 mV, $p = 0.043$ and 90 dB SPL: pre: 0.084 ± 0.023 vs. post: 0.043 ± 0.014 mV, $p = 0.031$). In addition to auditory-evoked amplitudes, peak latencies were also examined at 70 and 90 dB SPL before and after noise-induced hearing loss. A two-way repeated-measures ANOVA revealed main effects of sound intensity and time, as well as a significant interaction (see Table 6.1, section 1.2b). Follow-up post hoc t-tests revealed a significant increase in peak latency at 70 dB SPL ($p < 0.01$) and 90 dB SPL ($p < 0.01$). As can be seen in Figure 6.7, similar results were observed at the other electrode sites (i.e., electrode sites 1, 3, and 4; see Table 6.1 for statistical analyses), whereby noise exposure decreased the amplitude of the auditory-evoked responses across all intensities as well as an increase peak latency. Taken together, these results demonstrate that noise-induced hearing loss resulted in an immediate loss of hearing sensitivity at both the level of the brainstem and the cortex.

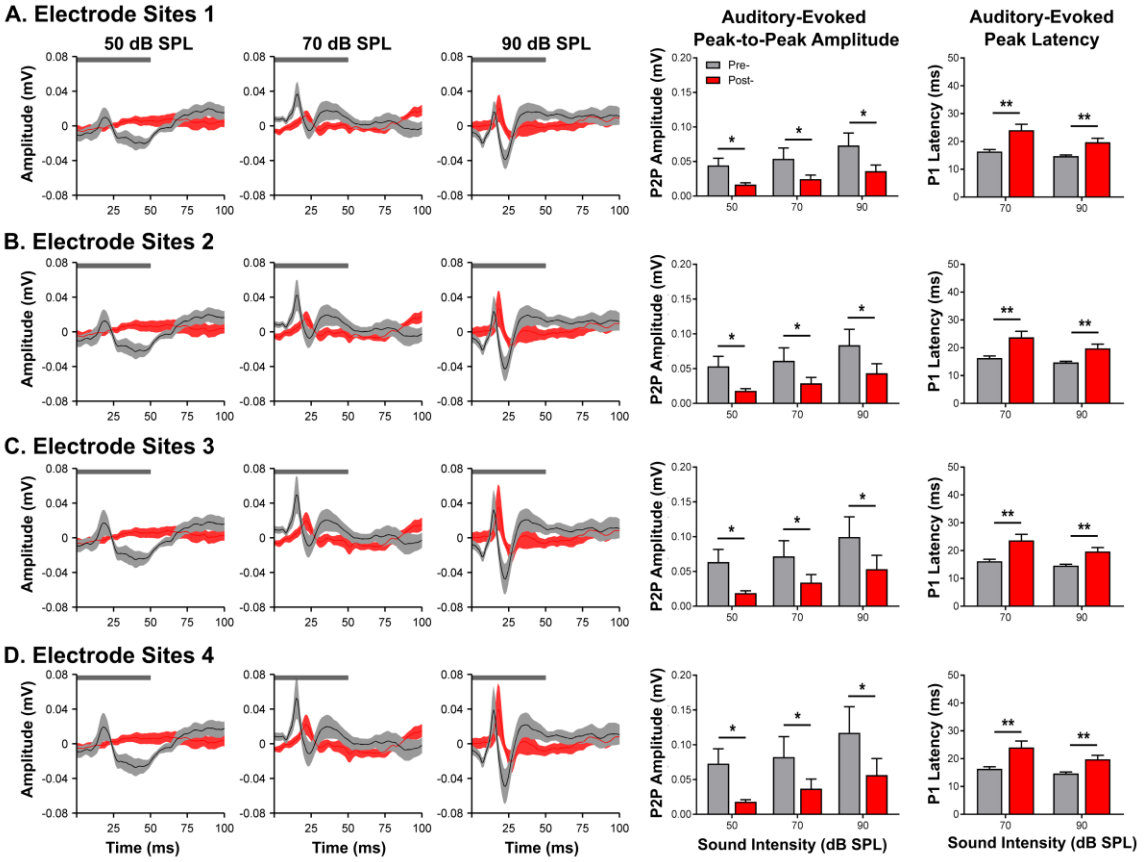

Figure 6.7. Decrease in auditory-evoked amplitudes following noise-induced hearing loss across the higher-order sensory cortices.

*Average LFP waveforms from the first (A), second (B), third (C) and fourth (D) series of electrode sites in response to auditory stimuli at 50 dB, 70 dB and 90 dB SPL (from left to right). The horizontal grey bar denotes the presentation of the auditory stimulus, and the dark line represents the group mean and shading represents the SEM for the recordings completed pre-noise (light grey; n = 6) and post-exposure (red; n = 6). An analysis of peak-to-peak (P2P) amplitudes (first set of bar graphs) shows a decrease in auditory-evoked amplitude across all stimulus intensities. Consistent across all electrode sites, there was an increase in peak latency in response to the 70 dB and 90 dB SPL stimuli (bar graphs on the far right). Values are mean ± SEM for the noise exposed rats pre-exposure (n = 6) and post-exposure (n = 6). *p < 0.05, **p < 0.017.*

Table 6.1. Statistical analysis of auditory-evoked data by two-way rmANOVA

Factor	F-value	p value
Electrode Sites 1:		
(1.1a) Effect of noise on auditory-evoked P2P amplitude		
Stimulus Intensity	$F_{(2,10)} = 7.1$	< 0.05
Time	$F_{(1,5)} = 9.8$	< 0.05
Stimulus Intensity x Time	$F_{(2,10)} = 0.7$	0.519
(1.1b) Effect of noise on auditory-evoked peak latency		
Stimulus Intensity	$F_{(1,5)} = 20.7$	< 0.01
Time	$F_{(1,5)} = 20.7$	< 0.01
Stimulus Intensity x Time	$F_{(1,5)} = 13.7$	< 0.05
Electrode Sites 2:		
(1.2a) Effect of noise on auditory-evoked P2P amplitude		
Stimulus Intensity	$F_{(1.1,5.4)} = 5.6$	0.059
Time	$F_{(1,5)} = 10.2$	< 0.05
Stimulus Intensity x Time	$F_{(2,10)} = 0.36$	0.708
(1.2b) Effect of noise on auditory-evoked peak latency		
Stimulus Intensity	$F_{(1,5)} = 19.7$	< 0.01
Time	$F_{(1,5)} = 18.1$	< 0.01
Stimulus Intensity x Time	$F_{(1,5)} = 16.5$	< 0.01
Electrode Sites 3:		
1.3a) Effect of noise on auditory-evoked P2P amplitude		
Stimulus Intensity	$F_{(1.0,5.2)} = 5.1$	0.070
Time	$F_{(1,5)} = 10.9$	< 0.05
Stimulus Intensity x Time	$F_{(1.1,5.4)} = 0.32$	0.613
(1.3b) Effect of noise on auditory-evoked peak latency		
Stimulus Intensity	$F_{(1,5)} = 17.5$	< 0.01
Time	$F_{(1,5)} = 18.7$	< 0.01
Stimulus Intensity x Time	$F_{(1,5)} = 20.2$	< 0.01
Electrode Sites 4:		
(1.4a) Effect of noise on auditory-evoked P2P amplitude		
Stimulus Intensity	$F_{(1.0,5.2)} = 3.8$	0.106
Time	$F_{(1,5)} = 9.9$	< 0.05
Stimulus Intensity x Time	$F_{(1.2,5.9)} = 0.77$	0.488
(1.4b) Effect of noise on auditory-evoked peak latency		
Stimulus Intensity	$F_{(1,5)} = 19.2$	< 0.01
Time	$F_{(1,5)} = 18.5$	< 0.01
Stimulus Intensity x Time	$F_{(1,5)} = 10.5$	< 0.05

6.3.2.3 Crossmodal Plasticity Observed Immediately following Noise-Induced Hearing Loss

To investigate the timing of noise-induced crossmodal plasticity, visual-evoked amplitudes across the audiovisual cortex were examined before and after exposure to a loud noise. Peak amplitudes were calculated for each of the four averaged electrode sites at three different visual intensities (i.e., 3, 33, and 73 lux). In contrast to auditory-evoked responses, a two-way repeated-measures ANOVA revealed effects of time and stimulus intensity across all electrode sites (see Table 6.2 for detailed statistical values). An analysis of the amplitudes for the second series of electrode sites (i.e., electrode sites 2) revealed a significant increase in peak amplitude in response to the brightest stimulus (i.e., 73 lux; pre: 0.088 ± 0.019 vs. post: 0.133 ± 0.029 mV, $p < 0.017$) and a modest increase in response to the middle stimulus intensity (i.e., 33 lux; pre: 0.086 ± 0.015 vs. post: 0.124 ± 0.027 mV, $p = 0.034$). Interestingly, the dim visual stimulus (i.e., 3 lux) demonstrated no change in visual-evoked amplitude ($p = 0.304$), indicating that there is a stimulus-dependent enhancement of visual-evoked activity immediately following noise exposure. To further investigate the effects of noise-induced crossmodal plasticity, visual-evoked peak latency was calculated for all visual stimuli. For peak latency at electrode sites 2, a two-way repeated-measures ANOVA revealed significant effects of stimulus intensity and time (see Table 6.2, section 2.2.b). As can be seen in Figure 6.8A, there was a significant decrease in visual-evoked peak latency in response to the 33 lux visual stimulus (pre: 46.83 ± 1.58 vs. post: 41.30 ± 1.02 ms, $p < 0.01$) and the 73 lux visual stimulus (pre: 44.58 ± 1.19 vs. post: 41.17± 1.21 ms, $p < 0.01$). To summarize, noise-induced hearing loss resulted in an increase visual responsiveness, and a decrease in peak latency of ~5 ms at 33 lux, ~3 ms at 73 lux. Similar to the auditory-evoked activity, a consistent trend was observed across the other electrode sites (i.e., electrode sites 1, 3, and 4), demonstrating that all regions of the V2L cortex showed a consistent increase in peak amplitude and a decrease in peak latency in response to visual stimulation (Fig. 6.8). Overall, these collective results provide the first evidence that noise-induced crossmodal plasticity occurs rapidly following exposure, and this is characterized by an increase in visual-evoked amplitude and response latency.

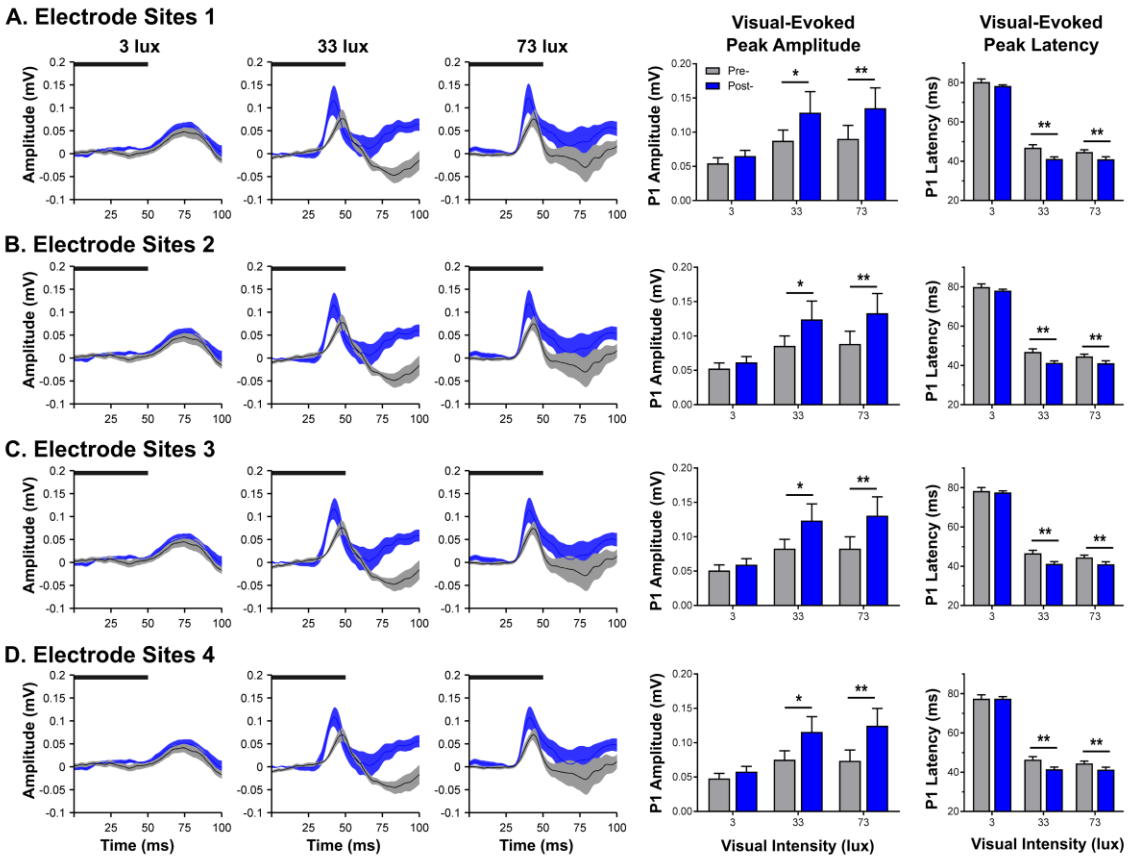

Figure 6.8. Enhancement of visual-evoked amplitudes following adult-onset hearing loss within higher-order sensory cortices.

*Average LFP waveforms from the first (A), second (B), third (C) and fourth (D) series of electrode sites in response to visual stimuli at 3, 33 and 73 lux (from left to right). The horizontal black bar denotes the presentation of the visual stimulus, and the dark line represents the group mean and shading represents the SEM for the recordings completed pre-noise (light grey; n = 6) and post-exposure (blue; n = 6). Immediately following the noise exposure, there was an increase in peak amplitudes (first set of bar graphs) in response to two of the stimulus intensities (i.e., 33 and 73 lux). Furthermore, there is a decrease in peak latency following exposure to the loud noise (bar graphs on the far right). Values are mean ± SEM for the noise exposed rats pre-exposure (n = 6) and post-exposure (n = 6). *p < 0.05, **p < 0.017.*

Table 6.2. Statistical analysis of visual-evoked data by two-way rmANOVA

Factor	F-value	p value
Electrode Sites 1:		
(2.1a) Effect of noise on visual-evoked peak amplitude		
Stimulus Intensity	$F_{(2,10)} = 7.1$	< 0.05
Time	$F_{(1,5)} = 12.9$	< 0.05
Stimulus Intensity x Time	$F_{(2,10)} = 3.1$	0.089
(2.1b) Effect of noise on visual-evoked peak latency		
Stimulus Intensity	$F_{(2,10)} = 371.4$	< 0.001
Time	$F_{(1,5)} = 83.1$	< 0.001
Stimulus Intensity x Time	$F_{(2,10)} = 1.8$	0.209
Electrode Sites 2:		
(2.2a) Effect of noise on visual-evoked peak amplitude		
Stimulus Intensity	$F_{(2,10)} = 8.4$	< 0.01
Time	$F_{(1,5)} = 14.6$	< 0.05
Stimulus Intensity x Time	$F_{(2,10)} = 3.6$	0.065
(2.2b) Effect of noise on visual-evoked peak latency		
Stimulus Intensity	$F_{(2,10)} = 351.4$	< 0.001
Time	$F_{(1,5)} = 73.4$	< 0.001
Stimulus Intensity x Time	$F_{(2,10)} = 2.1$	0.177
Electrode Sites 3:		
(2.3a) Effect of noise on visual-evoked peak amplitude		
Stimulus Intensity	$F_{(2,10)} = 9.9$	< 0.01
Time	$F_{(1,5)} = 18.5$	< 0.01
Stimulus Intensity x Time	$F_{(2,10)} = 4.8$	< 0.05
(2.3b) Effect of noise on visual-evoked peak latency		
Stimulus Intensity	$F_{(1.1,5.5)} = 259.6$	< 0.001
Time	$F_{(1,5)} = 299.7$	< 0.001
Stimulus Intensity x Time	$F_{(2,10)} = 3.2$	0.084
Electrode Sites 4:		
(2.4a) Effect of noise on visual-evoked peak amplitude		
Stimulus Intensity	$F_{(2,10)} = 8.6$	< 0.01
Time	$F_{(1,5)} = 24.5$	< 0.01
Stimulus Intensity x Time	$F_{(2,10)} = 5.1$	< 0.05
2.4b) Effect of noise on visual-evoked peak latency		
Stimulus Intensity	$F_{(1.1,5.5)} = 217.1$	< 0.001
Time	$F_{(1,5)} = 42.2$	< 0.001
Stimulus Intensity x Time	$F_{(2,10)} = 4.1$	< 0.05

6.3.2.4 Differential Sensory Responsiveness following Adult-onset Hearing Loss

To ensure that the visual enhancement that was observed was not a confounding result due to time under anesthesia, the degree of change from baseline was calculated for auditory and visual-evoked amplitudes in both the sham and noise exposed groups. For both auditory and visual-evoked amplitudes, separate two-way repeated-measures ANOVAs revealed a main effect of group ($F[1,7] = 24.1$, $p < 0.01$; $F[1,7] = 79.1$, $p < 0.001$, respectively), indicating that the observed effects were due to the noise exposure. As can be seen in Figure 6.9A, there was a significant decrease in the change from baseline when compared to sham exposed rats in response to auditory stimulation ($p < 0.01$). Interestingly, there was a consistent decrease in the change from baseline across all three auditory intensities (50 dB SPL: -58.5 ± 9.9 %; 70 dB SPL: -49.8 ± 7.2%; 90 dB SPL: -47.8 ± 10.3 %). An opposite pattern emerged in response to visual stimulation, where there was a significant increase in the change from baseline when compared to the sham exposed rats at 33 lux ($p < 0.01$) and 73 lux ($p < 0.001$). Furthermore, as can be seen in Figure 6.9B, the brightest visual stimulus evoked the largest degree of change compared to the other stimulus intensities (3 lux: 24.4 ± 12.6%; 33 lux: 46.8 ± 8.9%; 73 lux: 57.8 ± 11.3%). Therefore, noise-induced crossmodal plasticity resulted in a differential change from baseline between auditory and visual stimulation. Moreover, there may be intensity-specific effects in response to visual stimulation immediately following noise exposure, whereby the brighter the stimulus evokes greatest change from baseline.

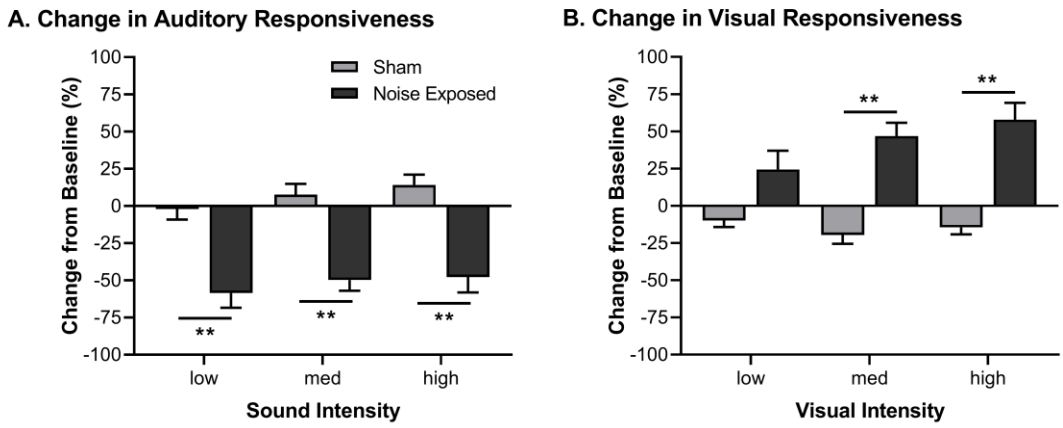

Figure 6.9. Effect of stimulus intensity on sensory-evoked activity following noise-induced hearing loss.

*Percent change from baseline was calculated in response to auditory (A) and visual (B) stimulation for noise exposed as well as sham exposed rats. Consistent across all sound intensities, there is approximately a 50% decrease in auditory-evoked amplitudes immediately following noise-induced hearing loss ($p < 0.01$). In contrast, there was an increase in visual-evoked amplitudes following hearing loss, with the brightest visual stimulus evoking the greatest change from baseline. Values are mean ± SEM for the noise exposed ($n = 6$) and sham exposed ($n = 3$) groups. *$p < 0.05$, **$p < 0.017$.*

6.4 Discussion

In the present study, we conducted the first investigation of altered thalamocortical processing in the audiovisual cortex following adult-onset hearing loss. To do so, we compared auditory- and visual-evoked postsynaptic activity in noise exposed rats versus age-matched controls, to assess the sensory- and layer-specific effects of noise-induced crossmodal plasticity (Experiment 1). Using a previously established technique to investigate the thalamocortical components of stimulus-induced excitation within the cortex (Happel et al., 2010, 2014; Lippert et al., 2013), we revealed that there was a layer-specific enhancement of visual input within the multisensory zone of the V2L cortex. Surprisingly, despite the enhancement of visual-evoked granular sink amplitudes, there

was no change in the overall strength of the postsynaptic activity between the control and noise exposed groups, suggesting that there was a re-allocation of inputs following noise-induced hearing loss. Additionally, we performed the first characterization of crossmodal plasticity immediately following acoustic trauma across the higher-order sensory cortices. More specifically, auditory- and visual-evoked LFP activity at several stimulus intensities was compared between sham and noise exposed rats to determine the timing of noise-induced crossmodal plasticity (Experiment 2). Interestingly, noise exposure resulted in a loss of auditory responsiveness across all sound intensities, as well as an immediate manifestation of crossmodal plasticity—characterized as an increase in visual-evoked amplitudes and a decrease in response latency—across all recording sites. Taken together, our results have shown for the first time that noise-induced crossmodal plasticity alters thalamocortical processing of visual stimuli and manifests soon after acoustic trauma within the higher-order sensory cortices; findings in support of the working hypothesis that crossmodal plasticity manifests, at least in part, by the unmasking of pre-existing connections.

6.4.1 Layer-Specific Effects of Sensory Deprivation

Recent electrophysiological studies have demonstrated that noise-induced hearing loss results in crossmodal plasticity across several regions of the V2L cortex (i.e., V2L-Az and V2L-Mz). More specifically, Schormans et al. (2018) revealed that crossmodal plasticity was observed across multiple cortical layers—characterized by an increase in visual responsiveness, suggesting that crossmodal plasticity results in intracortical and thalamocortical alterations. However, at the synaptic level, differential effects in synaptic transmission have been observed within specific cortical layers and sensory regions (Lee and Whitt, 2015). For example, within the supragranular layers (i.e., layer 2/3), there is an overall reduction in the postsynaptic strength of excitatory synaptic transmission in the primary auditory and barrel cortex of visually-deprived mice (Goel et al., 2006). Whereas, there was a global increase in the strength of excitatory synapses within the deprived visual cortex, indicating that homeostatic mechanisms may underlie the altered activity levels in each of the sensory cortices (Whitt et al., 2014). Thus, these previous results demonstrate that deprivation leads to opposite changes in the strength of the excitatory synapses within

the superficial layers of the primary sensory cortices, whereby they are decreased in the spared regions, and increased in the deprived cortical areas (Lee and Whitt, 2015).

In addition to alterations in synaptic plasticity within the superficial layers of the cortex, alterations in the thalamocortical recipient layer (i.e., layer 4) have also been observed. Even though, thalamocortical connections were originally believed to be less plastic later in life, several studies have demonstrated that thalamocortical plasticity can be reactivated later in life following sensory deprivation (Oberlaender et al., 2012; Yu et al., 2012). Indeed, visual deprivation in adults strengthened thalamocortical synapses in the auditory cortex but not in the primary visual cortex (Petrus et al., 2014). Furthermore, this effect was not restricted to visual deprivation, as deafening resulted in an enhancement of layer 4 synapses within the primary visual cortex (Petrus et al., 2014). Interestingly, in the present study, there was an increase in sink amplitudes within the granular layer of the V2L-Mz cortex (Fig. 6.4), which is consistent with the plasticity observed in the primary visual cortex following deafening. Moreover, the enhancement of granular layer activity (i.e., layer 4), was sensory-specific, as only an increase in visual-evoked activity was observed. Layer-specific plasticity has also been observed following short-term dark exposure whereby deprivation potentiated synapses from layer 4 to layer 2/3 within the auditory cortex (i.e., spared cortical region) and strengthened intracortical inputs to the primary visual cortex (i.e., deprived cortex) (Petrus et al., 2015). Overall, the collective studies demonstrated that there is an enhancement of activity within the thalamocortical recipient layer (i.e., granular layer), as well as a global decrease of excitatory synapses within layer 2/3 following sensory deprivation within the spared cortex, suggesting a shift towards feedforward processing at the expense of intracortical processing (Petrus et al., 2015). Despite the growing evidence of differential synaptic plasticity between the primary sensory regions, future studies are needed in order to determine whether the higher-order sensory cortices show synaptic changes consistent with the deprived or spared sensory cortex following partial deprivation.

6.4.2 The Audiovisual Cortex: Spared or Deprived Cortical Region?

It is important to note that the majority of the studies investigating crossmodal plasticity following sensory deprivation have been focused on changes within the primary sensory cortices. Because the audiovisual cortex (i.e., the multisensory zone of the V2L cortex) is a region of the brain that is capable of processing both auditory and visual stimuli (Barth et al., 1995; Hirokawa et al., 2008; Schormans et al., 2017b; Toldi et al., 1986; Wallace et al., 2004), it could be defined as either a deprived area (due to the loss of auditory input) or a spared area (due to the maintenance visual input) following a hearing impairment. Based on our current results as well as previous studies, we suggest that the audiovisual cortex takes on characteristics consistent with the spared sensory cortex following noise-induced hearing loss.

Following sensory deprivation, several alterations have been observed within the spared sensory regions, such as strengthening of thalamocortical synapses (Petrus et al., 2014, 2015), reduced activity within the superficial layers (Goel et al., 2006; He et al., 2012), as well as an expansion of sensory responsiveness (Elbert et al., 2002; Foeller et al., 2005; Pascual-Leone and Torres, 1993; Sterr et al., 1998). In the present study, we found that noise-induced crossmodal plasticity resulted in an enhancement of visual-evoked activity specifically within the granular layer (Fig. 6.4), which is consistent with the strengthening of thalamocortical synapses within the visual cortex following deafness (Petrus et al., 2014). While the thalamocortical recipient layer demonstrated an enhancement, several studies have demonstrated that the superficial layers show an overall reduction (Goel et al., 2006; He et al., 2012). More specifically, in visually-deprived mice the spared cortices show a global reduction in the postsynaptic strength of excitatory synaptic transmission (Goel et al., 2006; He et al., 2012). Interestingly, Schormans et al. (2017a) demonstrated that single-neurons within the most dorsally-located region of V2L (i.e., V2L-Vz) had a lower firing rate in response to visual stimulation following noise-induced hearing loss. Taken together, the synaptic plasticity observed within the thalamocortical and superficial layers of the spared sensory cortices are similar to the single-unit and cortical-microcircuit plasticity observed in the audiovisual cortex. Furthermore, noise-induced hearing loss has

been shown to increase the proportion of neurons responsive to visual stimuli within the V2L cortex of the rat, indicative of an expansion of visual responses (Schormans et al., 2017a), consistent with observations in blind individuals (Elbert et al., 2002; Pascual-Leone and Torres, 1993). More specifically, blind individuals who are proficient braille readers, show an expansion of the cortical area that is devoted to the representation of the fingers (Pascual-Leone and Torres, 1993), as well as an expansion for the cortical areas which respond to auditory stimuli (Elbert et al., 2002). Therefore, consistent with the spared cortices of blind individuals (i.e., touch and audition), the amount of space allocated to visual processing expands within the higher-order sensory cortices following hearing loss.

Finally, a well-characterized consequence of hearing loss is the resultant hyperactivity within the primary auditory cortex (Meredith et al., 2012; Popelar et al., 2008; Salvi et al., 2000). Until recently, it was unknown whether this hyperactivity extended beyond the auditory cortex (i.e., deprived cortical region) into neighbouring cortical areas. Surprisingly, the neuronal hyperactivity (i.e., central gain enhancement) observed in rats with adult-onset hearing loss was found to be restricted to auditory cortical regions (Schormans et al., 2018), indicating that the V2L cortex does not inherit the properties of the deprived region. Furthermore, single-unit recordings within the V2L cortex of noise exposed rats demonstrated a loss of auditory responsiveness, which is inconsistent with the enhancement of sensory responsiveness observed in the primary auditory cortex (Meredith et al., 2012). Ultimately, the aforementioned studies demonstrate that following noise-induced hearing loss, the V2L cortex demonstrates similar plasticity with that of spared sensory areas.

6.4.3 Rapid Manifestation of Crossmodal Plasticity following Sensory Deprivation

At present, it is relatively unknown whether the crossmodal plasticity occurs due to changes in existing neural networks or from the formation of new neural connections (Singh et al., 2018). While these are not likely the sole mechanisms, the immediate enhancement of visual activity following noise-induced hearing loss observed in the present study (see Fig. 6.8, 6.9), would suggest an unmasking of existing connections may

underlie these changes. Support for the rapid manifestation of cortical plasticity, can be seen in repetitive transcranial magnetic stimulation (rTMS) studies, whereby rTMS applied over the somatosensory cortex in early blind subjects revealed an increase in the regional cerebral blood flow (rCBF) within the striate and extrastriate visual areas using positron emission tomography (Wittenberg et al., 2004). Moreover, healthy subjects that were blindfolded for five days demonstrated greater activation of the bilateral region of the occipital cortex in response to tactile stimulation immediately following the procedure (Merabet et al., 2008). Based on the rapid onset of these neuroplastic changes, these studies suggest that crossmodal plasticity may be due to the unmasking of normally inhibited connections. While a few studies have examined crossmodal plasticity shortly after the onset of deprivation, to our knowledge the present study represents the first examination of cortical plasticity immediately following auditory deprivation. Therefore, it remains unknown whether this rapid enhancement of the intact sensory modalities is maintained, or if the degree of enhancement decreases over time.

6.5 References

Allman, B.L., and Meredith, M.A. (2007). Multisensory Processing in “Unimodal” Neurons: Cross-Modal Subthreshold Auditory Effects in Cat Extrastriate Visual Cortex. *J. Neurophysiol.* 98, 545–549.

Allman, B.L., Bittencourt-Navarrete, R.E., Keniston, L.P., Medina, A.E., Wang, M.Y., and Meredith, M.A. (2008). Do Cross-Modal Projections Always Result in Multisensory Integration? *Cereb. Cortex* 18, 2066–2076.

Allman, B.L., Keniston, L.P., and Meredith, M.A. (2009). Adult deafness induces somatosensory conversion of ferret auditory cortex. *Proc. Natl. Acad. Sci.* 106, 5925–5930.

Auer, E.T., Bernstein, L.E., Sungkarat, W., and Singh, M. (2007). Vibrotactile Activation of the Auditory Cortices in Deaf versus Hearing Adults. *Neuroreport* 18, 645–648.

Barth, D.S., Goldberg, N., Brett, B., and Di, S. (1995). The spatiotemporal organization of auditory, visual, and auditory-visual evoked potentials in rat cortex. *Brain Res.* 678, 177–190.

Bavelier, D., and Neville, H.J. (2002). Cross-modal plasticity: where and how? *Nat. Rev. Neurosci.* 3, 443–452.

Bavelier, D., Dye, M.W.G., and Hauser, P.C. (2006). Do deaf individuals see better? *Trends Cogn. Sci.* 10, 512–518.

Burkhalter, A. (2016). The Network for Intracortical Communication in Mouse Visual Cortex. In Micro-, Meso- and Macro-Connectomics of the Brain, H. Kennedy, D.C.V. Essen, and Y. Christen, eds. (Springer International Publishing), pp. 31–43.

Campbell, J., and Sharma, A. (2013). Compensatory changes in cortical resource allocation in adults with hearing loss. *Front. Syst. Neurosci.* 7, 71.

Campbell, J., and Sharma, A. (2014). Cross-Modal Re-Organization in Adults with Early Stage Hearing Loss. *PLOS ONE* 9, e90594.

Cardon, G., and Sharma, A. (2018). Somatosensory Cross-Modal Reorganization in Adults With Age-Related, Early-Stage Hearing Loss. *Front. Hum. Neurosci.* 12.

Einevoll, G.T., Kayser, C., Logothetis, N.K., and Panzeri, S. (2013). Modelling and analysis of local field potentials for studying the function of cortical circuits. *Nat. Rev. Neurosci. Lond.* 14, 770–785.

Elbert, T., Sterr, A., Rockstroh, B., Pantev, C., Müller, M.M., and Taub, E. (2002). Expansion of the Tonotopic Area in the Auditory Cortex of the Blind. *J. Neurosci.* 22, 9941–9944.

Foeller, E., Celikel, T., and Feldman, D.E. (2005). Inhibitory Sharpening of Receptive Fields Contributes to Whisker Map Plasticity in Rat Somatosensory Cortex. *J. Neurophysiol.* 94, 4387–4400.

Frasnelli, J., Collignon, O., Voss, P., and Lepore, F. (2011). Chapter 15 - Crossmodal plasticity in sensory loss. In *Progress in Brain Research*, eds. A.M. Green, C.E. Chapman, J.F. Kalaska, and F. Lepore, (Amsterdam, Netherlands: Elsevier), 233–249.

Freeman, B., and Singer, W. (1983). Direct and indirect visual inputs to superficial layers of cat superior colliculus: a current source-density analysis of electrically evoked potentials. *J. Neurophysiol*. 49, 1075–1091.

Givre, S.J., Schroeder, C.E., and Arezzo, J.C. (1994). Contribution of extrastriate area V4 to the surface-recorded flash VEP in the awake macaque. *Vision Res.* 34, 415–428.

Goel, A., Jiang, B., Xu, L.W., Song, L., Kirkwood, A., and Lee, H.-K. (2006). Cross-modal regulation of synaptic AMPA receptors in primary sensory cortices by visual experience. *Nat. Neurosci.* 9, 1001–1003.

Happel, M.F.K., Jeschke, M., and Ohl, F.W. (2010). Spectral Integration in Primary Auditory Cortex Attributable to Temporally Precise Convergence of Thalamocortical and Intracortical Input. *J. Neurosci.* 30, 11114–11127.

Happel, M.F.K., Deliano, M., Handschuh, J., and Ohl, F.W. (2014). Dopamine-modulated recurrent corticoefferent feedback in primary sensory cortex promotes detection of behaviorally relevant stimuli. *J. Neurosci.* 34, 1234–1247.

He, K., Petrus, E., Gammon, N., and Lee, H.-K. (2012). Distinct Sensory Requirements for Unimodal and Cross-Modal Homeostatic Synaptic Plasticity. *J. Neurosci*. 32, 8469–8474.

Heimler, B., Weisz, N., and Collignon, O. (2014). Revisiting the adaptive and maladaptive effects of crossmodal plasticity. *Neuroscience* 283, 44–63.

Hirokawa, J., Bosch, M., Sakata, S., Sakurai, Y., and Yamamori, T. (2008). Functional role of the secondary visual cortex in multisensory facilitation in rats. *Neuroscience* 153, 1402–1417.

Hunt, D.L., Yamoah, E.N., and Krubitzer, L. (2006). Multisensory plasticity in congenitally deaf mice: How are cortical areas functionally specified? *Neuroscience* 139, 1507–1524.

Konerding, W.S., Froriep, U.P., Kral, A., and Baumhoff, P. (2018). New thin-film surface electrode array enables brain mapping with high spatial acuity in rodents. *Sci. Rep.* 8, 3825.

Kral, A., and Eggermont, J.J. (2007). What's to lose and what's to learn: Development under auditory deprivation, cochlear implants and limits of cortical plasticity. *Brain Res. Rev*. 56, 259–269.

Kujawa, S.G., and Liberman, M.C. (2009). Adding Insult to Injury: Cochlear Nerve Degeneration after "Temporary" Noise-Induced Hearing Loss. *J. Neurosci*. 29, 14077–14085.

Lambertz, N., Gizewski, E.R., de Greiff, A., and Forsting, M. (2005). Cross-modal plasticity in deaf subjects dependent on the extent of hearing loss. *Cogn. Brain Res.* 25, 884–890.

Lee, H.-K., and Whitt, J.L. (2015). Cross-modal synaptic plasticity in adult primary sensory cortices. *Curr. Opin. Neurobiol*. 35, 119–126.

Lippert, M.T., Takagaki, K., Kayser, C., and Ohl, F.W. (2013). Asymmetric Multisensory Interactions of Visual and Somatosensory Responses in a Region of the Rat Parietal Cortex. *PLOS ONE* 8, e63631.

Liu, B., Wu, G.K., Arbuckle, R., Tao, H.W., and Zhang, L.I. (2007). Defining cortical frequency tuning with recurrent excitatory circuitry. *Nat. Neurosci.* 10, 1594–1600.

Merabet, L.B., and Pascual-Leone, A. (2010). Neural reorganization following sensory loss: the opportunity of change. *Nat. Rev. Neurosci*. 11, 44–52.

Merabet, L.B., Hamilton, R., Schlaug, G., Swisher, J.D., Kiriakopoulos, E.T., Pitskel, N.B., Kauffman, T., and Pascual-Leone, A. (2008). Rapid and Reversible Recruitment of Early Visual Cortex for Touch. *PLOS ONE* 3, e3046.

Meredith, M.A., and Allman, B.L. (2009). Subthreshold multisensory processing in cat auditory cortex. *Neuroreport* 20, 126–131.

Meredith, M.A., and Allman, B.L. (2012). Early Hearing-Impairment Results in Crossmodal Reorganization of Ferret Core Auditory Cortex. *Neural Plast*. 2012, e601591.

Meredith, M.A., and Allman, B.L. (2015). Single-unit analysis of somatosensory processing in the core auditory cortex of hearing ferrets. *Eur. J. Neurosci*. 41, 686–698.

Meredith, M.A., and Lomber, S.G. (2011). Somatosensory and visual crossmodal plasticity in the anterior auditory field of early-deaf cats. *Hear. Res*. 280, 38–47.

Meredith, M.A., Keniston, L.P., and Allman, B.L. (2012). Multisensory dysfunction accompanies crossmodal plasticity following adult hearing impairment. *Neuroscience* 214, 136–148.

Mitzdorf, U. (1985). Current source-density method and application in cat cerebral cortex: investigation of evoked potentials and EEG phenomena. *Physiol. Rev*. 65, 37–100.

Mitzdorf, U., and Singer, W. (1977). Laminar segregation of afferents to lateral geniculate nucleus of the cat: an analysis of current source density. J. *Neurophysiol*. 40, 1227–1244.

Mitzdorf, U., and Singer, W. (1980). Monocular activation of visual cortex in normal and monocularly deprived cats: an analysis of evoked potentials. *J. Physiol*. 304, 203–220.

Moeller, C.K., Kurt, S., Happel, M.F.K., and Schulze, H. (2010). Long-range effects of GABAergic inhibition in gerbil primary auditory cortex. *Eur. J. Neurosci*. 31, 49–59.

Nicholson, C., and Freeman, J.A. (1975). Theory of current source-density analysis and determination of conductivity tensor for anuran cerebellum. *J. Neurophysiol*. 38, 356–368.

Oberlaender, M., Ramirez, A., and Bruno, R.M. (2012). Sensory Experience Restructures Thalamocortical Axons during Adulthood. *Neuron* 74, 648–655.

Olsen, G.M., and Witter, M.P. (2016). Posterior parietal cortex of the rat: Architectural delineation and thalamic differentiation. *J. Comp. Neurol*. 524:18, 3774-3809

Pascual-Leone, A., and Torres, F. (1993). Plasticity of the sensorimotor cortex representation of the reading finger in Braille readers. *Brain* 116, 39–52.

Pavani, F., and Roder, B. (2012). "Crossmodal plasticity as a consequence of sensory loss: insights from blindness and deafness." In *The New Handbook for Multisensory Processes*, eds. B. Stein (Cambridge, MA: MIT Press) 737–759.

Petrus, E., Isaiah, A., Jones, A.P., Li, D., Wang, H., Lee, H.-K., and Kanold, P.O. (2014). Crossmodal Induction of Thalamocortical Potentiation Leads to Enhanced Information Processing in the Auditory Cortex. *Neuron* 81, 664–673.

Petrus, E., Rodriguez, G., Patterson, R., Connor, B., Kanold, P.O., and Lee, H.-K. (2015). Vision Loss Shifts the Balance of Feedforward and Intracortical Circuits in Opposite Directions in Mouse Primary Auditory and Visual Cortices. *J. Neurosci*. 35, 8790–8801.

Popelar, J., Grecova, J., Rybalko, N., and Syka, J. (2008). Comparison of noise-induced changes of auditory brainstem and middle latency response amplitudes in rats. *Hear. Res*. 245, 82–91.

Sakata, S., and Harris, K.D. (2009). Laminar Structure of Spontaneous and Sensory-Evoked Population Activity in Auditory Cortex. *Neuron* 64, 404–418.

Salvi, R.J., Wang, J., and Ding, D. (2000). Auditory plasticity and hyperactivity following cochlear damage. *Hear. Res.* 147, 261–274.

Schormans, A.L., Typlt, M., and Allman, B.L. (2017a). Crossmodal plasticity in auditory, visual and multisensory cortical areas following noise-induced hearing loss in adulthood. *Hear. Res.* 343, 92–107.

Schormans, A.L., Scott, K.E., Vo, A.M.Q., Tyker, A., Typlt, M., Stolzberg, D., and Allman, B.L. (2017b). Audiovisual Temporal Processing and Synchrony Perception in the Rat. *Front. Behav. Neurosci.* 10.

Schormans, A.L., Typlt, M., and Allman, B.L. (2018). Adult-Onset Hearing Impairment Induces Layer-Specific Cortical Reorganization: Evidence of Crossmodal Plasticity and Central Gain Enhancement. *Cereb. Cortex*, bhy067

Schroeder, C.E., Javitt, D.C., Steinschneider, M., Mehta, A.D., Givre, S.J., Jr, H.G.V., and Arezzo, J.C. (1997). N-methyl-d-aspartate enhancement of phasic responses in primate neocortex. *Exp. Brain Res.* 114, 271–278.

Schroeder, C.E., Mehta, A.D., and Givre, S.J. (1998). A spatiotemporal profile of visual system activation revealed by current source density analysis in the awake macaque. *Cereb. Cortex* 8, 575–592.

Schroeder, C.E., Lindsley, R.W., Specht, C., Marcovici, A., Smiley, J.F., and Javitt, D.C. (2001). Somatosensory Input to Auditory Association Cortex in the Macaque Monkey. *J. Neurophysiol.* 85, 1322–1327.

Singh, A.K., Phillips, F., Merabet, L.B., and Sinha, P. (2018). Why Does the Cortex Reorganize after Sensory Loss? *Trends Cogn. Sci.* 22, 569–582.

Sterr, A., Müller, M.M., Elbert, T., Rockstroh, B., Pantev, C., and Taub, E. (1998). Perceptual Correlates of Changes in Cortical Representation of Fingers in Blind Multifinger Braille Readers. *J. Neurosci.* 18, 4417–4423.

Stolzberg, D., Chrostowski, M., Salvi, R.J., and Allman, B.L. (2012). Intracortical circuits amplify sound-evokes activity in primary auditory cortex following systemic injection of salicylate in the rat. *J. Neurophysiol.* 108, 200–214.

Szymanski, F.D., Garcia-Lazaro, J.A., and Schnupp, J.W.H. (2009). Current Source Density Profiles of Stimulus-Specific Adaptation in Rat Auditory Cortex. *J. Neurophysiol.* 102, 1483–1490.

Toldi, J., Fehér, O., and Wolff, J.R. (1986). Sensory interactive zones in the rat cerebral cortex. *Neuroscience* 18, 461–465.

Wallace, M.T., Ramachandran, R., and Stein, B.E. (2004). A revised view of sensory cortical parcellation. *Proc. Natl. Acad. Sci.* 101, 2167–2172.

Whitt, J.L., Petrus, E., and Lee, H.-K. (2014). Experience-dependent homeostatic synaptic plasticity in neocortex. *Neuropharmacology* 78, 45–54.

Wittenberg, G.F., Werhahn, K.J., Wassermann, E.M., Herscovitch, P., and Cohen, L.G. (2004). Functional connectivity between somatosensory and visual cortex in early blind humans. *Eur. J. Neurosci.* 20, 1923–1927.

Xu, J., Sun, X., Zhou, X., Zhang, J., and Yu, L. (2014). The cortical distribution of multisensory neurons was modulated by multisensory experience. *Neuroscience* 272, 1–9.

Yamauchi, T., Hori, T., and Takahashi, T. (2000). Presynaptic inhibition by muscimol through GABAB receptors. *Eur. J. Neurosci.* 12, 3433–3436.

Yu, X., Chung, S., Chen, D.-Y., Wang, S., Dodd, S.J., Walters, J.R., Isaac, J.T.R., and Koretsky, A.P. (2012). Thalamocortical Inputs Show Post-Critical-Period Plasticity. *Neuron* 74, 731–742.

Chapter 7

7 General Discussion

7.1 Summary of Main Findings

The collection of studies presented in this thesis were performed to examine the consequences of noise-induced hearing loss on audiovisual processing in higher-order sensory cortices. To accomplish this, electrophysiological recordings and pharmacological manipulations were completed within the rat lateral extrastriate visual cortex (V2L) and/or the dorsal auditory cortex (AuD). Moreover, novel behavioural paradigms were developed for rats to examine the perceptual changes in audiovisual temporal acuity following noise exposure. Ultimately, the work presented herein has provided the first comprehensive investigation into the consequences of noise-induced plasticity within higher-order sensory cortices at the level of single neurons, local cortical microcircuits and audiovisual perception.

7.1.1 Mapping the Sensory Domains within the V2L Cortex in the Rat

Throughout the mammalian cortex there exist functionally-specialized regions that are largely populated by neurons capable of integrating information from more than one sensory modality. As this thesis aimed to investigate the cortical consequences of hearing loss on audiovisual processing and perception, we first needed to profile the response characteristics of single neurons within the V2L cortex of the rat—a region known to be capable of processing both auditory and visual information (Barth et al., 1995; Toldi et al., 1986; Wallace et al., 2004; Xu et al., 2014). Consistent with previous studies (Xu et al., 2014), approximately 50% of the neurons recorded in V2L were found to be classified as multisensory, with more neurons showing bimodal response characteristics than subthreshold multisensory effects. Based the distribution of responses observed in the electrophysiological recordings completed in Chapter 2 and 3, the V2L cortex could be sub-divided into 3 sensory domains: (1) a region which predominantly responds to visual stimuli (i.e., the visual zone of the V2L cortex; V2L-Vz), (2) a region which responds to both auditory and visual stimuli (i.e., the multisensory zone of the V2L cortex; V2L-Mz),

and (3) a region which predominantly responds to auditory stimuli (i.e., the auditory zone of the V2L cortex; V2L-Az). In addition to characterizing the neuronal profile of the V2L cortex, I also examined the laminar profile of each of the regions of the V2L cortex using current source density analyses (Chapter 3). Consistent with the laminar profile of the primary auditory cortex (Happel et al., 2010, 2014; Stolzberg et al., 2012), the V2L cortex displayed current sinks within the supragranular, granular and infragranular layers in response to sensory stimulation. Based on this extensive characterization in normal-hearing animals, I was then able to thoroughly examine the cortical consequences of noise-induced hearing loss within the V2L cortex, as well as the neighbouring AuD cortex (Chapters 2 through 6).

7.1.2 Crossmodal Plasticity in Auditory, Visual and Multisensory Cortical Areas following Noise-Induced Hearing Loss

Complete or partial hearing loss results in an increased responsiveness of neurons in the core auditory cortex of numerous species to visual and/or tactile stimuli (i.e., crossmodal plasticity) (Allman et al., 2009; Campbell and Sharma, 2014; Cardon and Sharma, 2018; Meredith and Allman, 2012; Meredith et al., 2011, 2012). However, at the time I began my thesis work, it was uncertain how adult-onset partial hearing loss affected higher-order cortical areas that normally integrate audiovisual information. To that end, extracellular electrophysiological recordings were performed under anesthesia in noise-exposed rats two weeks post-exposure (0.8-20 kHz at 120 dB SPL for 2 h) and age-matched controls to characterize the nature and extent of crossmodal plasticity in the AuD, an area outside of the auditory core, as well as in the neighbouring V2L, an area known to contribute to audiovisual processing. Computer-generated auditory (noise burst), visual (light flash) and combined audiovisual stimuli were delivered, and the associated spiking activity was used to determine the response profile of each neuron sampled (i.e., unisensory, subthreshold multisensory or bimodal). In both the AuD cortex and the multisensory zone of the V2L cortex, the maximum firing rates were unchanged following noise exposure, and there was a relative increase in the proportion of neurons responsive to visual stimuli, with a concomitant decrease in the number of neurons that were solely responsive to auditory stimuli despite adjusting the sound intensity to account for each rat's hearing threshold.

These neighbouring cortical areas differed, however, in how noise-induced hearing loss affected audiovisual processing; the total proportion of multisensory neurons significantly decreased in the V2L cortex, and dramatically increased in the AuD cortex. Thus, following noise exposure, the cortical area showing the greatest relative degree of multisensory convergence transitioned ventrally, away from the audiovisual area, V2L, toward the predominantly auditory area, AuD. Overall, the collective findings of the present study support the suggestion that crossmodal plasticity induced by adult-onset hearing impairment manifests in higher-order cortical areas as a transition in the functional border of the audiovisual cortex. This work was published in *Hearing Research* (Schormans et al., 2017a).

7.1.3 Adult-Onset Hearing Impairment Induces Layer-Specific Cortical Reorganization: Evidence of Crossmodal Plasticity and Central Gain Enhancement

Adult-onset hearing impairment can lead to hyperactivity in the auditory pathway (i.e., central gain enhancement) (Popelar et al., 1995, 2008; Salvi et al., 2000; Syka and Rybalko, 2000) as well as increased cortical responsiveness to non-auditory stimuli (i.e., crossmodal plasticity) (Meredith and Allman, 2012; Meredith et al., 2012). It was unclear, however, to what extent hearing loss-induced hyperactivity gets relayed beyond the auditory cortex, and thus, whether central gain enhancement competes or coexists with crossmodal plasticity throughout the distinct layers of the audiovisual cortex. To that end, I investigated the effects of partial hearing loss on laminar processing in the auditory, visual and audiovisual cortices of adult rats using extracellular electrophysiological recordings performed two weeks after loud noise exposure. Current source density analyses revealed that central gain enhancement was not relayed to the audiovisual cortex (V2L) and was instead restricted to the granular layer of the higher-order auditory area, AuD. In contrast, crossmodal plasticity was evident across multiple cortical layers within V2L, and also manifested in AuD, consistent with the results of Chapter 2. Surprisingly, despite this coexistence of central gain enhancement and crossmodal plasticity, noise exposure did not disrupt the responsiveness of these neighbouring cortical regions to combined audiovisual stimuli. Overall, we have shown for the first time that adult-onset hearing impairment causes a complex assortment of intramodal and crossmodal changes across the layers of

higher-order sensory cortices. This work was published in *Cerebral Cortex* (Schormans et al., 2018).

7.1.4 Behavioural Plasticity of Audiovisual Perception: Rapid Recalibration of Temporal Sensitivity but not Perceptual Binding following Adult-Onset Hearing Loss

The ability to accurately integrate or bind stimuli from more than one sensory modality is highly dependent on the features of the stimuli, such as their intensity and relative timing (Stein and Meredith, 1993). Previous studies have demonstrated that the ability to perceptually bind stimuli is impaired in various clinical conditions such as autism, dyslexia, schizophrenia, as well as aging (Bedard and Barnett-Cowan, 2016; Brooks et al., 2018; Wallace and Stevenson, 2014). However, it was unclear if adult-onset hearing loss, separate from aging, influences audiovisual temporal acuity—the perceptual ability to accurately judge the relative timing of auditory and visual stimulation. In the present study, rats were trained using appetitive operant conditioning to perform an audiovisual temporal order judgment (TOJ) task or synchrony judgment (SJ) task in order to investigate the nature and extent that audiovisual temporal acuity is affected by adult-onset hearing loss, with a specific focus on the time-course of perceptual changes following loud noise exposure. In my first series of experiments, I found that audiovisual temporal acuity in normal-hearing rats was influenced by sound intensity, such that when a quieter sound was presented, the rats were biased to perceive the audiovisual stimuli as asynchronous (SJ task), or as though the visual stimulus was presented first (TOJ task), consistent with previous studies demonstrating the effect of stimulus intensity on audiovisual perception (Boenke et al., 2009; Krueger Fister et al., 2016; Smith, 1933). Psychophysical testing demonstrated that noise-induced hearing loss did not alter the rats' temporal sensitivity 2-3 weeks post-noise exposure, despite rats showing an initial difficulty in differentiating the temporal order of audiovisual stimuli. Furthermore, consistent with normal-hearing rats, the timing at which the stimuli were perceived as simultaneous (i.e., the point of subjective simultaneity; PSS) remained sensitive to sound intensity following hearing loss. Contrary to the TOJ task, hearing loss resulted in persistent impairments in asynchrony detection during the SJ task, such that a greater proportion of trials were now perceived as synchronous. Moreover, psychophysical testing found that noise-exposed rats had altered

audiovisual synchrony perception, consistent with impaired audiovisual perceptual binding (e.g., an increase in the temporal window of integration on the right side of simultaneity; right TBW). Finally, despite their hearing impairment, rats trained on both behavioural tasks remained sensitive to the intensity of the auditory stimulus presented. Ultimately, my collective results show for the first time that adult-onset hearing loss leads to behavioural plasticity of audiovisual perception, characterized by a rapid recalibration of temporal sensitivity but a persistent impairment in the perceptual binding of audiovisual stimuli. This work was published in *Frontiers in Behavioral Neuroscience* (Schormans and Allman, 2018), following my initial development and validation of these novel behavioural paradigms (Schormans et al., 2017b).

7.1.5 Compensatory Plasticity within the Lateral Extrastriate Visual Cortex Preserves Audiovisual Temporal Processing Following Adult-Onset Hearing Loss

Partial hearing loss can cause neurons in the auditory and audiovisual cortices to increase their responsiveness to visual stimuli (Campbell and Sharma, 2014; Meredith et al., 2012; Chapter 2, 3); however, behavioural studies in hearing-impaired humans and rats have found that the perceptual ability to accurately judge the relative timing of auditory and visual stimuli is largely unaffected (Başkent and Bazo, 2011; Butera et al., 2018; Hay-McCutcheon et al., 2009). To investigate the neurophysiological basis of how audiovisual temporal acuity may be preserved in the presence of hearing loss-induced crossmodal plasticity, I exposed adult rats to loud noise, and two weeks later performed *in vivo* electrophysiological recordings in two neighbouring regions within the lateral extrastriate visual (V2L) cortex; a multisensory zone known to be responsive to audiovisual stimuli (V2L-Mz), and a predominantly-auditory zone (V2L-Az). To examine the cortical layer-specific effects at the level of postsynaptic potentials, a current source density analysis was applied to the local field potential data recorded in response to auditory and visual stimuli presented at various stimulus onset asynchronies (SOAs). As predicted, differential effects were observed in the neighbouring cortical regions post-noise exposure. Most notably, an analysis of the strength of multisensory response interactions revealed that the V2L-Mz lost its sensitivity to the relative timing of the auditory and visual stimuli, due to an increased responsiveness to visual stimulation that produced a prominent audiovisual

response irrespective of the SOA. In contrast, the V2L-Az in noise exposed rats not only became more responsive to visual stimuli, but neurons in this region also inherited the capacity to process audiovisual stimuli with the temporal precision and specificity that was previously restricted to the V2L-Mz. Thus, this study provided the first demonstration that audiovisual temporal processing can be preserved following moderate hearing loss via compensatory plasticity in the higher-order sensory cortices that is ultimately characterized by a functional transition in the cortical region capable of temporal sensitivity. This work has been accepted for publication in *Neural Plasticity* (Schormans et al., In Press).

7.1.6 Noise-Induced Crossmodal Plasticity within the Audiovisual Cortex: Layer-Specific Enhancement, and Rapid Manifestation of Visual-Evoked Activity

Visual deprivation has been shown to result in layer-specific synaptic changes within both the spared and deprived sensory cortices, including a strengthening of thalamocortical synapses within the spared sensory region (Lee and Whitt, 2015; Petrus et al., 2014, 2015). Similarly, noise-induced plasticity in the lateral extrastriate visual cortex (V2L) manifested as layer-specific changes in visual-evoked activity (Chapter 3). However, it was unknown whether this crossmodal plasticity observed in cortical microcircuits manifests solely from intrinsic changes in the cortex itself, or whether partial hearing impairment leads to increased visual responsiveness via a combination of altered intracortical processing as well as thalamocortical plasticity. To that end, laminar electrophysiological recordings were performed in noise exposed rats and age-matched controls before and after pharmacological cortical silencing to examine the thalamocortical contributions of noise-induced crossmodal plasticity within the multisensory zone of the V2L cortex. A detailed current source density (CSD) analysis revealed an enhancement of visual-evoked activity within the granular layer of the multisensory zone of the V2L cortex following noise-induced hearing loss. Moreover, despite adjusting for the degree of hearing loss in each of the noise exposed rats, there was no change in auditory-evoked activity following pharmacological silencing across all cortical layers. In addition to examining the thalamocortical contributions to crossmodal plasticity, we also sought to investigate the working hypothesis that the characteristic increase in visual responsiveness observed following partial hearing loss occurs, at least in part, because of pre-existing connections

that are unmasked following auditory deprivation. To that end, we used an epidural electrode array that spanned the higher-order sensory cortices. An analysis of visual-evoked responses before and immediately after acoustic trauma revealed a rapid emergence of crossmodal plasticity within the higher-order sensory cortices, which was characterized by an increase in visual responsiveness and a decrease in response latency. Interestingly, the rapid onset of crossmodal plasticity appeared to be dependent on the intensity of the stimuli, as the brighter the visual stimulus, the greater the relative change from baseline following hearing loss. Overall, these collective results demonstrate for the first time that noise-induced crossmodal plasticity manifests rapidly following acoustic trauma, and ultimately results in thalamocortical changes consistent with the effects observed previously in the spared cortices following complete sensory deprivation (e.g., deafness). This work is currently being prepared into a manuscript for future submission (Schormans et al., in preparation).

7.2 Experimental Limitations

Collectively, the work presented in this thesis provides an extensive overview of the consequences of noise-induced hearing loss on audiovisual processing and perception; however, it is worth considering a few experimental limitations inherent in these studies.

Firstly, all of the experiments were performed on adult male Sprague-Dawley rats. Although cats and ferrets have been the primary model to explore cortical crossmodal plasticity, I decided to use the rat because it offers various methodological advantages, such as well characterized sensory receptive fields (Montero et al., 1973; Sally and Kelly, 1988; Wallace et al., 2004). Moreover, because the rat cortex is lissencephalic (i.e., no cortical convolutions), this allows for a straightforward examination of the functional transition across multiple sensory areas (Wallace et al., 2004)—a principal finding of the present work. Although the rodent represents an excellent model to examine alterations in sensory processing, there are a few anatomical differences within the visual system of rodents when compared to other mammals (e.g., humans). For example, rats demonstrate no indication of a foveal depression (LeVere, 1978), which, in humans contains only cone photoreceptors, as well as a lack bipolar and ganglion cells which are pushed to one side, which ultimately allows for the sharpest vision (Hendrickson and Yuodelis, 1984; Moyes

and Schulte, 2008). Despite rats lacking a fovea, several studies have revealed that their visual system is capable of detailed vision (Lashley, 1932; LeVere, 1978; Vincent, 1912). In addition to the absence of a fovea, rodents have dichromatic vision in which there are only two types of cone photoceptors within the retina, whereas humans have trichromatic vision (Jacobs, 1993). Although the visual system of the rodent is organized differently than other mammals (e.g., humans), they represent an excellent model for behavioural and electrophysiological research. However, future studies should examine the translatability of rodent research for human clinical populations as the sensory system which is predominantly utilized varies between mammals (e.g., human are more reliant on vision, whereas rodents predominantly utilize audition, somatosensation and/or olfaction). Thus, future studies are needed to investigate whether the degree of deprivation-induced plasticity is dependent on which sense is lost (i.e., if a most important sense is lost, does the sense which is not as well-developed compensate more by becoming more dominant?).

At the time of commencing this thesis, I had elected to study only male rats due to the known effects of estrogen on auditory brainstem responses (ABR), such as the increase in the latency of wave III and wave V that occurs in the high estrogen state at the mid-cycle phase of the menstrual cycle (Elkind-Hirsch et al., 1992), and the increase in wave V latencies and shorter wave I to wave V intervals in females (Watson, 1996). Despite these sex differences observed in humans, it is worth noting that a recent study on rats from our lab revealed that there were no differences in hearing thresholds between sexes, as well as no differences in the amplitude and latency of the ABR waves (Scott et al., 2018). Ultimately, it will be important for future studies investigating cortical crossmodal plasticity in animal models use both males and females in order to provide an accurate representation of the consequences of hearing loss on the entire population.

Additionally, the stimulus used to assess general hearing sensitivity was a 0.1 ms click stimulus. This stimulus was selected because it activates a large range of the cochlea (i.e., approximately 1-10 kHz), and provides consistent waveforms in order to assess the amplitude and latency of each of the ABR waves. However, because a broadband noise was used during the electrophysiological recordings (1-32 kHz) and for the noise exposure (0.8-20 kHz), future studies should consider assessing hearing sensitivity using a noise

burst stimulus to determine the change in hearing sensitivity with respect to the frequencies presented during the noise exposure.

Lastly, in Chapter 6, I used a previously-established cortical silencing technique to dissociate the intracortical and thalamocortical components of cortical stimulus-evoked excitation (Happel et al., 2010; Liu et al., 2007; Yamauchi et al., 2000). Electrophysiological studies have demonstrated that the concentrations used in the present work exclusively influenced intracortical potentials (Edeline et al., 2002; Kaur et al., 2004), as well as block psychophysical detection of pure tones in rats (Talwar et al., 2001). Furthermore, using this technique, synaptic activities driven by intracortical activity should be silenced completely following the application of muscimol, whereas bottom-up thalamocortical input should not be blocked (Kaur et al., 2004). However, while bottom-up processing may be preserved, long-range intracortical afferents such as contralateral projections may also be preserved. Despite this possibility, several studies have demonstrated that the primary auditory cortex, as well as multisensory cortices receive a characteristic feedforward pattern of innervation, with afferent thalamocortical projections terminating in the granular layer (i.e. layers III/IV) and intracortical connections projecting to supragranular and infragranular layers (Laramée et al., 2011, 2013; Olsen and Witter, 2016; Sakata and Harris, 2009; Schroeder and Foxe, 2002; Schroeder et al., 1998). Therefore, consistent with the analyses completed in Chapter 6, previous studies restricted the analyses to the granular layer to exclusively examine changes in the thalamocortical projections (Happel et al., 2010, 2014). Despite these advanced experimental and analytical methods, future studies are needed in order to further examine thalamocortical plasticity following noise-induced hearing loss across the sensory cortices.

7.3 Future Directions

Based on the results of Chapters 2 through 6, there are a few questions that have emerged which warrant future consideration, such as the effect of perceptual training on audiovisual temporal acuity, and the role of cortical inhibition on crossmodal plasticity (both discussed below).

7.3.1 Effect of Perceptual Training on Temporal Perception following Noise-Induced Hearing Loss

The behavioural results of the TOJ task from Chapter 4 revealed that noise-induced hearing loss resulted in an initial impairment in the rats' perceptual ability to accurately identify the temporal order of audiovisual stimuli. More specifically, there was a decrease in performance on auditory-first trials following noise exposure, which rapidly improved and ultimately reached post-sham performance after 3 days of training. Based on this initial impairment and rapid recalibration, it is reasonable to question whether training played a role in the preservation (restoration) of audiovisual temporal perception. Therefore, future studies should consider the effect of training on temporal perception in hearing-impaired subjects, especially since the temporal binding window (TBW) has been shown to improve following perceptual training (De Niear et al., 2016, 2018; Powers et al., 2009). Moreover, exposure to asynchronous stimuli presented prior to psychophysical testing has been shown to alter ones' perception of audiovisual stimuli (Fujisaki et al., 2004; Navarra et al., 2005). Overall, based on the results of Chapter 4 and the results of perceptual training studies, it is reasonable to predict that following noise-induced hearing loss, rats will show an impairment in their ability to perceive the simultaneity of audiovisual stimuli if no training is completed prior to experimental testing.

7.3.2 Is a Loss of Inhibition Sufficient to Induce Crossmodal Plasticity?

Based on the rapid manifestation of crossmodal plasticity observed in Chapter 6, it is reasonable to suggest that the plasticity observed in the higher-order sensory cortices may be due to an unmasking of existing inputs (Merabet et al., 2008; Rauschecker, 1995; Singh et al., 2018) and/or alterations in GABAergic inhibition (Yang et al., 2012). Changes in the expression of GABA markers have been observed following hearing loss within the auditory pathway (Browne et al., 2012; Burianova et al., 2009; Kotak et al., 2008; Sarro et al., 2008). Because the auditory cortex has direct connections with the primary visual cortex as well as the V2L cortex (Henschke et al., 2015; Iurilli et al., 2012; Laramée et al., 2011), I predict that the loss of inhibition within the auditory cortex may underlie the enhanced visual responsiveness observed within the higher-order sensory cortices.

Ultimately, to investigate this hypothesis, future studies are needed to determine whether a loss of inhibition within the auditory cortex is sufficient to induce crossmodal plasticity.

7.4 Conclusion

Overall, the work in this thesis characterized sensory responsiveness across the cortical micro-circuit and at the level of single neurons within the V2L cortex of noise-exposed rats and age-matched controls. These studies demonstrated that cortical plasticity occurs within higher-order sensory cortices, such as the V2L cortex; an area capable of processing both auditory and visual stimuli in normal-hearing animals. Following noise-induced hearing loss, crossmodal plasticity was observed within the V2L cortex, which was characterized by an increase in the proportion of visual neurons (Chapter 2), as well as an increase in visual input across most of the cortical layers (Chapter 3). Despite this increase in visual responsiveness and loss of temporal sensitivity in the multisensory zone of V2L following noise exposure, the neighbouring, once-predominantly auditory region (i.e., V2L-Az) inherited the temporal profile consistent the V2L-Mz of normal-hearing rats; findings which indicate a shift in the cortical region with the greatest level of multisensory convergence (Chapter 5). Furthermore, we revealed that the crossmodal plasticity observed within the V2L cortex was not restricted to intrinsic changes as there was also an increase in visual-evoked thalamocortical input to the granular layer (Chapter 6). In addition to characterizing the V2L cortex, the dorsal auditory cortex (AuD) was also examined in normal-hearing and noise exposed rats. Following noise exposure, the AuD cortex, which responded predominantly to auditory stimuli in controls, now demonstrated an increase in audiovisual responsiveness (Chapter 2) as well as central gain enhancement (Chapter 3); evidence of a complex assortment of crossmodal and intramodal plasticity induced by adult-onset hearing loss. Overall, these studies demonstrate for the first time that there is a differential effect of noise-induced hearing loss on higher-order sensory cortices. Despite the extensive cortical plasticity throughout these higher-order sensory regions, audiovisual temporal acuity was relatively preserved following noise-induced hearing loss (Chapter 4). Taken together, these studies provide new insight into the cortical consequences of excessive noise exposure; an all-too-common recreational and workplace hazard which permanently damages the hearing of millions of people every year.

7.5 References

Allman, B.L., Keniston, L.P., and Meredith, M.A. (2009). Adult deafness induces somatosensory conversion of ferret auditory cortex. *Proc. Natl. Acad. Sci.* 106, 5925–5930.

Barth, D.S., Goldberg, N., Brett, B., and Di, S. (1995). The spatiotemporal organization of auditory, visual, and auditory-visual evoked potentials in rat cortex. *Brain Res*. 678, 177–190.

Başkent, D., and Bazo, D. (2011). Audiovisual asynchrony detection and speech intelligibility in noise with moderate to severe sensorineural hearing impairment. *Ear Hear*. 32, 582–592.

Bedard, G., and Barnett-Cowan, M. (2016). Impaired timing of audiovisual events in the elderly. *Exp. Brain Res*. 234, 331–340.

Boenke, L.T., Deliano, M., and Ohl, F.W. (2009). Stimulus duration influences perceived simultaneity in audiovisual temporal-order judgment. *Exp. Brain Res*. 198, 233–244.

Brooks, C.J., Chan, Y.M., Anderson, A.J., and McKendrick, A.M. (2018). Audiovisual Temporal Perception in Aging: The Role of Multisensory Integration and Age-Related Sensory Loss. *Front. Hum. Neurosci*. 12.

Browne, C.J., Morley, J.W., and Parsons, C.H. (2012). Tracking the Expression of Excitatory and Inhibitory Neurotransmission-Related Proteins and Neuroplasticity Markers after Noise Induced Hearing Loss. *PLOS ONE* 7, e33272.

Burianova, J., Ouda, L., Profant, O., and Syka, J. (2009). Age-related changes in GAD levels in the central auditory system of the rat. *Exp. Gerontol.* 44, 161–169.

Butera, I.M., Stevenson, R.A., Mangus, B.D., Woynaroski, T.G., Gifford, R.H., and Wallace, M.T. (2018). Audiovisual Temporal Processing in Postlingually Deafened Adults with Cochlear Implants. *Sci. Rep.* 8, 11345.

Campbell, J., and Sharma, A. (2014). Cross-Modal Re-Organization in Adults with Early Stage Hearing Loss. *PLOS ONE* 9, e90594.

Cardon, G., and Sharma, A. (2018). Somatosensory Cross-Modal Reorganization in Adults With Age-Related, Early-Stage Hearing Loss. *Front. Hum. Neurosci.* 12.

De Niear, M.A., Koo, B., and Wallace, M.T. (2016). Multisensory perceptual learning is dependent upon task difficulty. *Exp. Brain Res.* 234, 3269–3277.

De Niear, M.A., Gupta, P.B., Baum, S.H., and Wallace, M.T. (2018). Perceptual training enhances temporal acuity for multisensory speech. *Neurobiol. Learn. Mem.* 147, 9–17.

Edeline, J.-M., Hars, B., Hennevin, E., and Cotillon, N. (2002). Muscimol diffusion after intracerebral microinjections: a reevaluation based on electrophysiological and autoradiographic quantifications. *Neurobiol. Learn. Mem.* 78, 100–124.

Elkind-Hirsch, K.E., Stoner, W.R., Stach, B.A., and Jerger, J.F. (1992). Estrogen influences auditory brainstem responses during the normal menstrual cycle - ScienceDirect. *Hear. Res*. 60, 143–148.

Fujisaki, W., Shimojo, S., Kashino, M., and Nishida, S. (2004). Recalibration of audiovisual simultaneity. *Nat. Neurosci.* 7, 773–778.

Happel, M.F.K., Jeschke, M., and Ohl, F.W. (2010). Spectral Integration in Primary Auditory Cortex Attributable to Temporally Precise Convergence of Thalamocortical and Intracortical Input. *J. Neurosci.* 30, 11114–11127.

Happel, M.F.K., Deliano, M., Handschuh, J., and Ohl, F.W. (2014). Dopamine-modulated recurrent corticoefferent feedback in primary sensory cortex promotes detection of behaviorally relevant stimuli. *J. Neurosci.* 34, 1234–1247.

Hendrickson, A.E., and Yuodelis, C. (1984). The Morphological Development of the Human Fovea. *Ophthalmology 91*, 603–612.

Hay-McCutcheon, M.J., Pisoni, D.B., and Hunt, K.K. (2009). Audiovisual Asynchrony Detection and Speech Perception in Hearing-Impaired Listeners with Cochlear Implants: A Preliminary Analysis. *Int. J. Audiol.* 48, 321–333.

Henschke, J.U., Noesselt, T., Scheich, H., and Budinger, E. (2015). Possible anatomical pathways for short-latency multisensory integration processes in primary sensory cortices. *Brain Struct. Funct.* 220, 955–977.

Iurilli, G., Ghezzi, D., Olcese, U., Lassi, G., Nazzaro, C., Tonini, R., Tucci, V., Benfenati, F., and Medini, P. (2012). Sound-Driven Synaptic Inhibition in Primary Visual Cortex. *Neuron* 73, 814–828.

Jacobs, G.H. (1993). The Distribution and Nature of Colour Vision Among the Mammals. *Biol. Rev. 68*, 413–471.

Kaur, S., Lazar, R., and Metherate, R. (2004). Intracortical Pathways Determine Breadth of Subthreshold Frequency Receptive Fields in Primary Auditory Cortex. *J. Neurophysiol.* 91, 2551–2567.

Kotak, V.C., Takesian, A.E., and Sanes, D.H. (2008). Hearing Loss Prevents the Maturation of GABAergic Transmission in the Auditory Cortex. *Cereb. Cortex* 18, 2098–2108.

Krueger Fister, J., Stevenson, R.A., Nidiffer, A.R., Barnett, Z.P., and Wallace, M.T. (2016). Stimulus intensity modulates multisensory temporal processing. *Neuropsychologia* 88, 92–100.

Laramée, M.E., Kurotani, T., Rockland, K.S., Bronchti, G., and Boire, D. (2011). Indirect pathway between the primary auditory and visual cortices through layer V pyramidal neurons in V2L in mouse and the effects of bilateral enucleation. *Eur. J. Neurosci.* 34, 65–78.

Laramée, M.E., Rockland, K.S., Prince, S., Bronchti, G., and Boire, D. (2013). Principal component and cluster analysis of layer V pyramidal cells in visual and non-visual cortical areas projecting to the primary visual cortex of the mouse. *Cereb. Cortex* N. Y. N 1991 23, 714–728.

Lashley, K.S. (1932). The mechanism of vision. V. The structure and image-forming power of the rat's eye. *J. Comp. Psychol. 13*, 173–200.

Lee, H.-K., and Whitt, J.L. (2015). Cross-modal synaptic plasticity in adult primary sensory cortices. *Curr. Opin. Neurobiol.* 35, 119–126.

LeVere, T.E. (1978). The primary visual system of the rat: A primer of its anatomy. *Physiol. Psychol. 6*, 142–169.

Liu, B., Wu, G.K., Arbuckle, R., Tao, H.W., and Zhang, L.I. (2007). Defining cortical frequency tuning with recurrent excitatory circuitry. *Nat. Neurosci*. 10, 1594–1600.

Merabet, L.B., Hamilton, R., Schlaug, G., Swisher, J.D., Kiriakopoulos, E.T., Pitskel, N.B., Kauffman, T., and Pascual-Leone, A. (2008). Rapid and Reversible Recruitment of Early Visual Cortex for Touch. *PLOS ONE* 3, e3046.

Meredith, M.A., and Allman, B.L. (2012). Early Hearing-Impairment Results in Crossmodal Reorganization of Ferret Core Auditory Cortex. *Neural Plast*. 2012, e601591.

Meredith, M.A., Kryklywy, J., McMillan, A.J., Malhotra, S., Lum-Tai, R., and Lomber, S.G. (2011). Crossmodal reorganization in the early deaf switches sensory, but not behavioral roles of auditory cortex. *Proc. Natl. Acad. Sci.* 108, 8856–8861.

Meredith, M.A., Keniston, L.P., and Allman, B.L. (2012). Multisensory dysfunction accompanies crossmodal plasticity following adult hearing impairment. *Neuroscience* 214, 136–148.

Montero, V.M., Rojas, A., and Torrealba, F. (1973). Retinotopic organization of striate and peristriate visual cortex in the albino rat. *Brain Res.* 53, 197–201.

Moyes, C., and Schulte, P. (2008). Chapter 6- Sensory Systems. In Principles of Animal Physiology, (San Francisco, CA: Pearson Education Inc.), pp. 248–305.

Navarra, J., Vatakis, A., Zampini, M., Soto-Faraco, S., Humphreys, W., and Spence, C. (2005). Exposure to asynchronous audiovisual speech extends the temporal window for audiovisual integration. *Cogn. Brain Res*. 25, 499–507.

Olsen, G.M., and Witter, M.P. (2016). Posterior parietal cortex of the rat: Architectural delineation and thalamic differentiation. *J. Comp. Neurol*. 524:18, 3774-3809

Petrus, E., Isaiah, A., Jones, A.P., Li, D., Wang, H., Lee, H.-K., and Kanold, P.O. (2014). Crossmodal Induction of Thalamocortical Potentiation Leads to Enhanced Information Processing in the Auditory Cortex. *Neuron* 81, 664–673.

Petrus, E., Rodriguez, G., Patterson, R., Connor, B., Kanold, P.O., and Lee, H.-K. (2015). Vision Loss Shifts the Balance of Feedforward and Intracortical Circuits in Opposite Directions in Mouse Primary Auditory and Visual Cortices. *J. Neurosci.* 35, 8790–8801.

Popelar, J., Hartmann, R., Syka, J., and Klinke, R. (1995). Middle latency responses to acoustical and electrical stimulation of the cochlea in cats. *Hear. Res.* 92, 63–77.

Popelar, J., Grecova, J., Rybalko, N., and Syka, J. (2008). Comparison of noise-induced changes of auditory brainstem and middle latency response amplitudes in rats. *Hear. Res*. 245, 82–91.

Powers, A.R., Hillock, A.R., and Wallace, M.T. (2009). Perceptual Training Narrows the Temporal Window of Multisensory Binding. *J. Neurosci*. 29, 12265–12274.

Rauschecker, J.P. (1995). Compensatory plasticity and sensory substitution in the cerebral cortex. *Trends Neurosci*. 18, 36–43.

Sakata, S., and Harris, K.D. (2009). Laminar Structure of Spontaneous and Sensory-Evoked Population Activity in Auditory Cortex. *Neuron* 64, 404–418.

Sally, S.L., and Kelly, J.B. (1988). Organization of auditory cortex in the albino rat: sound frequency. *J. Neurophysiol.* 59, 1627–1638.

Salvi, R.J., Wang, J., and Ding, D. (2000). Auditory plasticity and hyperactivity following cochlear damage. *Hear. Res*. 147, 261–274.

Sarro, E.C., Kotak, V.C., Sanes, D.H., and Aoki, C. (2008). Hearing Loss Alters the Subcellular Distribution of Presynaptic GAD and Postsynaptic GABAA Receptors in the Auditory Cortex. *Cereb. Cortex* 18, 2855–2867.

Schormans, A.L., and Allman, B.L. (2018). Behavioral Plasticity of Audiovisual Perception: Rapid Recalibration of Temporal Sensitivity but Not Perceptual Binding Following Adult-Onset Hearing Loss. *Front. Behav. Neurosci.* 12.

Schormans, A.L., Typlt, M., and Allman, B.L. (2017a). Crossmodal plasticity in auditory, visual and multisensory cortical areas following noise-induced hearing loss in adulthood. *Hear. Res.* 343, 92–107.

Schormans, A.L., Scott, K.E., Vo, A.M.Q., Tyker, A., Typlt, M., Stolzberg, D., and Allman, B.L. (2017b). Audiovisual Temporal Processing and Synchrony Perception in the Rat. *Front. Behav. Neurosci*. 10.

Schormans, A.L., Typlt, M., and Allman, B.L. (2018). Adult-Onset Hearing Impairment Induces Layer-Specific Cortical Reorganization: Evidence of Crossmodal Plasticity and Central Gain Enhancement. *Cereb. Cortex*, bhy067

Schroeder, C.E., and Foxe, J.J. (2002). The timing and laminar profile of converging inputs to multisensory areas of the macaque neocortex. *Cogn. Brain Res*. 14, 187–198.

Schroeder, C.E., Mehta, A.D., and Givre, S.J. (1998). A spatiotemporal profile of visual system activation revealed by current source density analysis in the awake macaque. *Cereb. Cortex* 8, 575–592.

Scott, K.E., Schormans, A.L., Pacoli, K.Y., Oliveira, C.D., Allman, B.L., and Schmid, S. (2018). Altered Auditory Processing, Filtering, and Reactivity in the Cntnap2 Knock-Out Rat Model for Neurodevelopmental Disorders. *J. Neurosci*. 38, 8588–8604.

Singh, A.K., Phillips, F., Merabet, L.B., and Sinha, P. (2018). Why Does the Cortex Reorganize after Sensory Loss? *Trends Cogn. Sci.* 22, 569–582.

Smith, W.F. (1933). The relative quickness of visual and auditory perception. *J. Exp. Psychol.* 16, 239–257.

Stein, B.E., and Meredith, M.A. (1993). The merging of the senses (Cambridge, MA, US: The MIT Press).

Stolzberg, D., Chrostowski, M., Salvi, R.J., and Allman, B.L. (2012). Intracortical circuits amplify sound-evoked activity in primary auditory cortex following systemic injection of salicylate in the rat. *J. Neurophysiol.* 108, 200–214.

Syka, J., and Rybalko, N. (2000). Threshold shifts and enhancement of cortical evoked responses after noise exposure in rats. *Hear. Res*. 139, 59–68.

Talwar, S.K., Musial, P.G., and Gerstein, G.L. (2001). Role of Mammalian Auditory Cortex in the Perception of Elementary Sound Properties. *J. Neurophysiol.* 85, 2350–2358.

Toldi, J., Fehér, O., and Wolff, J.R. (1986). Sensory interactive zones in the rat cerebral cortex. *Neuroscience* 18, 461–465.

Vincent, S.B. (1912). The mammalian eye. *J. Anim. Behav. 2*, 249–255.

Wallace, M.T., and Stevenson, R.A. (2014). The construct of the multisensory temporal binding window and its dysregulation in developmental disabilities. *Neuropsychologia* 64, 105–123.

Wallace, M.T., Ramachandran, R., and Stein, B.E. (2004). A revised view of sensory cortical parcellation. *Proc. Natl. Acad. Sci.* 101, 2167–2172.

Watson, D.R. (1996). The Effects of Cochlear Hearing Loss, Age and Sex on the Auditory Brainstem Response. *Audiology* 35, 246–258.

Xu, J., Sun, X., Zhou, X., Zhang, J., and Yu, L. (2014). The cortical distribution of multisensory neurons was modulated by multisensory experience. *Neuroscience* 272, 1–9.

Yamauchi, T., Hori, T., and Takahashi, T. (2000). Presynaptic inhibition by muscimol through GABAB receptors. *Eur. J. Neurosci.* 12, 3433–3436.

Yang, S., Su, W., and Bao, S. (2012). Long-term, but not transient, threshold shifts alter the morphology and increase the excitability of cortical pyramidal neurons. *J. Neurophysiol.* 108, 1567–1574.

Appendices

Appendix A: Development and validation of a rodent model of audiovisual temporal and synchrony perception

This work was published in *Frontiers in Behavioral Neuroscience* in January of 2017 and provides a detailed description of the training protocol for both audiovisual temporal order judgment (TOJ) and synchrony judgment (SJ) tasks.

AUDIOVISUAL TEMPORAL PROCESSING AND SYNCHRONY PERCEPTION IN THE RAT

ABSTRACT:

Extensive research on humans has improved our understanding of how the brain integrates information from our different senses, and has begun to uncover the brain regions and large-scale neural activity that contributes to an observer's ability to perceive the relative timing of auditory and visual stimuli. In the present study, we developed the first behavioural tasks to assess the perception of audiovisual temporal synchrony in rats. Modeled after the parameters used in human studies, separate groups of rats were trained to perform 1) a simultaneity judgement task in which they reported whether audiovisual stimuli at various stimulus onset asynchronies (SOAs) were presented simultaneously or not, and 2) a temporal order judgement task in which they reported whether they perceived the auditory or visual stimulus to have been presented first. Furthermore, using *in vivo* electrophysiological recordings in the lateral extrastriate visual (V2L) cortex of anesthetized rats, we performed the first investigation of how neurons in the rat multisensory cortex integrate audiovisual stimuli presented at different SOAs. As predicted, rats (n=7) trained to perform the simultaneity judgement task could accurately (~80%) identify synchronous versus asynchronous (200 ms SOA) trials. Moreover, the rats judged trials at 10 ms SOA to be synchronous, whereas the majority (~70%) of trials at 100 ms SOA were perceived to be asynchronous. During the temporal order judgement task, rats (n=7) perceived the synchronous audiovisual stimuli to be "visual first" for ~52% of the trials, and calculation of the smallest timing interval between the auditory and visual

stimuli that could be detected in each rat (i.e., the *just noticeable difference*) ranged from 77 to 122 ms. Neurons in the rat V2L cortex were sensitive to the timing of audiovisual stimuli, such that spiking activity was greatest during trials when the visual stimulus preceded the auditory by 20 to 40 ms. Ultimately, given that our behavioural and electrophysiological results were consistent with studies conducted on human participants and previous recordings made in multisensory brain regions of different species, we suggest that the rat represents an effective model for studying audiovisual temporal synchrony at both the neuronal and perceptual level.

1. INTRODUCTION:

Within the mammalian brain, there exist functionally-specialized regions, such as the superior colliculus and higher-order cortical areas, which are populated by neurons capable of merging information from more than one sensory modality (e.g., hearing and vision) (Allman, 2009; Barth et al., 1995; Meredith and Stein, 1986; Stein and Meredith, 1993; Stein and Stanford, 2008; Wallace et al., 2004; Xu et al., 2014; Allman et al., 2008a; Schroeder and Foxe, 2002; Ghazanfar and Schroeder, 2006). As shown in numerous species (for review see Stein and Meredith, 1993), the successful integration of auditory and visual information allows for behavioural improvements in the detection, localization and identification of the stimuli (Gleiss and Kayser, 2012; Hershenson, 1962; Hirokawa et al., 2008; Raposo et al., 2012; Siemann et al., 2014). For example, consistent with studies on humans (Calvert et al., 2000; Diederich and Colonius, 2004), rats are able to more quickly detect auditory and visual stimuli when the cues are presented in combination compared to when either cue is presented alone (Gleiss and Kayser, 2012; Hirokawa et al., 2008). Related to this, the lateral extrastriate visual cortex (V2L) in rats has been identified as a cortical area mediating the improved reaction time to detect audiovisual stimuli, as pharmacological deactivation of this region results in a loss of multisensory facilitation (Hirokawa et al., 2008).

In addition to studying various detection and localization tasks, psychophysical testing in humans has investigated the perceived temporal synchrony of audiovisual stimuli. Classically, two perceptual tasks have been used to probe an observer's ability to discern audiovisual temporal synchrony. In the temporal order judgement task, auditory and visual

stimuli are presented at various stimulus onset asynchronies (SOAs), and the observers must judge the relative timing of the stimuli by stating which one came first or which came second (Binder, 2015; Keetels and Vroomen, 2012; Spence et al., 2001; Stevenson et al., 2014; Stone et al., 2001; Vatakis et al., 2008b; Zampini et al., 2005a). The simultaneity judgement task also includes the presentation of audiovisual stimuli at various SOAs; however, the observers now judge whether they perceived the stimuli to have been presented at the same moment in time or not (Boenke et al., 2009; Keetels and Vroomen, 2012; Navarra et al., 2005; Spence et al., 2003; Vatakis et al., 2008b, 2007; Zampini et al., 2003). Performance in these tasks can be used to calculate (1) the observer's point of subjective simultaneity (PSS), which describes the actual timing of the audiovisual stimuli when the observer is most unsure of the temporal order, and; (2) the observer's just noticeable difference (JND), which represents the smallest interval between the separately presented auditory and visual stimuli that can be detected reliably (Keetels and Vroomen, 2012; Vatakis et al., 2008a; Vroomen and Stekelenburg, 2011).

In recent years, numerous studies have contributed to our understanding of the factors that influence one's perception of audiovisual temporal synchrony. For example, it is well established that the PSS and JND calculated from simultaneity- and temporal order judgement tasks can be significantly affected by a variety of experimental parameters, including the stimulus intensity (Boenke et al., 2009; Krueger Fister et al., 2016), stimulus duration (Boenke et al., 2009) and overall task conditions (Stevenson and Wallace, 2013; Zampini et al., 2005a, 2005b) as well as one's prior exposure to asynchronous stimuli (Fujisaki et al., 2004; Navarra et al., 2005; Vatakis et al., 2008b, 2007). At the same time, functional neuroimaging and electroencephalography studies have offered insight into the brain regions activated during audiovisual temporal synchrony tasks, as well as large-scale neural activity associated with the perceptual judgements (Binder, 2015; Bushara et al., 2001; Calvert and Thesen, 2004). Moreover, studies on various clinical populations (e.g., ASD, dyslexia and schizophrenia, for review see Wallace and Stevenson, 2014) have begun to identify the associated deficits that exist in audiovisual processing, as well as differences in brain activation during task performance. Despite the wealth of information gleaned from human studies, important issues remain to be fully resolved, such as the specific response properties of single neurons and their local circuits that contribute to the

perception of temporal synchrony, as well as the cellular mechanisms, neuronal responses and network properties underlying the altered perception in clinical populations. Given the considerable advances that have been made in neuron-specific activation/silencing using opto- and chemogenetics as well as the emergence of transgenic rats that model aspects of human neuropsychiatric disorders, it is reasonable to suggest that such experimental tools may help to reveal the neural substrates underlying the perception of synchrony between the senses. At present, however, a considerable hurdle exists as we are not aware of any studies that have established behavioural tasks in rats that probe for the perception of audiovisual temporal synchrony.

In the present study, we endeavored to design and implement the first simultaneity- and temporal order judgement tasks in rats. Using appetitive operant conditioning, we trained separate groups of adult rats to (1) differentiate whether audiovisual stimuli at various SOAs were presented synchronously or not (i.e., simultaneity judgement task) or (2) determine the temporal order of audiovisual stimuli presented at various SOAs (i.e., temporal order judgement task). Ultimately, psychophysical curves were generated for both of the behavioural paradigms, and the PSS and JND were calculated for the temporal order judgement task. Furthermore, prior to commencing the design of the novel behavioural tasks, we first performed *in vivo* electrophysiological recordings in the V2L cortex of anesthetized rats to assess the response characteristics of the constituent neurons to audiovisual stimuli presented at SOAs which are commonly used in human psychophysical studies. Not only did we intend to use these data to help determine which audiovisual SOAs would be included in the novel behavioural tasks, but to our knowledge, this would be the first investigation of how neurons in the rat multisensory cortex integrate audiovisual stimuli presented at different temporal onsets.

2.0 METHODS:

The present study included three experimental series that each used a separate group of adult male Sprague-Dawley rats (Charles River Laboratories, Inc., Wilmington, MA). Rats were housed on a 12-hour light-dark cycle with food and water ad libitum. All experimental procedures were approved by the University of Western Ontario Animal Care and Use

Committee and were in accordance with the guidelines established by the Canadian Council of Animal Care.

2.1 Experiment 1- Electrophysiological Recordings in the Lateral Extrastriate Visual Cortex (V2L)

2.1.1 Surgical Procedure:

Adult male rats (n = 7; body mass: 420 ± 11.8 g) were anaesthetized with ketamine (80 mg/kg; IP) and xylazine (5 mg/kg; IP) and fixed in a stereotaxic frame with blunt ear bars. The absence of a pedal withdrawal reflex was an indication of anesthetic depth, and supplemental doses of ketamine/xylazine were administered IM as needed. A midline incision was made in the skin of the scalp, and the tissue overlying the dorsal aspect of the skull was removed. A stainless-steel screw was inserted in the left frontal bone to serve as an anchor for a headpost and as an electrical ground. A stereotaxic micromanipulator was used to measure 5.5 mm caudal to bregma, which represents an approximate rostral-caudal location of the lateral extrastriate visual cortex (V2L) (Hirokawa et al., 2008; Schormans et al., 2016; Wallace et al., 2004; Xu et al., 2014), and a mark was made on the skull for later drilling. A craniotomy (2.5 x 3 mm; 4 – 7 mm caudal to bregma) was performed in the left parietal bone to expose the cortex. Following the surgical procedure, the right ear bar was removed to provide free-field auditory stimulation of the right ear during electrophysiological recordings in the contralateral cortex. The rat was held in position throughout the entire duration of the experiment within the stereotaxic frame using the left ear bar and the headpost.

2.1.2 Electrophysiological Recordings:

Extracellular electrophysiological recordings were performed in a dark, double-walled, sound-attenuating chamber (MDL 6060 ENV, WhisperRoom Inc., Knoxville, TN, USA). Neural signals were acquired using a 32-channel microelectrode array which consisted of a single shank with 32 recordings sites equally-spaced, spanning 1.5 mm in length (A1x32-10mm-50-177-A32; NeuroNexus Technologies, Ann Arbor, MI, USA). The microelectrode array was connected to a high-impedance headstage (NN32AC; Tucker-Davis Technologies, Alachua, FL, USA), and the electrophysiological signal was preamplified and digitized (two RA16SD Medusa preamplifiers; TDT), and sent to a RZ5

processing module via a fiber optic cable. The neuronal activity was detected online (digitally sampled at 25 kHz and bandpass filtered online at 300-3000 Hz) using a voltage threshold for spike detection of three standard deviations above the noise floor. The timing of the detected spikes and their associated waveforms were stored for offline analyses.

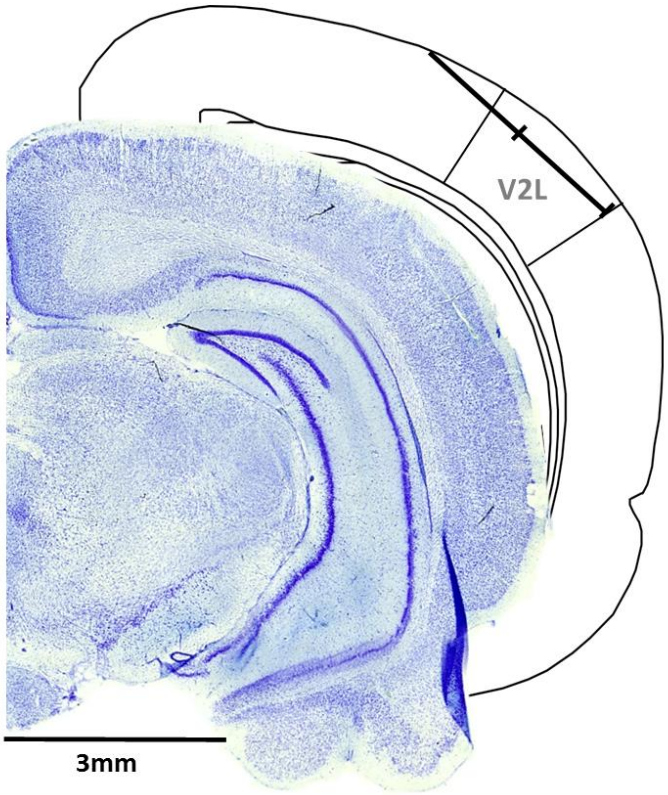

Figure 1. Representative recording penetration in the lateral extrastriate visual (V2L) cortex.

A schematic of the recording location from the pial surface (1.75 to 3.25mm) when the microelectrode array was advanced into the cortex at 5.5mm caudal to bregma using a dorsomedial-to-ventrolateral approach (40° angle). As shown in the coronal sections (Paxinos & Watson, 2007), the electrode array was positioned within the V2L cortex and was typically located within supragranular and granular layers.

A single penetration was completed in each experiment, whereby the microelectrode array was inserted in the cortex through a small slit in the dura using a dorsomedial-to-ventrolateral approach (40° angle), with the array entering the cortex 5.5 mm caudal to bregma and approximately 1 mm medial to the temporal ridge of the skull. The array was inserted into the cortex using a stereotaxic micromanipulator (World Precision Instruments, Sarasota, FL, USA) at a 40° angle until all recording sites were within the cortex (depth of 1.5 mm) based on visual confirmation using a surgical microscope equipped with a high-resolution camera. Once the electrode sites were no longer visible, a hydraulic microdrive (FHC, Bowdoinham, ME, USA) was used to slowly advance the array into the cortex until the 32 recording sites spanned a distance of 1.75 – 3.25 mm from the initial entry in the cortex. At this location, the recording sites were located within the lateral extrastriate visual cortex (V2L), a multisensory region responsive to auditory and visual stimuli (Barth et al., 1995; Hirokawa et al., 2008; Schormans et al., 2016; Toldi et al., 1986; Wallace et al., 2004; Xu et al., 2014) (Fig. 1).

2.1.3 Audiovisual Stimulation Paradigms:

Auditory stimuli consisted 50 ms noise bursts (1-32 kHz) from a speaker (MF1, TDT) positioned approximately 10 cm from the right pinna on a 30° angle from midline (i.e., speaker was positioned in the space contralateral to the electrode position). For each rat, the auditory stimulus (52.8 ± 1.5 dB sound pressure level, SPL) was presented at 30 dB above its threshold to a click (0.1 ms) stimulus (22.8 ± 1.5 dB SPL) as determined by an initial assessment of hearing sensitivity using our previously described auditory brainstem response paradigm (Schormans et al., 2016). Briefly, rats were anaesthetized with ketamine and xylazine (IP) and subdermal electrodes were positioned at the vertex, over the right mastoid and on the back. The auditory stimulus consisted of a click (0.1 ms) which was presented at decreasing intensities from 90 to 10 dB SPL, in 10 dB SPL steps. Near threshold, the stimulus intensity was then presented at 5 dB SPL steps, and ABR threshold was determined using the criteria of just noticeable deflection of the averaged electrical activity within the 10 ms window (Popelar et al., 2008). The sound stimuli were calibrated using a ¼-inch microphone (2530; Larson Davis, Depew, NY, USA) and preamplifier (2221; Larson Davis) and custom Matlab software (The MathWorks, Natick, MA, USA). The visual stimulus consisted of a 50 ms flash of light (11 lux; centered on the eye) from a

single LED (diameter: 0.8 cm) positioned adjacent the speaker. Based on pilot recordings and consistent with our earlier work (Schormans et al., 2016), a flash of light at 11 lux was chosen because it evoked a consistent, yet submaximal level of neuronal responsiveness, thereby allowing for the potential to observe enhanced multisensory responses during combined stimulus conditions (i.e., inverse effectiveness; Stein and Meredith, 1993).

Computer-triggered auditory and visual stimuli were presented alone or in combination using a TDT RZ6 processing module (100 kHz sampling rate) and custom Matlab software. Auditory and visual stimuli were presented alone in order to determine the sensory responsiveness of each of the multi-unit (MU) clusters sampled during the experiment. The combined audiovisual stimuli were presented at various stimulus onset asynchronies (SOAs) in which the visual stimulus was presented either 80, 60, 40 or 20 ms before the auditory stimulus, at the same time as the auditory stimulus (0 ms onset), or 20, 40, 60 or 80 ms after the auditory stimulus. In addition to the auditory alone, visual alone and nine audiovisual conditions, the paradigm also included trials in which no stimulus was presented in order to collect spontaneous activity. Overall, the trial conditions were presented in a pseudorandomized order, separated by an inter-trial interval of 3-5 s, and each condition was presented 50 times.

2.1.4 Multi-unit Analysis & Multisensory Enhancement:

At each of the 32 recording sites on the microelectrode array, MU activity was analyzed, and the results described in terms of each MU cluster's overall "sensory responsiveness" to the auditory and/or visual stimuli, as described previously (Schormans et al., 2016). For each MU cluster, custom Matlab scripts were used to generate rasters and PSTHs for each stimulus condition. To assess if a cluster was responsive to the auditory and/or visual stimuli, it had to demonstrate a significantly increased firing rate per trial compared to the spontaneous activity as determined with a paired t-test ($\alpha = 0.05$) (Allman et al., 2008a; Allman and Meredith, 2007; Schormans et al., 2016). Spontaneous activity was determined by first tallying the number of spikes within the 500-ms time window for each of the 50 trials, and then calculated by averaging the firing rate per trial over the 50 trials (SpontR; see Fig. 2 for representative values). Figure 2 shows representative examples of MU

clusters that were classified as being responsive to auditory (Fig. 2A), visual (Fig. 2B) or both auditory and visual stimuli (i.e., multisensory, Fig. 2C).

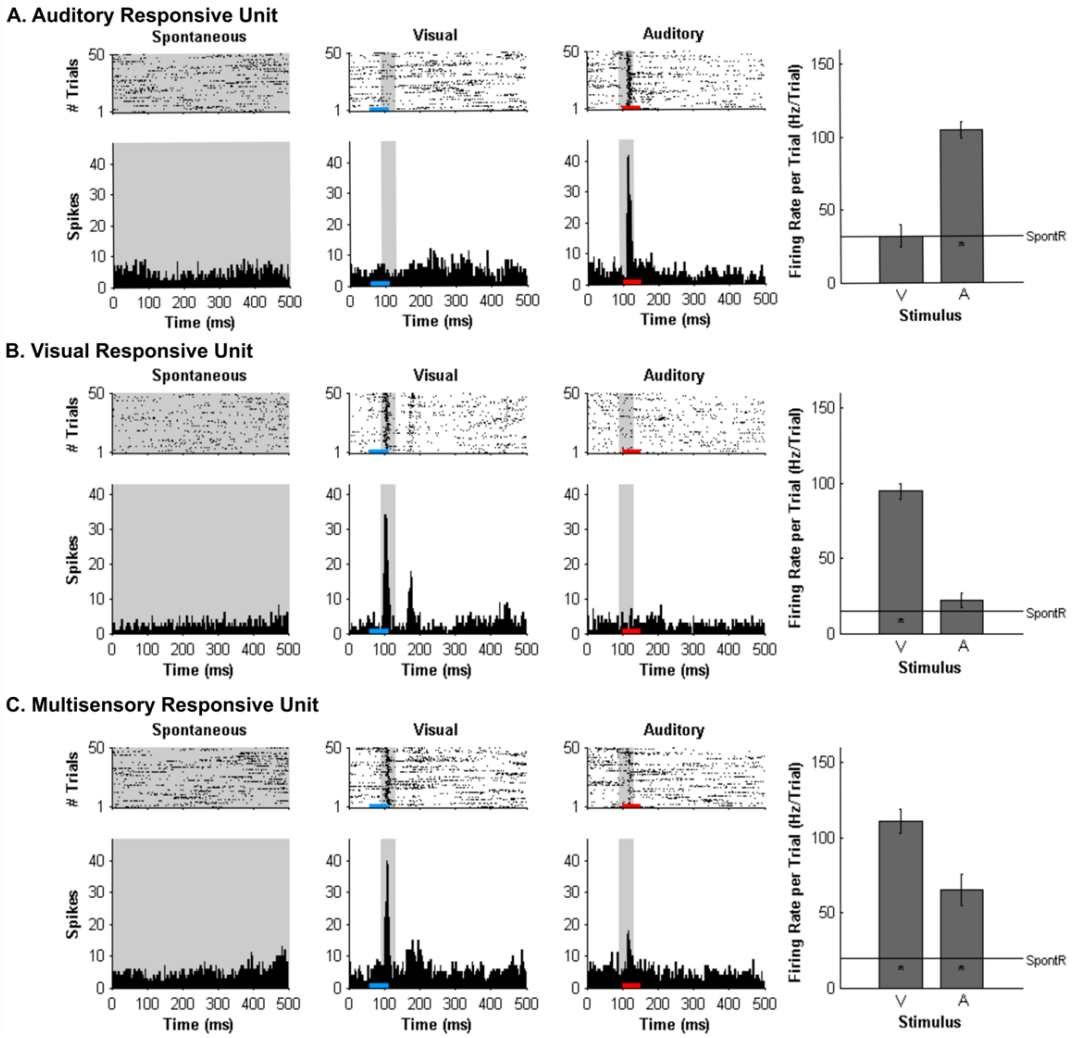

Figure 2. Responses of multi-unit clusters to auditory, visual and combined audiovisual stimuli.

For a representative multi-unit (MU) cluster, responses to no sensory stimulus (i.e., spontaneous activity; left panels), visual (50 ms LED flash at 11 lux, denoted by the blue horizontal bar; middle panels), and auditory [50 ms noise burst at 30 dB above click threshold, denoted by the red horizontal bar; right panels] are shown in the rasters (dot = spike; each row = 1 of 50 trials) and peri-stimulus time histograms (PSTH; 5 ms time bins). Spontaneous activity was determined in the no stimulus condition. For each MU cluster, firing rate in response to an auditory or visual stimulus was calculated within a 40 ms

window (gray shading on rasters and PSTH; 90 – 130ms) and average firing rate per trial ± SEM are shown in the bar graphs. In each bar graph, the "" appearing below the horizontal line (spontaneous activity; SpontR) denotes whether a particular stimulus was effective at eliciting an overt response (see Methods for details). The MU clusters shown were classified as being responsive to auditory (A), visual (B) or both auditory and visual stimuli (i.e., multisensory; C).*

Consistent with prior studies (King and Palmer, 1985; Lippert et al., 2013), all responsive MU clusters underwent analyses to determine its mean firing rate for each of the stimuli conditions using two methods: (1) a firing rate calculation based on latency of auditory responses (i.e., firing rate calculated from 90 – 130 ms from trial onset; "set window") and (2) a firing rate calculation window based on the latency of the peak firing rate irrespective of stimulus (i.e., firing rate calculated from 40 ms window centered around the peak firing rate within the overall 500 ms sampling time; "peak-centered window"). Figures 3 and 4 show representative calculation windows (i.e., gray shading on the rasters and PSTHs) for the mean firing rate derived from the "set window" and "peak-centered window" conditions, respectively. Table 1 shows the average start time for the 40 ms peak-centered window across all audiovisual SOAs presented. A "set window" of 90 to 130 ms was selected based on previous recordings within the V2L cortex, as this timing window captured the vast majority of auditory and visual responses of single- and multi-unit clusters (Schormans et al., 2016). Overall, a series of calculations were performed to generate an average response profile across all animals associated with the set window and peak-centered window analyses. Prior to the group calculations, the following steps were performed on MU clusters collected from each rat. First, using the set window for example, the firing rate per trial of a given auditory-responsive MU cluster (e.g., the one depicted in Fig. 3A) was divided by the firing rate per trial of the most effective unimodal stimulus condition (e.g., Fig. 2A, auditory response) to calculate the percent change in firing rate at each of the audiovisual SOAs (i.e., 0, ±20, ±40, ±60 and ±80 ms). This calculation was used to describe the degree of change due to the timing of the audiovisual stimuli, and presented as the level of multisensory enhancement. Next, for a given rat, all of its

auditory-responsive MU clusters were averaged at each of the SOAs for both the mean firing rate and the level of multisensory enhancement using the set window. Ultimately, the aforementioned series of calculations were performed on all of the auditory-, visual- and multisensory-responsive MU clusters sampled from each rat using both the set window and peak-centered window analyses. Finally, an average was derived from all seven rats at each of the audiovisual SOAs for the mean firing rate and multisensory enhancement.

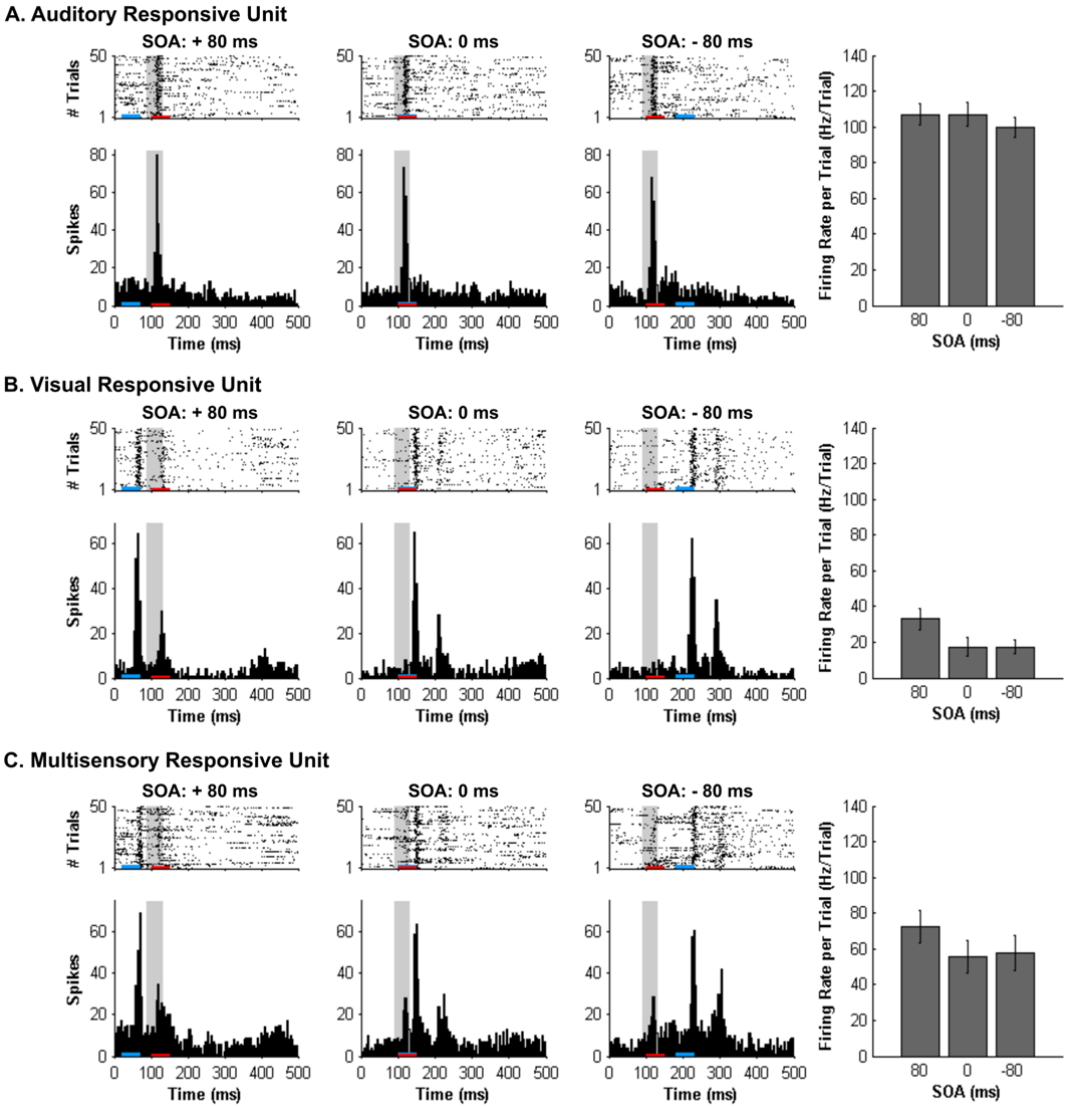

Figure 3. Spiking activity of multi-unit clusters at various audiovisual temporal onsets assessed using a set window analysis.

Rasters and PSTHs show the spiking activity of representative multi-unit (MU) clusters (A: auditory-responsive; B: visual-responsive; C: multisensory-responsive) to combined

auditory (50 ms noise burst; denoted by the red bar) and visual (50 ms LED flash, denoted by the blue bar) at three different stimulus onset asynchronies (SOAs). At a SOA of +80 ms, the onset of the visual stimulus preceded the auditory stimulus by 80 ms (left rasters and PSTHs), whereas a SOA of -80 ms indicates that auditory stimulus preceded the visual stimulus by 80 ms (right rasters and PSTHs). A temporal difference of 0 ms represents the simultaneous presentation of the auditory and visual stimuli (middle rasters and PSTHs). For each responsive MU cluster, mean firing rate per trial ± SEM (shown in the bar graphs) was calculated based on a 40-ms window fixed in time (i.e., set window). The set window analysis captured the majority of the spiking activity of auditory- and multisensory-responsive MU clusters; however, because the onset of the visual stimulus moved in time, the set window failed to consistently capture the maximal responsiveness of the visual MU cluster across all SOAs (note the low firing rates in bar graphs).

2.1.5 Histology:

Following the completion of the electrophysiological recordings, the rat was injected with sodium pentobarbital (100 mg/kg; IP) in preparation for a transcranial perfusion with 0.1 M phosphate buffer (PB), followed by 4% paraformaldehyde. The brain was then removed and post-fixed in paraformaldehyde for 12 hours, followed by storage in 30% sucrose. Coronal sections (40 µm) were cut using a freezing microtome (HM 430/34; Thermo Scientific, Waltham, MA). After staining with thionin, the coronal sections were imaged with an Axio Vert A1 inverted microscope (Carl Zeiss Microscopy GmbH, Jena, Germany). ZEN imaging software was used to reconstruct the location of each recording penetration (see Fig. 1 for representative image).

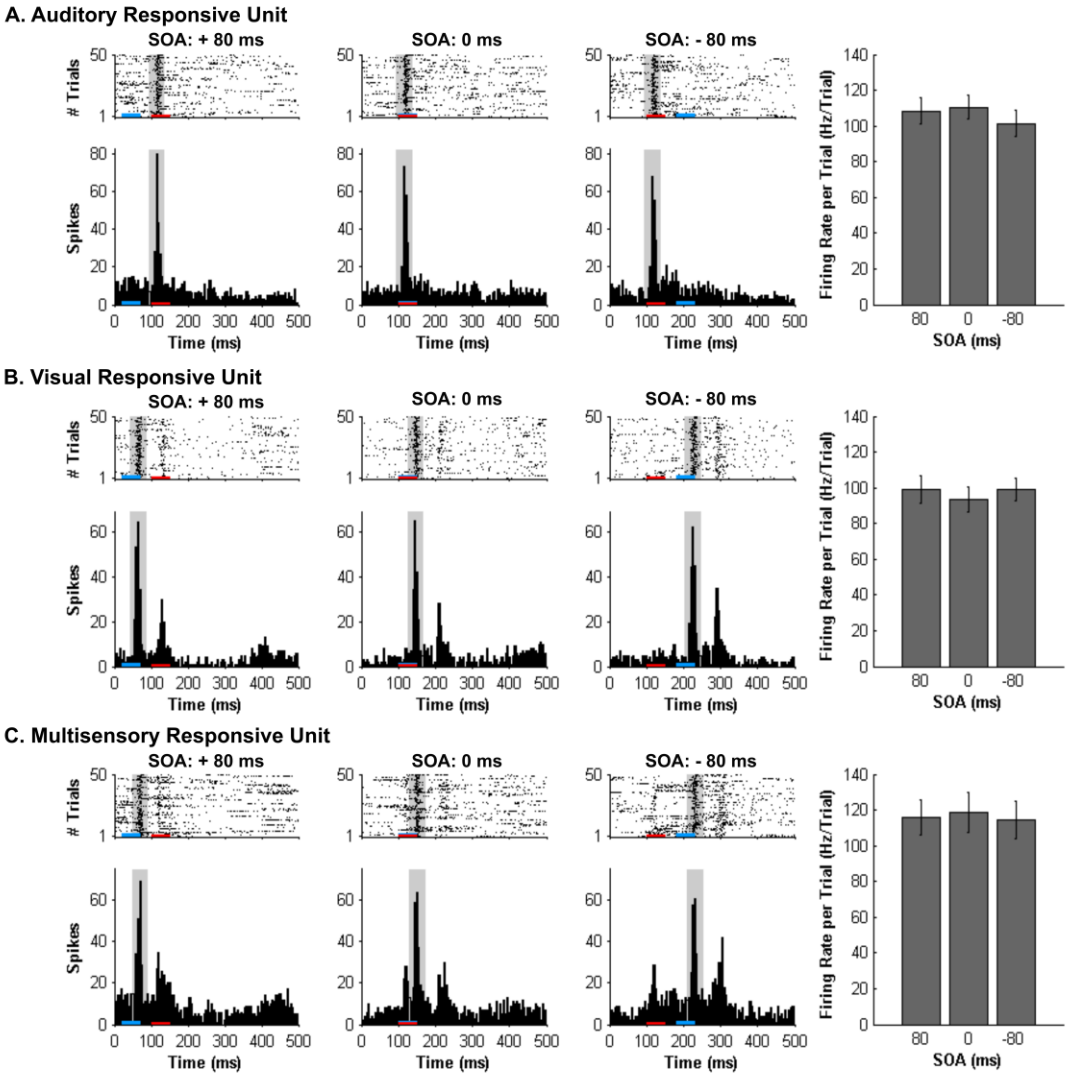

Figure 4. Spiking activity of multi-unit clusters at various audiovisual temporal onsets assessed using an analysis window centered on the peak firing rate.

Rasters and PSTHs show the spiking activity of the same representative multi-unit (MU) clusters shown in Fig. 3 (A: auditory-responsive; B: visual-responsive; C: multisensory-responsive) to combined auditory (50 ms noise burst; denoted by the red bar) and visual (50 ms LED flash, denoted by the blue bar) at three different stimulus onset asynchronies (SOAs). At a SOA of +80 ms, the onset of the visual stimulus preceded the auditory stimulus by 80 ms (left rasters and PSTHs), whereas a SOA of -80 ms indicates that auditory stimulus preceded the visual stimulus by 80 ms (right rasters and PSTHs). A temporal difference of 0 ms represents the simultaneous presentation of the auditory and visual

stimuli (middle rasters and PSTHs). For each responsive MU cluster, mean firing rate per trial ± SEM (shown in the bar graphs) was calculated based on a 40-ms window (gray shading on rasters and PSTH) centered on the peak firing rate within the sampling window. For example, the location of the 40 ms peak-centered window for the visual-responsive MU cluster was different at each SOA, given that the onset of the visual stimulus was moved in time with respect to the static auditory stimulus (presented 100 ms from the beginning of the trial). Consequently, the mean firing rate per trial ± SEM (seen in the bar graphs) of the visual-responsive MU cluster (B) was similar across SOAs, consistent with the auditory-responsive MU cluster (A).

Table 1. Start time of the 40ms peak-centered window across stimulus onset asynchronies (SOAs) for auditory, visual and multisensory multi-unit clusters.

	Auditory		**Visual**		**Multisensory**	
SOA	Mean (ms)	SEM	Mean (ms)	SEM	Mean (ms)	SEM
+ 80 ms	95.3	0.2	43.9	0.9	74.1	4.4
+ 60 ms	95.7	0.3	66.5	1.3	83.8	2.6
+ 40 ms	95.1	0.1	84.4	.8	91.9	0.8
+ 20 ms	95.5	0.2	102.8	0.5	100.7	0.8
0 ms	95.4	0.2	123.8	1.1	109.9	2.7
- 20 ms	97.4	1.9	141.6	1.4	117.8	4.1
- 40 ms	95.6	0.3	162.3	0.8	130.0	6.1
- 60 ms	95.7	0.2	181.9	1.4	136.3	7.7
- 80 ms	95.5	0.2	198.7	2.2	139.0	9.4

2.2 Experiment 2- Simultaneity Judgement Task

A separate group of adult male rats (n = 7; training began at 70 days old; body mass: 286 ± 4.4 g) were trained six days per week using a two-alternative forced-choice operant conditioning paradigm to differentiate between trials when a visual stimulus was presented simultaneously with an auditory stimulus (0 ms onset; synchronous), or when the visual stimulus preceded the auditory stimulus by 200 ms (i.e., asynchronous). As described in detail below, once the rats were proficient at the training task, occasional testing days occurred in which novel SOAs were also added to the paradigm whereby the visual stimulus preceded the auditory stimulus by 0, 10, 40, 100 or 200 ms. These testing days

took place when the rats were between six and eleven months of age (body mass at last day of testing: 449 ± 16.3 g), and allowed for the determination of each rat's judgement of simultaneity.

2.2.1 Behavioural Apparatus and Sensory Stimuli:

Behavioural training was performed using a standard modular test chamber (ENV-008CT; Med Associates Inc., St. Albans, VT, USA), which was housed in a sound-attenuating box (29" W by 23.5" H by 23.5" D, Med Associates Inc.). The behavioural chamber was illuminated by a house light located on the back wall, whereas the front wall was equipped with a center nose poke, a left feeder trough and a right feeder trough; each fitted with an infrared (IR) detector. Stimulus delivery, nose-poke responses and positive/negative reinforcement were controlled and monitored using custom Matlab behavioural protocols running in Matlab (EPsych Toolbox, dstolz.github.io/epsych/) which was interfaced with real-time processing hardware (RZ6, TDT). The visual stimulus consisted of a light flash (27 lux; 50 ms duration) from a LED (ENV-229M; Med Associates Inc.) located above the center nose poke. The intensity of the visual stimulus (as determined by a LED light meter; Model LT45, Extech Instruments, Nashua, NH, USA) was constrained by the hardware associated with the operant conditioning chamber (Med Associates Inc.). The auditory stimulus was a noise burst (1-32 kHz; 75 dB SPL; 50 ms duration) from a speaker (FT28D, Fostex, Tokyo, Japan) mounted on the ceiling of the behavioural chamber near the front wall. Pilot studies revealed that the rats had difficulty learning either paradigm to a performance criterion of 75% when a lower sound level (i.e., 60 dB SPL) was used; findings which are consistent with studies demonstrating improved audiovisual temporal discrimination with increasing sound intensities (Boenke et al., 2009; Krueger Fister et al., 2016). The intensity of the auditory stimulus was calibrated with custom Matlab software using a ¼-inch microphone (2530, Larson Davis) and preamplifier (2221; Larson Davis). The duration of the stimuli (i.e. 50 ms) was not varied in order to be consistent with electrophysiological recordings.

2.2.2 Behavioural Training:

Prior to commencing behavioural training, the rats were weighed daily and maintained on a food restricted diet until they reached 85% of their free feeding body mass. Initially, the

rats were habituated to the behavioural chamber for 30 min/day. During these habituation sessions, spontaneous nose pokes into the center port (detected by the IR beam) resulted in 1) the immediate presentation of an audiovisual stimulus combination that was either synchronous (i.e., 0 ms onset) or asynchronous (i.e., visual stimulus 400 ms prior to auditory stimulus), and 2) the delivery of a 45 mg food pellet (Bio-Serv, Frenchtown, NJ, USA) to the associated feeder trough (i.e., synchronous = left feeder trough; asynchronous = right feeder trough). Furthermore, if the rat went to the correct feeder trough following the stimuli presentation (as monitored with the IR detector), a second pellet was delivered so as to help the rat associate a given feeder trough with a particular audiovisual SOA.

Once the rats were able to frequently nose poke in the center port (typically within 3 days), the initial pellet reinforcement was removed, and now the pellet delivery was contingent on the rat poking its nose in the correct feeder trough in response to the given audiovisual SOA. At this stage, the audiovisual asynchronous stimuli onset remained at 400 ms. During each 30-min daily training session, correct feeder trough responses were reinforced with a food pellet, whereas incorrect responses resulted in the house light turning off for 15 s, during which time the rat was unable to initiate a new trial (Fig. 5A). Throughout the behavioural training, the amount of food provided in each rat's home cage was adjusted so that its body mass increased with age while still providing enough motivation for it to perform ~200 trials in a session (Stolzberg et al., 2013).

Rats remained on the 0 ms versus 400 ms SOA protocol until they correctly identified the synchronous and asynchronous audiovisual combinations with >75% accuracy. Upon achieving this performance criterion for three consecutive days, the asynchronous SOA was reduced to 300 ms. Training continued in sessions of 30 min/day or to the completion of 200 trials until a criterion of 75% correct was reached for both synchronous and asynchronous stimuli on five consecutive days. During the final training stage of the simultaneity judgement task, the asynchronous stimuli onset was reduced to 200 ms. As described below, after the rat had achieved >80% accuracy for five consecutive days on the final training stage (i.e., 0 ms vs. 200 ms SOA), "testing" days were performed approximately once a week.

2.2.3 Behavioural Testing & Analysis:

To determine each rat's perception of simultaneity (i.e., whether it judged a given audiovisual stimuli combination as being presented synchronously or asynchronously), novel SOAs were introduced. On average, rats underwent testing once a week, in which five SOAs were randomly presented (i.e., the visual stimulus preceded the auditory stimulus by 0, 10, 40, 100 or 200 ms; see Fig. 5B), whereas the other days of the week remained as training sessions (i.e., only 0 ms vs. 200 ms SOA). On testing days, the familiar 0 ms and 200 ms SOAs continued to be reinforced with food pellets for correct responses and 15-s timeouts for incorrect responses; however, the novel temporal onsets (i.e., 10, 40, and 100 ms SOA) were reinforced regardless of whether a correct or incorrect response was made. For the majority (70%) of trials on test days, the rats were presented with the 0 ms or 200 ms SOAs, whereas the remaining 30% of the trials were divided equally between the 10, 40 and 100 ms SOAs. Pilot testing revealed that this trial breakdown helped to prevent the rats from developing a side bias to the novel SOAs.

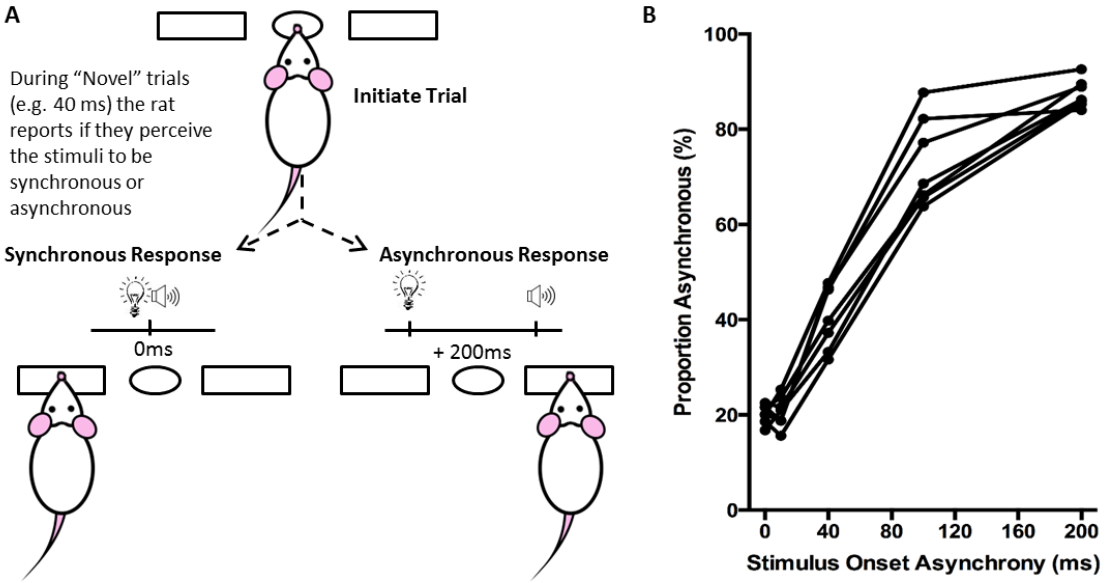

Figure 5. Overview of simultaneity judgement task.

(A) The simultaneity judgement task consisted of the rat initiating a trial by poking its nose into the center port, and holding for up 2 seconds. In response to the presentation of an audiovisual stimulus, the rat was trained to respond to the left feeder trough for the synchronous (0 ms SOA) trials and to the right feeder trough for the asynchronous (200

ms SOA) trials. On testing days, upon presentation of novel SOAs (0, 40 and 100 ms), the rat reported whether it judged the audiovisual stimuli to have been presented synchronously or asynchronously. (B) The behavioural performance of individual rats was plotted as the proportion of responses that the rat judged as asynchronous (i.e., right feeder trough). Each data point represents the average of five psychophysical testing sessions for an individual rat (n = 7).

Ultimately, the simultaneity judgement task was designed such that if the rat perceived the audiovisual stimuli to have been presented synchronously, it would respond by nose-poking the left feeder trough, whereas if it perceived the audiovisual stimuli to have presented asynchronously, it would respond by nose-poking the right feeder trough (Fig. 5A). Each rat completed a total of five test sessions over a two-month period, from which its performance on each of the SOAs (i.e., 0, 10, 40, 100 and 200 ms) was reported as the proportion of trials that were judged as asynchronous (i.e., % right feeder trough responses; Fig. 5B). Test days were repeated if the performance on the training SOAs (i.e., 0 and 200 ms) fell below the criterion of 70% correct. Finally, to determine each rat's baseline performance on the simultaneity judgement task, the results from the five successful test days were averaged for the various SOAs to create a psychophysical profile (Fig. 5B).

2.3 Experiment 3- Temporal Order Judgement Task

Using the same behavioural apparatus and sensory stimuli described in Experiment 2, a separate group of adult male rats (n = 7; training began at 70 days old; body mass: 310 ± 4.9 g) were trained six days per week using a two-alternative forced-choice operant conditioning paradigm to differentiate the temporal order of auditory and visual stimuli (i.e., which stimulus modality was presented first when separated by 400 ms). As outlined in the following sections, once the rats were proficient at the training task, occasional testing days occurred in which novel SOAs (i.e., 0, ±40 and ±100 ms) were also added to the paradigm. Ultimately, the testing days, which took place when the rats were between six and eight months of age (body mass at last day of testing: 422 ± 11.6 g), allowed for the determination of each rat's perception of audiovisual temporal order.

2.3.1 Behavioural Training:

Several aspects of the behavioural training were consistent with those described above in Experiment 2, such as the food deprivation, habituation, general nose-poking procedures, session duration (30 min/day or ~200 trials), frequency of training (6 days per week), positive/negative reinforcement, as well as an incremental progression through the various training stages. Importantly, in contrast to the simultaneity judgement task, rats in Experiment 3 received a food pellet for nose-poking the left feeder trough when the auditory stimulus preceded the visual stimulus by 400 ms, and for nose-poking the right feeder trough when the visual stimulus was presented 400 ms before the auditory stimulus (Fig. 6A). Once the rats reached the performance criterion of 75% correct for three consecutive days at a temporal onset of ±400 ms, the SOAs were reduced to ±300 ms. Moreover, when the rat scored >75% correct for five consecutive days, the SOAs were reduced to ±200 ms for the final training stage of the temporal order judgement task. As described below, behavioural testing days were performed approximately once a week after the rats had achieved >80% accuracy on five consecutive training days.

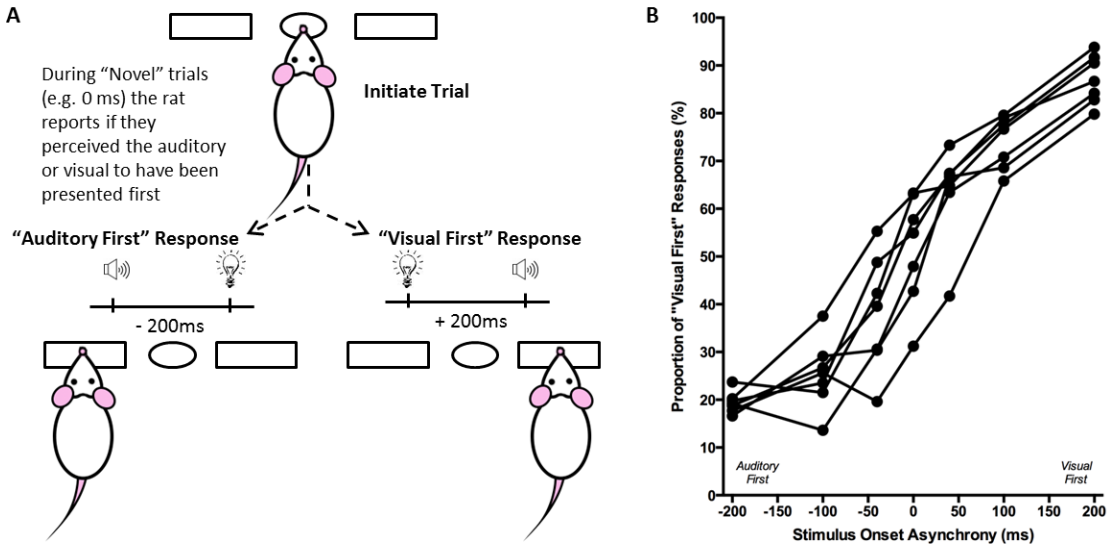

Figure 6. Overview of temporal order judgement task.

The temporal order judgement task consisted of the rat initiating a trial by poking its nose into the center port, and holding for up 2 seconds. In response to the presentation of an audiovisual stimulus, the rat was trained to respond to the left feeder trough on trials when the auditory stimulus preceded the visual (-200 ms SOA), and to the right feeder trough

when the visual stimulus was presented first (+200 ms SOA). On testing days, when the rat was presented novel SOAs (0, ±40 and ±100 ms), it reported whether it judged the audiovisual stimuli to have been "auditory first" or "visual first." (B) The behavioural performance of individual rats was plotted as the proportion of responses that the rat judged as "visual first" (i.e., right feeder trough). Each data point represents the average of five psychophysical testing sessions for an individual rat (n = 7).

2.3.2 Behavioural Testing & Analysis:

On testing days, novel SOAs were introduced so as to determine each rat's perception of the temporal order of the auditory and visual stimuli. On average, rats underwent testing days once a week, in which seven SOAs were randomly delivered (i.e. 0, ±40, ±100 and ±200 ms; see Fig. 6B), with the other days of the week remaining as training days (i.e., only the ±200 ms). On testing days, food pellets were delivered following the novel SOAs (i.e., 0, ±40 and ±100 ms) regardless of whether a correct or incorrect response was made. In contrast, the audiovisual stimuli conditions familiar to the rat through training (i.e., ±200 ms) continued to be reinforced with food pellets for correct responses and 15-s timeouts for incorrect responses. To help avoid the potential development of a side bias during testing days, the training stimuli were presented for the majority (70%) of the trials, with the other 30% of trials divided between the novel SOAs.

Performance at each of the SOAs was measured as the proportion of trials in which the rat responded on the right feeder trough (i.e., visual first; Fig. 6B). Test days were repeated if the trained stimuli (i.e. ±200 ms) did not reach the criterion of 70% correct. Ultimately, the results at the seven SOAs (i.e., 0, ±40, ±100 and ±200 ms) were averaged across the five successful test days to create a psychophysical profile of each rat's audiovisual temporal order judgement (Fig. 6B). Moreover, best-fitting straight lines were plotted between each of the neighbouring SOAs tested (e.g., -200 ms to -100 ms; -100 ms to -40 ms; etc.), and the associated slopes and intercept values were tabulated. From these values, the point of subjective simultaneity (PSS) was calculated by determining the SOA at which 50% of the responses were "visual first" (Vatakis et al., 2007). Similar to the PSS, the just noticeable detection (JND) was calculated by taking the difference between the SOAs at which 25%

and 75% of the responses were considered "visual-first" and then dividing by two (Vroomen and Stekelenburg, 2011). For each rat, PSS and JND were determined on the each of the five testing days, and the average PSS and JND values were calculated.

2.4 Statistics and Data Presentation:

Overall, the statistical analyses performed in the present study included one-way repeated-measures analysis of variance (ANOVA), and paired samples t-tests, depending on the comparison of interest (see Results section for the details of each specific comparison). If Mauchly's test of sphericity was violated within the repeated-measures ANOVA, the Greenhouse-Geisser correction was used. The level of statistical significance was set at $\alpha = 0.05$. When appropriate, Bonferroni post-hoc corrections were used to account for potential 'family-wise' error (Armstrong, 2014). SPSS software (version 20, IBM Corporation, Armonk, NY, USA) was used for the statistical analyses. Matlab and GraphPad Prism (GraphPad Software Inc., La Jolla, CA, USA) were used to plot the results. Data are presented as the mean values ± standard error of the mean (SEM).

3.0 RESULTS:

3.1 Experiment 1- Electrophysiological Recordings in the Lateral Extrastriate Visual Cortex (V2L)

All rats (n = 7) included in this experimental series underwent the same electrophysiology recording procedure, which consisted of a single penetration of the 32-channel microelectrode array into the lateral extrastriate visual cortex (V2L). In total, 224 waveform clusters were sampled, with 221 (98.7%) of these MU clusters being classified as responsive to at least one sensory modality. Of the MU clusters that were responsive to sensory stimuli, 97 (43.9%) were overtly responsive to only the visual stimulus, 90 (40.7%) were overtly responsive to only the auditory stimulus, and 34 (15.4%) were overtly responsive to both the auditory and visual stimuli (i.e., multisensory MU clusters). As described in the Methods, the mean firing rate and level of multisensory enhancement of each MU cluster were determined at the various audiovisual SOAs (i.e., 0, ±20, ±40, ±60 and ±80 ms). These calculations were performed when the analysis window was either fixed at a given time interval (i.e., set window: from 90 to 130 ms from the start of the trial) or when it was shifted according to the peak firing rate (i.e., peak-centered window).

3.1.1 Mean Firing Rate and Multisensory Enhancement Calculated from a Set Window:

As shown in Fig. 7A, separate one-way repeated-measures ANOVAs revealed that both the mean firing rates ($F[3.7, 22.1] = 0.693$, $p = 0.593$) and level of multisensory enhancement ($F[3.0, 18.1] = 0.666$, $p = 0.585$) of auditory-responsive MU clusters were not significantly affected by the various SOAs. This finding was not surprising given that the timing of the auditory stimulus did not vary during the SOA protocol; the onset of the visual stimulus shifted around the static auditory stimulus. Thus, because the spiking activity of the auditory-responsive MU clusters was consistently captured in the set window (see gray bars in Fig. 3A) and these neurons, by definition, did not show overt responsiveness to the visual stimulus, it was expected that the mean firing rates and level of multisensory enhancement would be largely unaffected by the varying SOAs.

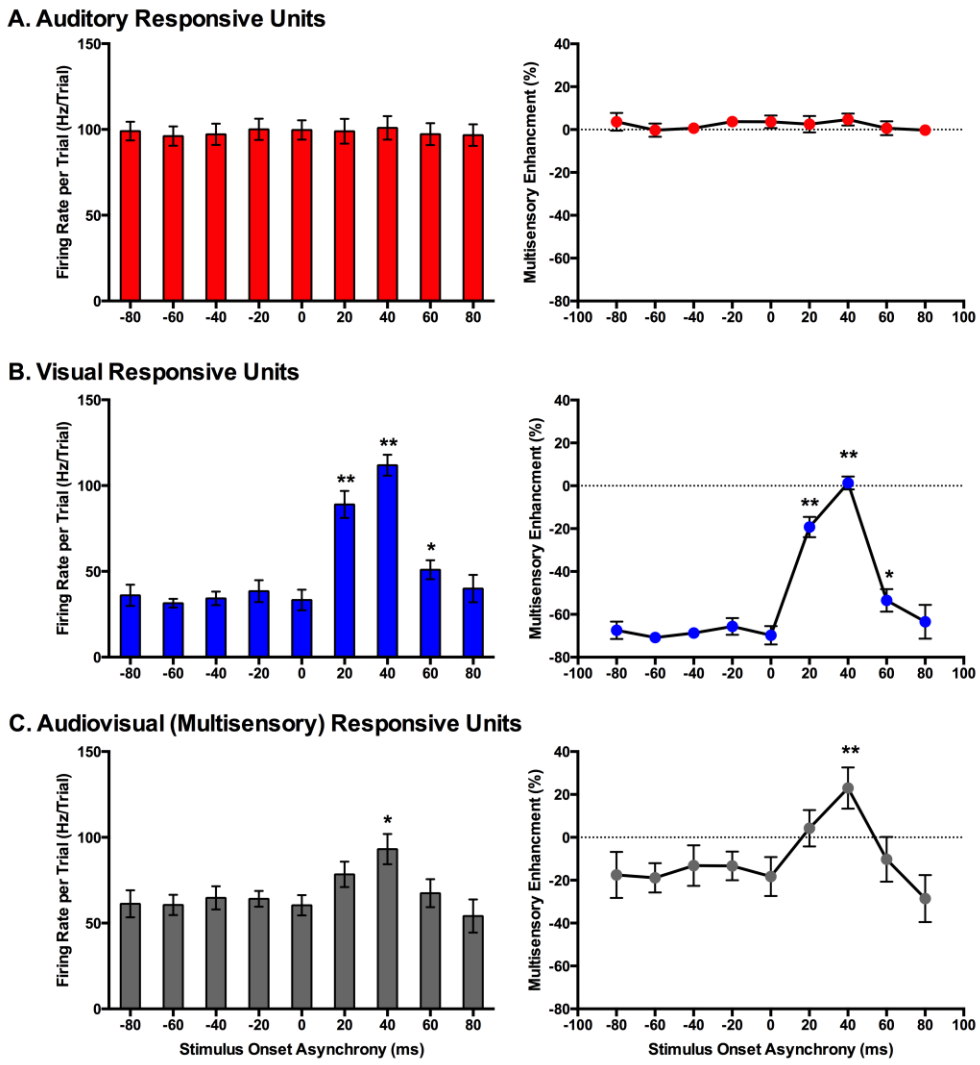

Figure 7. Use of a set window analysis to compare the spiking activity of multi-unit clusters evoked from audiovisual stimuli presented at various temporal onsets.

*For multi-unit (MU) clusters that were responsive to visual, auditory and both auditory and visual stimuli (i.e. multisensory), the group mean firing rate (left panels) and the level of multisensory enhancement (right panels) were determined based on a set window of analysis that was fixed at 90 to 130 ms from the start of the trial (see Fig. 3 for representative rasters and PSTHs). Auditory-responsive MU clusters (A) showed no effect of stimulus onset asynchrony (SOA), whereas clusters that exclusively responded to visual stimuli (B) showed an increase in mean firing rate and multisensory enhancement at a SOA of +20 (**p < 0.0125), +40 (**p < 0.0125) and +60 ms (*p < 0.05) when compared to the synchronous presentation of stimuli (i.e. 0 ms SOA). (C) Multisensory responsive*

*clusters showed an increase in mean firing rate (*p < 0.05) and multisensory enhancement (**p < 0.0125) at a SOA of +40 ms when compared to a SOA of 0 ms. Results are displayed as mean ± SEM, n = 7. Statistical comparisons are based on a repeated-measures ANOVA and Bonferroni corrected post-hoc tests in which the significant p-value was adjusted to **p < 0.0125 to account for the multiple comparisons.*

In contrast to the auditory-responsive MU clusters, the spiking profiles of neurons that responded exclusively to the visual stimulus were significantly affected by the set window analysis, as the fixed window often failed to capture the visually-evoked activity (see Fig. 3B; gray set window does not overlap maximum spiking response). Thus, it was not surprising that a one-way repeated-measures ANOVA revealed a significant effect of SOA on the mean firing rate ($F[3.1,18.6] = 64.186$, $p < 0.001$), and Bonferroni corrected post hoc analyses revealed that the mean firing rate was significantly greater at +20, +40 and +60 ms SOA compared to the synchronous presentation of the audiovisual stimuli (i.e., 0 ms onset). Similarly, the level of multisensory enhancement was significantly greater at the +20, +40 and +60 ms SOA than when the audiovisual stimuli were presented synchronously, as determined by a one-way repeated measures ANOVA ($F[3.2,18.9] = 57.049$, $p < 0.001$) and Bonferroni corrected post hoc testing ($p < 0.0125$). Notice, however, that the level of multisensory enhancement in the visually-responsive MU clusters was well below 0% for the majority of the SOAs; again, an expected result due to the set window of analysis failing to capture the spiking evoked by the visual stimulus that moved in time.

Based on the set window analysis (Fig. 7C), separate one-way repeated-measures ANOVAs revealed a significant effect of SOA on the mean firing rate ($F[2.3, 9.2] = 6.201$, $p < 0.02$) and level of multisensory enhancement ($F[2.2, 8.7] = 6.313$, $p < 0.02$) observed in multisensory-responsive MU clusters. Furthermore, post hoc analyses found a significant increase in mean firing rate ($p < 0.05$) and multisensory enhancement ($p < 0.01$) at +40 ms SOA compared to when the audiovisual stimuli were presented synchronously (0 ms SOA; Fig. 7C).

3.1.2 Mean Firing Rate and Multisensory Enhancement Calculated from a Peak-Centered Window:

Similar to the results found using a set window, separate one-way repeated measures ANOVAs revealed that both the mean firing rates ($F[3.5, 20.9] = 0.616$, $p = 0.635$) and level of multisensory enhancement ($F[2.9, 17.4] = 0.707$, $p = 0.556$) of auditory-responsive MU clusters did not significantly differ across the various SOAs when a peak-centered window of analysis was used (Fig. 8A). As shown in Figure 4B compared to Figure 3B, a peak-centered window of analysis better captured the stimulus-evoked spiking activity of visually-responsive MU clusters than a set window. Consequently, in contrast to Figure 7B (set window), separate one-way repeated-measures ANOVAs did not report a significant effect of SOA on the mean firing rates ($F[2.0, 12.2] = 1.177$, $p = 0.342$) or level of multisensory enhancement ($F[1.7, 9.9] = 1.853$, $p = 0.208$) observed in visually-responsive MU clusters (Fig. 8B). The lack of effect of SOA on auditory- or visual-responsive MU clusters was not surprising given that these neurons had only shown overt spiking activity in response to a single modality (see Fig. 2A and 2B for representative examples).

Consistent with the findings using the set window of analysis, multisensory-responsive MU clusters showed a sensitivity to SOAs when the visual stimulus preceded the auditory stimulus. Separate one-way repeated-measures ANOVAs revealed a significant effect of SOA on the mean firing rates ($F[1.9, 7.4] = 5.466$, $p < 0.05$) and level of multisensory enhancement ($F[2.4, 9.4] = 7.902$, $p < 0.01$) of multisensory-responsive MU clusters. Furthermore, post hoc analyses found an increase in mean firing rate and multisensory enhancement at +20 ms and +40 ms SOAs compared to when the audiovisual stimuli were presented synchronously (0 ms SOA; Fig. 8C). Based on these electrophysiological results, we aimed to design novel behavioural paradigms that would assess rats' ability to judge the simultaneity (Experiment 2) and temporal order (Experiment 3) of audiovisual stimuli specifically when the visual stimulus was presented 40 ms prior to the auditory stimulus.

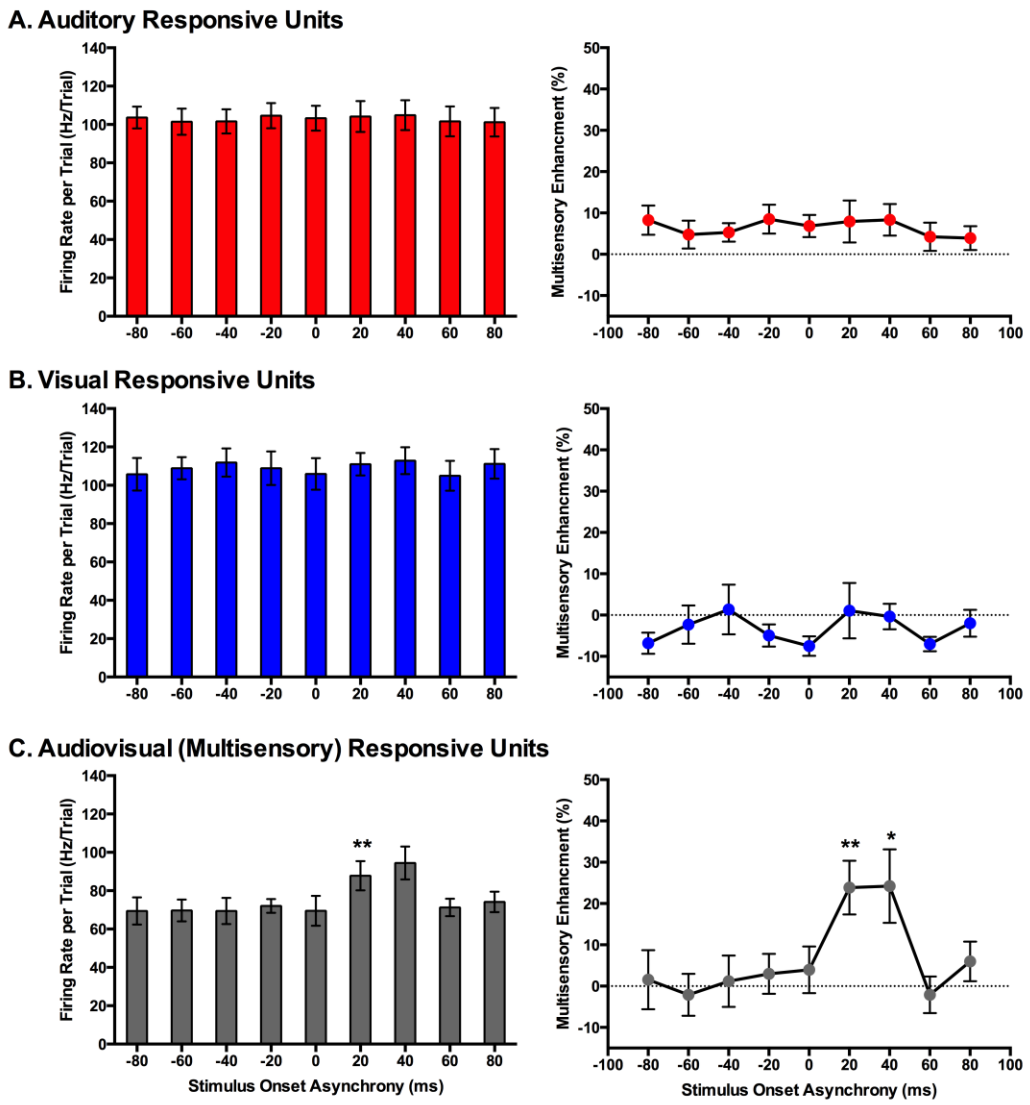

Figure 8. Use of an analysis window centered on the peak firing rate to compare spiking activity of multi-unit clusters evoked from audiovisual stimuli presented at various temporal onsets.

*For multi-unit (MU) clusters that were responsive to visual, auditory and both auditory and visual stimuli (i.e. multisensory), the group mean firing rate (left panels) and the level of multisensory enhancement (right panels) were determined based on the latency of the peak firing rate within the sampling window for each MU cluster. For MU clusters that exclusively responded to auditory (A) or visual (B) stimuli, there was no effect of SOA on either the mean firing rate or level of multisensory enhancement. (C) Multisensory-responsive MU clusters showed an increase in mean firing rate and multisensory enhancement at a SOA of +20 ms when compared to 0 ms (**p < 0.0125). Moreover, at*

*an SOA of +40 ms, an increase in multisensory enhancement was observed (*p < 0.05). Results are displayed as mean ± SEM, n = 7. Statistical comparisons are based on a repeated-measures ANOVA and Bonferroni corrected post-hoc tests in which the significant p-value was adjusted to **p < 0.0125 to account for the multiple comparisons.*

3.2 Experiment 2- Simultaneity Judgement Task

Over a series of stages, rats were trained using a two-alternative forced choice paradigm to differentiate between audiovisual stimuli that were presented synchronously (0 ms SOA) and when the onset of the visual stimulus preceded the auditory stimulus by 200 ms. On average, training took place over 131 ± 7 days before they were able to undergo the testing procedures. Once the rats had become proficient at the training paradigm, five testing days were performed over the next two to three months in which novel audiovisual temporal onsets (10, 40 and 100 ms SOA) were presented. At the 40 ms SOA, rats perceived the stimuli to be asynchronous on 40 ± 2.6% of the trials (Fig. 9A). A one-way repeated measures ANOVA revealed a significant main effect of SOA on the proportion of trials judged as asynchronous ($F[4,24] = 366.024$, $p < 0.001$), and Bonferroni corrected post hoc analyses found that the performance during the 40 ms SOA was significantly different from all of the other SOAs tested ($p < 0.001$; Fig. 9A). Moreover, the relatively short 10 ms SOA was also tested so that the face validity of the paradigm could be assessed, as human subjects judge audiovisual stimuli presented at 20 ms SOA to be synchronous (Zampini et al., 2005a). Consistent with these findings, the performance of the rats at the 10 ms SOA did not differ ($p = 0.654$) from that of the synchronous trials. Collectively, these results provide a psychophysical profile of simultaneity judgement in rats.

3.3 Experiment 3- Temporal Order Judgement Task

Although the results of Experiment 2 were largely consistent with previous studies on humans, it is important to note that the tasks differed between species; unlike human subjects, the rats were only required to judge the simultaneity of the audiovisual stimuli when the visual stimulus preceded the auditory stimulus, and not vice-versa. Thus, in Experiment 3, we trained a separate group of rats to perform a temporal order judgement task in which they learned to differentiate between trials when the auditory stimulus either

preceded or followed the visual stimulus by 200 ms. On average, the rats took 97 ± 7 days to reach the performance criterion required to advance to the five testing days, at which time additional SOAs were introduced (i.e., 0, ±40 and ±100 ms; see Fig. 6B). A one-way repeated measures ANOVA revealed a significant main effect of SOA on the proportion of trials judged as "visual first" ($F[2.4,14.6] = 138.460$, $p < 0.001$), and Bonferroni corrected post hoc analyses found that the performance during the 0 ms SOA was significantly different from both the -200 ms (auditory first) and +200 ms (visual first) SOA ($p < 0.001$; Fig. 9B). Rats perceived the synchronous audiovisual stimuli to be "visual first" for nearly half of the trials (51.6 ± 4.4%; Fig. 9B). When the auditory stimulus preceded or followed the visual stimulus by 100 ms, the rats were able to correctly judge the temporal order of the audiovisual stimuli on the majority of trials (-100 ms SOA: 74.3 ± 2.7%; +100 ms SOA: 74.1 ± 2.1%; Fig. 9B).

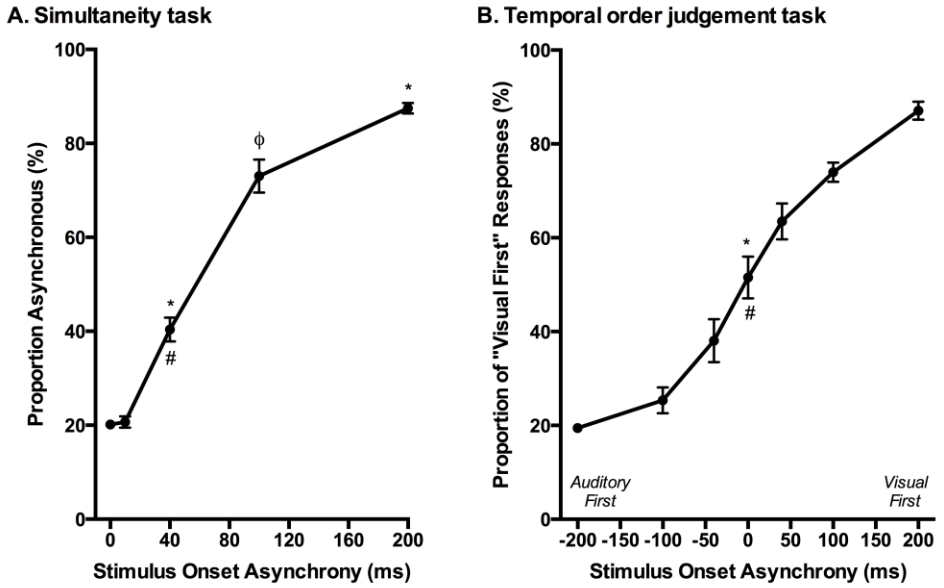

Figure 9. Psychophysical profiles for the simultaneity judgement task and temporal order judgement task.

*(A) Rats performing the simultaneity judgement task reported whether they perceived the audiovisual stimuli at various SOAs to have been presented synchronously or asynchronously (i.e., visual stimulus before the auditory). A significant difference in performance was observed between the simultaneous presentation of audiovisual stimuli (i.e., 0 ms) and 40 ms SOA (*p < 0.001) as well as 200 ms SOA (*p < 0.001); however, no*

*significant difference was found between 0 ms and 10 ms SOA (p = 0.654). Additional statistical comparisons demonstrated that the performance at 40 ms SOA was significantly different from 200 ms SOA (# p < 0.001) and 100 ms SOA (ϕ p < 0.001). (B) The temporal order judgement task required rats to report whether an auditory or visual stimulus was perceived to have been presented first in the audiovisual pair. When stimuli were presented synchronously (0 ms SOA), rats on average perceived the stimuli to be "visual first" 52% of the time, which was significantly different than their performance at -200 ms SOA (*p < 0.001) and +200 ms SOA (# p < 0.001). Results are displayed as mean ± SEM, n = 7.*

Similar to temporal order judgement tasks performed by humans (Chen and Vroomen, 2013; Keetels and Vroomen, 2012; Navarra et al., 2005; Vroomen and Stekelenburg, 2011), the PSS and JND were calculated for each rat over its five testing days. As shown in Fig. 10A, the PSS varied across rats, with values ranging from -53 ms (auditory first) to 51 ms (visual first). On average, the PSS was -8.8 ± 13.6ms, which suggests that the rats tended to perceive the synchronously presented audiovisual stimuli as though the auditory stimulus was delivered slightly in advance of the visual stimulus. When averaged across all seven rats, the JND was 105 ± 7 ms, with values ranging from 77 to 122 ms (Fig. 10B).

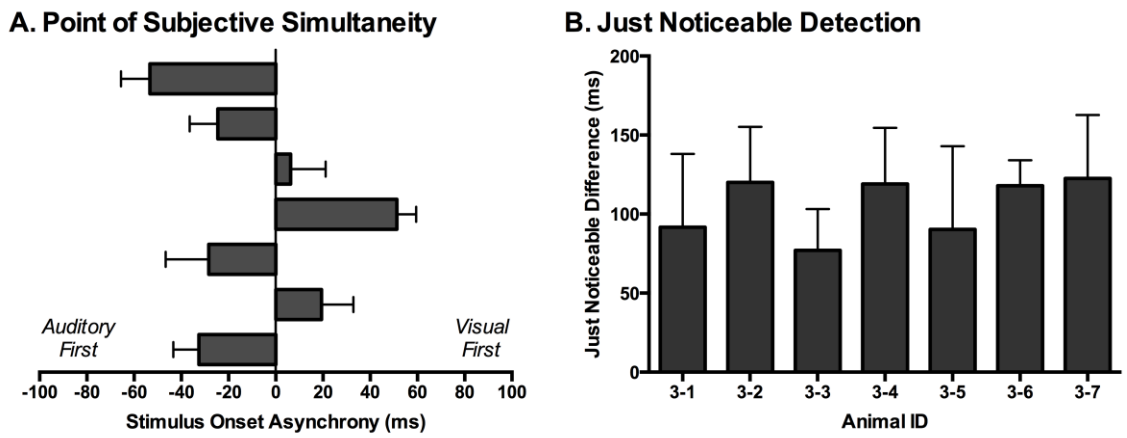

Figure 10. The point of subjective simultaneity and just noticeable difference derived from the temporal order judgement task.

(A) For each rat (n=7; 3-1 to 3-7, plotted in ascending order), its point of subjective simultaneity (PSS; i.e., the actual timing of the audiovisual stimuli when the observer is most unsure of the temporal order (Keetels and Vroomen, 2012) was determined. (B) For each rat (n=7; 3-1 to 3-7), the metric of just noticeable detection (JND; i.e., the smallest interval between the separately presented auditory and visual stimuli that can be detected reliably) was calculated by taking the difference between the SOAs at which 25% and 75% of the responses were considered "visual-first" and then dividing by two (Vroomen and Stekelenburg, 2011). The PSS and JND were determined for each of the five testing days, and then averaged to provide a representative metric for each rat. Results are displayed as mean ± SEM.

4.0 DISCUSSION:

To our knowledge, the present study represents the first investigation into the development and implementation of behavioural paradigms to assess the perception of audiovisual temporal synchrony in rodents. Using operant conditioning, rats were trained to perform 1) a simultaneity judgement task in which they reported whether audiovisual stimuli at various SOAs were presented at the same moment in time or at different times, and 2) a temporal order judgement task in which they reported whether they perceived the auditory or visual stimulus to be presented first. Rats were able to learn both tasks, and the resultant psychophysical curves were similar to those reported in humans (Vatakis et al., 2008b;

Zampini et al., 2005a). In addition, we conducted the first investigation of how neurons in the rat multisensory cortex integrate audiovisual stimuli presented at different SOAs. By comparing the spiking activity in response to the audiovisual stimuli presented at the various SOAs, we confirmed that the profile of neuronal activity in the rat V2L cortex was similar to that recorded in various multisensory brain regions of different species. Overall, our collective findings suggest that the rat represents an effective model for studying audiovisual temporal synchrony at both the neuronal and perceptual level.

4.1 Behavioural Assessments of Audiovisual Temporal Synchrony

A variety of experimental procedures have been developed to assess the ability of humans to determine the relative timing of combined auditory and visual stimuli presented at different SOAs by using a method of constant stimuli (Spence et al., 2001). The two procedures that have been used most often are the simultaneity judgement task and the temporal order judgement task. Although both of these tasks can assess an observer's perception of the temporal synchrony of audiovisual stimuli, it is thought that these tasks reflect different underlying mechanisms (Love et al., 2013; Vatakis et al., 2008b) and may be subject to different kinds of response biases (Schneider and Bavelier, 2003; Vatakis et al., 2008b; Vatakis and Spence, 2007).

Typically, the simultaneity judgement task asks observers to judge whether audiovisual stimuli were presented at the same moment in time (i.e., synchronous) or at different moments in time (i.e., asynchronous), irrespective of whether the auditory or visual stimulus was presented first (Binder, 2015; Spence et al., 2001; Stevenson et al., 2014; Stone et al., 2001; Vatakis et al., 2008b; Zampini et al., 2005a). In contrast, although our simultaneity judgement task (Experiment 2) also required that rats judge whether the audiovisual stimuli were presented synchronously or asynchronously, we elected to have the visual stimulus always precede the auditory stimulus (and never vice-versa). This protocol choice was made because numerous studies on humans have shown that the PSS typically occurs when visual stimulus precedes the auditory stimulus by approximately 50 ms (Boenke et al., 2009; Stevenson et al., 2014; Stone et al., 2001; Vatakis and Spence, 2008; Vroomen and Stekelenburg, 2011; Zampini et al., 2005a). Although the experimental procedures differed between species, the performance results of the rats in

the present study were similar to those of humans when compared to the "visual first" SOAs (Stevenson et al., 2014; Vatakis et al., 2008b; Zampini et al., 2005a). As predicted, rats were able to accurately (~80%) detect the difference between trials when audiovisual stimuli were presented synchronously versus when the visual stimulus preceded the auditory by 200 ms (Fig. 5B), and their performance scaled according to the interposed audiovisual SOAs. For example, similar to humans (Zampini et al., 2005a), the rats judged trials with a 10 ms SOA to be synchronous, whereas the majority (~70%) of trials at 100 ms SOA were perceived to be asynchronous (Fig. 9A). Collectively, these results provide support for the face validity of our newly-developed simultaneity judgement task for rats. It is worth noting, however, that rats training on the simultaneity judgement task were susceptible to developing a response bias, which resulted in a longer-than-expected training duration. Interestingly, Vatakis and Spence (2007) described that response bias may manifest more when humans perform simultaneity judgement tasks compared to temporal order judgement tasks. Thus, in an effort to lessen the potential for response bias, and to evaluate the perception of temporal synchrony when an auditory stimulus was presented before- or after a visual stimulus, we developed a novel temporal order judgement task for rats.

In Experiment 3, the ability of rats to judge temporal order was assessed at SOAs of 0, ±40, ±100, ±200 ms, as these timing onsets not only matched those used in Experiment 2 but were similar to the SOAs used in testing human participants. Consistent with humans (Vatakis et al., 2008a, 2008b), rats in the present study were able to accurately differentiate which modality was presented first when the SOAs were ±200 ms (Fig. 6B). Moreover, when the timing difference between the stimuli was incrementally reduced, the rats showed a commensurate decline in performance toward chance levels (Fig. 9B; see ~50% proportion of "visual first" responses when SOA was 0 ms). In addition to examining the psychophysical curve of response accuracy (Fig. 9B), the PSS and JND were calculated from the temporal order judgement task. As shown in Fig. 10A, the PSS values of the rats were variable, ranging from -53 ms ("auditory first") to 51 ms ("visual first"); findings within the range of values reported in experiments conducted on humans (Navarra et al., 2005; Vatakis et al., 2008b; Vatakis and Spence, 2007; Zampini et al., 2003). Similar to Vatakis et al. (2008), who found that the mean PSS value was 1 ms and -6 ms for

synchronous and asynchronous speech monitoring, respectively, the mean PSS value for the rats was -8 ms (i.e., auditory was judged to precede visual). Moreover, the average JND value of 105 ± 7 ms indicates that rats were able to determine the temporal order of different sensory modalities similar to humans (Navarra et al., 2005; Vatakis et al., 2008a, 2008b).

4.2 Neural Basis of Audiovisual Temporal Processing?

Neuroimaging studies have provided insight into the brain regions activated during audiovisual processing tasks. For example, the insula, ventrolateral prefrontal cortex, and inferior parietal lobe (predominantly within the right hemisphere) have been shown to be engaged in the perception of audiovisual simultaneity (Adhikari et al., 2013; Binder, 2015; Bushara et al., 2001) and multisensory perception (Calvert and Thesen, 2004). Investigations into audiovisual temporal synchrony perception have found differences in the networks activated in response to synchronous and asynchronous stimuli. Consistent with temporal order judgement tasks in the visual domain (Davis et al., 2009), activation of both the left and right temporal parietal junction (TPJ) was observed, where the right temporal and parietal cortices, TPJ, as well as the right frontal and left parietal cortices showed greater activation to asynchronous perception in comparison to the synchronous perception of audiovisual stimuli (Adhikari et al., 2013). While differences in the degree of activation have been observed between synchronous and asynchronous perception, Binder (2015) demonstrated that simultaneity judgement tasks and temporal order judgement tasks activate similar cortical networks; however, the temporal order judgement task requires a greater amount of activation within the prefrontal, parietal lobules and occipito-temporal regions. This higher degree of neuronal activation is thought to be due to the additional cognitive operations that are required to judge which stimulus was presented first (Binder, 2015).

At this time, it is not possible to be certain which brain areas in the rat are responsible for audiovisual temporal synchrony perception, and whether these neuronal networks and patterns of activity differ during simultaneity- versus temporal order judgement tasks. It is, however, reasonable to speculate that the V2L cortex may contribute to task performance. For example, as shown in the present study (Experiment 1), the rat V2L

cortex—a well-established area responsive to audiovisual stimuli (Barth et al., 1995; Hirokawa et al., 2008; Schormans et al., 2016; Toldi et al., 1986; Wallace et al., 2004; Xu et al., 2014)—is sensitive to differences in the timing of combined audiovisual stimuli, such that spiking activity was greatest during trials when the visual stimulus preceded the auditory by 20 to 40 ms (Fig. 7C and 8C). These results are fairly consistent with previous studies that recorded audiovisual-evoked spiking activity in the superior colliculus [cat (Meredith et al., 1987; Meredith and Stein, 1996, 1986, Perrault et al., 2012, 2005; Stanford et al., 2005) and guinea pig (King and Palmer, 1985)] as well as multisensory cortices [cat PLLS (Allman, 2009; Allman et al., 2008b; Allman and Meredith, 2007) and cat FAES (Meredith and Allman, 2009)], and further confirm that the timing of the stimuli play a critical role in the ability of the neurons to integrate the different sensory modalities (King and Palmer, 1985; Meredith and Stein, 1986; Miller et al., 2015; Perrault et al., 2005; Stanford et al., 2005). Although the V2L cortex has been shown to play an important role in audiovisual processing, future investigations are needed in order to assess audiovisual temporal processing at the single neuron level. As additional support of the potential role of the V2L cortex in the audiovisual temporal synchrony tasks, Hirokawa and colleagues (2008) demonstrated using local pharmacological inactivation that the V2L cortex was responsible for the improved reaction time to detect audiovisual stimulation (i.e., multisensory facilitation). That said, given the extra demands of decision-making in the audiovisual temporal synchrony tasks developed in the present study, it is likely that, in addition to the V2L cortex, areas of the prefrontal and posterior parietal cortices also influence perceptual judgements. Indeed, Raposo and colleagues demonstrated that the neurons in the posterior parietal cortex of rats dynamically-contributed to the performance of a multisensory decision-making task (Raposo et al., 2014). Ultimately, our future studies will seek record the neural activity in the V2L cortex as rats perform the simultaneity- and temporal judgement tasks so as to further investigate the putative neural substrates contributing to the perception of audiovisual temporal synchrony.

5.0 REFERENCES:

Adhikari, B.M., Goshorn, E.S., Lamichhane, B., Dhamala, M., (2013). Temporal-Order Judgment of Audiovisual Events Involves Network Activity Between Parietal and Prefrontal Cortices. *Brain Connect.* 3, 536–545.

Allman, B., (2009). Not Just for Bimodal Neurons Anymore: The Contribution of Unimodal Neurons to Cortical Multisensory Processing. *Brain Topogr.* 21, 157–167.

Allman, B.L., Bittencourt-Navarrete, R.E., Keniston, L.P., Medina, A.E., Wang, M.Y., Meredith, M.A., (2008a). Do Cross-Modal Projections Always Result in Multisensory Integration? *Cereb. Cortex* 18, 2066–2076.

Allman, B.L., Keniston, L.P., Meredith, M.A., (2008b). Subthreshold auditory inputs to extrastriate visual neurons are responsive to parametric changes in stimulus quality: Sensory-specific versus non-specific coding. *Brain Res.* 1242, 95–101.

Allman, B.L., Meredith, M.A., (2007). Multisensory Processing in "Unimodal" Neurons: Cross-Modal Subthreshold Auditory Effects in Cat Extrastriate Visual Cortex. *J. Neurophysiol.* 98, 545–549.

Armstrong, R.A., (2014). When to use the Bonferroni correction. *Ophthalmic Physiol. Opt.* 34, 502–508.

Barth, D.S., Goldberg, N., Brett, B., Di, S., (1995). The spatiotemporal organization of auditory, visual, and auditory-visual evoked potentials in rat cortex. *Brain Res.* 678, 177–190.

Binder, M., (2015). Neural correlates of audiovisual temporal processing – Comparison of temporal order and simultaneity judgments. *Neuroscience* 300, 432–447.

Boenke, L.T., Deliano, M., Ohl, F.W., (2009). Stimulus duration influences perceived simultaneity in audiovisual temporal-order judgment. *Exp. Brain Res.* 198, 233–244.

Bushara, K.O., Grafman, J., Hallett, M., (2001). Neural Correlates of Auditory–Visual Stimulus Onset Asynchrony Detection. *J. Neurosci.* 21, 300–304.

Calvert, G.A., Campbell, R., Brammer, M.J., (2000). Evidence from functional magnetic resonance imaging of crossmodal binding in the human heteromodal cortex. *Curr. Biol.* 10, 649–657.

Calvert, G.A., Thesen, T., (2004). Multisensory integration: methodological approaches and emerging principles in the human brain. *J. Physiol.-Paris* 98, 191–205.

Chen, L., Vroomen, J., (2013). Intersensory binding across space and time: a tutorial review. *Atten. Percept. Psychophys.* 75, 790–811.

Davis, B., Christie, J., Rorden, C., (2009). Temporal Order Judgments Activate Temporal Parietal Junction. *J. Neurosci.* 29, 3182–3188.

Diederich, A., Colonius, H., (2004). Bimodal and trimodal multisensory enhancement: Effects of stimulus onset and intensity on reaction time. *Percept. Psychophys.* 66, 1388–1404.

Fujisaki, W., Shimojo, S., Kashino, M., Nishida, S., (2004). Recalibration of audiovisual simultaneity. *Nat. Neurosci.* 7, 773–778.

Ghazanfar, A.A, Schroeder, C.E., (2006) Is neocortex essentially multisensory? *Trends in Cognitive Sciences.* 10 (6), 278-285

Gleiss, S., Kayser, C., (2012). Audio-Visual Detection Benefits in the Rat. *PLoS ONE* 7, e45677.

Hershenson, M., (1962). Reaction time as a measure of intersensory facilitation. *J. Exp. Psychol.* 63, 289–293.

Hirokawa, J., Bosch, M., Sakata, S., Sakurai, Y., Yamamori, T., (2008). Functional role of the secondary visual cortex in multisensory facilitation in rats. *Neuroscience* 153, 1402–1417.

Keetels, M., Vroomen, J., (2012). Perception of Synchrony between the Senses. CRC Press/Taylor & Francis.

King, A.J., Palmer, A.R., (1985). Integration of visual and auditory information in bimodal neurones in the guinea-pig superior colliculus. *Exp. Brain Res.* 60, 492–500.

Krueger Fister, J., Stevenson, R.A., Nidiffer, A.R., Barnett, Z.P., Wallace, M.T., (2016). Stimulus intensity modulates multisensory temporal processing. *Neuropsychologia* 88, 92–100.

Lippert, M.T., Takagaki, K., Kayser, C., Ohl, F.W., (2013). Asymmetric Multisensory Interactions of Visual and Somatosensory Responses in a Region of the Rat Parietal Cortex. *PLoS ONE* 8, e63631.

Love, S.A., Petrini, K., Cheng, A., Pollick, F.E., (2013). A psychophysical investigation of differences between synchrony and temporal order judgments. *PLoS ONE* 8, e54798.

Meredith, M.A., Allman, B.L., (2009). Subthreshold multisensory processing in cat auditory cortex. *Neuroreport* 20, 126–131.

Meredith, M.A., Nemitz, J.W., Stein, B.E., (1987). Determinants of multisensory integration in superior colliculus neurons. I. Temporal factors. *J. Neurosci.* 7, 3215–3229.

Meredith, M.A., Stein, B.E., (1996). Spatial determinants of multisensory integration in cat superior colliculus neurons. *J. Neurophysiol.* 75, 1843–1857.

Meredith, M.A., Stein, B.E., (1986). Visual, auditory, and somatosensory convergence on cells in superior colliculus results in multisensory integration. *J. Neurophysiol*. 56, 640–662.

Miller, R.L., Pluta, S.R., Stein, B.E., Rowland, B.A., (2015). Relative unisensory strength and timing predict their multisensory product. *J. Neurosci.* 35, 5213–5220.

Navarra, J., Vatakis, A., Zampini, M., Soto-Faraco, S., Humphreys, W., Spence, C., (2005). Exposure to asynchronous audiovisual speech extends the temporal window for audiovisual integration. *Cogn. Brain Res.* 25, 499–507.

Paxinos, G., Watson, C., (2007). The rat brain in stereotaxic coordinates, 6th ed. Elsevier Inc., Burlington, MA.

Perrault, T.J., Rowland, B.A., Stein, B.E., (2012). "The Organization and Plasticity of Multisensory Integration in the Midbrain", In *The Neural Bases of Multisensory Processes.* eds, Murray, M.M., Wallace, M.T. (Boca Raton, FL.: CRC Press/Taylor Francis), 279-300.

Perrault, T.J., Vaughan, J.W., Stein, B.E., Wallace, M.T., (2005). Superior Colliculus Neurons Use Distinct Operational Modes in the Integration of Multisensory Stimuli. *J. Neurophysiol*. 93, 2575–2586.

Popelar, J., Grecova, J., Rybalko, N., Syka, J., (2008) Comparison of noise-induced changes of auditory brainstem and middle latency response amplitudes in rats. *Hear. Res.* 245, 82-91.

Raposo, D., Kaufman, M.T., Churchland, A.K., (2014). A category-free neural population supports evolving demands during decision-making. *Nat. Neurosci*. 17, 1784–1792.

Raposo, D., Sheppard, J.P., Schrater, P.R., Churchland, A.K., (2012). Multisensory Decision-Making in Rats and Humans. *J. Neurosci*. 32, 3726–3735.

Schneider, K.A., Bavelier, D., (2003). Components of visual prior entry. *Cognit. Psychol.* 47, 333–366.

Schormans, A.L., Typlt, M., Allman, B.L., (2016). Crossmodal plasticity in auditory, visual and multisensory cortical areas following noise-induced hearing loss in adulthood. *Hear. Res.* 343: 93-107

Schroeder C.E., Foxe, J.J., (2002) The timing and laminar profile of converging inputs to multisensory areas of the macaque neocortex. *Cognitive Brain Res*. 14, 187-198

Seimann, J.K., Muller, C.L., Bamberger, G., Allison, J.D., Veenstra-VanderWeele, J., Wallace, M.T., (2014) A novel behavioral paradigm to asses multisensory processing in mice. *Frontiers in Behavioral Neuroscience*. 8: 456.

Spence, C., Baddeley, R., Zampini, M., James, R., Shore, D.I., (2003). Multisensory temporal order judgments: When two locations are better than one. *Percept. Psychophys*. 65, 318–328.

Spence, C., Shore, D.I., Klein, R.M., (2001). Multisensory prior entry. *J. Exp. Psychol. Gen.* 130, 799–832.

Stanford, T.R., Quessy, S., Stein, B.E., (2005). Evaluating the operations underlying multisensory integration in the cat superior colliculus. *J. Neurosci.*. 25, 6499–6508.

Stein, B.E., Meredith, M.A., (1993). The merging of the senses, Cognitive neuroscience. The MIT Press, Cambridge, MA, US.

Stein, B.E., Stanford, T.R., (2008). Multisensory integration: current issues from the perspective of the single neuron. *Nat. Rev. Neurosci.* 9, 255–266.

Stevenson, R.A., Siemann, J.K., Schneider, B.C., Eberly, H.E., Woynaroski, T.G., Camarata, S.M., Wallace, M.T., (2014). Multisensory temporal integration in autism spectrum disorders. *J. Neurosci.* 34, 691–697.

Stevenson, R.A., Wallace, M.T., (2013). Multisensory temporal integration: task and stimulus dependencies. *Exp. Brain Res*. 227, 249–261. doi:10.1007/s00221-013-3507-3

Stolzberg, D., Hayes, S.H., Kashanian, N., Radziwon, K., Salvi, R.J., Allman, B.L., (2013). A novel behavioral assay for the assessment of acute tinnitus in rats optimized for simultaneous recording of oscillatory neural activity. *J. Neurosci. Methods* 219, 224–232.

Stone, J.V., Hunkin, N.M., Porrill, J., Wood, R., Keeler, V., Beanland, M., Port, M., Porter, N.R., (2001). When is now? Perception of simultaneity. *Proc. Biol. Sci.* 268, 31–38.

Toldi, J., Fehér, O., Wolff, J.R., (1986). Sensory interactive zones in the rat cerebral cortex. *Neuroscience* 18, 461–465.

Vatakis, A., Bayliss, L., Zampini, M., Spence, C., (2007). The influence of synchronous audiovisual distractors on audiovisual temporal order judgments. *Percept. Psychophys.* 69, 298–309.

Vatakis, A., Ghazanfar, A.A., Spence, C., (2008a). Facilitation of multisensory integration by the “unity effect” reveals that speech is special. *J. Vis.* 8, 14.1-11.

Vatakis, A., Navarra, J., Soto-Faraco, S., Spence, C., (2008b). Audiovisual temporal adaptation of speech: temporal order versus simultaneity judgments. *Exp. Brain Res.* 185, 521–529.

Vatakis, A., Spence, C., (2008). Evaluating the influence of the “unity assumption” on the temporal perception of realistic audiovisual stimuli. *Acta Psychol. (Amst.)* 127, 12–23.

Vatakis, A., Spence, C., (2007). Crossmodal binding: evaluating the “unity assumption” using audiovisual speech stimuli. *Percept. Psychophys*. 69, 744–756.

Vroomen, J., Stekelenburg, J.J., (2011). Perception of intersensory synchrony in audiovisual speech: Not that special. Cognition 118, 75–83.

Wallace, M.T., Ramachandran, R., Stein, B.E., (2004). A revised view of sensory cortical parcellation. *Proc. Natl. Acad. Sci.* 101, 2167–2172.

Wallace, M.T., Stevenson, R.A., (2014). The construct of the multisensory temporal binding window and its dysregulation in developmental disabilities. *Neuropsychologia* 64, 105–123.

Xu, J., Sun, X., Zhou, X., Zhang, J., Yu, L., (2014). The cortical distribution of multisensory neurons was modulated by multisensory experience. *Neuroscience* 272, 1–9.

Zampini, M., Guest, S., Shore, D.I., Spence, C., (2005a). Audio-visual simultaneity judgments. *Percept. Psychophys*. 67, 531–544.

Zampini, M., Shore, D.I., Spence, C., (2005b). Audiovisual prior entry. *Neurosci. Lett.* 381, 217–222.

Zampini, M., Shore, D.I., Spence, C., (2003). Audiovisual temporal order judgments. *Exp. Brain Res*. 152, 198–210.

Appendix B: Ethics Approvals

Western

2013-020::1:

AUP Number: 2013-020
AUP Title: Neurophysiological Basis of Multisensory Processing
Yearly Renewal Date: 08/01/2014

The YEARLY RENEWAL to Animal Use Protocol (AUP) 2013-020 has been approved, and will be approved for one year following the above review date.

1. This AUP number must be indicated when ordering animals for this project.
2. Animals for other projects may not be ordered under this AUP number.
3. Purchases of animals other than through this system must be cleared through the ACVS office. Health certificates will be required.

REQUIREMENTS/COMMENTS
Please ensure that individual(s) performing procedures on live animals, as described in this protocol, are familiar with the contents of this document.

The holder of this Animal Use Protocol is responsible to ensure that all associated safety components (biosafety, radiation safety, general laboratory safety) comply with institutional safety standards and have received all necessary approvals. Please consult directly with your institutional safety officers.

Submitted by: Kinchlea, Will D
on behalf of the Animal Use Subcommittee

Western

AUP Number: 2017-162
PI Name: Allman, Brian
AUP Title: Neurophysiological Basis of Multisensory Processing
Approval Date: 12/01/2017

Official Notice of Animal Care Committee (ACC) Approval:
Your new Animal Use Protocol (AUP) 2017-162:1: entitled " Neurophysiological Basis of Multisensory Processing"
has been APPROVED by the Animal Care Committee of the University Council on Animal Care. This approval, although valid for up to four years, is subject to annua

Prior to commencing animal work, please review your AUP with your research team to ensure full understanding by everyone listed within this AUP.

As per your declaration within this approved AUP, you are obligated to ensure that:

1) Animals used in this research project will be cared for in alignment with:
   a) Western's Senate MAPPs 7.12, 7.10, and 7.15
   http://www.uwo.ca/univsec/policies_procedures/research.html

   b) University Council on Animal Care Policies and related Animal Care Committee procedures
   http://uwo.ca/research/services/animalethics/animal_care_and_use_policies.htm
2) As per UCAC's Animal Use Protocols Policy,
   a) this AUP accurately represents intended animal use;
   b) external approvals associated with this AUP, including permits and scientific/departmental peer approvals, are complete and accurate;
   c) any divergence from this AUP will not be undertaken until the related Protocol Modification is approved by the ACC; and
   d) AUP form submissions - Annual Protocol Renewals and Full AUP Renewals - will be submitted and attended to within timeframes outline
   e) http://uwo.ca/research/services/animalethics/animal_use_protocols.html

3) As per MAPP 7.10 all individuals listed within this AUP as having any hands-on animal contact will
   a) be made familiar with and have direct access to this AUP;
   b) complete all required CCAC mandatory training
   c) be overseen by me to ensure appropriate care and use of animals.
4) As per MAPP 7.15,
   a) Practice will align with approved AUP elements;
   b) Unrestricted access to all animal areas will be given to ACVS Veterinarians and ACC Leaders;
   c) UCAC policies and related ACC procedures will be followed, including but not limited to:
      i) Research Animal Procurement
      ii) Animal Care and Use Records
      iii) Sick Animal Response
      iv) Continuing Care Visits
5) As per institutional OH&S policies, all individuals listed within this AUP who will be using or potentially exposed to
hazardous materials will have completed in advance the appropriate institutional OH&S training, facility-level training, and reviewed related (M)SDS Sheets
http://www.uwo.ca/hr/learning/required/index.html

Submitted by: Copeman, Laura
on behalf of the Animal Care Committee
University Council on Animal Care

Appendix C: Copyright Permissions

OXFORD UNIVERSITY PRESS LICENSE
TERMS AND CONDITIONS

Dec 01, 2018

This Agreement between 1 Grosvenor St. ("You") and Oxford University Press ("Oxford University Press") consists of your license details and the terms and conditions provided by Oxford University Press and Copyright Clearance Center.

License Number	4480051291570
License date	Dec 01, 2018
Licensed content publisher	Oxford University Press
Licensed content publication	Cerebral Cortex
Licensed content title	Adult-Onset Hearing Impairment Induces Layer-Specific Cortical Reorganization: Evidence of Crossmodal Plasticity and Central Gain Enhancement
Licensed content author	Schormans, Ashley L; Typlt, Marei
Licensed content date	Apr 13, 2018
Type of Use	Thesis/Dissertation
Institution name	
Title of your work	Adult-Onset Hearing Impairment Induces Layer-Specific Cortical Reorganization: Evidence of Crossmodal Plasticity and Central Gain Enhancement
Publisher of your work	University of Western Ontario
Expected publication date	Feb 2019
Permissions cost	0.00 CAD
Value added tax	0.00 CAD
Total	0.00 CAD
Title	Adult-Onset Hearing Impairment Induces Layer-Specific Cortical Reorganization: Evidence of Crossmodal Plasticity and Central Gain Enhancement
Institution name	University of Western Ontario
Expected presentation date	Feb 2019
Portions	Entire text
Requestor Location	

Publisher Tax ID	GB125506730
Billing Type	Invoice
Billing Address	

Curriculum Vitae

Name:	Ashley Schormans
Post-secondary Education and Degrees:	University of Waterloo Waterloo, Ontario, Canada 2008-2013 B.Sc. Biology The University of Western Ontario London, Ontario, Canada 2013 - 2019 Ph.D. Anatomy and Cell Biology
Honours and Awards:	Queen Elizabeth II Graduate Scholarship in Science and Technology 2015-2018 Gabriel G. Altman Research Award – PhD Department of Anatomy and Cell Biology 2015 CIHR Silver Prize Poster Presentation Canadian Student Health Research Forum 2018
Related Work Experience	Research Assistant, Biology University of Waterloo 2010 Environmental Assistant, National Guidelines and Safety Office Environment Canada 2012 Teaching Assistant, Human Physiology University of Waterloo 2013 Teaching Assistant, Systemic Human Anatomy The University of Western Ontario 2013-2014, 2015-2016 Teaching Assistant, Integrative Neuroscience The University of Western Ontario 2014, 2016-2017

Publications:

Schormans, A. L., Typlt, M. & Allman, B. L. (2016) Crossmodal plasticity in Auditory, Visual and Multisensory Cortical Regions Following Noise-Induced Hearing Loss in Adulthood. *Hearing Research.* 343, 92-107

Abitbol, J.M., Kelly, J.J., Barr, K., **Schormans, A.L.**, Laird, D.W., Allman, B.L. (2016) Differential Effects of Pannexins on Noise-Induced Hearing Loss. *Journal of Biochemistry.* 473:24, 4665-4680

Allman, B.L., **Schormans, A.L.**, Typlt, M., Lobarinas, E. (2016) Past, Present and Future Pharmacological Therapies for Tinnitus", In: *Springer Handbook of Auditory Sciences: Translational Research in Audiology and Hearing Sciences.* Chpt. 7, 165-195

Schormans, A.L., Scott, K.E., Vo, A.M.Q., Tyker, A., Typlt, M., Stolzberg, D., Allman, B.L. (2017) Audiovisual Temporal Processing and Synchrony Perception in the Rat. *Frontiers in Behavioural Neuroscience*. 10:246, 1-18

Schormans, A.L., Typlt, M., Allman, B.L. (2018) Adult-onset hearing impairment induces layer-specific cortical reorganization: Evidence of crossmodal plasticity and central gain enhancement. *Cerebral Cortex*. bhy067

Scott, K.E., **Schormans, A.L.**, Pacoli, K., De Olivera, C., Allman, B.L., Schmid, S. (2018) Altered auditory processing, filtering, and reactivity in the Cntnap2 knockout model for neurodevelopmental disorders. *Journal of Neuroscience*, 0759-18

Schormans, A.L., Allman, B.L. (2018) Behavioral plasticity of audiovisual perception: rapid recalibration of temporal sensitivity but not perceptual binding following adult-onset hearing loss. *Frontiers in Behavioral Neuroscience.* 12:256, 1-18

Schormans, A.L., Allman, B.L. (2019) Compensatory plasticity in the lateral extrastriate visual cortex preserves audiovisual temporal processing following adult-onset hearing loss. *Neural Plasticity* [In Press].